THE UNIVERSITY *of* EDINBURGH

The role of PrP^C glycosylation in health and disease

Kayleigh Iremonger

Ph.D. by Research
The University of Edinburgh
2013

Declaration

I declare that this thesis has been composed entirely by myself and that the work presented herein is my own, except where otherwise stated. All experiments were designed by myself, in collaboration with my supervisors. No part of this thesis has been, or will be, submitted for any other degree, diploma or qualification

Kayleigh Iremonger

Acknowledgements

I would like to express my thanks to my supervisors **Professor Jean Manson**, **Dr. Wilfred Goldmann** and **Dr. Enrico Cancellotti** for their help and guidance throughout this PhD, for giving me the opportunity to develop my ideas and present it to a wider audience.

I would like to thank the following people for provision of material, skills and knowledge:

Sue Godsave (NKI, Netherlands) for all of your help with the electron microscopy and gold quantification and for your rapid responses to my many emails.

Peter Peters (NKI, Netherlands) for giving me the opportunity to visit Amsterdam and experience the EM protocol.

Sandra McCutcheon for provision of many of the anti-PrP antibodies tested, including BC6, which was used throughout.

Dr. Richard Alejo-Blanco and **James Alibhai** for producing and providing recombinant PrP for the QuIC assay

James Alibhai for teaching me the QuIC assay, for all of your QuIC advice and checking it over the weekend.

Dr. Rona Wilson and **Dr. Herbert Baybutt** for teaching me to prepare and culture cells

Susie Aungier for providing protocols and teaching me RNA extraction and rt-qPCR

I would like to thank all of the animal house staff who have helped me along the way, particularly **Irene McConnell**, and **Simon Cumming** for providing me with mouse tissues and **Mary Brady** for collection of embryos for cell culture experiments.

I would like to thank all of the **Manson group members** for all of your advice and scientific discussion during lab meetings, for not laughing at my half-baked ideas and for always pointing me in the right direction.

Thanks to **Boon chin Tan** and **Chris de Wolf** for all of your science discussions and immunoblot problem solving sessions and for letting me borrow reagents when mine didn't like the science.

A big thank you to **Sandra McCutcheon** for help and support for both work and non-work related issues. Thanks for your encouragement and helping me to 'sell myself and my science' during my PhD. More importantly thanks for all of our play dates and listening to all things baby when everyone else has glazed over and gone to sleep.

Many thanks to **Abi Diack** for being 'my post-doc' and proof reading my thesis. Thank you for answering all of my silly questions. You have been like family to me and have kept me sane for the last four years.

Many thanks to **Charmaine Love** for your friendship and being my running buddy. We went on some adventures and most ended up with us covered in mud!

To all of the **PhD students**, thank you for all of your conversations and understanding of the challenges of a PhD and thank you for all of the chocolate and cake in the final push.

And finally, a huge thank you to **my families** for sharing the highs and for the never ending encouragement through the lows. Your pride in me means so much. Thank you to my wonderful husband **James**, for taking on a 'dirty student' and for believing in me when I didn't believe in myself. **Harriet**, my beautiful little girly you have kept me going through the final year. You have made life much more complicated but every day has been an adventure with you. It doesn't matter how bad the day has been you always make me smile and forget my worries.

Abstract

Glycosylation is the most abundant post-translational modification of proteins and has the ability to change the physical properties of the protein and its cell biology. The cellular prion protein (PrP^C) is a membrane bound host glycoprotein present in a number of isoforms *in vivo* due to variable occupancy of the two *N*-linked glycosylation sites. The function of PrP^C is still unclear but it is essential for disease in transmissible spongiform encephalopathies (TSEs). The significance of the PrP glycoforms in the physiological function is unknown. Gene targeted mice have been created with point mutations that selectively abolish the glycosylation sites of PrP^C. These GlycoD mutants have been used to study the effect of glycosylation at the different sites on the cell biology of PrP^C.

This study showed that both glycosylation sites played a role in the cell biology of PrP^C. Removal of a single or both glycosylation sites significantly reduced total PrP^C protein. The relative amount of the truncated protein produced through proteolytic cleaving was slightly reduced in the GlycoD mutants; however the proportion of truncated to full length PrP was increased, further reducing full length protein. The maintenance of truncated protein levels indicates a potential importance of the fragment in PrP^C function. Wild type PrP is predominantly diglycosylated and localised to the cell surface. In this study it was shown that all GlycoD mutants had reduced amounts of cell surface PrP^C and an increased proportion of PrP^C associated with the secretory pathway. Removal of either the first or the second glycosylation site produced changes in cell biology that were almost indistinguishable from each other whilst disruption of both glycosylation sites produces a more extreme phenotype than removal of a single site.

Previous studies have shown an altered susceptibility for TSE disease GlycoD mice. An *in vitro* conversion assay was used to investigate the ability of the glycoforms to initiate conversion from PrP^C to the disease associated PrP^{Sc}. Mice which had only the second site abolished were much more efficient at seeding conversion than all other glycoforms. This may reflect the difference in susceptibility between the two

monoglycosylated PrPs but does not explain the increased resistance compared to wild type mice. All other GlycoD mutants had similar seeding times to wild type mice despite having increased TSE resistance. The differences observed in the cell biology of PrP^{C} of the GlycoD mutants may go some way to explaining the differences in TSE susceptibilities seen with these mice.

Abbreviations

Asn	Asparagine (amino acid)
APP	Amyloid precursor protein
BCA	Bicinchoninic acid
BSA	Bovine serum albumen
BSE	Bovine spongiform encephalopathy
CD	Circular dichroism
CDG	Congenital disorder of glycosylation
cDNA	Complementary DNA
CETP	Cholesteryl ester transfer protein
CFC	Cell free conversion assay
CJD	Creutzfeldt Jakob disease
CNS	Central nervous system
Co-IP	Co-immunoprecipitation
^{Ctm}PrP	C-terminal transmembrane PrP
CWD	Chronic Wasting Disease
DAPI	4'6-diamidino-2-phenylindole, a fluorescent dye that binds to DNA
DELFIA	Dissociation enhanced lanthanide fluoroimmunoassay
dH_2O	Deionised water
DMSO	Dimethyl sulphoxide
DPBS	Dulbecco's phosphate buffered saline
DTT	DithiothreitolEDTA Ethylenediaminetetraacetic acid
Endo H	Endo-β-N-acetylglucosaminidase H, Endoglycosidase
ER	Endoplasmic reticulum
ERAD	Endoplasmic reticulum associated degradation
ERK	Extracellular regulated kinase
EGF	Epidermal growth factor
EGTA	Ethylene glycol tetraacetic acid
EM	Electron microscopy
fFI	Fatal Familial Insomnia

FGFb	Fibroblast growth factor b
Flot-1	Flotillin
FSE	Feline spongiform encephalopathy
G1	PrP glycosylation deficient transgenic, lacking the first N-glycan attachment site (N180T)
G2	PrP glycosylation deficient transgenic, lacking the second N-glycan attachment site (N196T)
G3	PrP glycosylation deficient transgenic, lacking both N-glycan attachment sites (N180T, N196T)
GABA	Gamma-aminobutyric acid
GFAP	GLial fibrillary acidic protein
GlycoD	PrP glycosylation deficient transgenic (either G1, G2 or G3)
Gnd HCl	Guanidine hydrochloride
GPI	Glycosylphosphatidylinisotol
GSS	Gerstmann-Sträussler-Scheinker syndrome
HBSS	Hanks balanced salt solution
ICC	Immunocytochemistry
IgG	Immunoglobulin G
IHC	Immunohistochemistry
IL-6	Interleukin 6
kDa	Kilo dalton
LN_2	Liquid nitrogen
mAb	Monoclonal antibody
MAP-2	Microtubule associated protein 2
MBS	MES buffered saline
MES	2-(N-morpholino)ethanesulfonic acid
Met	Methionine (amino acid)
mRNA	Messenger RNA
NEM	N- ethylmaleimide
NMR	Nuclear magnetic resonance
^{Ntm}PtP	N-terminal transmembrane PrP
o/n	Over night

ORF	Open reading frame
OST	Oligosaccharyl transferase complex
PAGE	Polyacrylamide gel electrophoresis
PI-PLC	Phosphatidylinositol-Specific Phospholipase C
PBS	Phosphate buffered saline
PBS-G	PBS 0.02% Glycine
PCR	Polymerase chain reaction
PFA	Paraformaldehyde
PK	Proteinase K
PMCA	Protein misfolding cyclic amplification
PMSF	Phenylmethanesulfonyl fluoride
PNGase F	Peptide -N-Glycosidase F
PNS	Peripheral nervous system
Prn-p	Gene encoding the murine prion protein
PrP	Any isoform of the prion protein
PrP^{C}	PrP- cellular; native, uninfectious form of PrP
PrP^{res}	PK resistant PrP, not necessarily associated with infectivity
PrP^{Sc}	PrP- scrapie; infectious form of PrP
PrP^{spon}	PrP^{res} spontaneously generated without PrP^{Sc} seeding during *in vitro* assays
PVDF	Polyvinylidine fluoride
qPCR	quantitative polymerase chain reaction
QuIC	Quaking induced conversion
ROS	Reactive oxygen species
sCJD	Sporadic CJD
SDS	Sodium dodecyl sulphate
Sem	Standard error of the mean
Ser	Serine (amino acid)
sFI	Sporadic fatal insomnia
SSCA	Scrapie cell conversion assay
Stip 1	Stress-inducible protein 1
TBS	Tris buffered saline

TBST	TBS 1% Tween
TfR	Transferrin receptor
Thr	Threonine (amino acid)
Tg	Transgenic
TME	Transmissible Mink Encephalopathy
t-PA	Tissue plasminogen activator
TSE	Transmissible spongiform encephalopathy
UPR	Unfolded protein response
Val	Valine (amino acid)
VEGF	Vascular endothelial growth factor
v/v	volume per volume
Wt	Wild type mice on 129/ola background
w/v	weight per volume

Contents

Figures

Chapter 1

Chapter 2

Chapter 3

Chapter 4

Chapter 5

Tables

Chapter 1

Chapter 2

Chapter 3

Chapter 5

1 Introduction

The transmissible spongiform encephalopathies (TSEs) are a group of rare, fatal neurodegenerative diseases which affect a variety of hosts, such as Creutzfeldt-Jakob disease (CJD) in humans, scrapie in sheep and bovine spongiform encephalopathy (BSE) in cattle. Disease is characterised by long incubation periods before a clinical phase with neurological symptoms such as ataxia, dementia, hallucinations, depression, anxiety and insomnia. There are currently no cures or treatments for TSEs.

The central event in TSE disease is the conversion of the host cellular prion protein (PrP^{C}) into a disease associated conformer, PrP^{Sc}. Several different strains of TSE can exist within the same host species, which is thought to be due to different conformations of PrP^{Sc}. Mice are not natural hosts for TSEs but have been used as models to investigate TSE diseases using strains adapted from different sources.

Both PrP^{C} and PrP^{Sc} contain two glycosylation sites which can be variably occupied to produce four glycoforms *in vivo*. The glycosylation has been shown to influence TSE disease susceptibility and pathology in transgenic mice that have the glycosylation sites of PrP^{C} abolished. Most research has focused on PrP^{Sc} thus very little is known about the function and biological relevance of the cellular protein. The influence of the glycosylation on the normal cell biology of PrP^{C} may indicate whether the glycoforms have different functions and may give an insight into the altered TSE disease phenotype observed when glycosylation is disrupted.

1.1 The cellular prion protein

PrP^{C} was first identified in 1985 during the search for the infectious agent of the TSEs (Oesch et al., 1985). The scrapie agent was purified and the N-terminal sequence obtained (Prusiner et al., 1984). It was found that the sequence of PrP^{C} and the scrapie agent, PrP^{Sc} did not differ indicating that the differences between the cellular protein

and disease associated protein are due to post-translational modification (Basler et al., 1986).

1.1.1 Prnp

The cellular prion protein (PrP^C) is encoded by a small, single copy gene, *Prnp*. The PrP open reading frame (ORF) is encoded within a single exon although the gene itself comprises two to three exons depending upon the species (Basler et al., 1986, Gabriel et al., 1992). Other exons contain the 5' untranslated region including the GC rich promoter. PrP^C belongs to the prion protein family which also includes the paralogues *Prnd* which produces doppel and *Sprn* which produces shadoo. PrP is highly conserved between species. Orthologs of *Prnp* have been identified in many species and their loci mapped (Ryou, 2007).

In mice *Prnp* is located on chromosome 2 (Oesch et al., 1985, Siracusa et al., 1990), spans 16kb and is made up of 3 exons (Lee et al., 1998). Mice have three distinct alleles of *Prnp*, a, b and c which differ at two codons (108 and 189) (Westaway et al., 1987, Brown et al., 2000, Lloyd et al., 2004).

Prnp mRNA is developmentally regulated and increases in response to neuronal differentiation (Lazarini et al., 1994). *In situ* hybridisation shows mRNA can be detected in the murine brain as early as embryonic day 9 (E9) (Miele et al., 2003). Levels of mRNA are low at birth and rise steadily to increase by four fold at postnatal day 20 (P20) to a level maintained in adult mice (Lazarini et al., 1991). Increased expression correlates with brain development and neuronal differentiation but not astroglial differentiation. During development mRNA expression is detected in brain areas with highly active cell proliferation, such as the ventricular zones containing multipotent neural stem cells and the marginal zone of the superficial cortical plate. By E16.5 mRNA can also be detected in non-neuronal tissues (Benvegnu et al., 2010).

In adult mice *Prnp* mRNA is constitutively expressed and highly expressed in the central nervous system (CNS) (Manson et al., 1992, Miele et al., 2003). Several

effectors cause a change in mRNA expression but there is very little understanding of the mechanisms and pathways involved in the cell responses that lead to changes in *Prnp* mRNA. Cellular stresses have been shown to upregulate *Prnp* mRNA although the mechanisms are unknown. Heat shock in neuroblastoma cells increased Hsp-70 and *Prnp* mRNA. Hyperbaric oxygen, hypoglycaemia and chronic copper overload also upregulate PrP^C by interacting with the heat shock element of the *Prnp* promoter (Shyu et al., 2005, Shyu et al., 2004, Armendariz et al., 2004). Upregulation of *Prnp* mRNA in response to different cytokines *in vitro* is neuronal cell-type specific (Lazarini et al., 1994).

1.1.2 Structure of PrPC

Mature PrP^C is a glycosylated, glycosylphospatidylinositol (GPI) anchored protein found in lipid-rich membrane rafts on the extracellular side of the plasma membrane (Naslavsky et al., 1997, Taylor and Hooper, 2006).

Murine *Prnp* mRNA encodes a 254 amino acid protein containing two signal peptides. Upon entering the endoplasmic reticulum the 22 amino acid N-terminal signal peptide is cleaved off. Once translated a C-terminal signal peptide (22 amino acids) is cleaved off and a GPI anchor is attached to the terminal serine of the protein to leave a 210 amino acid protein attached to the membrane.

The protein can be separated into two distinct domains; the globular C-terminal domain (amino acids 127-231) and the flexible N-terminal domain (amino acids 23-124) (Figure 1.1). The structure of the globular domain is identical in mammals, as expected for the high degree of sequence similarity (Lysek et al., 2005). The structure of PrP in non-mammalian species is surprisingly well preserved despite the low sequence identity (Calzolai et al., 2005).

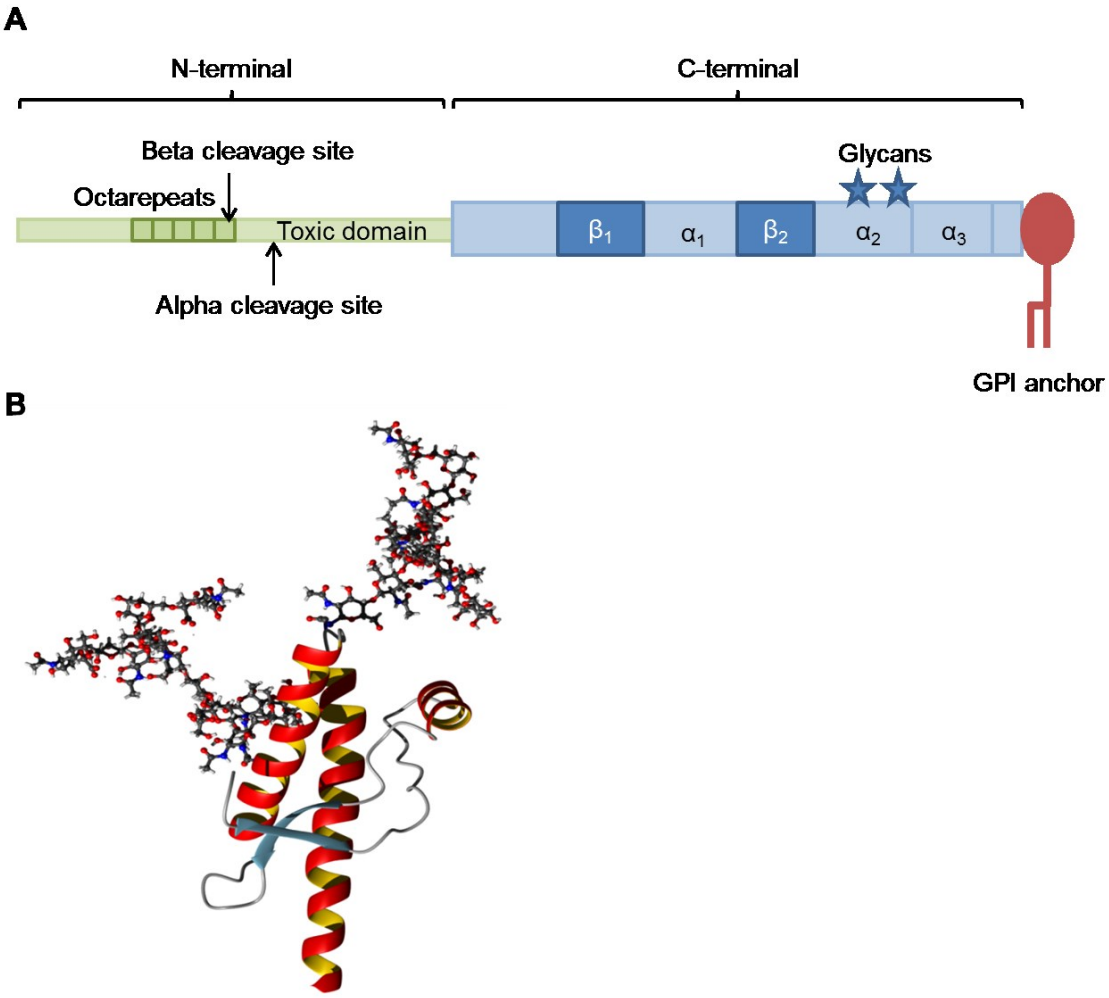

Figure 1.1 Structure of murine cellular prion protein
(A) Cartoon depicting the regions of $PrP^{C.}$ A GPI anchor tethers the protein to the membrane. There are 2 distinct regions to the protein; the flexible N-terminal and the globular C-terminal. The N-terminal of the protein (23-124) is highly flexible and lacks any identifiable structure in the absence of Cu^{2+}. There are 5 octarepeats (PH/QGGGWGQ) that bind copper ions and a toxic domain that is important during TSE disease. The C-terminal domain is highly structured and consists of 2 short antiparallel β-strands (aa 128-131 and 161-164) and 3 longer α-helices (aa144-154, 173-194 and 200-228). There are two *N*-linked glycosylation sites (aa 180 and 196) and a disulphide bridge is formed between C179 and C214. (B) Computer generated model of the structure of the C-terminal domain with two glycans. Helices are shown in red and yellow and β-sheets in blue. Produced by A. Gill, The Roslin Institute.

The N-terminal domain of the protein is highly flexible and lacks any identifiable structure in the absence of Cu^{2+} (Donne et al., 1997, Whittal et al., 2000). There are 5 octarepeats (PH/QGGGWGQ) in this domain that bind metal ions, with a high affinity for copper ions (Aronoff-Spencer et al., 2000). The N-terminal also contains a neurotoxic domain, which is important during TSE disease (Forloni et al., 1993, Chen et al., 1995, Solomon et al., 2011).

The C-terminal domain is highly structured and highly conserved in mammals due to the sequence similarities. It consists of two short antiparallel β-strands (128-131 and 161-164) forming a β sheet and three α-helices (144-154, 173-194 and 200-228) (Linden et al., 2008, Riek et al., 1996). The C-terminal is selectively glycosylated at residues Asn-180 and Asn-196 and a single disulphide bond is formed between cysteine residues 179 and 214 (Jackson et al., 1999).

The GPI anchor and interactions with the membrane lipids may play a role in the secondary structure of PrP^C. Recombinant PrP^C interacts with acidic lipid containing membranes under acidic conditions and showed a consistent shift in circular dichroism (CD) spectrum. The C-terminal domain becomes destabilised and the N-terminal shows significant ordering (Morillas et al., 1999). However bacterially expressed recombinant bovine PrP, which lacks glycosylation and the GPI anchor shows an indistinguishable CD spectra to PrP^C isolated from calf brain, suggesting that the GPI anchor alone does not necessarily affect tertiary structure (Hornemann et al., 2004).

1.1.3 Distribution of PrPC

PrP^C protein can be detected in all adult tissues with the exception of liver and kidney (Miele et al., 2003). The highest levels of PrP^C are found in the brain (Miele et al., 2003). Within the brain there are various different cell types, both neuronal and glial, which show varying levels of PrP^C. Levels of mRNA do not always correlate with levels of protein suggesting a high degree of post-translational control (Manson et al., 1992, Ford et al., 2002a). Astrocytes and oligodendrocytes have detectable levels of *Prnp* mRNA yet little or no detectable PrP^C is detected in glia (Ford et al., 2002a, Moser et al., 1995). Neuronal subtypes have varying levels of PrP^C; GABAergic neurons display high levels of PrP^C, cholinergic neurons have low levels of PrP^C and dopaminergic neurons little detectable protein (Ford et al., 2002a).

It has previously been shown that there are differing levels of PrP^C in different brain regions in hamsters and mice (Ford et al., 2002a). High PrP^C levels were detected in the hippocampus and the thalamolimbic system (Benvegnu et al., 2010). This likely reflects

the differing amounts of PrP^C produced by the different neuronal subpopulations found in each region. Most cells in grey matter areas contain PrP^C whereas myelinated fibre tracts in white matter areas show little evidence of PrP^C (Ford et al., 2002a). Within grey matter regions, basket and stellate cells were intensely positive for PrP^C. In the deep cerebellar nuclei all cells expressed high levels of PrP^C (Ford et al., 2002a). In the white matter of the cerebellum the majority of axons were PrP^C negative but a minor population of axons from GABA positive Purkinje cells have high levels of PrP^C.

PrP^C has been reported to have a physiological role at the synapse and is localised primarily to synapses (Fournier et al., 1995, Moya et al., 2000). This is reflected in the hippocampus, with synaptic layers expressing high levels of PrP^C and no detectable PrP^C in the cell bodies (Beringue et al., 2003, Moya et al., 2000).

1.1.4 Trafficking of PrPC

PrP^C is a cell surface protein synthesised and modified through the secretory pathway and trafficked to the plasma membrane. The N-terminal of PrP^C contains a signal peptide, which causes translocation to the endoplasmic reticulum (ER) to be further translated. Upon entry into the ER lumen the signal peptide is cleaved off. PrP^C can be found in 3 different topologies. The majority of protein produced (>90%) is GPI anchored to the plasma membrane. A small minority (<10%) is either an N-terminal (^{Ntm}PrP) or C-terminal (^{Ctm}PrP) transmembrane form due to a hydrophobic pocket (Holscher et al., 2001, Kim and Hegde, 2002).

PrP^C undergoes several post-translational modifications whilst in the ER. High mannose, endoglycosidase H (Endo H) sensitive *N*-linked oligosaccharides are added co-translationally. A single disulphide bond is also created between C179 and C214. The GPI anchor is added after removal of a C-terminal signal peptide upon translation, which causes association with the lipid rafts, low-density, detergent insoluble regions of the membrane rich in cholesterol and sphingolipids (Taylor and Hooper, 2006). The glycans are further modified in the Golgi by adding sialic acid to create mature PrP^C that is Endo H resistant (Harris, 2003).

Once it has reached the plasma membrane PrP^C is constitutively cycled between the membrane and endosomal compartments, with >95% of endocytosed protein returned to the membrane (Shyng et al., 1993). PrP^C is rapidly cycled between the cell surface and internal membranes. Once internalised the majority of the PrP^C is recycled to the surface, however some protein is degraded by lysosomes and some is secreted into the extracellular medium with exosomes (Vetrugno et al., 2005, Porto-Carreiro et al., 2005, Robertson et al., 2006).

PrP^C lacks a transmembrane domain and therefore relies on binding partners to interact with cytosolic proteins required for internalisation. Endocytosis occurs either by caveolae-like domains (Prado et al., 2004) or via clathrin coated pits (Shyng et al., 1994). GPI anchored proteins are typically endocytosed via caveosomes formed from lipid rafts however disruption of clathrin dependent endocytosis reduced PrP internalisation. Blocking clathrin dependent endocytosis does not completely prevent endocytosis suggesting a combination of methods are employed, depending upon the cell type and the binding partner initiating internalisation. For clathrin dependant endocytosis PrP^C has to move out of lipid raft domains and into non-raft membranes by binding ligands. Deletion of the N-terminal portion of PrP^C reduces internalisation and turnover, suggesting an important role of the highly conserved N-terminal in trafficking of the protein (Nunziante et al., 2003). The N-terminal domain has been proposed as the ligand binding domain for partners such as LRP1 (Parkyn et al., 2008) and NCAM (Schmitt-Ulms et al., 2001). Ligands that bind to PrP^C may also activate signalling pathways leading to neuronal survival or neuritic outgrowth (Pantera et al., 2009, Santuccione et al., 2005).

1.1.5 Cleavage of PrP^C

PrP^C can undergo several different cleavage events *in vivo* to produce both membrane attached and soluble fragments. There are three main cleavage events described in brain; alpha and beta cleavage and C-terminal shedding (Figure 1.2).

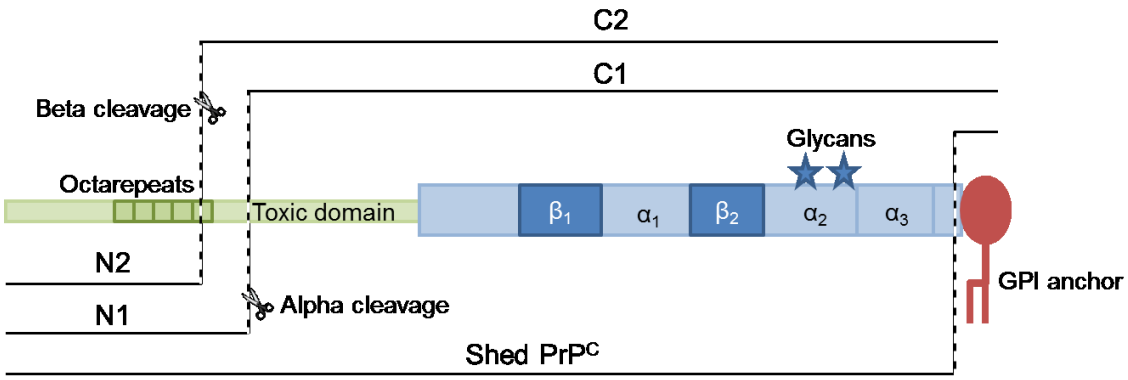

Figure 1.2 PrP^C cleavage sites
PrP^C can be cleaved at 3 different cleavage sites. PrP is shed by removal of the GPI anchor and releasing soluble full length PrP from the membrane. Proteolytic cleavage can occur at two sites in the N-terminal region. Alpha cleavage cuts at 110/111, producing C1 and N1 fragments and beta cleavage cuts at 90/91, producing C2 and N2 fragments. Both C1 and C2 fragments are membrane bound, GPI anchored and glycosylated. The N1 and N2 fragments are released from the cell surface.

1.1.5.1 Alpha cleavage

Alpha cleavage occurs between residues 110/111 to produce a 17 kDa C1 fragment and a 9 kDa N1 fragment (Mange et al., 2004). C1 remains GPI anchored to the membrane and retains both glycans whilst N1 is most likely secreted from the cell. C1 has been reported for different species, such as human, sheep and mice (Chen et al., 1995, Nieznanski et al., 2005b, Laffont-Proust et al., 2006, Kuczius et al., 2007a, Kuczius et al., 2007b).

Defining the location of alpha cleavage has been challenging due to the constant recycling of the protein. It has been suggested that cleavage occurs in the late Golgi before PrP^C reaches the cell surface (Walmsley et al., 2009). This study showed that disruption of exit from the secretory pathway increased C1 levels whilst retention in the

ER lowered C1 levels. There is also evidence that cleavage could occur in endocytic vesicles, once PrP^C has been internalised (Shyng et al., 1993). Alpha cleavage was reduced by lysosomal protease inhibitors and raising the pH of endocytic compartments suggesting cleavage in an acidic endocytic vesicle after internalisation from the cell surface.

Very little is known about the cleavage event and there is conflicting evidence in the literature regarding the enzymes responsible. Several metalloproteases from the ADAM family (A Disintegrin And Metalloproteinase) have been suggested as candidate enzymes which carry out alpha cleavage, including ADAM 9, 10 and 17. It has been shown that the presence of active ADAM10 was associated with high C1 levels in human brain and inhibition of metalloproteases ADAM 10 and 17 reduced N1 formation *in vitro* (Laffont-Proust et al., 2005, Vincent et al., 2001). However, Taylor *et al.* (2009) showed that ADAM10 was responsible for shedding of the protein rather than alpha cleavage and ADAM10 knockdown in neurons did not reduce C1 (Altmeppen et al., 2011). The ADAMs may indirectly modulate cleavage by regulating an unidentified protease responsible for alpha cleavage. It has been shown that purified plasminogen can interact with recombinant PrP^C *in vitro* and cleave it to produce a C1 like fragment (Kornblatt et al., 2003). This was accelerated by the presence of plasmin. N1 could potentially augment PrP^C alpha cleavage through enhanced plasminogen activation to produce more N1 (Praus et al., 2003). However, plasminogen-deficient mice showed no alteration in cleavage patterns, suggesting that plasmin has no role in cleavage *in vivo* (Barnewitz et al., 2006). Protein kinase C upregulated alpha cleavage (Vincent et al., 2000, Alfa Cisse et al., 2007).

Alpha cleavage of PrP^C is believed to be important in the physiological functions. A series of mutants with portions of the N-terminal have been created (Shmerling et al., 1998, Li et al., 2007) (Figure 1.4). Some mutants, but not all, showed spontaneous neurodegeneration with the absence of accumulated misfolded protein. There was a strong correlation between the absence of alpha cleavage and neurotoxicity caused by the truncated PrP [reviewed in (Yusa et al., 2012)]. Mutants that showed C1 did not

develop spontaneous neurological disease whilst mutants that had at least residues 105-125 deleted lacked detectable C1 and developed disease.

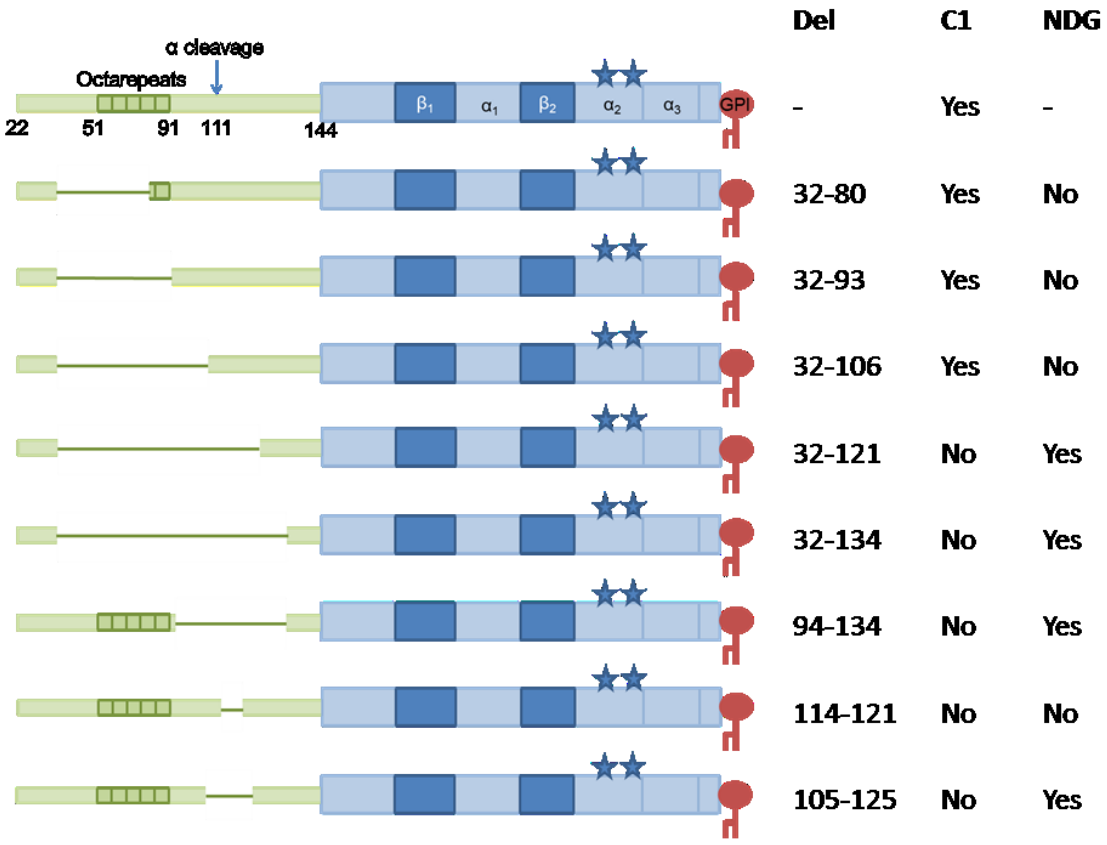

Figure 1.3 PrP deletion mutants and their neurodegenerative phenotype
Wild type PrP with the domains (shown in figure 1.1) is shown at the top. Deleted domains are shown with a solid line and the deleted amino acids indicated to the right (Del). The presence of C1 is indicated for each mutant to demonstrate whether it is able to undergo cleavage. NDG shows whether the mutants show spontaneous neurodegeneration. Data from (Yusa et al., 2012)

Both C1 and N1 have also been shown to be biologically active fragments both *in vitro* and *in vivo*. It has been suggested that C1 acts as a pro-apoptotic signal, pushing a cell towards apoptosis. Cells overexpressing C1 had an enhanced apoptotic effect when treated with staurosporine through positively regulating caspase-3 activation in a p53-depedent mechanism (Sunyach et al., 2007). However, transgenic mice expressing only C1 did not display neurological changes showing that C1 is not neurotoxic (Westergard et al., 2011). In contrast it is believed that N1 exerts a neuroprotective effect on the cell, preventing cell death (Guillot-Sestier et al., 2009). Alpha cleavage may be linked to

signal transduction. Increased alpha cleavage in response to membrane perturbation increased signal transduction through MAPK intermediates (Haigh et al., 2009).

1.1.5.2 Beta cleavage

Beta cleavage of PrP^C occurs upstream of the alpha cleavage site at the end of the octarepeat region (around aa 90) to produce a membrane bound 20 kDa fragment (C2) and a 9 kDa secreted fragment (N2). Cleavage occurs at the cell surface in response to reactive oxygen species (ROS) and is dependent upon the octarepeat region (McMahon et al., 2001, Watt et al., 2005). Copper binds to the octarepeat region and can promote formation of a hydroxyl radical from H_2O_2 resulting in peptide bond cleavage. Cleavage is prevented by hydroxyl radical trapping by dimethyl sulphoxide and by removal of the octarepeat region (Watt et al., 2005).

In contract to C1, the C2 fragment has not been demonstrated to have a biological function (Sunyach et al., 2007). Beta cleavage has been proposed to be a mechanism for the protective role of PrP^C against oxidative stress. PrP^C may act as an external sensor for external ROS and cleavage is the first response in a cascade of cellular events against increased oxidative stress. Failure to undergo beta cleavage correlated with an increased sensitivity of cells to oxidative stress (Watt et al., 2005).

Beta cleavage of PrP^C occurs at low levels and C2 is rarely observed in healthy mice. Enhanced beta cleavage is associated with TSE disease (Chen et al., 1995). Unlike PrP^C, PrP^{Sc} is cleaved by calpain to produce a protease resistant C2-like fragment.

1.1.5.3 Extreme C-terminal shedding

Soluble full length PrP lacking the GPI anchor has been identified both *in vitro* and *in vivo* (Zhao et al., 2006). A small proportion of PrP^C is shed into the medium by cultured cells (Borchelt et al., 1993) and soluble PrP^C has been identified in human cerebrospinal fluid (Tagliavini et al., 1992) and released from human platelets (Perini et al., 1996).

The soluble PrP^C was recognised by antibodies to the extreme C-terminal and did not change molecular weight when treated with hydrofluoric acid to remove the GPI anchor, indicating that the protein was full length but lacked the entire GPI anchor (Borchelt et al., 1993). Naturally shed PrP^C has been shown to be cleaved between Gly 228/Arg 229, close to the GPI anchor by a zinc metalloproteinase (Parkin et al., 2004, Taylor et al., 2009). Disruption of the lipid rafts with filipin and methyl-β-cyclodextrin stimulates cleavage within the GPI anchor possibly by a phospholipase (Parkin et al., 2004).

1.1.6 Functions of PrPC in the CNS

Several different null mice were created on different mouse backgrounds in order to elucidate the function of PrP^C (Bueler et al., 1992, Manson et al., 1994a, Sakaguchi et al., 1996, Moore et al., 1999, Rossi et al., 2001). Initial screening of PrP null mice showed no overt phenotype, no gross anatomical abnormalities, fully functioning immune systems and no impairment of learning when tested with several complex behavioural tests (Bueler et al., 1992, Manson et al., 1994a). Later knockouts showed normal development but developed ataxia and Purkinje cell degeneration with age, however this was due to overexpression of doppel caused by the deletion of *Prnp* (Moore et al., 1999, Sakaguchi et al., 1996, Rossi et al., 2001). The lack of phenotype hindered identifying the function and suggests that PrP^C is not essential for development or that there is a redundant protein that compensates for the loss of PrP^C.

However, later studies with PrP null mice have shown subtle changes. Null mice had a slight increase in locomotor activity (Roesler et al., 1999) and a decrease in anxiety during acute stress (Nico et al., 2005). Electrophysiology studies found subtle changes in circadian rhythm and sleep (Tobler et al., 1996), weakened GABA-A (gamma-aminobutyric acid type A) receptor-mediated fast inhibition and impaired long-term potentiation (Collinge et al., 1994, Coitinho et al., 2003).

Another method of elucidating the function of PrP^C has been to identify the proteins and molecules with which PrP^C interacts. Identifying binding partners allows potential

physiological pathways of PrP^C to be identified. Several binding partners have been identified through yeast two hybrid systems, co-immunoprecipitation (Co-IP) and cross linking. PrP binds many different molecules *in vitro* and some of these are localised to the cytoplasm so would not be able to interact directly with PrP^C *in vivo*, bringing into question the validity of some of the binding partners (Table 1.1). Some of the binding partners may interact through intermediate proteins.

PrP^C has been proposed to be involved in neuroprotection by an anti-apoptotic activity. PrP^C protects cells against apoptosis induced by serum deprivation, TNF-α, doppel and Bax-mediated apoptosis (Bounhar et al., 2001, Kuwahara et al., 1999, Diarra-Mehrpour et al., 2004, Drisaldi et al., 2004, Qin et al., 2006). PrP^C also protects against Bax-mediated apoptosis in yeast systems (Li and Harris, 2005, Bounhar et al., 2006). The N1 fragment produced by proteolytic cleavage has been shown to have neuroprotective properties both *in vitro* and *in vivo* (Guillot-Sestier et al., 2009). Mice which lack a portion of the N-terminal, encompassing at least residues 105-125 develop neurodegeneration which is rescued by introduction of full length PrP. This deletion prevents alpha cleavage and production of the N1 fragment.

Table 1.1 PrP^C ligands

Binding partner	Function	Location	Identification method	Ref
Bcl2	Anti-apoptotic activator	Cytoplasm, (mitochondria and ER)	Yeast two-hybrid	(Kurschner and Morgan, 1995, Kurschner and Morgan, 1996)
Caveolin	Caveolar coat for endocytosis	Cytosolic plasma membrane	Co-IP	(Mouillet-Richard et al., 2000)
Grb2	Adaptor protein in signal transduction	Cytoplasm	Yeast two-hybrid; co-IP	(Spielhaupter and Schatzl, 2001)
Hsp60	Chaperone	Cytoplasm	Yeast two-hybrid	(Edenhofer et al., 1996)
Laminin receptor precursor (LRP)	Extracellular matrix protein	Cytoplasm, plasma membrane?	Yeast two-hybrid	(Gauczynski et al., 2001, Hundt et al., 2001)
Neural cell adhesion molecule (N-CAM)	Extracellular matrix protein	Plasma membrane	Cross linking	(Santuccione et al., 2005, Schmitt-Ulms et al., 2001)
Neurotrophin receptor-interacting MAGE homologue (NRAGE)	Apoptosis activator	Cytoplasm	Yeast two-hybrid; Co-IP	(Bragason and Palsdottir, 2005)
Pint1	Unknown	Cytoplasm	Yeast two-hybrid; co-IP	(Spielhaupter and Schatzl, 2001)
Stress inducible protein (STI-1)	Heat shock protein	Cytoplasm, plasma membrane?	Co-IP	(Zanata et al., 2002)
Synapsin-1b	Synaptic vesicle trafficking	Cytoplasm (synaptic vesicles)	Yeast two-hybrid; co-IP	(Spielhaupter and Schatzl, 2001)
Trek	K^+ channel	Plasma membrane (ransmembrane)	Yeast two-hybrid; co-IP	(Azzalin et al., 2006)
Tubulin	Microtubule subunit	Cytoplasm	Cross linking	(Nieznanski et al., 2005a)

PrP^C may also protect against oxidative stress. Mice lacking PrP^C are more susceptible to oxidative stress and brain lesions induced by hypoxia or ischemia are larger than in wild type mice (McLennan et al., 2004, Spudich et al., 2005). Cultured PrP null neurons are more susceptible to treatments that induce oxidative stress (Brown et al., 2002). The protective mechanism of PrP^C is not known, but PrP^C may activate signalling pathways or upregulate other proteins that detoxify ROS. It has been proposed that PrP^C monitors the levels of oxidative stress and initiates protective signal cascades under conditions of high stress through beta cleavage (Watt et al., 2005).

PrP^C has the ability to bind copper and other metal ions to the octarepeat region in the N terminal of the protein. PrP^C has also been implicated in copper homeostasis at the synaptic cleft. PrP^C binds copper at the cell surface which promotes endocytosis to allow maintenance of copper in the pre-synaptic cytosol and buffering against toxic levels of copper (Vassallo and Herms, 2003).

PrP^C is localised to lipid raft regions of the membrane, which have been demonstrated to act as membrane scaffold for signal transduction (Tsui-Pierchala et al., 2002, Taylor and Hooper, 2006). Treatment of cells with recombinant PrP^C enhanced neurite outgrowth and neuronal survival through activation of fyn, PKC, PKA, PI-3 kinase/Akt and ERK (Kanaani et al., 2005, Chen et al., 2003). PrP^C is on the outer membrane of the cell and does not contain any transmembrane domains and therefore must interact with proteins with a transmembrane domain to be able to initiate signal transduction. Several signalling proteins have been identified as binding partners for PrP^C (Spielhaupter and Schatzl, 2001). Antibody-mediated cross linking of PrP^C stimulated the non-receptor tyrosine kinase, fyn *in vitro* and caused downstream stimulation of NADPH oxidase and extracellular regulated kinases (ERKs) (Mouillet-Richard et al., 2000, Schneider et al., 2003). STI-1 is a co-chaperone for heat shock proteins and binds to PrP^C to stimulate neurite outgrowth through the MAPK pathway and neuroprotection through the activation of the PKA pathway (Lopes et al., 2005). Interactions of PrP^C with N-CAM recruited to lipid rafts activate fyn kinase to promote neurite outgrowth (Santuccione et al., 2005).

PrP^C interacts with several proteins involved in cell adhesion, such as the laminin receptor and N-CAM. Laminin has a significant role in neurite outgrowth and aids cell migration (Graner et al., 2000a). Removal of cell surface PrP causes disruption of laminin-induced differentiation and retraction of neurites (Graner et al., 2000b).

The localisation of PrP^C at the synapses has led to the proposal of the involvement of PrP^C in neuronal communication. PrP^C promotes neurite outgrowth and increases the number of synaptic contacts suggesting it could regulate synapse formation (Kanaani et al., 2005). The synaptic role of PrP^C is supported by the electrophysiological changes seen in null mice (Tobler et al., 1996, Colling et al., 1996, Colling et al., 1997).

PrP^C has also been shown to have functions in the peripheral nervous system (PNS) that are separate from the CNS functions. PrP^C has also been shown to have a role in peripheral myelin maintenance which is dependent upon the cleavage of PrP^C to produce C1/N1 fragments (Bremer et al., 2010).

1.2 *N*-linked glycosylation of proteins

Glycosylation of proteins occurs in both prokaryotes and eukaryotes and has a huge biological and functional significance. It is the most common post-translational modification; over half of all human proteins are glycosylated. Proteins can possess more than one glycosylation site and a mixture of *N*-linked or *O*-linked glycosylation sites, which may be occupied with an array of complex and heterogeneous glycan structures. Only *N*-linked glycosylation in eukaryotes will be discussed in this thesis.

The addition of glycans is usually in the secretory pathway in eukaryotes and has three conserved steps.

1. A core of sugars are synthesised on the cytoplasmic membrane and transferred to the ER lumen. Glycans are assembled from nucleotide-activated building blocks on a lipid carrier anchored to the membrane through stepwise

incorporation of oligosaccharides by glycosyl-transferases. The core is then re-oriented into the luminal side and may be further extended

2. Proteins are translated in the ER with an *N*-linked glycosylation sites, usually encoded by Asn-X-Ser/Thr (where X is any amino acid except proline). This consensus acts as an acceptor for glycosylation.
3. The conserved oligosaccharide core (Glc_3-Man_9-$GlcNAc_2$) is added to the asparagine side chain by the oligosaccharyl transferase complex (OST).

The glycans are then processed by a series of trimming and elongation reactions in the ER and Golgi by glycoenzymes to produce mature glycans, which can be either high mannose, complex or hybrid, depending upon the sugar composition (Marino et al., 2010). There are nine monosaccharides which are used in the process of glycosylation in mammals. Due to the number of OH groups available on each monosaccharide many glycosidic links can potentially be formed producing diverse branching with different types of linkage. The diversity of the glycans is determined by the enzymes present in the cell; glycosyltransferases and glycosylhydrolases recognise the different linkages and work together to modify basic glycan structures. This allows for species-specific and cell-type specific glycosylation. The availability of these enzymes can change depending upon cellular conditions, such as in aging or in disease (Ohtsubo and Marth, 2006) to produce differences in glycosylation and subsequently the properties of the glycoproteins. The structure of the protein backbone and the position of the glycosylation site will also limit and regulate glycosylation, allowing a protein to direct its own pattern of glycosylation. Each glycosylation site may accommodate different glycans, producing a subset of glycoforms. The properties of a protein can be altered by the heterogeneous oligosaccharides attached to a glycosylation site, which allows extra diversity not encoded by the genome.

1.2.1 Functions of glycosylation

Glycosylation can influence many aspects of a protein; the properties, localisation, function, stability and activity can be altered by the presence or absence of glycans (Table 1.2). Glycosylation many alter just one of these aspects or may affect more than

one, depending upon the protein. Most glycans attached are large, flexible and cover large areas of proteins.

Table 1.2 Influences of glycans on proteins

Type	Function
Physico-chemical	Assist protein folding in the ER Modify • Solubility • Charge • Mass • Size Protection against proteolysis Conformational and thermal stability
Biological	Regulate trafficking Determine localisation Change half-life of protein Modulate activity of enzymes Act as cell surface receptors Assist with cell-cell interactions

Not all glycosylation consensus sites are occupied; a site may never be glycosylated or sometimes it may be selectively glycosylated, leading to a number of different glycoforms existing *in vivo*. Although different glycoforms can exist the significance of having multiple glycoforms is poorly understood for most proteins.

Most glycoproteins studied have a high level of site occupancy and under-glycosylation is associated with disease, such as cancer and congenital disorders of glycosylation (CDG) (Table 1.3). The level of site occupancy correlates with the severity of the disease (Hulsmeier et al., 2007). Glycophorin A, CD52 and CD45 are all fully glycosylated on the extracellular regions of the protein (Tomita et al., 1978, Treumann et al., 1995). Transferrin and α_1-antitrypsin have a normal physiological range of 99-100% glycan site occupancy and a reduction in site occupancy is associated with CGD. Thy-1 is a GPI anchored protein with three *N*-glycosylation sites. GPI anchored partially glycosylated Thy-1 is not detected on the cell surface and is believed to be

retained in the ER and degraded. When the GPI anchor is removed all sites are variable occupied and a range of glycoforms are detected (Devasahayam et al., 1999).

Site occupancy is influenced by several factors; both from the protein itself and from the local environment. The sequence around the glycosylation site can prevent glycosylation. The presence of a proline flanking or in the middle of the glycosylation site prevents glycan attachment. The peptide sequence can prevent efficient glycosylation due to folding occurring so rapidly that glycosylation sites become inaccessible to the dolichol-linked precursor or glycosylation enzymes (Go et al., 2008, Fujii et al., 1990). A disulphide bridge near the glycosylation site can hinder glycosylation as seen with interleukin-6 (IL-6) (Hasegawa et al., 1992). Glycosylation sites close to the amino or carboxy terminals are less efficiently glycosylated (Livi et al., 1991) potentially due to accessibility of the glycosylation enzymes. The availability of the dolichol-linked precursor and oligosaccharyl transferases also influences the levels of glycosylation.

Table 1.3 Effect of altered *N*-linked glycosylation of glycoproteins

Glycoprotein	Function	Effect of lack or alteration of glycosylation
Most lysosomal enzymes	Enzyme	Loss of targeting signal for lysosomes
β-glucosidase		Loss of enzymatic activity
Lipoprotein lipase		Core glycosylation important for secretion and activity
Hepatic lipase		Reduced secretion
Propain		Loss of transport and secretion
α-antitypsin		Altered CD and spectrum leading to aggregation
Pancreatic ribonuclease		Increased susceptibility to proteases
Granulocyte/macrophage colony stimulating factor	Growth factor	Increased activity and binding but increased antigenicity and clearance
Vascular endothelial growth factor		Decreased rate and efficiency of secretion
Erythropoietin	Hormone	Loss of secretion and decreased stability and activity
Interleukin-4	Cytokine	Increased activity
Immunoglobulins		Complex effects dependent upon Ig. Altered secretion and enhanced antigen binding if glycosylation is in variable region
Plasminogen	Plasma protein	Altered cell surface binding, half-life and fibrinolytic activity
Fibronectin	Matrix protein	Increased susceptibility to proteases
Low density lipoprotein receptor	Membrane receptor	Redistribution of intracellular and surface protein. Decrease in ligand binding capacity
Interferon gamma receptor		Loss of ligand binding in the cell

1.2.1.1 Protein folding and degradation

N-linked glycosylation is important for quality control of protein folding in the secretory pathway. Glycosylation occurs concomitantly with translocation into the ER lumen before the protein is fully synthesised or folded. Some subunits of the OST interact with the translocon and ribosome and are thought to modulate or prevent protein folding, allowing glycosylation of the nascent polypeptides before potential glycosylation sites become buried (Wilson et al., 2005, Chavan et al., 2005).

Terminal glucoses and mannoses in combination with lectin receptors assist in protein folding and can direct misfolded proteins towards degradation. Removal of two glucoses by glucosidase II from the core glycan allows recognition by ER chaperones which prevent misfolding and aggregation (Aebi et al., 2010). Calnexin and calreticulin bind and recruit the lectin-associated oxidoreductase ERp57, which catalyses the formation of native disulfide bonds. If the protein is misfolded it is detected and rebinds the chaperones until it is either refolded correctly or targeted for ER associated degradation (ERAD). Abnormally folded proteins can still sometimes be secreted, but usually have impaired biological function and the effect is dependent upon the location of the glycosylation site.

1.2.1.2 Physico-chemical functions

The *N*-linked triose core added cotranslationally can improve both kinetics and thermodynamics of a protein. Glycosylation can increase the thermodynamic stability by reducing the disorder of the unfolded protein (Imperiali and O'Connor, 1999). Glycans form hydrogen bonds with the protein, giving it a more rigid structure (Hanson et al., 2009). A mutation resulting in an under-glycosylated tyrosinase observed in mouse melanocytes has been shown to be active but at the same time to be more heat sensitive and more susceptible to rapid inactivation (Halaban et al., 1988).

The addition of glycans can change the overall charge of the protein, with the negative charges of sialic acids and sulphate groups increasing solubility (Sola and Griebenow, 2009).

Most glycans are large and have a degree of rotational flexibility, allowing large areas of the protein to be shielded by the glycans. The core oligosaccharides are close to the surface of the protein and are responsible for structural functions of the glycans, whereas the distal oligosaccharides are responsible for interactions with lectins and receptors (Drickamer and Taylor, 1998). It does not matter which core oligosaccharides are attached, as long as they are present, to help shield the protein. Glycan shielding is more commonly employed by pathogens, particularly viruses to subvert the host immune system and prevent recognition of the surface proteins (Kobayashi and Suzuki, 2012).

Different glycosylation sites on the same protein may impart different features and influence other glycosylation sites. Human protein C has four potential glycosylation sites which each impart different features. Glycosylation at Asn97 is critical for secretion of the protein but also influences the level of core glycosylation at Asn329. Glycosylation at Asn248 affects the intra-molecular cleavage of the peptide required for activation and a lack of glycosylation at Asn313 enhances the peptides binding affinity, increasing its catalytic ability (Grinnell et al., 1991).

1.2.1.3 Biological functions

Glycosylation can determine the trafficking of a protein, which in turn influences the localisation and degradation. Glycans can act as an ER export signal for assisting proteins to move through the ER and into the Golgi. Glycosylation of the potassium ion channel kv1.4 is essential for the efficient cell surface expression of the protein (Watanabe et al., 2004).

On the cell surface glycans are able to interact with other molecules which can change the localisation and sorting of the proteins. Glycosylation of a protein generates binding sites for galactose-specific lectins (galectins). Galectins cross-link glycoproteins forming dynamic microdomains or lattices that regulate various mediators of cell adhesion, migration, proliferation, survival and differentiation. The interactions of glycoproteins and galectins at the cell surface are dynamic and allow the cell to adapt and respond to cellular conditions.

Glycans allow proteins to interact with other molecules to carry out functions. Glycoproteins provide a scaffold for cell adhesion. In addition to interacting with galectins the glycans can also prevent interactions with other glycoproteins on the cell surface. The size and rotational flexibility of the glycans can shield areas of the polypeptide. A mutation in the epidermal growth factor receptor (EGFR) deletes a domain and four glycosylation sites and increases ligand independent homodimerisation (Fernandes et al., 2001, Tsuda et al., 2000). The glycans appear to insulate against dimerisation by restricting the approaches between monomeric EGFR. The glycans of ErbB3 play a role in negative regulation of receptor dimerisation and activation (Takahashi et al., 2008).

Separate functions for individual glycoforms have not been reported for variable glycosylated proteins although a change in the ability to carry out a function has been observed. Plasma cholesteryl ester transfer protein (CETP) has multiple glycosylation sites but is found as two glycoforms *in vivo* depending upon site occupancy at Asn341. CETP lacking the glycan has a higher activity than the protein with a glycan at this site, possibly due to charge alteration or a decrease in steric hindrance in proximity to the active site (Stevenson et al., 1993). Glycosylation of tissue plasminogen activator (t-PA) is variably glycosylated at Asn184. Glycosylation decreases the activity of the enzyme, possibly by steric hindrance of the active site in the kringle domain (Berg et al., 1993). Plasminogen is found naturally in two different forms, type I and II, which differ in the presence of *N*-linked glycosylation in the kringle 3 domain and have different functional activity (Aisina et al., 2005).

1.2.2 Glycosylation of PrPC in health

In wild type mice diglycosylated PrP is the predominant form and other glycoforms are minor forms. The oligosaccharides added to PrP are large and heterogeneous, with over 50 different carbohydrate species found on hamster PrP (Rudd et al., 2001). Comparison of the glycans for the different sites in wild type mice show differing populations of glycans at each site (Stimson et al., 1999). The major oligosaccharides are present at both sites and many sialylated bi- and triantennary structures are common to both sites but some of the larger tetraantennary glycans were not detected at the first site. The majority of glycans at the first glycosylation site have a mass between 1660-2340 Da whilst glycans at the second site have a mass of 2000-3020 Da (Stimson et al., 1999).

The role of the glycans remains elusive. The N-glycans do not appear to impart structural features on PrP^C. Recombinant PrP, which lacks post-translational modifications, shows the same structure as native, glycosylated PrP^C using CD and nuclear magnetic resonance (NMR) spectroscopy (Hornemann et al., 2004, DeMarco and Daggett, 2009).

Several ligands have been demonstrated to bind to PrP and initiate signalling cascades to promote neuritogenesis and neuronal survival (Santuccione et al., 2005, Martins et al., 2001). The N-glycosidic link is flexible, allowing large areas of PrP to be shielded, possibly to protect from proteases and to prevent non-specific protein-protein interactions (Rudd et al., 2001, Ermonval et al., 2003). The oligosaccharides interact with the environment so may also play a role in trafficking and ligand binding (Varki, 1993).

It is not known whether the different glycoforms of PrP^C have different functions but the diverse functions proposed for PrP^C and the multiple isoforms may indicate separate functions for different isoforms. Methods used to investigate PrP^C captures PrP in all stages of its life cycle therefore it cannot be ruled out that incompletely glycosylated PrP represents immature PrP which will become diglycosylated before being trafficked to the surface, rather than an isoform with a distinct function. Several physiological

functions have been suggested for PrP^C from modulating synaptic plasticity, a role in cell differentiation and protection against oxidative stress. Neurons with high levels of PrP^C are less susceptible to oxidative stress than those that have little PrP^C (Ford et al., 2002a).

Unglycosylated proteins have been reported to have a different localisation and to aggregate more readily (Powell and Pain, 1992, Kayser et al., 2011), potentially causing a toxic species. Cytoplasmic PrP^C has been shown to be toxic *in vitro* (Wang et al., 2009, Norstrom et al., 2007) and unglycosylated PrP provokes apoptosis *in vitro* (Yang et al., 2009). However, studies with a mouse model producing only unglycosylated PrP^C show an altered localisation of PrP^C but no spontaneous disease or overt phenotype (Cancellotti et al., 2005).

1.3 PrP Glycosylation deficient mouse models

1.3.1 Gene targeted mouse models

Gene-targeted transgenic mouse lines were developed to investigate the influence of PrP glycosylation on host susceptibility and TSE disease susceptibility. GlycoD mice have a *Prnp* gene replacement containing point mutations at codons 180 (G1), 196 (G2) or both (G3) that replace asparagine (N) with threonine (T) thereby abolishing N-linked glycosylation (Cancellotti et al., 2005).

The endogenous murine *Prnp* gene is replaced by homologous recombination with the gene containing the point mutation. The altered PrP allele is in the correct genomic location and under control of the endogenous promoter and transcriptional controls. PrP mRNA is expressed in the same tissues and at the same levels as wild type mice. All 3 lines of gene targeted mice are on an inbred 129/Ola line, allowing any alteration in host susceptibility or TSE disease process to be attributed to the mutation of the PrP gene or altered glycosylation status of the host. It also allows a direct comparison between the different GlycoD mice.

Western blot analysis has shown that G1 and G2 mice only express mono- and unglycosylated PrP, while G3 mice express only unglycosylated PrP^C (Figure 1.4). Deglycosylation with N-Glycosidase F (PNGase F), which removes all carbohydrates from glycosylated asparagine residues, showed all transgenic mice with a single unglycosylated product. This demonstrated that the isoforms with heavier molecular weight are due to the addition of glycans and that the point mutations are preventing glycosylation.

The GlycoD mice showed no overt phenotype due to a lack of PrP glycosylation. Mice were fertile and aged normally. G3 mice aged to 850 days did not show any signs of neurodegeneration, vacuolation or gliosis (Cancellotti et al., 2005).

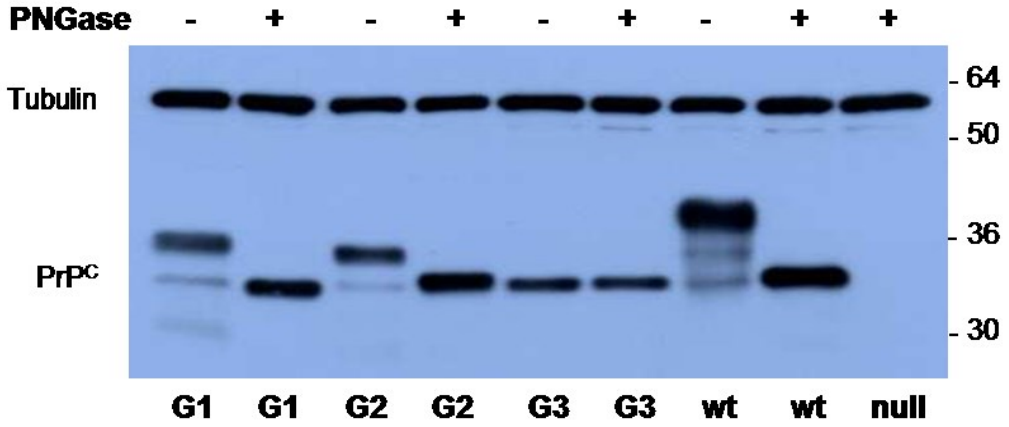

Figure 1.4 PrP isoforms present in each PrP glycosylation deficient mouse line
Normally glycosylated wild type mice express un, mono or diglycosylated PrP. Treatment with PNGase F to remove N linked glycans leaving only the unglycosylated band, showing that the different isoforms are due to attachment of carbohydrates. The PrP glycosylation deficient mice demonstrate that mutation at one or both of the glycosylation sites prevents glycosylation as the diglycosylated isoforms are not present in any of the mutants. Taken from (Cancellotti et al., 2005)

1.3.2 Localisation of PrPC in PrP glycosylation deficient models

Glycosylation of PrP^C may influence localisation of the protein *in vivo* (Cancellotti et al., 2007). A study performed using fixed brain tissues from the GlycoD mice have shown that PrP from G1 and G2 mice localised on the cell surface in a pattern

indistinguishable from wild type mice. Unglycosylated PrP from the G3 mice appeared to be intracellular (Figure 1.5).

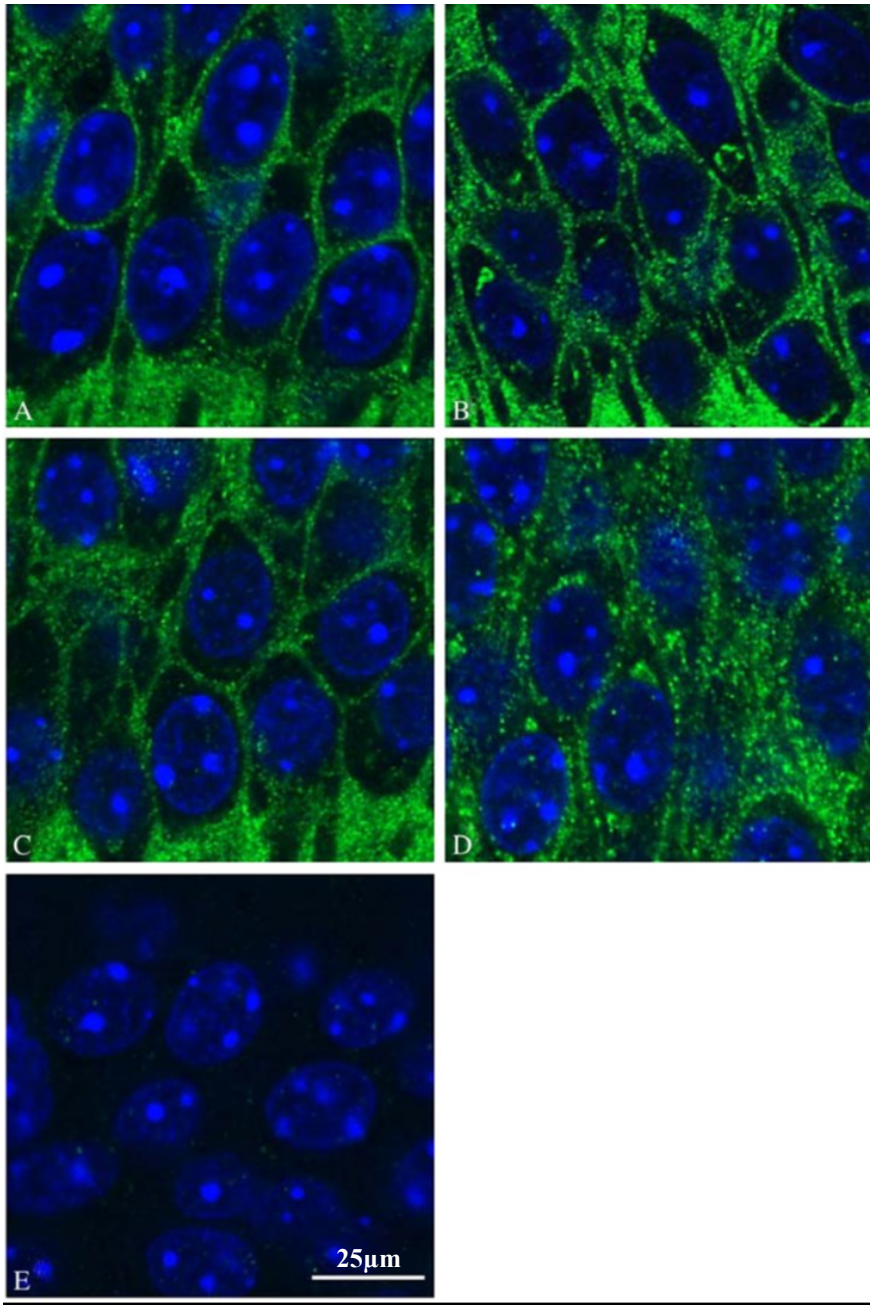

Figure 1.5 Localisation of PrP^C glycotypes in brain sections
Immunofluorescence on brain sections (A) wild type, (B) G1, (C) G2, (D) G3 and (E) PrP null. G1 and G2 PrP have similar cell surface localisation as wt PrP. G3 PrP appears to be mainly intracellular. Figure taken from (Cancellotti et al., 2007).

Co-localisation with ER (ErP60) and Golgi (23C β–cop) markers showed that G1 and G2 mice had a high cell surface localisation but an increased proportion of intracellular PrP compared to wild type mice (Cancellotti et al., 2005). PrP^C in the GlycoD mutants did not co-localise with the ER marker, showing that glycosylation did not prevent PrP from exiting the ER. The Golgi marker surrounded a significant portion of the intracellular PrP in all genotypes, suggesting presence in the Golgi (Cancellotti et al., 2005).

In other studies it has been observed that accumulation of intracellular PrP causes severe toxicity in cultured cells and leads to ataxia, neurodegeneration and gliosis in mice (Ma et al., 2002), however G3 mice develop normally despite relocation of PrP^C (Cancellotti et al., 2005).

1.3.3 Effect of amino acid substitution in GlycoD mutants

There is a potential that any changes in cell biology seen in the GlycoD mice are due not to the glycosylation state of PrP but to the amino acid substitution. In order to abolish the glycosylation in the GlycoD mutants the Asn of the glycosylation site is substituted with a Thr. This amino acid change has the potential to change the physical properties of the protein, such as stability or solubility, which can in turn affect the cell biology.

Glycosylation has been abolished in an epithelial cell line expressing ovine PrP^C by substitution of asparagine at either site with 5 different amino acids, including threonine (Salamat et al., 2011). Immunoblots show the same expected profiles and there is no reported difference between the different amino acid substitutions. Although PrP^C was not quantified there appears to be a reduced expression of PrP for all of the different substitutions. This suggests that the replacement of Asn with Thr does not have an effect and that the changes in protein level are due to the lack of glycosylation.

1.4 Transmissible spongiform encephalopathies

The cellular prion protein plays a central role in the transmissible spongiform encephalopathies (TSEs), a group of infectious fatal neurodegenerative diseases that affect a variety of mammals (Table 1.4). These include Creutzfeldt-Jakob disease (CJD) in humans, scrapie in sheep and bovine spongiform encephalopathy (BSE) in cattle.

Table 1.4 TSE diseases and their hosts

Disease	Host	Aetiology	First Described
Sporadic Creutzfeldt-Jakob disease (sCJD)	Human	Idiopathic	1920
Familial Creutzfeldt-Jakob disease	Human	Familial mutations in *PRNP*	1930
Iatrogenic Creutzfeldt-Jakob disease	Human	Medical exposure to infected human tissues (Dura mater graft, corneal transplant and human growth hormone)	1974
Variant CJD (vCJD)	Human	Consumption of BSE contaminated beef or blood transfusion from vCJD infected donor	1996
Gerstmann-Straussler-Scheinker disease (GSS)	Human	Familial mutations in *PRNP*	1938
Kuru	Human	Ritualistic cannibalism	1957
Fatal Familial Insomnia (FFI)	Human	Mutation in *PRNP* (D178N linked to 129M)	1986
Sporadic Fatal Insomnia (sFI)	Human	Idiopathic	1999
Scrapie	Sheep, moufflon and goats	Infectious, Unknown	1750
Atypical Scrapie	Sheep	Unknown	2003
Bovine Spongiform Encephalopathy (BSE)	Cattle	Consumption of BSE contaminated feed	1985
Atypical BSE (L and H type)	Cattle	Unknown	2004
Chronic Wasting Disease (CWD)	Deer, elk and moose	Infectious, Unknown	1967
Transmissible Mink Encephalopathy (TME)	Mink	Consumption of contaminated feed, putatively scrapie or L-type BSE	1947
Feline Spongiform Encephalopathy (FSE)	Domestic and captive wild cats	Consumption of BSE contaminated feed	1990
Exotic Ungulate Encephalopathy	Nyala and kudu	Consumption of BSE contaminated feed	1986

1.4.1 Clinical signs

Clinical signs are limited to the CNS and reflect the areas of the brain damaged due to vacuolation and PrP^{Sc} deposition (Brown et al., 1994, Santuccione et al., 2005). TSEs are characterised by a long incubation period, typically months for rodents and years for larger species, such as sheep and cattle. Clinical signs are usually only evident in older animals due to the long incubation times. A short clinical phase of progressive neurological deterioration leads invariably to death.

Clinical signs are heterogeneous and vary between TSEs. The differences in clinical signs are used to differentiate the strain of TSE, alongside molecular typing of PrP^{Sc}, the misfolded form of PrP^{C}, and genotyping of the PrP encoding gene.

Classic CJD is a heterogeneous group of diseases due to their sporadic, familial or iatrogenic nature (Table 1.5). There are different disease associated mutations which can give rise to different clinical signs, ages of onset and duration times. Clinical presentation is influenced by the 129 codon of the *PRNP* gene and the PrP^{Sc} subtype of the patient (type 1 or 2 depending upon the size of the PK resistant core when run on an immunoblot).

Variant CJD presents with earlier symptoms consisting of psychiatric disturbances, such as depression, anxiety and insomnia, peripheral sensory disturbances and cerebellar ataxia. Neurological symptoms appear much later in the disease. The average duration is also much longer than classic CJD, at 14 months. The median illness duration was 14 months (range, 8-38 months) and the median age at death was 29 years (range, 18-53 years) (Ward et al., 2003).

Table 1.5 Clinical signs of different sub-strains of sporadic CJD

Genotype		Average age of onset (range)	Clinical duration (range)	Signs
Typical	MM-1 MV-1	65 years (42-91 years)	4 months (1-18 months)	Early signs include cognitive impairment such as memory loss and confusion. Cognitive impairment, ataxia, myoclonus and pyramidal signs become very common in more advanced stages of the disease
Early onset	VV-1	39 years (24-49 years)	15 months (14-16 months)	Presentation is characterised by fronto-temporal dementia. Myoclonus and pyramidal signs eventually appear as disease progresses
Long duration	MM-2	65 years (49-77 years)	16 months (9-36 months)	Presentation is dominated by cognitive impairment followed by aphasia. As disease progresses myoclonus and pyramidal signs also become common, and Parkinsonism, apraxia and seizures are present in about 30% of the cases
Kuru plaques	MV-2	60 years (40-81 years)	17 months (5-72 months)	Ataxia is the most common presenting sign, with cognitive and mental signs also present. As disease progresses myoclonus and pyramidal signs are also common as are aphasia and apraxia
Ataxic	VV-2	60 years (41-81 years)	6 months (3-18 months)	Ataxia is the most common presenting sign. As disease progresses dementia, myoclonus and pyramidal signs are seen in most patients

Data from (Gambetti et al., 2003)

Clinical symptoms of scrapie vary depending upon the strain and the genotype of the infected animal (Williams, 2003). The most common symptom is intense pruritis leading to rubbing, scraping and wool loss. Behavioural changes, blindness and tremors may also occur. In atypical scrapie pruritis is uncommon and instead the dominant symptoms are ataxia and incoordination.

The clinical signs of BSE include tremors, hind limb ataxia, aggressive behaviour and hyper-reactivity to stimuli. The most common sign of CWD is the chronic weight loss of the affected animal along with a deterioration of the coat condition and patchy

retention of the winter coat in summer (Williams, 2003). Animals also show ataxia, excessive salivation and regurgitation of ruminal fluid. Behavioural changes also occur, such as loss of fear of humans and repetitive walking.

1.4.2 Pathological features

As with clinical signs, pathological features are heterogeneous and vary with strain of TSE. Broad pathological features include spongiform change, characterised by diffuse or focally clustered vacuoles in the neuropil of the deep cortical layers, cerebellar cortex or subcortical grey matter (Budka et al., 1995), neuronal death, gliosis and PrP^{Sc} deposition in the brain (Manson et al., 2006, Caughey and Baron, 2006).

Deposition of the abnormally folded, disease associated PrP^{Sc} is an early event and precedes vacuolation. PrP^{Sc} is most commonly deposited as diffuse aggregates on or within the neurons but in some strains, such as GSS, PrP^{Sc} is associated with amyloid plaque deposits (DeArmond and Prusiner, 2003). The pattern and type of PrP^{Sc} deposition is influenced by both host PrP^{C} and TSE strain in a characteristic pattern and is commonly used to distinguish between strains.

Vacuolation is a defining characteristic of TSEs and causes the spongiform appearance in the brain (Brownlee, 1940). In some models vacuolation is closely associated with PrP deposition whilst in others there is a clear dissociation between vacuolation and deposition. In some models there are high levels of vacuolation with little or no detectable PrP^{Sc} (Barron et al., 2007) whilst other models have PrP^{Sc} deposition with little vacuolation observed.

Neuronal dysfunction and neurodegeneration are very poorly understood in TSEs. Synaptic loss and dendritic abnormalities in the CNS are early disease events and can precede PrP^{Sc} deposition (Jamieson et al., 2001). Gamma-aminobutyric acid (GABAergic) neurons are particularly susceptible to TSEs and changes in these are often the first detectable neuropathological change. At terminal stages of disease there is a significant decrease of [3H]-GABA from GABAergic neurons that corresponds to the

accumulation of PrP^{Sc} (Bouzamondo-Bernstein et al., 2004). PrP null mice show weakened GABA receptor-mediated fast inhibitions and impaired long-term potentiation (Collinge et al., 1994) which indicates a loss of function of PrP^{C} may be responsible for some of the clinical phenotypes.

A glial response is seen very early on in disease and is characteristic for all TSE strains; however hosts fail to mount an inflammatory response to the abnormal protein and anti-prion antibodies are not detected during the disease (Aguzzi and Heikenwalder, 2005). As with other protein misfolding diseases, it is uncertain of the exact role of the glia in disease; whether it is protective or detrimental. Microglia express low levels of anti-inflammatory cytokines prior to neuronal loss but in association with synaptic loss (Cunningham et al., 2003). The profile of the microglia appears to be benign but primed. They can become abnormally activated with systemic inflammation, which is a common occurrence in clinical disease, where they switch to an aggressive inflammatory phenotype and can exacerbate disease symptoms (Ransohoff and Perry, 2009). It has been postulated that microglia undergo a switch in an attempt to phagocytose or degrade the PrP deposits.

Although a clinical disease of the CNS, PrP^{Sc} can often be found in the lymphoreticular system, particularly spleen before neural invasion (Kimberlin and Walker, 1979, Farquhar et al., 1994) depending upon the strain and route of infection. There is prominent and uniform PrP^{Sc} deposition in lymphoid tissue, particularly in the tonsils of patients with vCJD, whilst PrP^{Sc} is very rarely found in lymphoid tissues of patients with sCJD and at very low levels (Peden and Ironside, 2004). Despite accumulation of PrP^{Sc} there is a lack of phenotype in peripheral tissues.

1.4.3 Nature of the infectious agent

The infectious agent has not been formally defined and several theories have been proposed over the years. Initially it was believed that TSEs were caused by a slow virus, due to the long incubation periods; however the infectious agent was difficult to identify because it was resistant to formaldehyde, ethanol, nucleases, UV and ionising radiation,

unlike any other known pathogens (Alper et al., 1967, Latarjet et al., 1970). It is however sensitive to phenol, proteases and urea (Hunter and Millson, 1967, Hunter et al., 1969). These properties led to the notion that the infectious agent may not have a nucleic-acid genome (Griffith, 1967).

The lack of evidence for genetic material led to the proposal of the 'protein only' hypothesis by Alper (Alper et al., 1967) and Gibbons (Gibbons and Hunter, 1967), which was developed by Prusiner, who coined the term prion (Prusiner, 1982, Prusiner, 1998), which is now the most widely accepted theory. The prion hypothesis suggested that the transmissible agent was composed entirely of a modified host protein, the prion protein (PrP), which was partially resistant to proteolytic degradation, with no nucleic acid component (Prusiner, 1982). During disease host prion protein (PrP^{C}) is converted to the abnormal isoform PrP^{Sc} in an autocatalytic manner leading to neurodegeneration. Some have suggested that nucleic acid or unknown co-factors are required but these have not yet been identified (Chesebro, 1998).

One feature of prion diseases is the existence of several different TSE strains within the same species (Pattison and Millson, 1961, Beringue et al., 2006). Each strain has distinct phenotypic properties which are reproducible when transmitted to another animal of the same species. Strains are characterised by the incubation time, neuropathology and physicochemical properties such as susceptibility to proteinase K (PK), electrophoretic mobility after PK digestion and the ratio of the glycoforms (glycotype) (Kuczius and Groschup, 1999, Collinge et al., 1996, Telling et al., 1996). As only a single PrP^{C} sequence is shared by all strains the different strains are believed to arise from different conformations of aggregated PrP^{Sc}. Two strains that have been used in this thesis are 79A and ME7, which are mouse-adapted scrapie strains from two different isolates of natural scrapie (Zlotnik and Rennie, 1963, Kimberlin et al., 1989).

It is unclear whether or not the prion protein is the infectious agent but the cellular prion protein (PrP^{C}) is essential for disease (Weissmann et al., 1994, Manson et al., 1994b) and the aberrant folding is present in all TSE diseases. The amount of PrP^{C} influences the incubation period of disease but not the pathology at terminal disease (Manson et

al., 1994b). Heterozygous mice carrying a single wild type PrP allele (*Prnp* $^{+/-}$) had 50% *Prnp* mRNA, significantly reduced PrP^{C} and longer incubation times. Overexpression of PrP in mice also showed an inverse correlation between incubation period and steady state PrP^{C} levels (Scott et al., 1989, Westaway et al., 1991) (Vilotte et al., 2001).

1.4.4 Transmissibility of TSEs

Transmissible spongiform encephalopathies are unusual for protein misfolding diseases in that they can be acquired from external sources and are transmissible between animals. They can also be inherited although the majority of human cases are sporadic, with the cause of disease unknown.

Approximately 10-15% of all human TSEs are caused by an inherited autosomal dominant mutation in the *PRNP* gene (Wadsworth and Collinge, 2007, Weissmann, 2002, Mead, 2006). Mutations are thought to destabilise PrP^{C}, allowing a more ready conversion to PrP^{Sc} without an external source of PrP^{Sc}. Mutations can introduce a premature stop codon, insert additional octapeptide repeats or cause a point mutation leading to a single amino acid change (van der Kamp and Daggett, 2011). Amino acid changes are found at 28 different locations and effect protein stability, cell processing and function (van der Kamp and Daggett, 2009).

Although no familial TSEs or disease causing mutations have been identified for any species other than humans, polymorphisms in the PrP gene play a role in disease progression and susceptibility, such as in sheep and goats.

1.4.5 Conversion of PrPC to PrPSc

The central event in disease is the conversion of host PrP^{C} to the disease associated PrP^{Sc}. PrP^{C} undergoes post-translational modification and conformational change to become the pathogenic PrP^{Sc}, which shares the same amino acid sequence as PrP^{C} but is structurally different (Table 1.6).

PrP^{Sc} is composed of 40% beta-sheets and only ~30% is alpha-helical, compared to the 40% alpha-helical and 3% beta-sheet structure of PrP^{C} (Baldwin et al., 1994, Pan et al., 1993). The high beta-sheet content increases propensity to aggregate and form amyloid fibrils. The altered structure also makes it more detergent insoluble and resistant to the activity of proteases.

Table 1.6 A comparison of the structure and properties PrP^{C} and PrP^{Sc}

	PrP^{C}	PrP^{Sc}
Structure	40% alpha helical 3% beta sheet	30% alpha helical 40% beta sheet
GPI anchor	Yes	Yes
PI-PLC sensitive	Yes	No
Solubility	Detergent soluble	Detergent insoluble
Protease sensitivity	Sensitive	Resistant

1.4.5.1 Interaction of PrPC with PrPSc

It has been proposed that there must be a direct interaction between the PrP^{Sc} template and the PrP^{C} substrate to drive the formation of nascent infectious prions (Prusiner, 1998, Horiuchi and Caughey, 1999). The C-terminal (residues 90-231) of PrP^{Sc} contains beta-sheets which form hydrogen bonds with beta-sheets from other PrP^{Sc} molecules to form a cross-β core (Chiti and Dobson, 2006, Collinge, 2001).

Originally it was proposed that the propagation of PrP^{Sc} was by a heterodimeric interaction between PrP^{C} and PrP^{Sc} monomers (Prusiner, 1991). The conversion was proposed to act in a two stage process; firstly PrP^{C} binds to PrP^{Sc} and then PrP^{C} undergoes a conformational change into PrP^{Sc}. However, there is no evidence of a stable PrP^{Sc} monomer and conversion is associated with PrP^{Sc} aggregation and seeding with PrP^{Sc} aggregates making it unlikely that conversion is by a heterodimeric interaction. An alternative theory, the nucleated polymerisation mechanism states that conformational change to PrP^{Sc} only occurs when there is an oligomer large enough to

act as a stable nucleus (Jarrett and Lansbury, 1993, Harper and Lansbury, 1997, Come et al., 1993). This also supports the maintenance of prion strains as monomeric proteins are unlikely to adopt different stable conformations however aggregates can stably form many different conformations (Faber and Matthews, 1990).

Helix 2 and 3 are important regions for amyloid formation and are believed to be the initiation sites of PrP^{C} to PrP^{Sc} transition (Yamaguchi et al., 2008, Chen and Thirumalai, 2013). The first glycosylation site lies within helix 2 and presence of the glycan has been shown to reduce the rate of fibril formation by stabilising the intermolecular disulphide bond formation (Bosques and Imperiali, 2003) therefore unglycosylated PrP^{C} is more readily converted to PrP^{Sc}.

The N-terminal undergoes conformational change (Peretz et al., 1997) however the entire N-terminal is not required for conversion. Deletions of the N-terminal do not prevent conversion to PrP^{Sc} but prevent efficient conversion and change pathology (Flechsig et al., 2000, Fischer et al., 1996). Peptides of residues 109-122 have been shown to exhibit high beta-sheet structure and form amyloid (Gasset et al., 1992). Conversion is also dependent upon the central domain of the prion protein. Deletions of residues 114-121, 95-107 or 108-121 prevent conversion to PrP^{Sc} in cultured cells and transgenic mice (Holscher et al., 1998, Muramoto et al., 1997).

The sequence homogeneity between PrP^{C} and PrP^{Sc} is important for conversion and may contribute to the interspecies barrier observed with some TSEs (Kocisko et al., 1995). Homogenous seeding is more effective than heterogeneous seeding, thus seeding mouse PrP^{C} with mouse PrP^{Sc} gives more efficient conversion than seeding hamster PrP^{C} with mouse PrP^{Sc} (Kocisko et al., 1995). The effect of glycosylation homogeneity is significant but is secondary to PrP sequence in determining compatibility for conversion (Priola and Lawson, 2001). The ratios of the glycoforms have also been shown to affect the efficiency of conversion *in vitro* in a species and/or strain specific manner (Nishina et al., 2006).

Conversion has different efficiencies with different isoforms of PrP^{C} and the interactions between isoforms may also influence conversion. Truncated C1 is not able to convert to PrP^{Sc} *in vivo* but acts as a dominant negative inhibitor for early stages of conversion (Westergard et al., 2011).

1.4.5.2 Site of conversion

The exact PrP^{C}/PrP^{Sc} conversion site has not been defined. It has been proposed that PrP^{C} undergoes conversion either on the cell surface or following endocytosis of PrP^{C} (Borchelt et al., 1992, Beranger et al., 2002, Veith et al., 2009). The site of conversion may occur at multiple sites and may be strain dependent.

Localisation to the cell membrane is important for conversion. The plasma membrane is believed to be the primary site of conversion. Fluorescent epitope tagging has demonstrated rapid conversion of PrP^{C} after one minute of exposure to PrP^{Sc} at the cell surface (Goold et al., 2011). Infectivity is reduced on exposure to anti-PrP antibodies or if PrP is released from the cell surface by removal of the GPI anchor (Borchelt et al., 1992, Campana et al., 2005) or if trafficking to the cell surface is altered (Gilch et al., 2001) suggesting that PrP^{C} must go to the cell membrane before conversion can occur.

In addition to conversion at the cell surface PrP^{C} may act as a receptor allowing internalisation of PrP^{Sc} and intracellular conversion. Studies have shown that conversion may occur in endosomal compartments. In cell culture, exosomes are infectious and PrP^{Sc} can be secreted into the media to infect other cells (Fevrier et al., 2004). Dominant negative peptides that disrupt trafficking have shown that in more than one cell line early and late endosomes do not take part in conversion but endosomal recycling compartments do (Marijanovic et al., 2009). Blocking endocytosis by lowering the temperature inhibits PrP^{Sc} formation (Borchelt et al., 1992).
PrP^{Sc} can undergo retrograde transport to the Golgi apparatus or ER, where it can form new PrP^{Sc} from newly synthesised immature PrP^{C} (Campana et al., 2005). Stimulation of retrograde transport and intracellular accumulation by the small GTPase Rab6a

showed an increase in PrP^{Sc} in infected cells (Beranger et al., 2002). Immature PrP^{C} may be a better substrate for conversion than mature PrP^{C} because it is easier to misfold (Campana et al., 2005). The ER is thought to play a key role in conversion of PrP^{C} mutants in familial TSEs. Studies have shown that PrP^{C} containing some familial mutations convert spontaneously to PrP^{Sc} soon after synthesis and are much slower to leave the ER, suggesting accumulation in the ER rather than the cytoplasm is important in this set of familial TSEs (Harris, 2003, Gu et al., 2003).

Efficient conversion of PrP is dependent upon membrane tethered PrP^{C}. Cell cultures that expressed only GPI anchorless PrP were resistant to TSEs (McNally et al., 2009). Mice that express PrP lacking the GPI anchor do not have PrP^{C} on the cell surface (Chesebro et al., 2005). The anchorless PrP is processed through the secretory pathway but remains mostly unglycosylated and is secreted from the cell surface. These mice are still susceptible to TSEs; however they show PrP^{Sc} positive amyloid plaques rather than diffuse deposition and live a normal lifespan. Transmission of TSEs to GPI anchorless animals was much more inefficient than in mice with GPI anchored PrP (Chesebro et al., 2005).

1.4.5.3 In vitro conversion assays

In order to understand the prion hypothesis several *in vitro* conversion assays have been developed to amplify PrP^{Sc}. These assays can aid in identifying the infectious agent and are being developed as a sensitive diagnostic test for natural TSE diseases. These assays use a small seed from infectious material as a template to induce refolding and fibrillisation of PrP^{C} under different biophysical conditions. The conversion product is PK resistant but not necessarily the same as PrP^{Sc} generated in disease as it does not always cause disease when inoculated into mice.

The first assay developed was the cell free conversion (CFC) assay. Radiolabelled PrP^{C} is incubated with brain derived PrP^{Sc} in the presence of guanidine to induce conversion to a similarly protease resistant protein (Kocisko et al., 1994). Cell free conversion is

highly specific, correlating with species transmission and strains (Raymond et al., 2000, Kocisko et al., 1995, Bossers et al., 1997). Very little PrP^{Sc} is generated from this single round conversion; therefore assays with repeated rounds of conversion were developed to improve sensitivity.

Two other *in vitro* conversion assays were developed to amplify small amounts of PrP^{Sc} in an excess of PrP^{C} substrate using alternating cycles of incubation to allow PrP^{Sc} aggregates to grow and disruption of the aggregates to provide new aggregates for further conversion. The level of amplification can be increased by increasing the number of cycles and is only limited by the availability of PrP^{C} and other essential cofactors. Protein misfolding cyclic amplification (PMCA) and the quaking induced conversion (QuIC) assay work on the same principle as each other but use different sources of PrP^{C} substrate and different methods of disruption.

PMCA uses uninfected brain homogenate as the source of the PrP^{C} substrate for conversion and PrP^{Sc} aggregates are broken into smaller aggregates by sonication. It is difficult to standardise the conditions in PMCA and the assay has varying success at the hands of different laboratories. The QuIC assay uses recombinant PrP at a known concentration as the substrate and rapid shaking to disrupt the aggregates.

The PMCA product is tested for amplification by immunoblot. Initially the QuIC assay amplification was measured by immunoblotting products (Atarashi et al., 2008); however the technique was improved by the addition of thioflavin T (Orru et al., 2009). When PrP^{res} forms amyloid fibrils the thioflavin T binds and fluorescence is enhanced. Fluorescence is measured throughout the incubation, giving a real time measurement of amplification.

1.4.6 Loss of function versus gain of function

The roles of PrP^{C} and PrP^{Sc} in neurodegeneration are not understood. Toxicity could be due to a gain of function of PrP^{Sc} or loss of function of PrP^{C} (Figure 1.6).

PrP^{Sc} may possess toxic properties that are not related to the normal function of PrP^{C}, such as aggregates interfering with synaptic function or triggering apoptotic pathways. It has been proposed that prion neurotoxicity is linked to PrP^{Sc} oligomers, which translocate to the cytosol and inhibit the ubiquitin-proteosome system (Kristiansen et al., 2007). The $PrP_{106-126}$ fragment has been shown to be neurotoxic to cells expressing PrP^{C} both *in vitro* and *in vivo* (Forloni et al., 1993, Ettaiche et al., 2000). The neurotoxic peptide has a propensity to aggregate and form amyloid like fibrils (Forloni et al., 1993). Reactive gliosis is a feature of prion diseases but is also common in other protein mis-folding diseases, such as Alzheimer's disease. The $PrP_{106-126}$ peptide neurotoxicity is dependent upon the presence of microglia, which are stimulated by the peptide into overproducing oxygen radicals (Brown et al., 1996).

Despite this evidence for PrP^{Sc} as the toxic species several studies have shown that there is no correlation between PrP^{Sc} deposition and neurodegeneration. Models exist with abundant deposits of PrP^{Sc} amyloid but lacking clinical signs (Chesebro et al., 2005). This does not discount PrP^{Sc} as the toxic species, but rather suggests that the toxic species may be a particular conformation of PrP^{Sc}, such as a small oligomer.

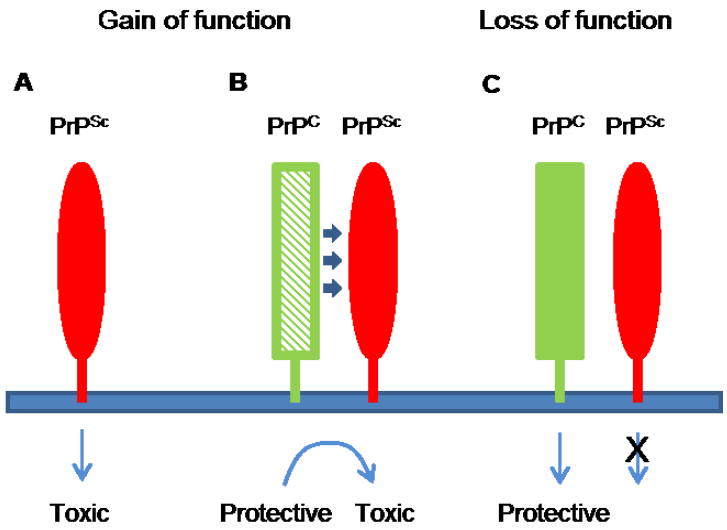

Figure 1.6 Gain or loss of function mechanisms for PrP neurotoxicity
Gain of function mechanism (A) PrP^{Sc} possesses toxic properties independent of PrP^{C} function or (B) Conversion to PrP^{Sc} subverts the protective function of PrP^{C} to the toxic function of PrP^{Sc}. Loss of function mechanism (C) PrP^{Sc} is inert but neuronal death is caused by the loss of protective function from PrP^{C}.

The loss of biological activity of PrP^{C} could be responsible for neurotoxicity. PrP^{C} has been proposed to be involved with anti-apoptotic activity and neuroprotection (Roucou et al., 2004). Loss of this neuroprotection could lead to neurodegeneration thus understanding the function of PrP^{C} may be important in elucidating the neurotoxic mechanisms. However the lack of phenotype in PrP null mice is strong evidence against the loss of function mechanism.

As arguments exist for both loss and gain of function it may be that the neurodegeneration is a result of both. A build-up of PrP^{Sc} causes stress on the cell, which is unable to respond effectively due to loss of function of PrP^{C} leading to neuronal dysfunction and neurodegeneration. PrP^{C} has been implicated in several signal transduction cascades. Binding of PrP^{Sc} to PrP^{C} could alter the binding ability and initiate a toxic signalling cascade.

1.5 Glycosylation of PrP in TSE disease

Glycosylation can influence conformation of a protein and interactions with other glycoproteins therefore the glycans have the potential to influence conversion of PrP^{C} to

PrP^{Sc}. Glycosylation is not essential for conversion however the glycosylation status of both host PrP^{C} and donor PrP^{Sc} influence TSE disease outcome (Taraboulos et al., 1990, Tuzi et al., 2008, Cancellotti et al., 2013).

Glycosylation is used as a tool to distinguish between TSE strains. PrP glycotype analysis forms part of the molecular classification and looks at the ratio of the different glycoforms and the size of the PK digested cleavage fragment of unglycosylated PrP^{Sc}. Glycosylation alone does not define a strain as some strains share the same glycotype, yet display unique clinical and pathological features. Therefore, strains are distinguished by a combination of molecular, pathological and clinical classifications (Bruce, 2003, Beck et al., 2012, Gavier-Widen et al., 2005).

Strains may have different requirements of host glycosylation in order to cause disease. Subtle changes in the stoichiometry of host PrP^{C} glycoforms can significantly impact prion conversion during *in vitro* amplification in a species- and strain-specific manner (Nishina et al., 2006). Unglycosylated PrP as a substrate for conversion by PMCA was essential for the formation of RML mouse PrP^{Sc}, while diglycosylated PrP was required for hamster PrP^{Sc} formation. Disease incubation period varies with host glycosylation status *in vivo* (discussed in detail in 1.5.1) indicating that glycosylation assists in conversion (Tuzi et al., 2008, Cancellotti et al., 2013).

Glycosylation may determine the targeting of different strains to different brain regions due to neuronal-specific differences in PrP glycosylation (Hecker et al., 1992, DeArmond et al., 1999). Glycosylation at the first site did not influence strain targeting, as vacuolation patterns seen in wild type mice and mice lacking glycans at this site were the same for three strains. However, vacuolation patterns were altered in 79A infected G1 mice indicating that the second site may contribute to strain targeting (Tuzi et al., 2008).

In TSE disease, strains show precise regional variation of PrP^{Sc} deposition, suggesting strain specific targeting of neuronal populations. When glycosylation is disrupted the pattern of PrP^{Sc} deposition can be changed therefore it has been proposed that

glycosylation can influence targeting (Cancellotti et al., 2010). The degree of glycosylation of PrP^{Sc} in TSE disease varies with brain region (Somerville et al., 2005), which may reflect the degree of glycosylation of PrP^{C}. Regional differences in the PrP^{C} glycoforms have been observed (Beringue et al., 2003) and the stoichiometry of the PrP^{C} glycoforms has been shown to influence the efficiency of conversion in a strain dependent manner (Nishina et al., 2006) therefore the glycoforms available in different regions may determine the efficiency of conversion and deposition for the different strains.

The glycosylation status of the host and glycosylation of PrP^{Sc} can allow selection of a strain (Cancellotti et al., 2013). When 79A from the PrP glycosylation deficient mice were tested in a strain typing panel of mice (C57, VM and the F1 cross) the vacuolation profile and incubation period order was different between mouse strains (Tuzi et al., 2008, Cancellotti et al., 2013). G3 79A showed a similar profile to wild type 79A, but G2 79A appeared to be more similar to the 139A strain. The scrapie cell conversion assay (SSCA) also showed G2 to have a 139A phenotype. G1 79A showed a different phenotype from wild type mice both in the strain typing panel and the SSCA which may represent a novel strain (Cancellotti et al., 2013). There was no change in phenotype seen in G2 ME7 or G2 301C. 79A may be a less stable strain and is able to switch between 79A and 139A, depending upon host PrP.

1.5.1 Susceptibility of GlycoD mice to TSE disease

The GlycoD mice have been used to study the effect of glycosylation on the TSE disease process. Several different strains, both mouse adapted and non-adapted have been used in the GlycoD mice to assess the influence of host glycosylation status (Table 1.7**Table 1.7**). PrP^{Sc} from the GlycoD mice was also used to assess the effect of glycosylation of the PrP^{Sc} on strain properties.

All GlycoD mice were susceptible to at least one strain of TSE; however the susceptibilities varied according to glycosylation status of the host and the TSE agent (Figure 1.7). The susceptibility of G3 mice to at least one strain shows that

glycosylation is not essential to support TSE disease. G1 and G3 mice are resistant to most strains tested, with the exception of 79A where they are susceptible but with an increased incubation time. Both of these mouse lines lack glycans at the first glycosylation site suggesting that the presence of carbohydrates at the first site are important for determining susceptibility. G2 mice were susceptible to all strains tested, although they had increased incubation times for some strains. G2 mice were the only strain to be susceptible to sCJD.

Glycosylation of PrP^{Sc} is not required for infection as brain material from unglycosylated mice infected with 79A was able to cause disease in wild type mice. Moreover the infected GlycoD mice, which only have mono or unglycosylated PrP^{Sc}; when used to inoculate wild type mice demonstrated the presence of diglycosylated PrP^{Sc} in the host (Tuzi et al., 2008) demonstrating that the host dictates the glycosylation of the PrP^{Sc} rather than the donor.

Glycosylation appears to have a strain dependent influence on disease susceptibility. All GlycoD mice were susceptible to 79A but both G1 and G2 mice had an increased incubation period. G3 mice showed a dramatically reduced susceptibility, only 4 out of 21 mice showed clinical disease and the incubation time was more than tripled compared to wild type mice. The prolonged incubation in the GlycoD mice suggests that both glycosylation sites facilitate infection by 79A.

It is likely that the glycan at the first site is important for susceptibility to ME7 as mice lacking glycans at the first site were resistant to disease but mice with glycans present at the first site showed no difference in disease susceptibility and incubation time (Table 1.7). The difference in localisation of PrP^{C} in the GlycoD mice is not responsible for the increased resistance to ME7 as G1 and G2 mice have comparable localisations yet different susceptibilities.

The resistance of both G1 and G3 mice to five of the six TSE strains tested suggests that glycosylation at the first site is an important determinant for disease susceptibility. The G1 and G2 mice showed a similar decrease in cell surface PrP (Cancellotti et al., 2005)

therefore likely that the altered localisation of PrP^C is caused by the lack of glycosylation rather than altered localisation.

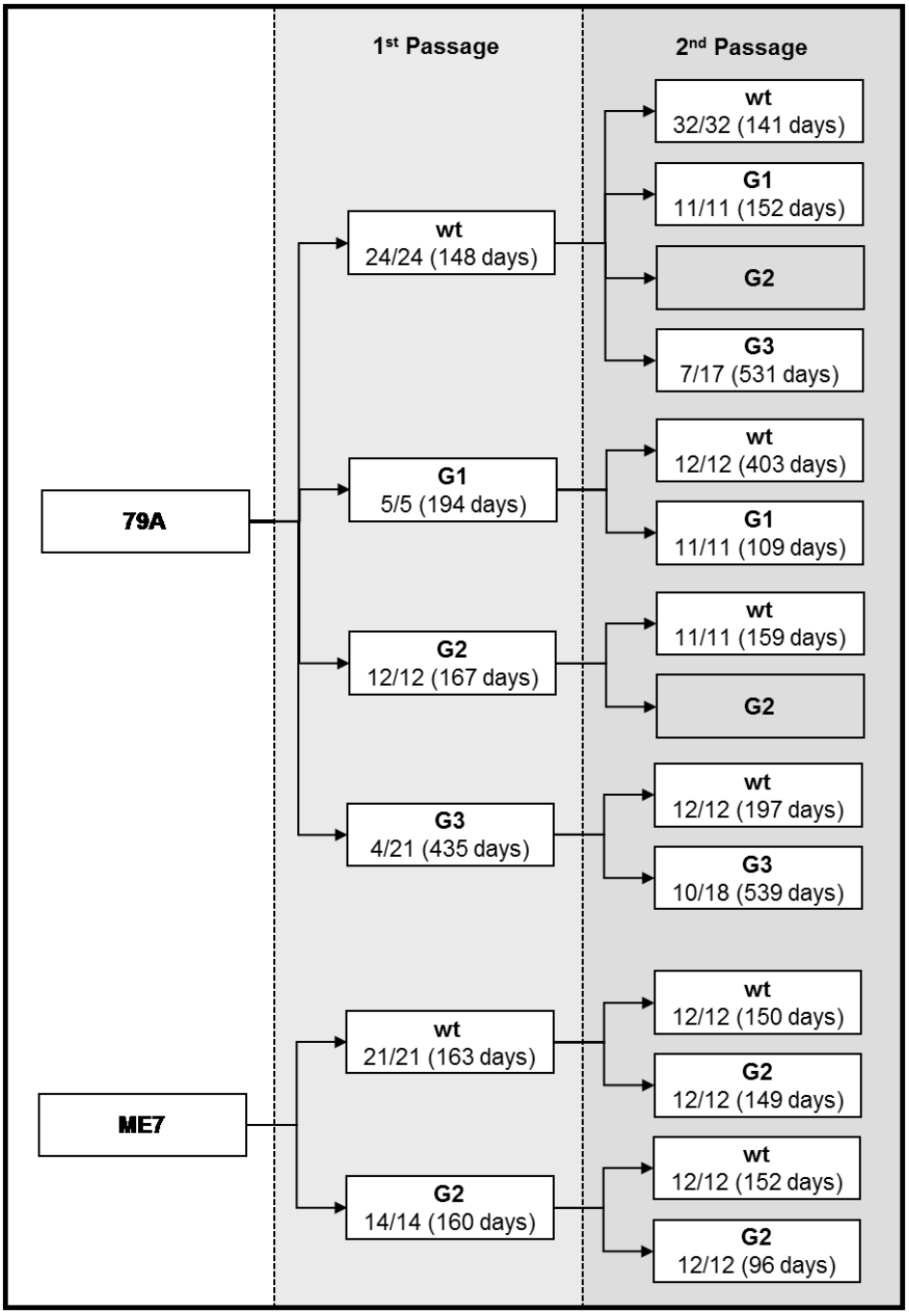

Figure 1.7 Susceptibility of GlycoD mice to mouse adapted TSE strains
The susceptibility of the GlycoD mice to 79A and ME7 is shown for primary and secondary passage. The number of mice susceptible (clinical and pathology positive) is shown with the total number of mice inoculated. Incubation period in days is shown in brackets. G1 and G3 mice were resistant to ME7. Data from (Tuzi et al., 2008) and (Cancellotti et al., 2013).

Table 1.7 Summary of susceptibilities and incubation periods for different TSE strains

TSE strain		129/Ola (wt)	G1	G2	G3
Mouse adapted strains	79A	24/24 (148 +/- 2.6 days)	5/5 (194 +/- 2.1 days)	12/12 (167 +/- 9.3 days)	4/21 (435 +/- 92 days)
	ME7	21/21 (163 +/- 2 days)	0/16 (600 < days)	14/14 (160 +/- 2.5 days)	0/18 (700 < days)
	301C	12/12 (166 +/- 1.5 days)	0/18 (700<days)	12/15 (354 +/- 5.3 days)	0/21 (700<days)
Non-mouse strains	vCJD	9/21 (491 +/- 24.5 days)	0/20 (600 < days)	5/18 (536 +/- 16 days)	0/22 (700 < days)
	sCJD (MM2)	0/19 (700 < days)	0/14 (600 < days)	7/14 (404 +/- 7.8 days)	0/21 (700 < days)
	263K	3/22	0/17	11/19	0/21

Susceptible	Incubation ↑	Incubation ↑ by 100 days or more	Resistant	† Subclinical

† Subclinical disease was determined as no clinical disease but by the presence of both PrP^{Sc} deposition and spongiform degeneration.

Each box shows the number of animals which were clinically and pathologically positive for TSE disease and the total number of animals in the group. The incubation period is also shown in brackets for each strain and genotype. Boxes are colour coded to allow easier visualisation of the susceptibility patterns.

The changes in disease susceptibility in the GlycoD mice may be due to the amino acid substitution rather than the absence of the glycans. However, there is a dramatic difference in TSE susceptibility between G3 mice and G1 or G2 mice. The G3 mice have the same amino acid substitution at position 180 as G1 mice yet G1-79A and G3-79A show a difference in phenotype. The G3 mice also share the amino acid substitution at position 196 as G2 mice yet G2-79A and G3-79A show differences in disease phenotype (Cancellotti et al., 2013), suggesting that the difference is caused by the lack of glycosylation rather than the amino acid substitution.

Studies using different amino acid substitutions showed that Asn substitution did not prevent TSE infection or PrP^{Sc} replication suggesting that Ans residues can be replaced without directly affecting disease susceptibility (Ikeda et al., 2008, Neuendorf et al., 2004). Studies using the GlycoD mice and other glycosylation deficient PrP mice with different amino acid substitutions produce similar results when inoculated with three different TSE strains (Tuzi et al., 2008, Neuendorf et al., 2004). Conversion of deglycosylated mouse PrP^{C} using serial PMCA showed no change in agent phenotype (Piro et al., 2009). This evidence suggests the effects are due to glycosylation deficiency but the effect of the amino acid substitution cannot be totally ruled out.

1.6 Aims

1. PrP^{C} possesses two glycosylation sites that can be variably glycosylated leading to 4 different glycoforms *in vivo*. Glycosylation of PrP^{C} plays an important role in TSE disease however the significance of the glycoforms is unknown for PrP^{C}. This thesis will investigate the effect the glycosylation of the two different sites have on the cell biology of PrP^{C}. It will also aim to determine whether the cell biology of the glycoforms can explain the differences in susceptibility in TSE disease in the GlycoD mice.

2. Investigate the cell biology of the different glycoforms of PrP^{C} using the different GlycoD mice to isolate glycoforms
    a. Establish whether glycosylation alters the steady state level of PrP^{C} in the brain
    b. Establish the distribution of the glycoforms throughout the brain
    c. Establish whether glycosylation affects susceptibility to the natural proteolytic cleavage events
    d. Determine exact localisation and quantity of PrP^{C} in the GlycoD mice

3. Assess the effect of glycosylation on the interaction between the PrP^{C} and PrP^{Sc} in an *in vitro* conversion assay (QuIC)

2 Materials and Methods

All chemicals are from BDH unless otherwise stated. All experiments were carried out at room temperature unless otherwise stated.

2.1 Animals used

All animal breeding and experimental work was carried out under the regulations of the UK Animals (Scientific Procedures) Act 1986 and approved by the local ethics Committee. All transgenic animals have been approved by the Health and Safety Executive.

3 different lines of PrP glycosylation deficient (GlycoD) mice were created using gene targeting methods and maintained on a 129/Ola background (Cancellotti et al., 2005).

- G1 carries the N180T mutation in PrP to abolish the first glycosylation site
- G2 carries the N196T mutation in PrP to abolish the second glycosylation site
- G3 carries the N180T and N196T mutations in PrP to abolish both glycosylation sites

All mice were 6 weeks or older and both sexes were used. No age or sex matching was carried out for the genotype groups.

2.2 Quantification of PrnP mRNA in mouse brain

2.2.1 Isolation of RNA

Half brains were weighed and homogenised in RNA-bee (1ml/50mg tissue) [Amsbio] in a gentleMACS dissociator [Miltenyi]. For every 1ml RNA-bee 0.2ml chloroform were added and shaken vigorously. Samples were incubated on ice for 5 minutes before centrifugation at 12,000 x g for 15 minutes at 4°C. The aqueous phase containing the

RNA was transferred to a new tube and 500 µl isopropanol added for 10 minutes at room temperature to precipitate the RNA. Precipitate was centrifuged at 12,000 x g for 5 minutes at 4 °C and the pellet washed twice with 75% ethanol and allowed to air dry. RNA was resuspended in RNase free water. Samples were treated with DNA-free [Ambion] to remove genomic DNA and RNA was stored at -80 °C long term.

2.2.2 cDNA synthesis

cDNA synthesis was carried out using a first strand cDNA synthesis kit [GE Healthcare] and a random hexamer primer ($pd(N)_6$). The RNA was measured using a NanoDrop spectrometer and diluted to 1000ng/µl. 5 µl RNA in 3 µl RNase free water was heated to 65 °C for 10 minutes to denature and then chilled on ice. 5 µl bulk reaction mix, 1 µl Dithiothreitol (DTT) solution and 1 µl pd(N)6 primer was added and incubated at 37 °C for 1 hour.

2.2.3 SYBR green Quantitative PCR (qPCR)

Quantitative PCR was carried out using the Platinum SYBR green supermix-UDG [Invitrogen]. Each sample was carried out in quadruplet with a no reverse transcriptase control and non template control included. Each cDNA was diluted 100 fold with nuclease-free water and 4.75 µl added to 7.75 µl qPCR master mix (6.25 µl SYBR green master mix, 0.625 µl forward primer, 0.625 µl reverse primer, 0.25 µl Rox reference dye). Primers for *Prnp* and the housekeeping gene, *β-actin* had been previously optimised and analysed by S. Aungier, The Roslin Institute. Samples were mixed by gentle vortexing and then centrifuged briefly to collect the liquid at the bottom of the wells.

Amplification was carried out on an Mx300 qPCR machine [Stratagene] using the MxPro software and the following thermal profile.

One cycle	50 °C	2 mins	UDG incubation
	96 °C	2 mins	Activated Taq polymerase
40 cycles	96 °C	15 secs	Denaturing
	60 °C	30 secs	Annealing and extension
One cycle	95 °C	1 min	Melting curve analysis
	60 °C	30 secs	
	95 °C	15 secs	
	25 °C	30 secs	

The ΔΔCT values were calculated to assess fold change in *Prnp* expression against the housekeeping gene β-actin compared to *Prnp* in wild type mice.

2.3 Preparation of protein from brain for biochemical analysis

2.3.1 Total protein extraction

Flash frozen whole brains or dissected regions of brain were weighed and appropriate volumes of ice cold lysis buffer [0.5% Nonidet NP-40 [Sigma], 0.5% sodium deoxycholate in PBS] added to give a 10% (v/w) homogenate. Protease inhibitors [phenylmethylsulfonyl fluoride (PMSF) final concentration 10 mM; N- ethylmaleimide (NEM) final concentration 10 mM] were added to prevent protein degradation by endogenous proteases. Brains were mechanically homogenised and centrifuged at 2000 x *g* for 10 minutes to remove the nuclei and cellular debris. Supernatants were removed, aliquoted and frozen in liquid nitrogen (LN_2). Homogenates were stored at -70 °C.

2.3.2 Protein extraction for lipid raft analysis

At 37 °C all membrane regions are soluble but at 4 °C lipid raft regions are insoluble, whilst non-raft regions are soluble. This can be used to isolate the lipid raft regions from the non-raft regions of the membrane. All stages carried out at 4 °C or on ice, using ice cold solutions and as quickly as possible.

Flash frozen brains were mechanically homogenised in 10 ml homogenisation buffer [150 mM sodium chloride, 20 mM sodium dihydrogen orthophosphate, 2 mM disodium

hydrogen phosphate, 1 mM EDTA, 20% glycerol in dH_2O] by 30 passes of a dounce homogeniser then passed through a 21 gauge needle 20 times. Homogenate was centrifuged at 5000 x *g* for 20 minutes to remove large debris. Supernatant was removed and centrifuged at 100,000 x *g* for 90 minutes to pellet the membranes. The resulting pellet was resuspended in 3 ml MES buffered saline (MBS) [25 mM MES and 0.15 M NaCl (pH 6.5 with HCl)] and further centrifuged at 100,000 x *g* for 90 minutes. The pellet was resuspended in 3 ml MBS with 2 mM EDTA and 2% (vol/vol) Triton X-100 and passed through a 21 gauge needle 15 times. It was then mixed at 4 °C for 2 hours to fully solubilise all membranes. Solubilised membranes were diluted with an equal volume of 80% (w/v) sucrose in MBS to give a 40% sucrose solution. 0.8 ml membrane solution was injected under a discontinuous sucrose gradient [2.4 ml 30% (wt/vol) sucrose and 0.8 ml 5% (w/v) sucrose in MBS containing 2 mM EDTA and 0.5% (v/v) Triton X-100] and centrifuged at 100,000 x *g* for 18 hours. 10 x 400 µl fractions were collected from the top of the gradient to the bottom. The pellet was resuspended in MBS with 2 mM EDTA and 2% (v/v) Triton X-100 with mild sonication. Fractions were stored at -70 °C until being probed by western blot.

Where necessary, individual fractions were concentrated in order to detect low-level proteins. Fractions were mixed with an equal volume of 40% (w/v) trichloroacetic acid and mixed at 4 °C for 1 hour to precipitate the protein. The protein was then pelleted by centrifugation at 11,600 x *g* for 5 minutes and the pellet resuspended in 100 µl 3M Tris-HCl (pH 7).

2.3.3 Micro dissection of mouse brain regions

Microcentrifuge tubes were labelled with the brain number and area of the brain and then weighed. Snap frozen brains were removed from LN_2 and allowed to partially thaw before dissection on a cold plate [Celltech]. The brain was sectioned coronally, starting from the brain stem, into 4 areas using a scalpel and forceps. Each section was then dissected into regions using the scalpel (Figure 2.1). The hippocampus was dissected using a punch method. A biopsy needle was used to punch out the hippocampus and a syringe used to blow the region out of the needle into a microcentrifuge tube. At least 4

punches were taken from each hippocampus. The brain regions were then flash frozen in LN_2. Frozen samples were then re-weighed and empty tube weights subtracted to calculate the total brain weight. 3 blank tubes were weighed before and after freezing to use as a correction factor for the other samples. Brain regions were stored at -70 °C.

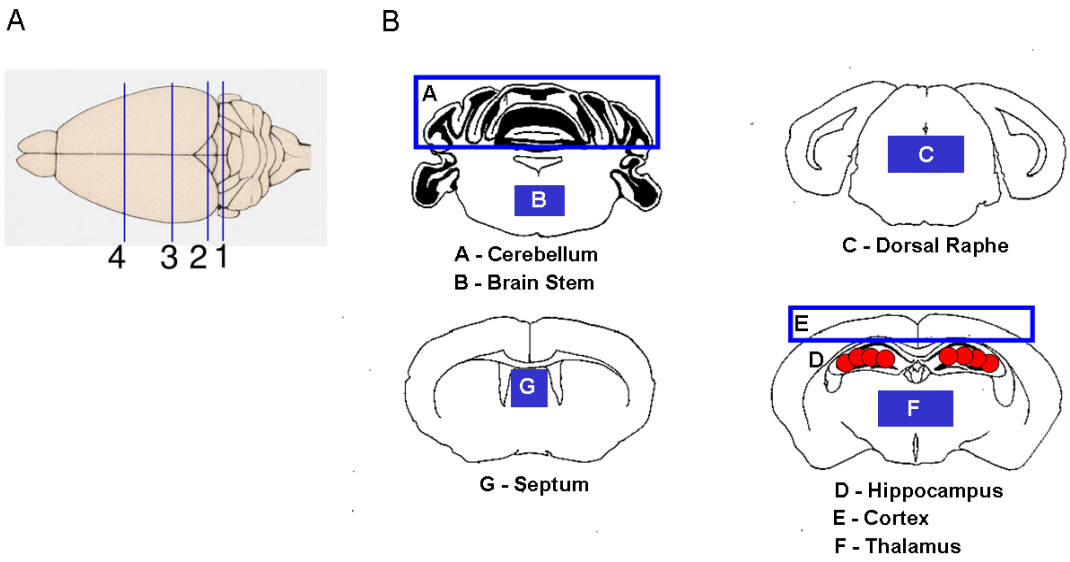

Figure 2.1. Dissected brain regions
(A) Coronal sections cut through mouse brain as described in (Barr et al., 2004) (B) Seven different brain regions throughout the brain were selected. Blue areas were cut with a scalpel whilst the red areas were dissected using at least 4 punches of a canula needle for each hippocampus.

2.3.4 Total protein estimation using the bicinchoninic acid assay

Total protein estimation was carried out using the bicinchoninic acid assay (BCA) assay kit [Pierce]. Protein standards were made with bovine serum albumen (BSA)[Pierce] diluted in the same buffer as the samples to give a range of concentrations. 3 µl homogenate was added to 57 µl buffer to give a 1:10 dilution of the original homogenate (6 µl homogenate added to 54 µl buffer to give a 1:20 dilution). 20 µl sample or standard was added in duplicate to a 96-well microtitre plate. Reagent A was mixed with reagent B [Peirce] 50:1 to create a working reagent. 180 µl working reagent was added to each well. The plate was incubated at 37 °C for 30 minutes then cooled to room temperature. The absorbance at 570 nm was read on a plate reader and analysed using Ascent software [Thermo Scientific]. Final absorbances were calculated by subtracting the blank reading (working reagent and sample buffer) and absorbances of

the BSA standards used to produce a standard curve. Concentrations of samples were derived using the standard curve.

2.3.5 Deglycosylation of proteins using PNGase F

20 µl 10% brain homogenate was denatured with 1 x glycoprotein denaturing buffer (0.5% sodium dodecylsulphate (SDS), 1% β-mercaptoethanol) [New England Biolabs] at 100 °C for 10 minutes before incubation with 1500 U of N-glycosidase F (PNGase F) [New England Biolabs] in 1 x G7 reaction buffer (50 mM $NaPO_4$, pH 7.5) [New England Biolabs], 1% NP-40 [New England Biolabs] and 2.5 M urea at 37 °C overnight with vigorous shaking. The reaction was stopped by freezing at -20 °C. 200 µl methanol, 100 µl chloroform and 150 µl dH_2O were added and centrifuged at 2,000 x *g* for 10 minutes to precipitate the proteins. The chloroform layer was removed and 200 µl methanol added to resuspend the precipitated proteins and stored at -20 °C. When samples were ready to be used for SDS gel electrophoresis they were centrifuged at 13,000 x *g* and supernatant discarded. Pellets allowed to air dry before being suspended in 20 µl lysis buffer.

2.3.6 Deglycosylation of proteins using Endoglycosidase H

40 µl 10% brain homogenate was denatured with 1 x glycoprotein denaturing buffer (0.5% sodium dodecylsulphate (SDS), 1% β-mercaptoethanol) [New England Biolabs] at 100 °C for 10 minutes. Samples were left to cool to room temperature and 1 x G5 reaction buffer (50 mM sodium citrate, pH 5.5) [New England Biolabs] added before splitting into two aliquots. 2500 U endoglycosidase H was added to one aliquot and dH_2O added to the other and incubated at 37 °C overnight with vigorous shaking. The reaction was stopped by freezing to -20 °C.

2.3.7 Proteinase K digestion

10% brain homogenate was incubated with 100 µg/ml Proteinase K [Roche] at 37 °C for 1 hour and 15 minutes with shaking. The reaction was stopped with 10 mM PMSF and 10 mM NEM.

2.3.8 Solubilisation in guanidine hydrochloride

10% brain homogenate in lysis buffer was added to equal volumes of 2 M guanidine hydrochloride (Gnd HCl) and homogenised with a dounce homogeniser. Insoluble proteins were separated from soluble proteins by centrifugation at 16,200 x *g* for 10 minutes. Supernatant contained proteins soluble in 1M Gnd HCl and stored at -20 °C. The resultant pellet was resuspended in 6M Gnd HCl and stored at -20 °C.

2.3.9 Phosphatidylinositol-specific phospholipase C removal of GPI anchor

A whole brain prepared as a 10% brain homogenate was centrifuged at 25,000 x *g* for 10 minutes at 4 °C to pellet membranes. Supernatant was retained and designated S_1. The pellet was resuspended in 500 µl PBS and split into two 250 µl aliquots. One aliquot was treated with 0.5 U Phosphatidylinositol-specific phospholipase C (PI-PLC) [Invitrogen] and the other dH_2O at 37 °C overnight. Samples were centrifuged at 16,000 x *g* for 15 minutes and supernatant retained as S_2. The pellet was resuspended in 500 µl. All fractions were frozen and stored short term at -20 °C.

2.4 Analysis of PrP^C by Western blot

2.4.1 Protein denaturation and separation by Sodium Dodecyl Sulphate Polyacrylamide gel electrophoresis (SDS-PAGE)

Total protein samples were denatured in 1x NuPage® LDS sample buffer [Invitrogen] and 1 x NuPage® sample reducing agent [Invitrogen] at 70 °C for 15 minutes. Proteins were then separated based on weight by gel electrophoresis at 200V for 40 minutes using NuPage® pre-cast 4-12% bis-tris gels [Invitrogen] in 1 x MES running buffer (MES 50 mM pH 7.2, Tris 50 mM, SDS 0.1%, EDTA 1 mM) [Invitrogen]. SeeBlue Plus2 prestained standard [Invitrogen] and MagicMark XP standard [Invitrogen] were used to estimate the molecular weight of the separated proteins.

For separation of monoglycosylated PrP in wt samples a tris-glycine system was used with a higher acrylamide percentage to increase separation. Total protein samples were denatured in 1x tris-glycine SDS sample buffer [Invitrogen] and 1 x NuPage® sample reducing agent [Invitrogen] at 90 °C for 10 minutes. Proteins were then separated based on weight by gel electrophoresis at 120 V for 30 minutes followed by 150 V for 2.5 hours using Novex® pre-cast 18% tris-glycine gels [Invitrogen] in 1 x tris-glycine running buffer (Tris 24 mM, Glycine 192 mM, SDS 0.1%).

2.4.2 Transfer of proteins to a membrane

Separated proteins were transferred to a polyvinylidene fluoride (PVDF) membrane [Fisher] at 25V for 1 hour using the NuPage® tank transfer system in 1 x NuPage® Transfer buffer (25 mM bicine, 25 mM Bis-Tris (free base), 1 mM EDTA, 0.05mM chlorobutanol) [Invitrogen], 10% methanol and NuPage® antioxidant [Invitrogen].

2.4.3 Coomassie staining of polyacrylamide gel

Coomassie brilliant blue stain was used to visualise proteins remaining on the gel after transfer to assess the efficiency of the transfer. Gels were incubated in coomassie brilliant blue stain (3 mM coomassie brilliant blue R-250, 50% methanol, 41% acetic acid) for 1 hour with agitation. The gel was then incubated for at least 2 hours or overnight if necessary with destain solution (23% ethanol, 7% acetic acid) with a minimum of 6 washes until the gel was clear.

2.4.4 Ponceau S staining of membrane bound proteins

The amount of protein bound to the membrane was visualised using Ponceau S solution to confirm that the transfer had been successful. The membrane was incubated in Ponceau S solution (0.1% Ponceau S, 5% acetic acid) [Sigma Aldrich] for 5 minutes so that protein bands were clearly visible. The membrane was then destained with Tris Buffered Saline with Tween (TBST) [50 mM Tris, 150 mM sodium chloride,1% tween 20; pH 7.5] until it was white again.

2.4.5 Identification of membrane bound proteins by immunodetection

Non-specific binding sites were blocked using 1% blocking solution [Roche Diagnostics] diluted in TBST for 1 hour at room temperature. Membranes were then incubated in primary antibody diluted (Table 2.1) in 0.5% blocking solution [Roche Diagnostics] for either an hour or overnight at room temperature with shaking. When two different antibodies of the same species were used then the primary antibodies were added together. Where two different antibodies of different species were used the membranes were cut at an appropriate marker and the separate pieces of membrane were processed separately. Excess primary antibody was washed off with 2 x 10 minute washes with TBST followed by 2 x 10 minute washes with 0.5% blocking solution. Membranes were incubated in species specific peroxidase conjugated AffiniPure antibodies [Stratech] at 0.05μg/ml diluted in 0.5% blocking solution for 30 minutes at room temperature. Membranes were washed 4 x 15 minutes in TBST to remove excess antibody. Bound secondary antibody was detected by light emission from SuperSignal West Dura Chemiluminescent Substrate [Fisher Scientific] using a Kodak 440 Image station with typical exposures of 1, 5 and 10 minutes. Membranes were also exposed to Lumi-Film Chemiluminescent Detection Film [Roche Diagnostics] and developed manually using developer and fixer [AGFA].

Table 2.1 Antibodies used in western blotting

Antibody	Antigen	Type	Epitope	Conc. (µg/ml)	Source
6H4	PrP	Mouse Monoclonal (IgG1)	aa. 144-152	0.1	Prionics
7A12	PrP	Mouse monoclonal (IgG1)	Conformational epitope	0.1	Gift of M S Sy, Case Western Reserve, USA
8H4	Prp	Mouse Monoclonal (IgG2b)	aa. 145-180	0.1	AbCam
AE11	PrP	Mouse monoclonal (IgG1)	aa. 140-145	0.1	Gifts of S. McCutcheon The Roslin Institute, University of Edinburgh
BC6			aa. 146-156	0.05-0.025	
BH1			aa. 143-154	0.1	
DE3			aa. 146-153	0.1	
EA6			unknown	0.1	
FD12			unknown	0.1	
FH10			aa. 202-210	0.1	
Ab-2	α tubulin	Mouse Monoclonal (IgG1)	aa. 426-450	0.01	Neomarkers
huTfR	Human transferrin receptor	Mouse monoclonal (IgG1)	aa. 3-28	0.2-0.4	Invitrogen
Flotillin	Flotillin-1	Rabbit polyclonal (IgG)	aa. 1-100	0.2	AbCam

2.4.6 Stripping of PVDF membrane

To allow re-probing of the membrane with a different antibody blots were stripped with Restore Western Blot stripping buffer [Thermo Scientific] for 2 x 15 minutes with shaking. Blots were then washed with TBS, TBST and 0.5% blocking solution before

being re-probed with another primary antibody using the same method for immunodetection.

2.4.7 Densitometry

Immunoblots were imaged using the Kodak Image station and Kodak MI software. Protein bands were selected manually by drawing around them and the sum intensity calculated. A blank region was also selected to measure the background intensity of the blot.

2.5 Culturing primary cell lines

All cell culture was carried out under aseptic conditions using a class 2 safety cabinet to prevent microbiological contamination. Cabinets were exposed to ultraviolet light when not in use and were cleaned with 70% ethanol before and after use. Cultures were incubated at 37 °C with 5% CO_2.

2.5.1 Preparation of media

Media was made up in 50ml batches and stored at 4 °C. One millitre of media was pipetted into a sterile culture flask and left in the incubator at 37 °C to check for microbiological contamination.

Neuronal media (1 x B27 serum-free supplement [Invitrogen], 2 mM L-glutamine [Invitrogen], 100 units/ml penicillin [Sigma], 100 µg/ml streptomycin [Sigma], 0.25 µg/ml amphotericin B [Sigma]; in Neurobasl media [Invitrogen]) was prepared for cells to be differentiated into neuronal cultures.

Glial media (1 x G5 supplement [Invitrogen], 2 mM L-glutamine [Invitrogen], 100 units/ml penicillin [Sigma], 100 µg/ml streptomycin [Sigma], 0.25 µg/ml amphotericin B [Sigma]; in Advanced D-MEM/F12 [Invitrogen] with 10% heat-inactivated foetal bovine serum [Invitrogen]) was prepared for cells to be differentiated into glial cultures.

2.5.2 Establishing cell suspensions to create primary cell cultures

Embryos from mice culled at day 17 after plug formation were collected and heads put into sterile Hanks Balanced Salt Solution (HBSS) [Sigma]. Embryo heads were then transferred from the animal facility to the laboratory on ice. Heads were removed from HBSS individually and brains were dissected out using sterile forceps. Brain material was put into fresh HBSS on ice. One skull from each litter was frozen at -20 °C and stored to confirm the genotype, the remaining skulls were discarded. 4-5 Brains were transferred to 1.5 ml TrypLE Express [Invitrogen] and incubated at 37 °C for 15 minutes to dissociate cells. TrypLE Express was removed and brains washed twice with HBSS. 10 ml media was added and cells dissociated into a single cell suspension by pipetting gently until the media was cloudy. Suspensions were left for 2 minutes to allow large debris to settle prior to cell counting.

Cell suspensions were used initially to create direct primary cell cultures but the method proved to be unreliable for neuronal cultures and cells would often not differentiate into neurons. Neurospheres were generated to create neuronal precursor cells that were dividing, which could then be further differentiated into neuronal cultures.

2.5.3 Establishing primary cell cultures directly

10 µl cell suspension was diluted 1:10 with fresh media and then 1:2 with trypan blue [Sigma]. Cells were counted under a light microscope using a haemocytometer and the number of live cells present per ml was calculated.

Sterile tissue culture plastics were pre-coated with poly-D-lysine hydrobromide [Sigma] and allowed to dry under a UV light overnight. Cell suspension was added so that there were 150,000 cells per well in 24 well plates or 6 million cells in a 10 cm culture dish. Media was added so that each well of a 24 well plate contains 500 µl in total and 10 ml total in a 10 cm dish.

2.5.4 Generation of Neurospheres

2 or 4 ml cell suspension was transferred into 25 cm tissue culture flasks [Fisher] and neuronal media with 10 nM epidermal growth factor (EGF) [Invitrogen] and 10 nM fibroblast growth factor basic (FGFb) [Invitrogen] added to make total volume up to 10 ml. Cultures were incubated for 3 days before media was transferred to a fresh flask to remove debris and adherent cells which had stuck to the plastic. Cultures were incubated for a further 2 days to allow neurospheres to form.

Once neurospheres were formed media was changed every 3-4 days by centrifuging cells at 2000 x *g* for 2 minutes then removing supernatant and re-suspending pelleted cells in 10 ml fresh media with EGF and FGF. Once neurospheres were too big, usually after 7-10 days, they started to adhere to the flask and differentiate. When a lot of large neurospheres were present they were incubated at 37 °C with TrypLe Express [Invitrogen] for 2 minutes then transferred to fresh media with EGF and FGF. Neurospheres were broken up into smaller neurospheres by gentle pipetting before being returned to flasks.

2.5.5 Freezing and storing cells

Neurospheres were broken up into small neurospheres before being frozen down to increase cell viability. Neurospheres were incubated at 37 °C with TrypLe Express for 2 minutes and transferred to freezing media (20% dimethyl sulphoxide (DMSO) in neurobasal media without growth factors). Cells were pipetted to dissociate large neurospheres and then frozen at -70 °C for 24 hours. Cells were stored at -150 °C long term.

2.5.6 Differentiating cells from neurospheres

One millitre culture containing neurospheres was removed from the flasks and incubated at 37 °C with TrypLE Express for 5 minutes. Neurospheres were put in fresh neuronal media and broken up into a single cell suspension. The cell suspension was

split into 24 well plates that were pre-treated with either 1% gelatine or poly-ornithine to help the cells to adhere to the plastic.

To differentiate the cells into neuronal cultures the EGF was removed from the media so that cells were cultured with neuronal media only containing FGF. Cultures were left for 5 days before they were checked for differentiation. Differentiation was monitored by looking at cell morphology.

2.6 Immunocytochemistry (ICC) on cultured cells

Media was removed from differentiated cells and cells were washed twice with Dulbeccos phosphate buffered saline (DPBS)[Invitrogen]. Cells were treated in fixative (4% paraformaldehyde and 0.25% gluteraldehyde in PBS) for 10 minutes at room temperature. Once cells were fixed they were removed from the safety cabinet and the rest of the protocol was carried out on the bench. The fixative was removed and excess washed off with 3 x 5 minute washes with PBS. Membranes were permeabilised with either 0.1% triton X-100 or 0.1% Saponin [Sigma] for 1 hour then rinsed 3 x 5 minutes with PBS. Non-specific binding sites were blocked with 3% BSA/PBS for 30 minutes. Cells were incubated in primary antibody (Table 2.2) in a humidified chamber for 1 hour. Excess antibody was washed off with 3 x 5 minutes with PBS before cells were incubated in species specific Alexafluor conjugated antibody [Invitrogen] for 1 hour. Excess antibody was washed off with 3 x 5 minute washes with PBS. DAPI was used as a nuclear counter stain for cells to identify cell bodies. Cells were incubated in DAPI (diluted 1:50,000 in dH_2O) for 5 minutes then washed twice with ultrapure water. Coverslips were allowed to air dry then were mounted onto glass slides using Vectashield hard-set mounting media for fluorescence [Vector labs]. Slides were stored at 4 °C in the dark for up to 2 months.

2.6.1 Confocal Imaging

Slides were imaged using a LSM 5 confocal microscope [Zeiss] with lasers at 405, 488 and 564nm. For PrP staining Null cells were used to set the laser strength in order to

reduce background fluorescence. The same microscope configuration was then used for all of the other genotypes to allow comparison between the genotypes. Images were captured using LSM imaging software [Zeiss]. A single image was captured by taking the mean values of 5 frame scans and a false colour was added. Images of the same section were overlayed using the LSM software to allow co-localisation of markers to be assessed.

Table 2.2 Antibodies used in ICC

Antibody	Antigen	Type	Epitope	Conc. (µg/ml)	Source
6H4	PrP	Mouse Monoclonal (IgG1)	aa. 147-155	0.1	Prionics
8H4	PrP	Mouse Monoclonal (IgG2b)	aa. 145-180	0.1	
BC6	PrP	Mouse monoclonal (IgG1)	aa. 146-156	0.05-0.025	Gift of S. McCutcheon The Roslin Institute, University of Edinburgh
BH1	PrP	Mouse monoclonal (IgG1)	aa. 143-154	1	
F4-31	PrP	Mouse monoclonal (IgG)	Bovine seq 101-241	0.1	Gift of S. Prusiner
GABA	GABA	Mouse monoclonal (IgG1)	Full length native protein	0.02	Abcam
GFAP	GFAP	Rabbit polyclonal	Full length native protein	0.1	Abcam
GS	Glutamine synthase	Rabbit monoclonal	-	0.1	Gift of S. Godsave NKI, Amsterdam
Iba1	Iba-1	Goat polyclonal (whole sera)	135-147 of Human Iba1	0.5	Abcam
MAP2	MAP2a + MAP2b	Mouse Monoclonal (IgG1)	Full length native protein	5	Abcam
VAMP2	VAMP2	Rabbit polyclonal	aa. 1-18 rat VAMP2	0.2	Abcam

2.7 Cryo-immunogold electron microscopy

Electron microscopy was performed in collaboration with Sue Godsave and Peter Peters (Netherlands Cancer Institute, Amsterdam). Cells were grown and fixed in Edinburgh then sent to Amsterdam for sectioning and electron microscopy.

2.7.1 Preparation of cells for electron microscopy

Primary neurons were grown on 10 cm tissue culture dishes at ~70% confluence, as described previously. Culture medium was replaced with 5 ml fresh media the day before fixation. Cultures were fixed in duplicate; one with just paraformaldehyde (PFA) and another with PFA and gluteraldehyde. 5 ml either PFA fixative (4 % PFA, 120 mM PIPES, 50 mM HEPES, 4 mM $MgCl_2$, 20 mM EGTA) or PFA/gluteraldehyde fixative (4% PFA, 0.4% gluteraldehyde, 120 mM PIPES, 50 mM HEPES, 4 mM $MgCl_2$, 20 mM EGTA) was added to each culture dish, without removing media. PFA fixative was left on the cultures for 24 hours while PFA/gluteraldehyde fixative was left on cultures for 2 hours. Fixative was removed and cells were washed twice with PBS+ (0.15 M glycine in PBS). Cells were coated in 3 ml 0.1% gelatine in PBS to protect membranes and cells were scraped off gently using a rubber cell scraper. The cells were pelleted by centrifugation at 3,000 x *g* for 3 minutes and washed twice in PBS to remove the gelatin. Cells were resuspended in 1 ml storage solution (0.5% PFA, 60 mM PIPES, 25 mM HEPES, 2 mM $MgCl_2$, 10 mM EGTA) then the tube was filled to the top to prevent the cells from drying out during transport.

Cells were mailed to Amsterdam in an airtight tube inside a polystyrene box at room temperature. Cells that have been frozen cannot be used for cryo electron microscopy so a temperature probe was included to monitor whether the cells were frozen during transport.

2.7.2 Cryosectioning

Blocks of cells were embedded in gelatin and frozen in LN_2. Sections were then cut on a cryotome. Semi-thin sections (200 nm) for light microscopy were picked up from the diamond knife and mounted onto a slide with 2.3 M sucrose. Ultra-thin sections (60 nm) were picked up from the diamond knife with 1% methyl cellulose 25cP in a 1.15 M sucrose solution and transferred to formvar/carbon-coated copper grids (hexagonal grid bars, spaced 200 μm across). Slides were stored at -20 °C until ready to be labelled.

2.7.3 Semi-thin fluorescent sections

8 semi-thin sections of the same genotype were mounted on each slide. 100 µl liquid was dropped on each section without covering another section so that multiple antibody combinations could be used on a single slide. Non-specific binding sites were blocked with 1% BSA in PBS with 0.02% glycine (PBS-G) for 15 minutes. Sections were incubated in primary antibody (Table 2.2) for 30 minutes. Excess antibody was washed off with 3 x 5 minute washes with PBS-G before being incubated with species specific secondary antibody conjugated to a fluorochrome dye. Excess antibody was washed off with 3 x 5 minute washes with PBS. DAPI was used as a nuclear counter stain for cells to identify cell bodies. Coverslips were mounted over sections using Vectashield mounting media for fluorescence [Vector Labs].

Sections were examined using a Zeiss Axiovert 100 TV inverted microscope. Micrographs were taken using a Photometrics Series 200 Black and White CCD camera with SmartCapture2 software, which adds false colours to the images.

2.7.4 Ultra-thin sections

Gelatin was removed from the grids by heating to 37 °C for 30 minutes on 2% gelatin plates. Grids were washed 5 x 2 minutes in PBS-G to remove any remaining gelatin. Grids were incubated with 1% BSA in PBS-G for 3 minutes to block any non-specific binding sites. Sections were then incubated with primary antibody (F4-31; diluted 1:100 in 1% BSA in PBS) for 1 hour. Excess antibody was washed off 3 x 5 minutes with PBS-G. A rabbit anti mouse bridging antibody [Pierce] was used so that the protein A-gold conjugate would be able to bind. Grids were incubated with the bridging antibody for 30 minutes then excess washed off 5 x 2 minutes with 0.1% BSA in PBS-G. Grids were blocked with 0.1% BSA in PBS-G before being incubated with Protein A conjugated to 10 nm gold particles [Utrecht Meedical Centre] in 1% BSA in PBS for 20 minutes. Excess antibody was washed off with 6 x 3 minutes washes with PBS. Sections were then fixed onto the grids with 1% gluteraldehyde in PBS for 5 minutes. Grids were washed 10 x 2 minutes with distilled water. In order to visualise the cells

and their organelles the grids were negatively stained with uranylacetate/ methylcellulose (pH4) for 5 minutes. The uranylacetate/ methylcellulose was removed by picking up the grid with a 6 mm wire loop and dragging it across thick filter paper until only a 1/3 was left as a fine coating. Grids were left to dry in the loops before being removed and viewed under the electron microscope. Labeled grids were examined using a Tecnai 12 G2 electron microscope [FEI] at 80 kV.

2.7.5 Quantification of gold labelling

Quantification of labelling was performed on areas selected by systematic random sampling. Starting close to a grid bar micrographs were taken at regular intervals from each block. PrP null cells were included as a control to look for non-specific labelling. Micrographs with a final magnification of 11,000 were taken from two cell blocks per genotype, and both were found to give similar results.

Gold particles labelling different structures were counted on micrographs. A structure was considered to be labelled if a gold particle was located within 20 nm. Ultrastructural features were used to distinguish between nuclei, mitochondria, Golgi apparatus (cisternae and vesicles) plasma membranes and internal membranes. For some internal membranes it was not possible to identify the structure due to the plane of sectioning so these were assigned to ‘other internal’.

The total lengths of each type of membrane (e.g. axonal plasma membrane or Golgi) were estimated by counting all intersections of each membrane type with grid lines 1.2 cm apart placed over the micrograph. Labelling density was measured using the following formula.

$$\text{Labelling density} = \text{gold}/(\text{grid intersections} * \text{distance between grid lines})$$

2.8 Quaking induced conversion assay (QuIC)

2.8.1 PrPSc seed preparation

10% brain homogenate was prepared in lysis buffer from TSE clinically and pathologically positive mice and treated with PK to remove PrP^{C}. Samples from all genotypes were then run on an immunoblot and PrP^{Sc} measured by densitometry. Samples were diluted with lysis buffer to the same concentration as the lowest genotype. Serial dilutions (1:10) were prepared by diluting brain homogenate in N2 media supplement.

2.8.2 Real-time QuIC reaction

All reagents were made fresh on the day of use and were filtered through a 0.2 µm filter prior to use. Frozen recombinant PrP was thawed on ice and filtered through a 0.2 µm filter and then concentration measured on a NanoDrop. 98 µl reaction mixture (0.1 mg/ml recombinant PrP, 300 mM NaCl, 1 mM EDTA, 0.01 mM thioflavin T in PBS) was added to each well of a 96 well optical bottom plate. 2 µl seed was added to each well and mixed by pipetting. The reaction was carried out on a double orbital plate reader [Fluoroskan, Omega] preheated to 42 °C. The shaking program was alternating 700 rpm double orbital for 1 minute with no shaking for 1 minute. Fluorescence was measured (excitation at 450 nm and emission 480 nm) every 15 minutes within a shaking kinetic cycle for 60 hours at 42 °C.

Each seed was carried out in 4-10 replicates per plate. All controls were included in quadruplet for each plate; positive control of a known positive seed, negative controls of normal brain homogenate from an uninfected animal and a recombinant PrP only (N2 supplement [Invitrogen] used as a seed).

Results were analysed using Mars data analysis software [BMG Labtech] and exported to an excel spreadsheet.

3 Expression of PrP^C in the brain

3.1 Aims

This chapter aims to measure the levels of PrP^C, in whole brain and different brain regions in order to identify whether disruption of one or both glycosylation site(s) alters PrP^C levels. Proteolytic processing may affect the overall levels of PrP therefore the level of alpha cleavage will be assessed. Individual glycoforms may possess separate functions therefore this chapter will also characterise the ratios of glycoforms to assess the influence of glycosylation at one site on the glycosylation of the other in order to establish whether a particular glycoform is favoured.

3.2 Introduction

Prnp mRNA is constitutively and highly expressed in the central nervous system (Manson et al., 1992). Studies using IHC have shown that PrP^C levels did not always correspond with mRNA levels (Manson et al., 1992, Ford et al., 2002a). An absence of protein was seen in some mRNA positive neurons whilst other neurons showed low levels of mRNA but substantial amounts of protein. This could represent a high degree of post-translational regulation of PrP^C. Glycosylation is a post-translational modification which can influence the cell biology of a protein through several mechanisms. The addition or removal of carbohydrates to a protein can have consequences for the stability of that protein and interactions with other proteins, which in turn can affect the turnover, and the overall levels. This chapter will assess whether the different GlycoD mice have differing levels PrP^C within the brain in order to understand the influence of glycosylation on the post translational regulation of PrP.

Previous characterisation of the expression of PrP^C in the GlycoD mice showed that there was a reduction of PrP by immunoblot, indicating that the glycosylation may assist in preventing degradation (Cancellotti et al., 2005). However, when quantified using the dissociation enhanced lanthanide fluoroimmunoassay (DELFIA) there was no significant difference in PrP^C levels between the GlycoD mice (Cancellotti et al., 2005).

This method showed that levels of PrP varied greatly depending upon the antibody pairs used [F. Wiseman; PhD thesis 2007]. A 10-fold reduction of PrP was observed with FH11, an N-terminal antibody that does not recognise cleaved isoforms in comparison to an antibody that recognises all cleavage products. FH11 was used as a capture antibody with two different detection antibodies; there was no significant difference between genotypes for one and a huge variability for the second, which also showed variability between wild type mice and the control line. This variability between the two pairs was likely caused by the low levels of PrP detected and may represent a limitation to DELFIA quantification.

In order to determine the total levels of PrP^C in the GlycoD mice PrP^C will be detected on immunoblot and the amount of PrP for each mouse will be compared to the levels in wild type mice. Several different antibodies with different epitopes will be assessed to ensure that the most appropriate antibody is used to measure PrP levels and that all isoforms are detected.

PrP^C naturally undergoes proteolytic cleavage *in vivo* and has been observed in several species. The glycans are some distance from the major cleavage site and are unlikely to shield the N-terminal but they may prevent proteolytic enzymes from interacting with PrP easily. A change in cleavage levels may influence the degradation and consequently the overall level of protein. It has recently been shown for ovine PrP^C that the level of alpha cleavage fragment in brain can vary with the amino acid present at 171 which is quite far from the cleavage site at 115 (Campbell et al., 2013). This supports the notion that the glycosylation sites could have an influence on cleavage. This chapter will investigate the level of alpha cleavage in the GlycoD mutants to establish whether the glycans can affect the proteolytic cleavage.

Alpha cleavage will be assessed at the same time as total protein levels by measuring the levels of one of the truncated fragments produced during alpha cleavage, C1, in brain homogenates. The N1 fragment is a soluble secreted protein and difficult to detect, however the C1 is membrane bound and all glycoforms can be detected on an immunoblot. The diglycosylated C1 fragment has a similar molecular weight to

unglycosylated full length PrP therefore all homogenates will be treated will the endoglycosidase, PNGase F to remove the glycans and render the PrP into unglycosylated isoforms which can easily be distinguished on an immunoblot.

It has been shown that there are differing levels of PrP^C protein in different brain regions in hamsters and mice (Benvegnu et al., 2010). The CNS consists of many neuronal subtypes which can be characterised by morphology or by the neurotransmitters expressed. Neurons in different brain regions are very diverse in order to carry out different functions and to interact with various other neurons. The difference in regional PrP may be due to the different cell types within the brain that express varying levels of PrP^C (Ford et al., 2002a). Glial cells have little or no detectable PrP^C and neuronal subtypes express varying levels of PrP^C. It has been proposed that different glycoforms are more abundant in different brain regions. Diglycosylated PrP was more predominant in the cortex, hippocampus, olfactory bulb and part of the cerebellum (Beringue et al., 2003, DeArmond et al., 1999). It is therefore possible that different neuronal cell sub-types may have different levels of total PrP^C or different ratios of glycoforms to satisfy the various functions of the cells.

This chapter will address whether certain isoforms are preferentially expressed in different brain regions using the GlycoD mice. This study will isolate brain regions through microdissection and PrP^C will be detected by immunoblot. PrP^C detection by IHC would allow the expression in different cell types to be assessed, however detection of PrP^C is difficult and low levels of PrP can make comparison of brain areas challenging, causing artefactual differences.

In addition to alpha cleavage, two other major cleavage events have been identified for PrP^C in brain to date; ectodomain shedding, alpha and beta cleavage (reviewed in (Liang and Kong, 2012, Altmeppen et al., 2012)). Enhanced beta cleavage is associated with TSE disease and is rarely observed in healthy animals (Chen et al., 1995). Beta cleavage occurs at the cell surface in response to reactive oxygen species (ROS) (McMahon et al., 2001). PrP^C has been implicated in neuroprotection against oxidative stress therefore an increased level of beta cleavage in the GlycoD mutants could indicate that these mice

have a higher level of oxidative stress and that glycosylation is important for the role of PrP^C in neuroprotection. Deglycosylation removes all of the glycoforms to leave unglycosylated isoform allowing the different truncated fragments to be identified. The C2 fragment will be identified and assessed to investigate whether it increases in the GlycoD mice.

PrP^C is anchored at the membrane and many of the proposed functions rely upon the membrane localisation, such as signal transduction. This chapter will confirm that PrP^C from the GlycoD mice is GPI anchored and that the mutations introduced do not prevent GPI attachment. Soluble full length PrP has been identified both *in vitro* and *in vivo* (Zhao et al., 2006). The significance of soluble PrP is not known, full length secreted PrP may represent an alternative degradation mechanism or may possess a unique function. There are two mechanisms of shedding PrP^C from the cell surface; cleavage at the GPI anchor possibly by phospholipases and cleavage close to the GPI anchor by metalloproteinases from the ADAM family (Parkin et al., 2004). The reduced total PrP in the GlycoD mice from might be due to increased ectodomain shedding leading to more rapid degradation. This chapter will isolate soluble proteins from membrane bound proteins to determine the amount of naturally cleaved, full length PrP shed from the cell in order to determine whether the glycans influence cleavage at the GPI anchor.

This chapter will identify the levels of both total and truncated PrP^C in the GlycoD mutants for whole brain and different brain regions in order to understand whether the glycosylation has a post-translational effect on protein levels.

3.3 Results

3.3.1 Microdissection of brain regions

Frozen brains from GlycoD mutants and wild type mice were dissected into 7 different regions; cerebellum, brain stem, dorsal raphe, hippocampus, cortex, thalamus and septum. These brain regions were selected as they represent different brain regions that can be targeted by different strains of TSE. Brain weights for the individual regions

were consistent between mice (Table 3.1) showing that microdissection is a reliable method for isolating brain regions (Barr et al., 2004).

Table 3.1 Weight and total protein concentrations of dissected brain regions (n=9 mice)

Brain region		Mean weight (mg)	sem	Mean protein (g/ml)	sem
Cerebellum	A	43.6	3.48	0.64	1.73
Brain Stem	B	23.9	2.45	0.05	1.62
Dorsal Raphe	C	10.6	2.95	0.65	0.61
Hippocampus	D	9.20	4.07	0.88	0.45
Cortex	E	22.3	3.85	0.63	0.92
Thalamus	F	13.6	3.98	0.46	0.97
Septum	G	10.5	3.88	0.88	0.65

Total protein levels for 10% w/v homogenates of each brain region were measured using the bicinchoninic acid (BCA) assay. There was no significant difference in protein levels between the brain regions.

3.3.2 Densitometry

Densitometry of immunoblots was carried out according to section 2.4.7 in Chapter 2. To assess the reproducibility of manually selecting the regions, densitometry was carried out on the same blot on several non-consecutive days (Figure 3.1). The maximum variability was 5% on repeated measurements of the same sample. Very little blot to blot variation was identified, showing that immunoblotting and manual densitometry is a reliable method for quantifying PrP^{C}.

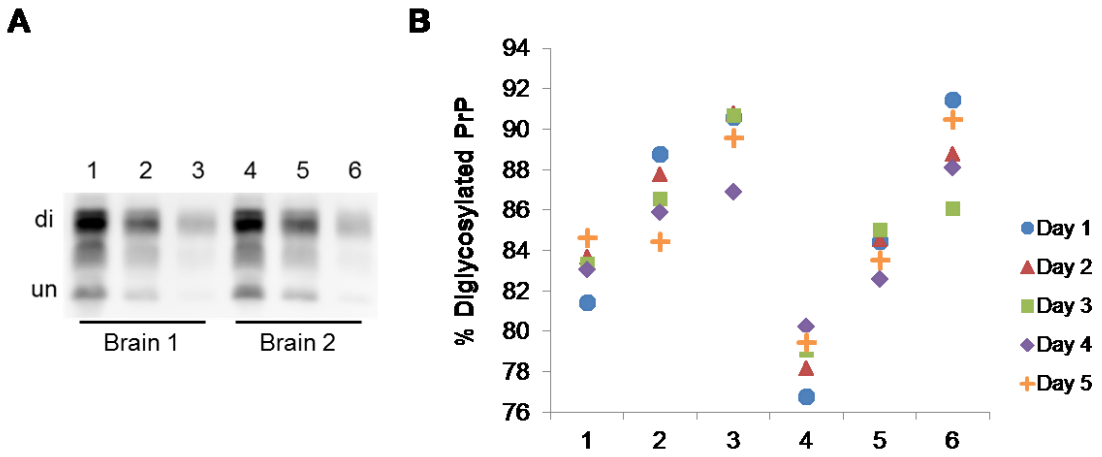

Figure 3.1 Variability of manually selecting bands for densitometry
Densitometry of the di and unglycosylated PrP bands was carried out on 5 non-consecutive days on the same immunoblot. (A) Lanes 1-3: a single wild type PrP homogenate at 10%, 5% and 2.5% w/v respectively. Lanes 5-6: a different homogenate at 10%, 5% and 2.5% v/w respectively. (B) Densitometry was carried out on diglycosylated and unglycosylated bands and the % diglycosylated PrP was calculated for each lane. A maximum difference of 5% was seen for each repeated measurement.

3.3.3 Monoclonal anti-PrP antibody screen

Some monoclonal antibodies used to detect PrP can have striking differences in the specificity for the glycoforms and truncated isoforms (Beringue et al., 2003) therefore it is essential to ensure an antibody chosen recognises all known isoforms. A range of antibodies with different epitopes were tested on immunoblots to assess whether the antibodies bind equally to all known isoforms or preferentially bind to a particular isoform. Epitopes of the antibodies chosen for this study are shown in Figure 3.2.

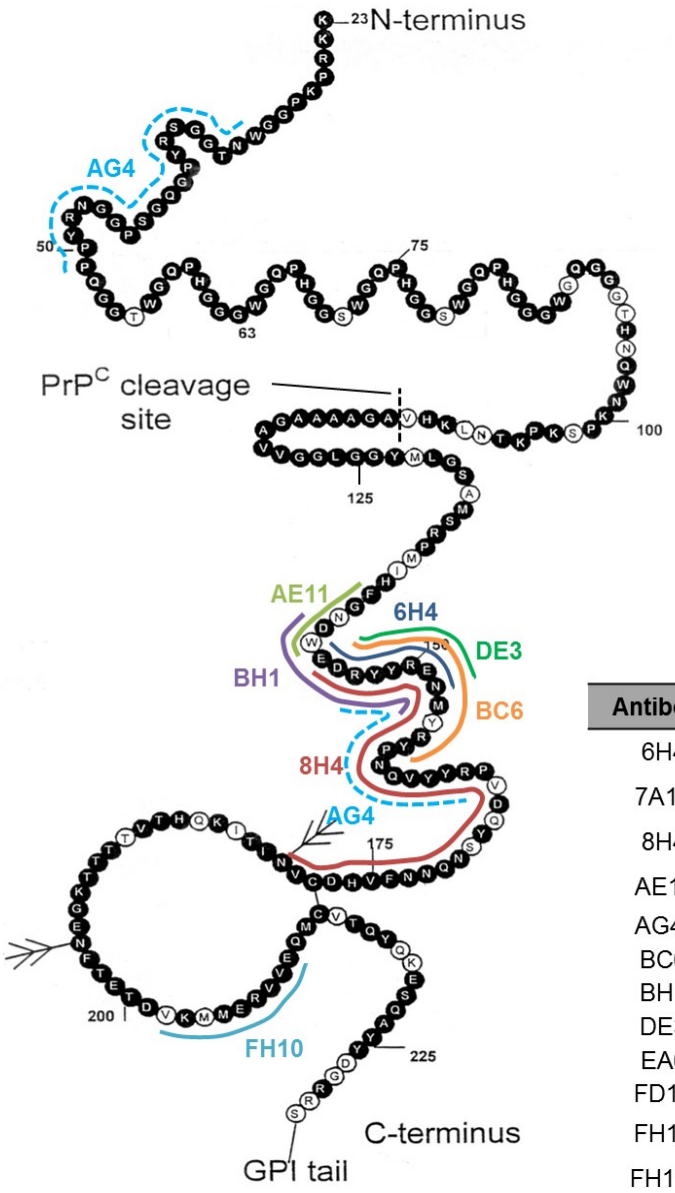

Antibody	Epitope
6H4	144-152
7A12	Conformational
8H4	145-180
AE11	140-145
AG4*	31-51 and 147-163
BC6	146-156
BH1	143-154
DE3	146-153
EA6	unknown
FD12	unknown
FH10	202-210
FH11*	N terminal

* Used for previous DELFIA analysis

Figure 3.2 Epitope map for the monoclonal antibodies used to detect PrP
PrP showing the location of the epitopes for the antibodies used to assess binding efficiency to the different glycoforms. The antibodies with an unmapped epitope (7A12, EA6 and FD12) recognise C1 fragments so have an epitope on the C-terminal between residues 111-230. Antibodies AG4 and FH11 were not used on immunoblots but were used as capture antibodies for previous DELFIA quantification [F. Wiseman; PhD thesis 2007].

Immunoblots were carried out on at least three different mouse brains of each genotype in duplicate, to account for mouse to mouse and blot to blot variation. All of the antibodies tested showed expected PrP profiles with binding to all isoforms (Figure 3.3).

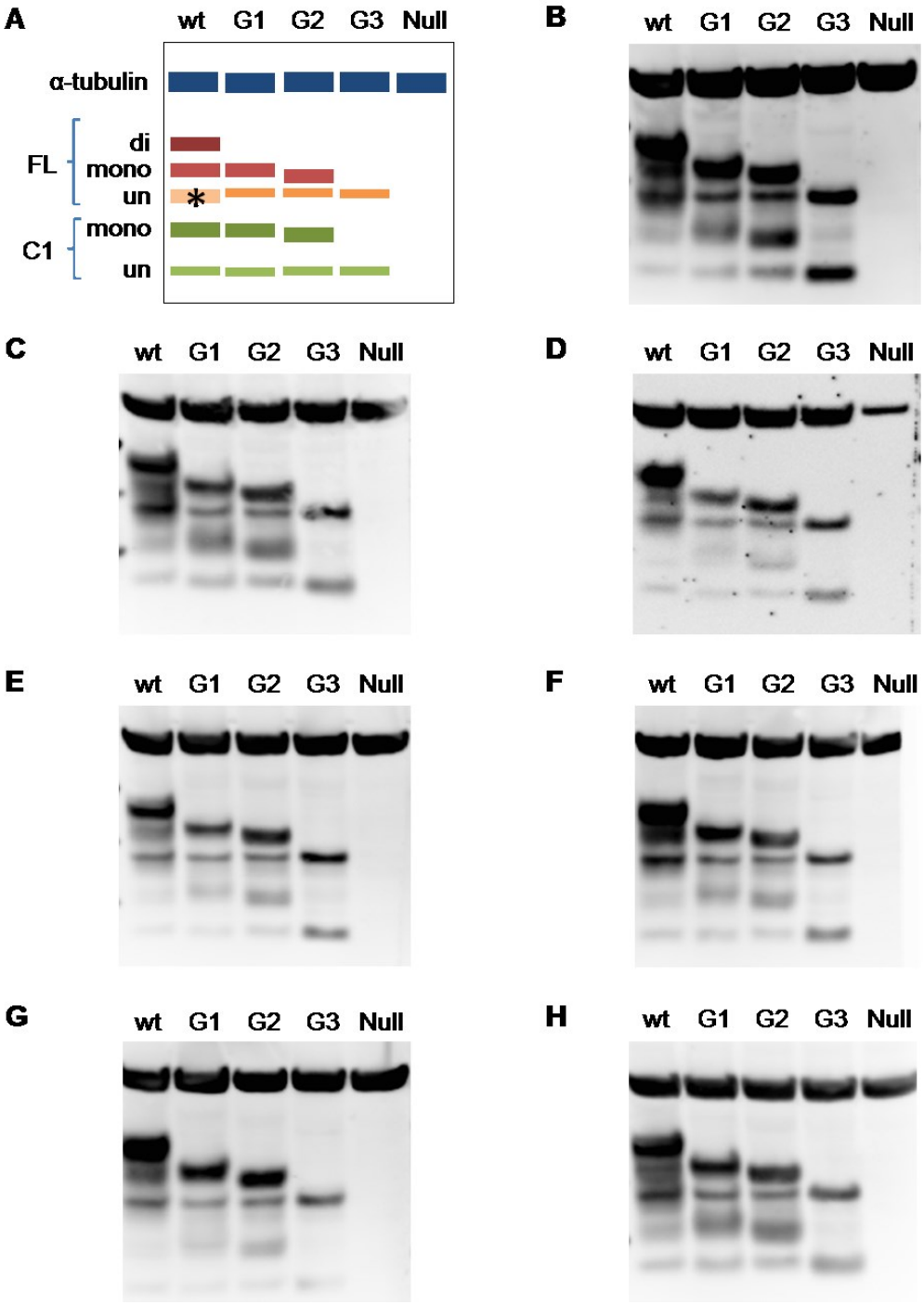

Figure 3.3 Immunoblots with different PrP antibodies
(A) Diagram showing the expected band pattern on an immunoblot produced by the different isoforms of PrP^{C} for each GlycoD mutant. The unglycosylated band in wild type mice, denoted by a star also contains the diglycosylated C1 fragment. (B-H) Immunoblots with 6 µg of 10% brain homogenate loaded per well and probed with different mAbs (B) 7A12 (C) DE3 (D) FH10 (E) AE11 (F) BC6 (G) FD12 and (H) BH1. All primary antibodies were probed at concentrations noted in Table 2.1 (Chapter 2).

Densitometry of the immunoblots in Figure 3.3 was carried out to measure the total PrP levels of each GlycoD mouse and compare it to wild type mice. All glycoforms of full length (FL) and C1 were included for each genotype. There was no significant difference in total PrP between the antibodies used suggesting that glycosylation does not influence the epitope binding of the antibodies tested. The different antibodies bind to all of the glycoforms with a similar affinity, suggesting that none of the antibodies are preferentially binding an isoform (Figure 3.4).

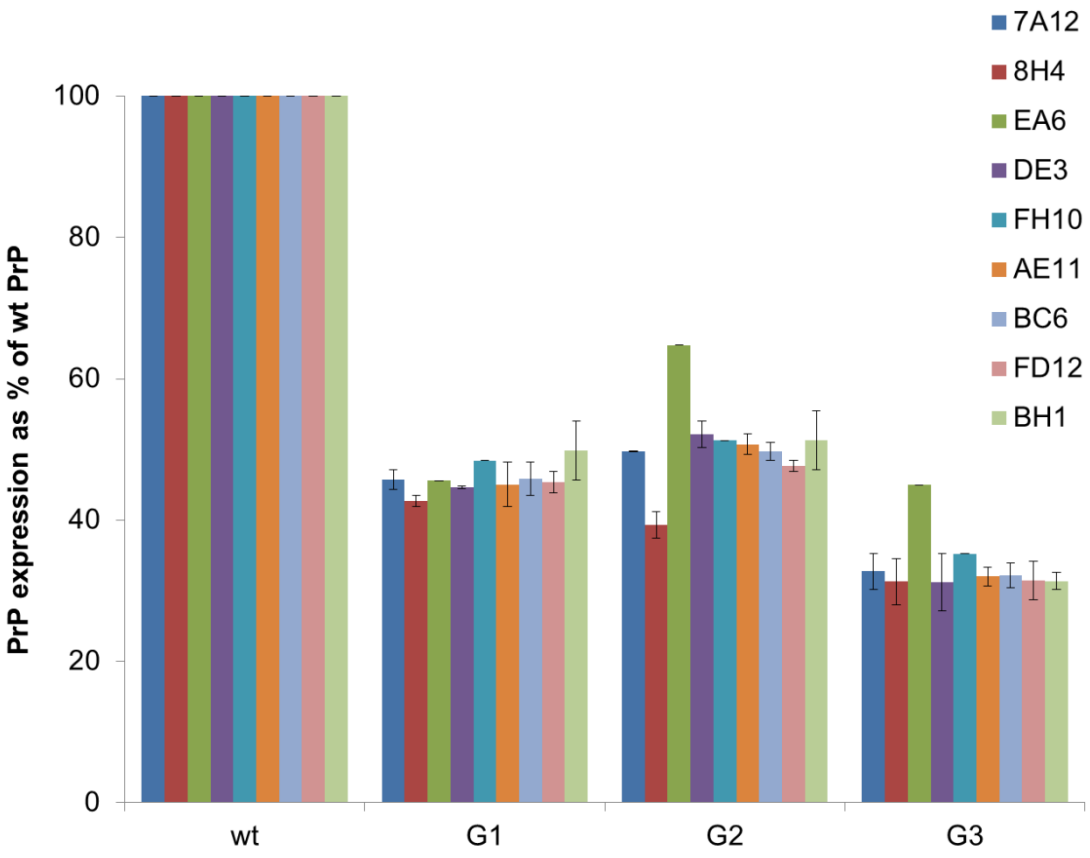

Figure 3.4. Assessment of anti PrP antibodies at detecting the glycoforms
Densitometry from western blots was used to measure the levels of PrP^C in the PrP glycosylation deficient mice in relation to the level of wild type PrP^C. A range of anti-PrP antibodies with different epitopes were used to assess whether any had a higher binding preference for a particular isoform or whether they bound all glycoforms equally. Each antibody was tested in duplicate on 3 different brains from a genotype. Monoclonal antibody EA6 was only carried out on a single immunoblot. There was no significant difference between the antibodies used for any of the glycoforms (ANOVA), suggesting that the carbohydrates are not involved in epitope recognition and all of the antibodies bind the glycoforms with equal affinity.

The consistency in expression levels with different antibodies allowed a single antibody to be used to analyse the PrP levels for the rest of the brain regions. The antibody BC6 was chosen to detect PrP^C for further experiments due to its high sensitivity as determined by antibody titrations carried out during optimisation.

3.3.4 Degradation of PrP^C

To allow C1 to be measured at the same time as total PrP all genotypes were treated with PNGase F to remove the glycans. C1 is not always observed or detected without deglycosylation treatment and may represent a degradation product or an artefact produced by PNGase treatment. Conditions used to deglycosylate PrP may increase natural degradation of the protein, increasing C1 levels.

A single homogenate was aliquoted and incubated with PNGase for different lengths of time to assess whether there was a steady state of C1 or whether it increased with time, indicating degradation. G3 mice were used as they do not have any glycans to remove and C1 levels can be compared with and without PNGase at the same time.

C1 calculated in PNGase treated samples accounted for around 60% of total PrP and did not increase with the length of incubation period at 37 °C, suggesting that C1 is not a degradation product (Figure 3.5). There was no difference between PNGase treated and untreated samples thus PNGase does not influence the degradation or levels of C1 observed.

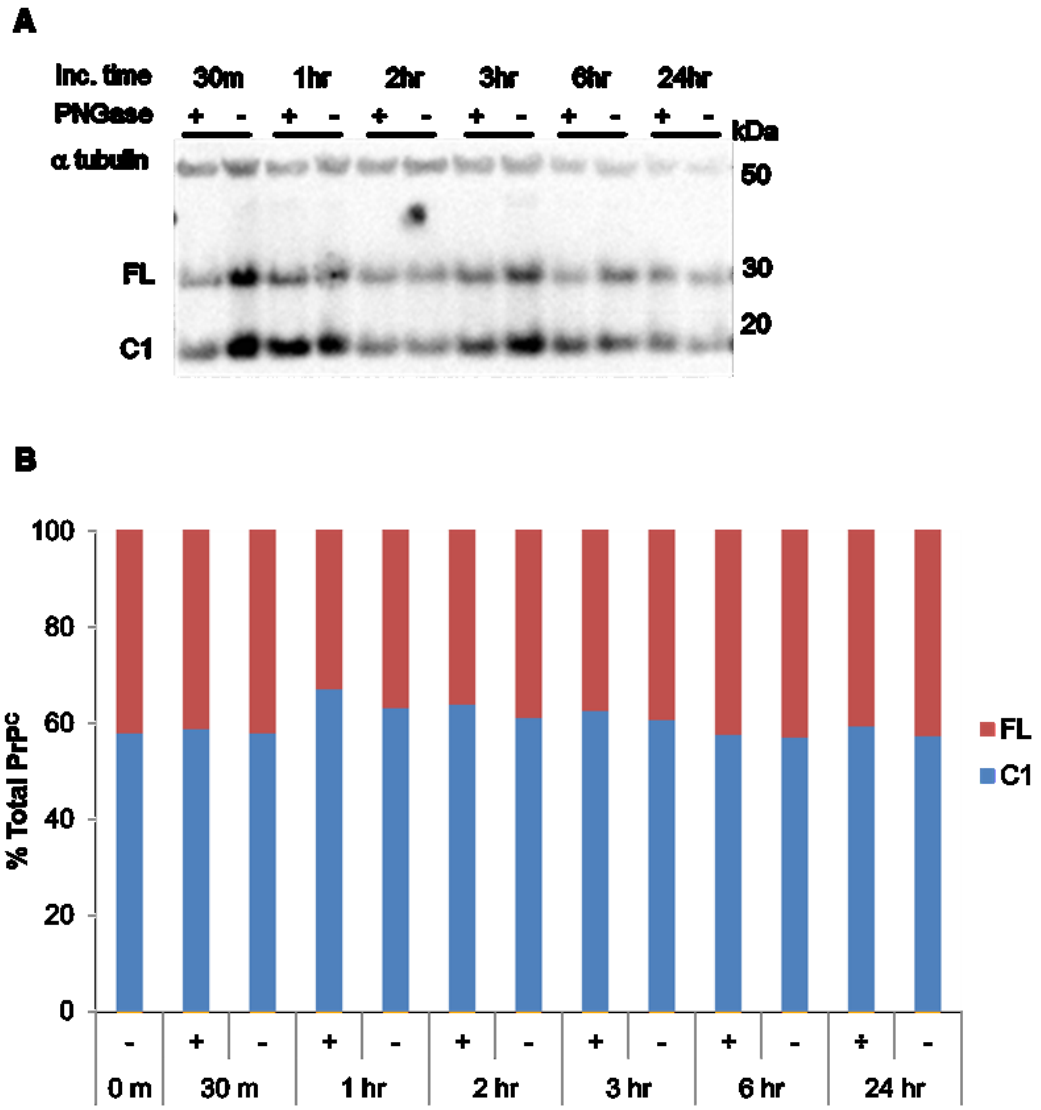

Figure 3.5 C1 levels do not increase with prolonged PNGase F treatment
(A) Immunoblot of PNGase deglycosylated PrP^C and undigested PrP^C in wild type 10% brain homogenate (20 µl sample and 1500 U of PNGase F) treated for different lengths of time. (B) Percentages of full length and C1 isoforms were calculated by densitometry for each time point.

3.3.5 Total PrPC levels in PrP GlycoD mice

To identify whether the change in glycosylation alters the overall expression of PrP^C, protein levels were measured in whole brain of the PrP glycosylation deficient mutants and wild type mice. PrP^C from brains were analysed by immunoblot and densitometry was carried out to quantify the amount of PrP relative to the wild type mice. Although densitometry on immunoblots is only semi-quantitative this method was chosen due to the ability to separate all of the isoforms so that they can be visually distinguished and

individually measured. An α tubulin loading control was used to determine the variation in amount of protein loaded onto the immunoblot and used to adjust the PrP levels accordingly.

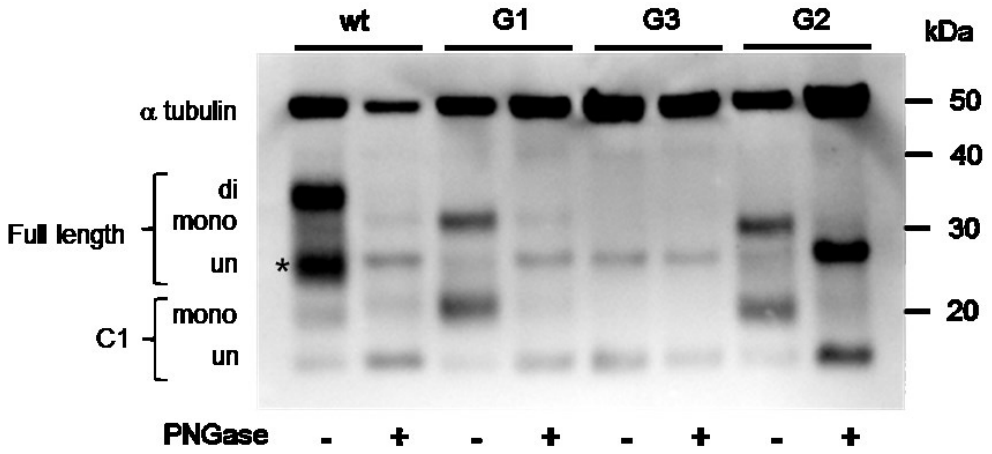

Figure 3.6 PrP from wild type and GlycoD mice detected on an immunoblot
10% brain homogenates were treated with PNGase F at 37°C overnight. PNGase F was used to de-glycosylate PrP^C to obtain two distinct bands of full length and C1 isoforms that could be measured easily. Treated and untreated homogenates were run on an immunoblot and PrP detected with anti-PrP mAB BC6 at 0.01 mg/ml. A protein loading control, α-tubulin (50 kDa) was included. PNGase treated homogenates show just the unglycosylated full length and C1 PrP. There is visibly less PrP in the GlycoD mutants.

The immunoblots showed the expected banding patterns for each of the mutants (Figure 3.6). As had been previously observed the two monoglycosylated PrP isoforms run at slightly different mobilities depending upon the glycosylation site occupied [F. Wiseman; PhD thesis 2007]. A doublet at the monoglycosylated band was also observed in TSE infected animals (Somerville, 1999) and has been postulated to correspond to glycosylation site occupancy. The major glycans attached to PrP^C are present at both sites however some larger tetra-antennary structures were only present at the second site (Stimson et al., 1999), therefore the monoglycosylated PrP in G1 mice with only the second site occupied had a slightly heavier molecular weight than the monoglycosylated G2.

Truncated PrP, designated C1 was seen for all of the mutants; both full length and C1 were included in the measurements for total PrP.

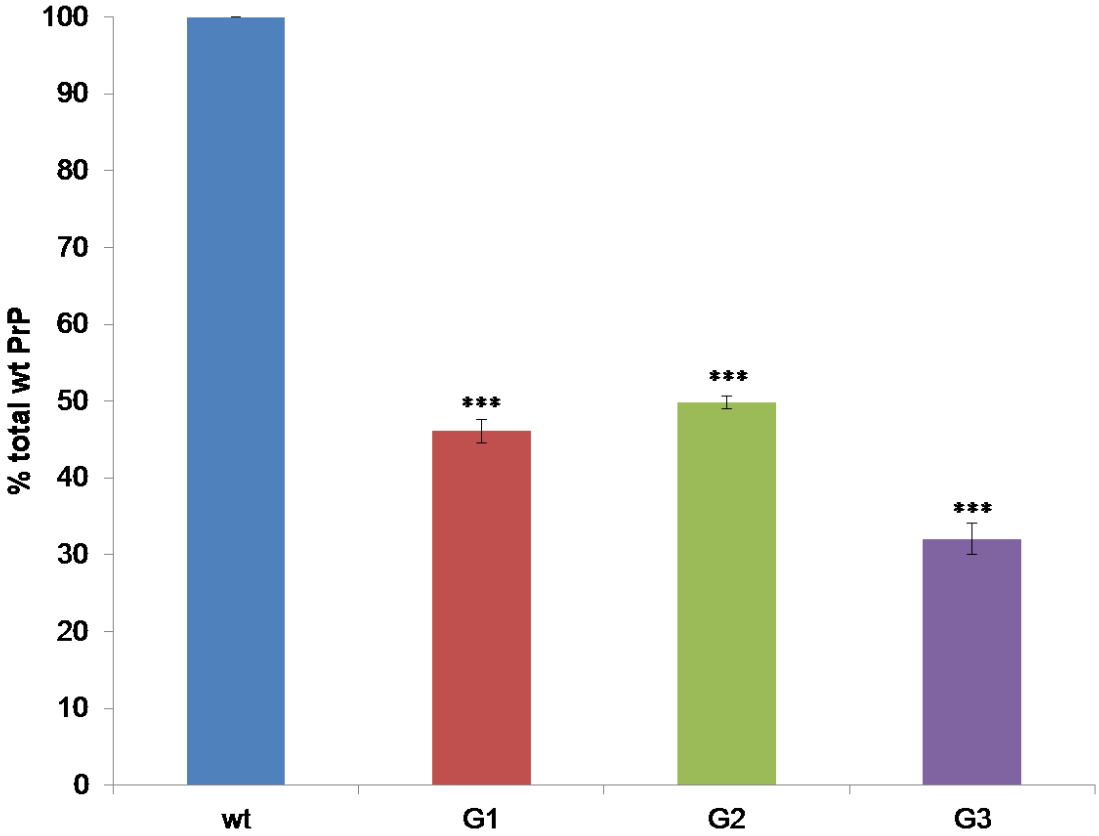

Figure 3.7 Total brain PrP levels as a % of total wild type PrP
5-7 brains per genotype were used to create 10% homogenates which were run on immunoblots in duplicate. Densitometry was carried out for PrP and normalised with an α-tubulin loading control. PrP from the GlycoD mutants were measured as a % wild type PrP^C. All GlycoD mutants had significantly less protein than the wild type mice (ANOVA, $p < 0.001$). There was no difference between G1 and G2 expression. G3 mutants had the lowest levels of PrP with significantly less than both G1 and G2 ($p < 0.01$).

All mutants had significantly less PrP^C than wild type controls (ANOVA, $p<0.001$); G1 and G2 mice have around 50% and G3 mice only have 32% PrP^C (Figure 3.7). This decrease in the PrP glycosylation deficient mice correlates with the decrease seen during the antibody screen. Although G1 mice have slightly less PrP than G2 mice this was not a significant difference. G3 mice had significantly less PrP^C than both G1 and G2 mice (ANOVA, $P<0.01$).

3.3.6 PrP mRNA levels in GlycoD mice

To determine whether the reduction of PrP^C was due to post-translational control of PrP^C or simply reflecting a reduction in mRNA levels, real time qPCR was used to measure mRNA levels in each of the GlycoD mice.

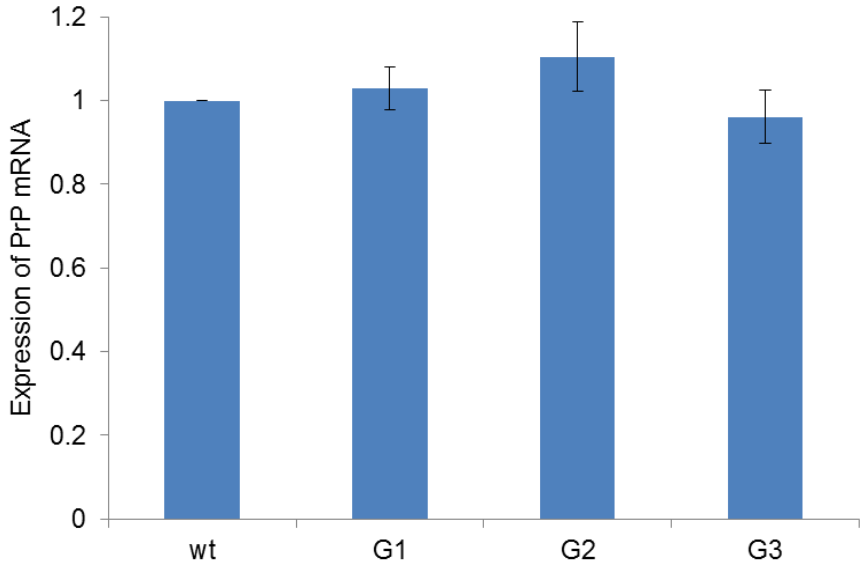

Figure 3.8 PrP^C mRNA levels measured by RT-PCR
mRNA was isolated from half brains, treated with DNAse I to remove genomic DNA and then converted into cDNA. *Prnp* from two different animals per genotype was amplified in multiples by qPCR (8 per brain). The housekeeping gene beta actin was also measured to normalise cDNA amounts for each sample. A sample of pure water and a sample of the RNA without cDNA conversion were included as a control and confirmed lack of contamination.

There was no significant difference in mRNA expression between any of the GlycoD or wild type mice (ANOVA), showing that they all expressed the same amount of *Prnp* mRNA (Figure 3.8). This result was expected due to the gene targeting method of creating these mice. However this is the first proof that there are no regulatory feedback loops that signal the decrease of PrP^C concentration.

3.3.7 Misfolded PrP in GlycoD mice

Expression of mutant PrP *in vivo* has led to development of spontaneous misfolding and disease (Chiesa et al., 1998, Hsiao et al., 1990). The reduction of PrP^C observed in the mutants could be due to the presence of misfolded PrP that spontaneously forms and has PrP^{Sc}-like properties. The different conformation adopted by misfolded PrP can cause

antigens to be lost or changed therefore misfolded PrP may not be detected during the standard protein preparation for immunoblot.

To establish whether there was any misfolded PrP with PrP^{Sc} properties present in the GlycoD mutants the solubility and PK resistance of PrP was assessed. Normal PrP^{C} is soluble in a weak guanidine hydrochloride solution (Gnd HCl; 1M) whilst misfolded PrP is insoluble. Brain homogenate was treated with 1M Gnd HCl to solubilise normal cellular PrP^{C}. The insoluble proteins, including misfolded PrP were solubilised in 6M Gnd HCl. (Figure 3.9).

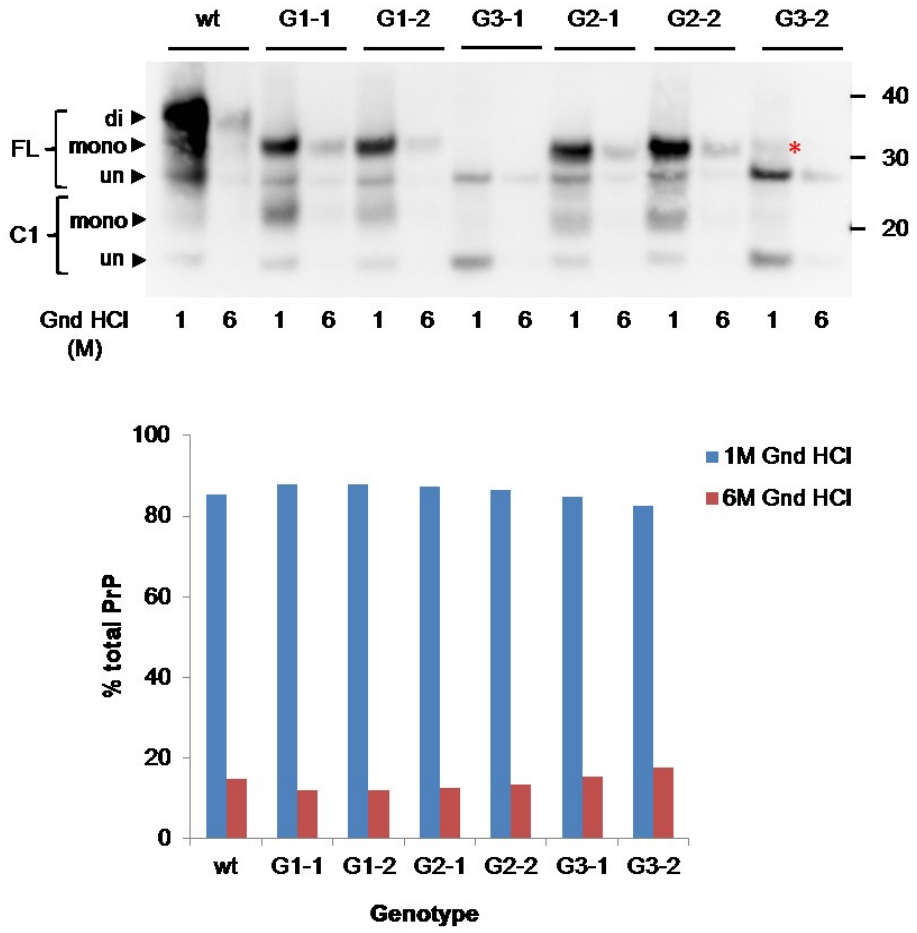

Figure 3.9 Soluble and insoluble PrP^{C} in murine brain
PrP was solubilised in 1M and 6M Gnd HCl to detect misfolded PrP^{C}. (A) 10% brain homogenates were treated with 1M Gnd HCl to solubilise normal PrP^{C} and insoluble proteins, including misfolded PrP then solubilised in 6M Gnd HCl. PrP was detected by immunoblot using anti PrP mAb BC6 at 0.01 µl/ml (B) Densitometry data shows that the predominant form of PrP^{C} is soluble in 1M but small amounts are seen at 6M for all genotypes.

Densitometry was carried out to quantify the ratios of soluble and insoluble protein. The majority of the PrP^C was soluble and detected in the 1M Gnd HCl fraction for all genotypes with a minority found in the insoluble fraction. There was no significant difference in the levels of PrP detected at 1M or 6M for any of the genotypes. Small amounts of PrP were detected for all genotypes, including the wild type control, in 6M Gnd HCl. A faint band was seen in the G3-2 sample at 1M Gnd HCl at the same molecular weight as G2 monoglycosylated full length PrP (shown by red asterisk in Figure 3.9). This is not seen in G3-1 and the sample does not show the expected pattern of a G2 homogenate. The monoglycosylated band was not included in calculation of soluble PrP^C.

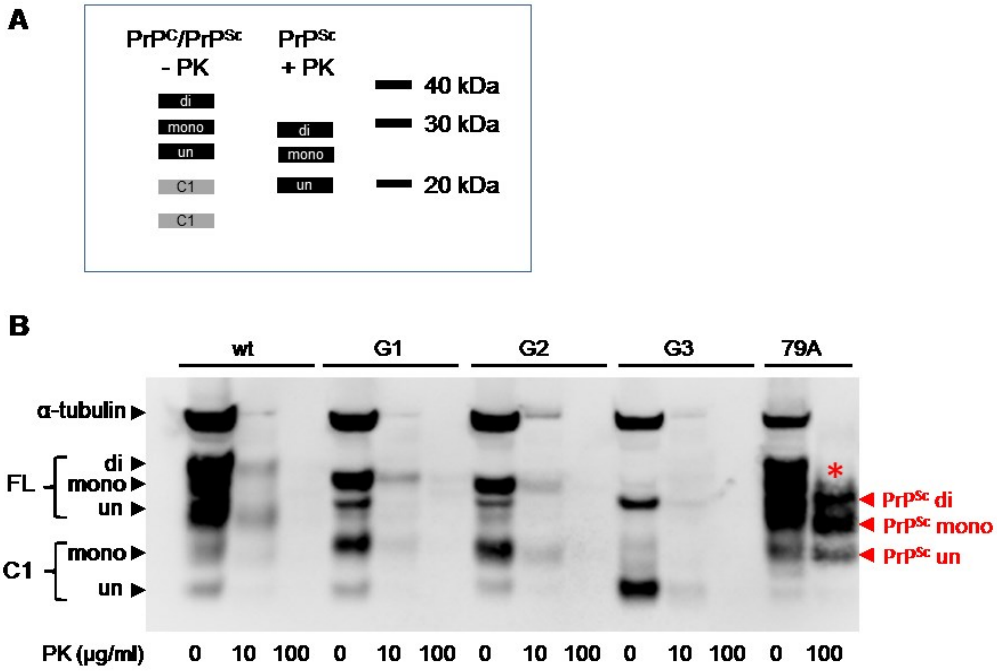

Figure 3.10 PK resistance in PrP glycosylation deficient mouse brain
(A) Expected molecular weights of PrP^C and the PK resistant core of PrP^{Sc}. C1 fragments are not seen with PK treated PrP^{Sc} (B) Total brain protein was treated with 10µg/ml or 100µg/ml of PK to remove PK sensitive PrP^C. Homogenate from a terminal mouse infected with 79A was used as a positive control to see the expected band shift of the PK resistant PrP core (asterisk). PrP^C was fully digested at 100µg/ml and incompletely digested at 10µg/ml, as was tubulin. Partial digestion showed all of the bands at the expected levels of PrP^C and no PrP^{Sc} bands.

In addition to its insolubility PrP^{Sc} is resistant to PK digestion and results in a PK resistant core. After PK digestion a shift in molecular weight from ~36 kDa to ~30 kDa is seen for diglycosylated PrP (Figure 3.10). Proteinase K digestion was used to see

whether there was any PK resistant PrP in normal brain homogenate. No PrP^{Sc} bands are seen in any of the GlycoD mice with 100 µg/ml PK thus all PrP^{C} present was PK sensitive. Incomplete digestion of PrP^{C} was seen with low levels of PK (10 µg/ml) as seen by a decrease in PrP^{C} and tubulin without a band shift indicating PrP^{Sc}.

There was no difference seen between the GlycoD and wild type mice in the solubility or PK sensitivity, suggesting that a lack of glycans do not cause PrP^{C} to spontaneously adopt any PrP^{Sc} properties.

3.3.8 Total levels of alpha cleavage in whole brain

The decrease in total PrP^{C} may be due to an increase in susceptibility to proteolytic degradation in PrP^{C} lacking glycans. The predominant cleavage event, alpha cleavage, produces truncated fragments which may have different half lives thus reducing protein levels. For each of the GlycoD mice densitometry was carried out to measure the ratio of full length PrP to C1 in PNGase treated homogenates (Figure 3.11).

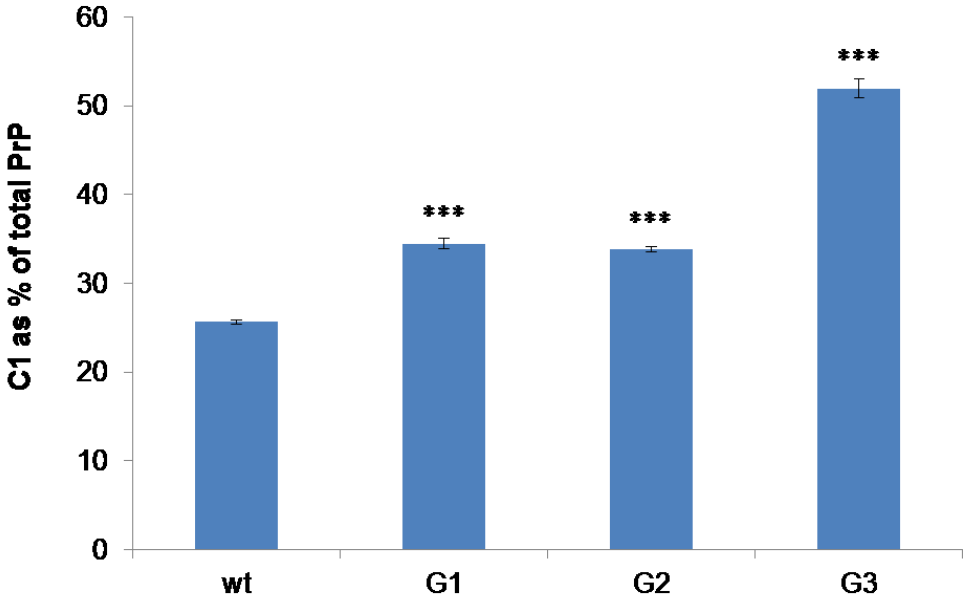

Figure 3.11. Cleavage levels in whole brain
Densitometry was used to measure full length and C1 bands. C1 was calculated as a percentage of total PrP^{C} for each genotype (n=7). In immunoblots where PrP^{C} was not fully deglycosylated partially deglycosylated bands were included in the appropriate fraction, either full length or C1.

25% of wild type PrP^C undergoes alpha cleavage whilst G1 and G2 mice showed 34% cleavage and G3 mice showed 52% cleavage. All glycosylation mutants have a significantly higher proportion of C1 than wild type mice (ANOVA; $F(3,24) = 180.4$, $p < 0.001$). G1 and G2 have similar levels of C1 and G3 mice have a significantly higher proportion of C1 than both G1 and G2 mice (Student's T-test, $p < 0.001$). As far as steady state levels are concerned over 50% of G3 brain PrP^C is present as C1 fragment.

The proportion of C1 PrP was increased in all GlycoD mice however they expressed less total PrP. The increased C1 could be due to increased propensity of the enzyme to cleave the protein in the absence of glycans. Conversely the relative levels of alpha cleavage and C1 could be the same for all genotypes and the full length PrP decreased.

The levels of C1 and FL were adjusted using the expression data collected in 3.3.5 to reflect the decreased overall expression to give a more accurate idea of the absolute levels of full length and C1 PrP in each GlycoD mutant. All values for C1 and full length PrP ware adjusted (Table 3.2) using the mean value of total brain expression for each genotype (G1, 46.1%; G2, 49.9%; G3, 32.1%).

Table 3.2 Adjusted PrP values to reflect expression levels of each isoform relative to total wild type PrP

PrP isoform	wt	G1	G2	G3
FL	74.4 (± 0.0)	30.2 (± 2.0)	33.0 (± 1.0)	15.4 (± 2.0)
C1	25.6 (± 0.0)	15.9 (± 0.3.0)	16.9 (± 0.3.0)	16.7 (± 0.5)
Total	100.0	46.1	49.9	32.1

The amount of C1 found in the GlycoD mutants was significantly less (7% decrease) than the wild type mice (ANOVA; $F(3,24) = 151.3$, $P = 0.001$,) when the data were adjusted to reflect the amount of PrP relative to wt PrP (Figure 3.12). There was no significant difference between the different GlycoD mice (ANOVA).

The reduction in full length PrP is much more pronounced (40-60%) and significantly less for all of the GlycoD mice than wild type mice (ANOVA; $F(3,24) = 4307$, $P<0.001$,). There is less than half the amount of full length PrP for G1 and G2 mice and only one fifth of the amount of full length wild type PrP in G3 mice (Figure 3.12).

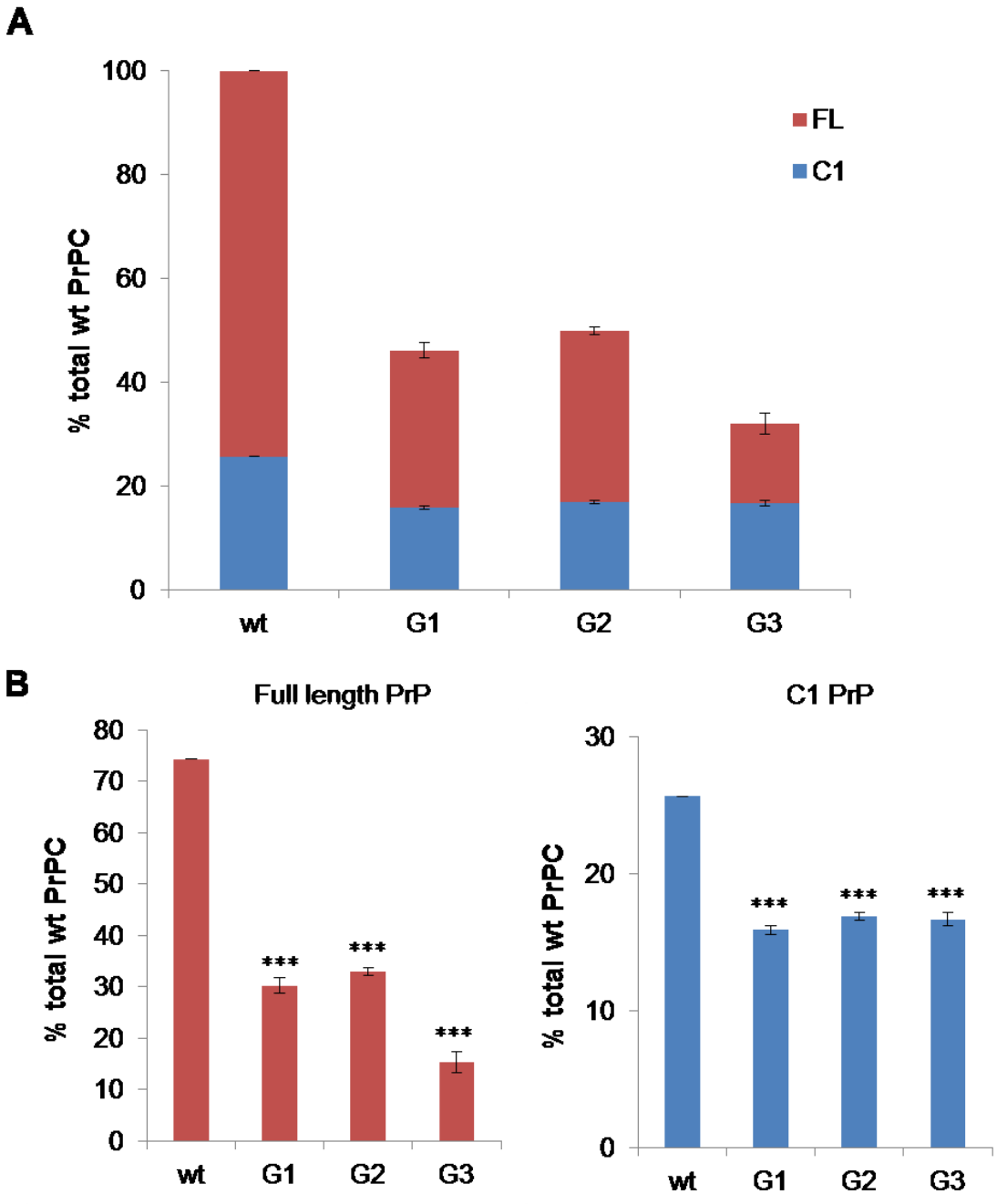

Figure 3.12 C1 levels corrected for overall PrP expression
The ratios of C1 and full length PrP were adjusted using the total expression data for each genotype (n=7) to reflect the relative amount of C1 and full length PrP for each genotype. (B) Relative amounts of full length PrP and C1 for each genotype.

3.3.9 PrPC distribution throughout the mouse brain

The lower levels of PrP protein in the mutants could be due to an overall reduction of PrP protein in all cell types or due to reduction of PrP in a specific neuronal population or brain region. To determine whether PrP is expressed equally throughout the brain, PrP levels were examined in seven different regions. An α-tubulin marker was used as a loading control so that PrP could be normalised to the amount of protein loaded onto the immunoblot. Densitometry was calculated as a percentage of the total PrP^C for that brain to measure the distribution of PrP.

Very small amounts of homogenate were produced for some brain regions due to the size of the mouse brain. Immunoblots were therefore only carried out in duplicate for each brain region of an animal. Samples were treated with PNGase to reduce the number of isoforms to two strong bands for improved quantification.

Full de-glycosylation was not achieved with wild type, G1 and G2 mouse tissue therefore partial PNGase digestion showed bands of monoglycosylated PrP. These bands were included when calculating total PrP. G3 mice do not have glycosylated PrP therefore only unglycosylated PrP^C is expected however for consistency between the genotypes the G3 mice were treated with PNGase.

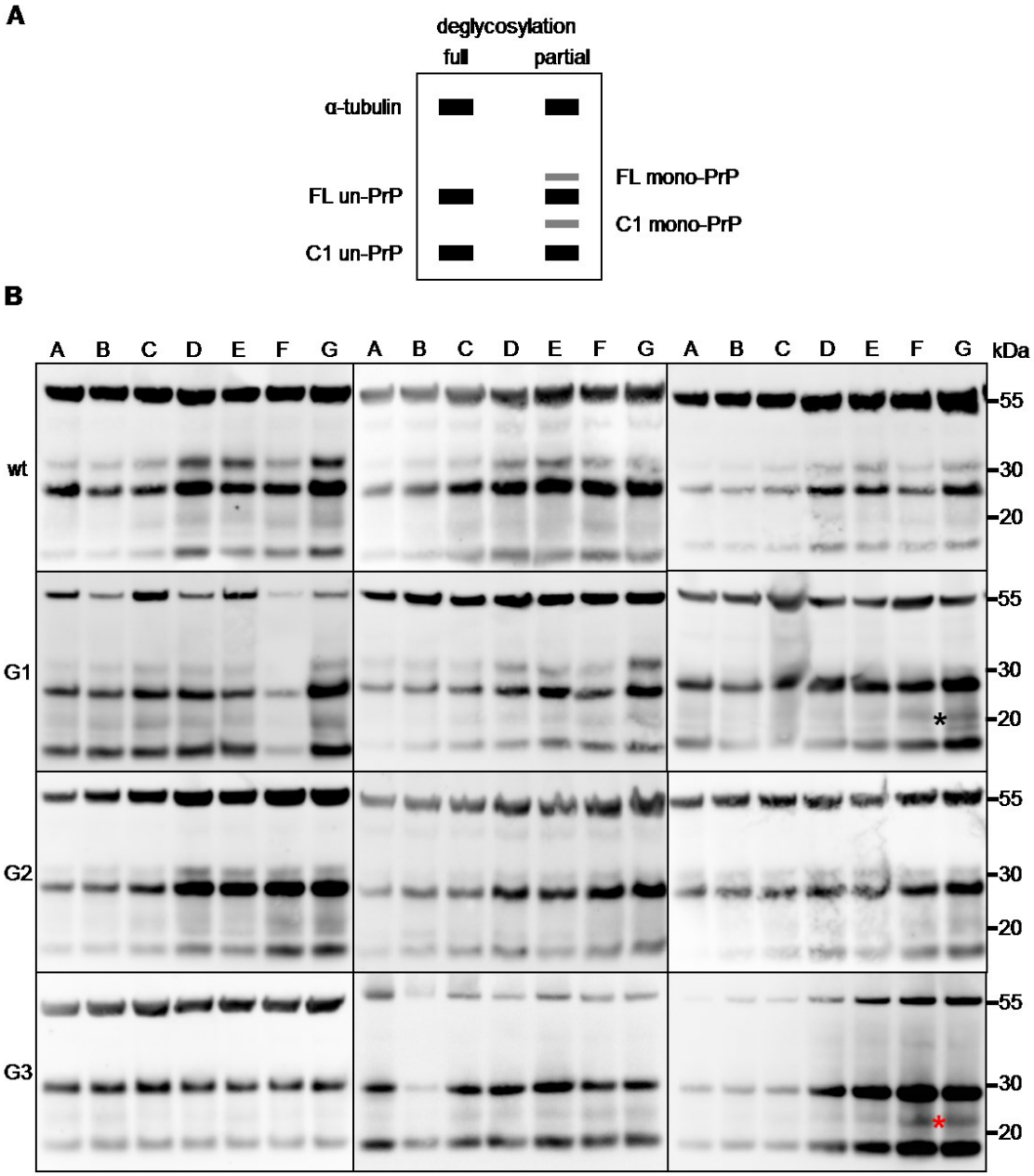

Figure 3.13. Immunoblots of PrP levels in different brain regions
10% Brain homogenates were treated with 1500 Units PNGase F to deglycosylate PrP. 6µl homogenate was run on an immunoblot and probed with mAb BC6 (0.01µg/ml). (A) Diagram showing the expected PrP bands. (B) Each immunoblot shows PrP^C from 7 different regions of the same brain represents a different mouse. Brain regions **A** Cerebellum, **B** Brain stem, **C** Dorsal Raphe, **D** Hippocampus, **E** Cortex, **F** Thalamus, **G** Septum. Unexpected bands were seen in some G3 blots (shown by a red asterisk) which could possibly represent C2 fragments. A faint band was also seen in a single G1 mouse, which may represent the C2 fragment (shown by a black asterisk).

Some of the brain regions with a high intensity of PrP show an extra band between the full length and C1 fragment (Figure 3.13, labelled with a red asterisk). This band could be the C2 fragment produced by beta-cleavage of PrP (Mange et al., 2004) or could be a

random degradation product of PrP^C. An antibody with an N-terminal epitope would need to be used to confirm that this fragment lacks the N-terminal and is not a degradation product with the same molecular weight as C2. A double band is also seen in one G1 mouse where a single band of monoglycosylated C1 is expected (Figure 3.13, labelled with a black asterisk). This is possibly a degradation product of PrP^C and was only observed in a single mouse. All bands detected with the PrP specific antibody BC6 were included in the densitometry.

Densitometry was used to calculate the total intensity of PrP for each brain. The intensities of PrP in each region were then used to calculate how much PrP was found in each region, showing the distribution of PrP throughout the brain (Table 3.3).

Table 3.3. Percentage of total PrP^C found in each brain region (n=5-7)

Brain region		% total brain PrP (sem)			
		wt	G1	G2	G3
Cerebellum	A	12.9 (0.6)	15.0 (2.5)	13.4 (0.4)	10.5 (1.7)
Brain stem	B	12.7 (0.8)	10.4 (1.2)	12.2 (0.9)	10.2 (2.6)
Dorsal Raphe	C	14.4 (0.3)	12.6 (1.6)	13.0 (1.2)	12.8 (1.6)
Hippocampus	D	13.8 (0.4)	16.5 (3.0)	13.4 (0.7)	17.3 (2.8)
Cortex	E	15.6 (0.8)	16.9 (3.0)	14.5 (0.6)	13.8 (2.2)
Thalamus	F	14.7 (0.8)	12.7 (2.4)	17.9 (2.1)	16.3 (3.6)
Septum	G	15.9 (0.5)	15.9 (3.1)	15.6 (2.2)	19.1 (6.8)

The distribution of PrP^C was uniform throughout the brain, with each of the seven regions assessed having similar amounts of PrP^C. There was no statistical difference between the brain regions within any of the GlycoD or wild type mice (Figure 3.14). A high level of animal to animal variation was seen with the GlycoD mice, especially in G3 mice. Although not significant there was a trend for increased PrP levels towards the front of the brain, with the brain stem and cerebellum having the lowest levels and the cortex, thalamus and septum having the highest. The brain stem had the lowest amount of PrP^C for all genotypes.

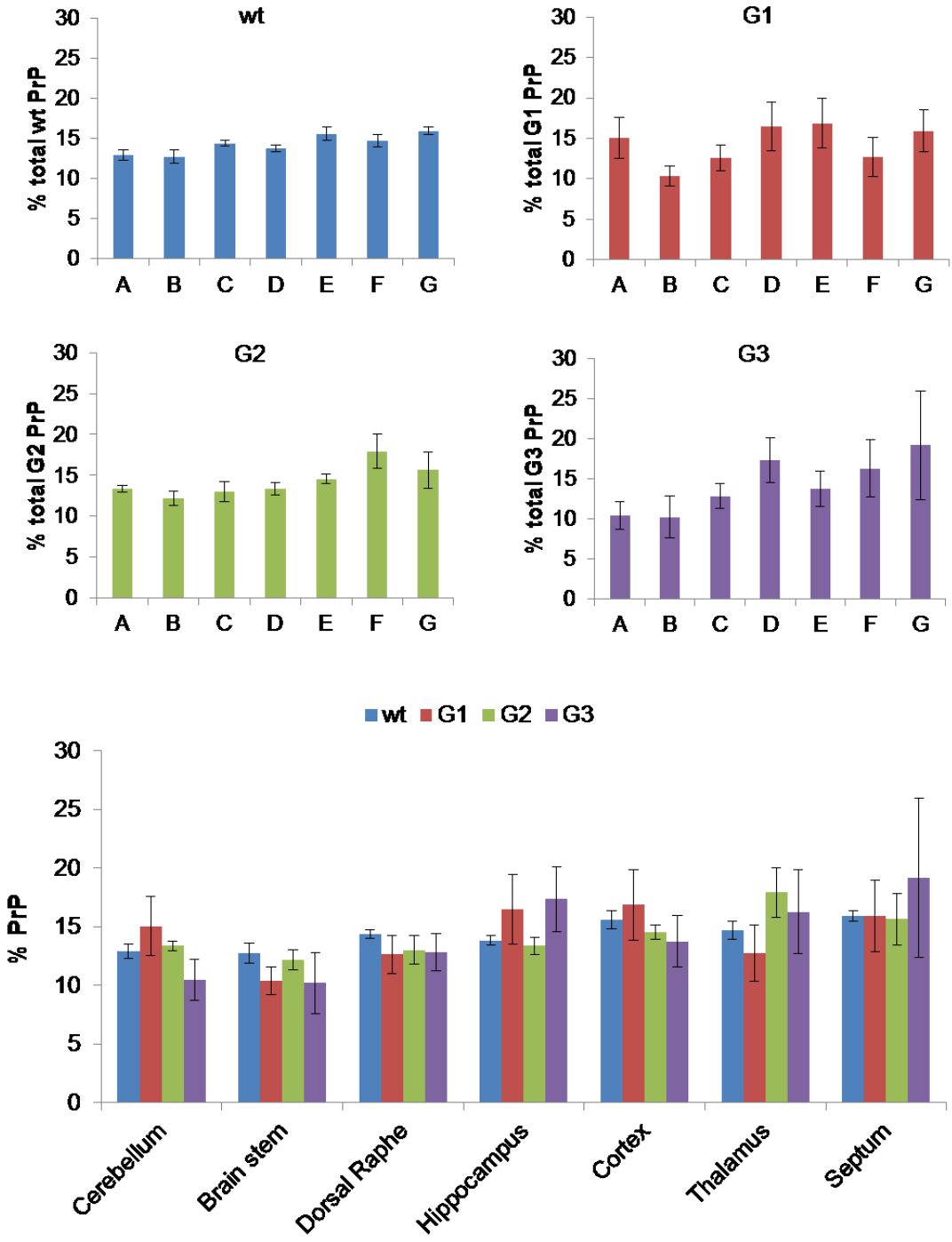

Figure 3.14. Distribution of PrP in different brain regions
Densitometry was carried out on immunoblots of different regions (4-8 brains per genotype carried out in duplicate) and protein loading normalised using an α-tubulin marker. The intensity of PrP was calculated for the whole brain and then intensities for each region used to calculate the percentage of PrP found in each region. There was no significant difference in expression of PrP between brain regions selected or between PrP glycosylation deficient mice (ANOVA). All areas have similar levels of PrP^C, regardless of the types of cells present in that area. There was a high level of mouse to mouse variation seen with the distribution of PrP throughout the

brain regions, especially in G3 mice. **A** Cerebellum, **B** Brain stem, **C** Dorsal Raphe, **D** Hippocampus, **E** Cortex, **F** Thalamus, **G** Septum

Alpha cleavage is probably caused by the action of a number of proteases and several metalloproteases have been put forward as candidate enzymes. Cleavage may vary from brain region to brain region depending upon the availability of cleavage enzymes. The proportion of C1 was measured from the same immunoblots used to measure total protein (Figure 3.13). Each brain region of each genotype was assessed to determine whether there were regional differences of cleavage (Table 3.4).

Table 3.4 C1 (as a percentage of total PrP) found in each brain region (n=5-7)

Brain region		% C1 (sem)			
		wt	G1	G2	G3
Cerebellum	A	24.7 (0.8)	33.7 (2.2)	31.8 (1.9)	53.5 (5.2)
Brain stem	B	24.5 (1.6)	36.1 (2.0)	35.3 (1.6)	54.6 (4.6)
Dorsal Raphe	C	26.2 (1.2)	36.5 (5.2)	33.5 (1.5)	46.3 (2.9)
Hippocampus	D	27.9 (1.2)	34.5 (3.7)	33.5 (2.0)	46.9 (5.6)
Cortex	E	24.7 (1.1)	32.8 (5.0)	33.3 (2.1)	53.4 (5.8)
Thalamus	F	25.6 (0.8)	32.8 (5.5)	33.6 (2.0)	55.8 (4.8)
Septum	G	25.9 (1.0)	34.8 (6.0)	36.0 (1.6)	53.1 (5.5)
Average		**25.6**	**34.5**	**33.8**	**51.9**

All brain regions within the same genotype showed similar cleavage levels (Figure 3.15). There was no significant difference in the cleavage levels throughout the brain for G1 (ANOVA; $F(6,28) = 0.11$, $p = 0.99$), G2 (ANOVA; $F(6,49) = 0.56$, $p = 0.78$), G3 (ANOVA; $F(6,49) = 0.57$, $p = 0.75$) or wild type mice (ANOVA; $F(6,42) = 1.21$, $p = 0.32$).

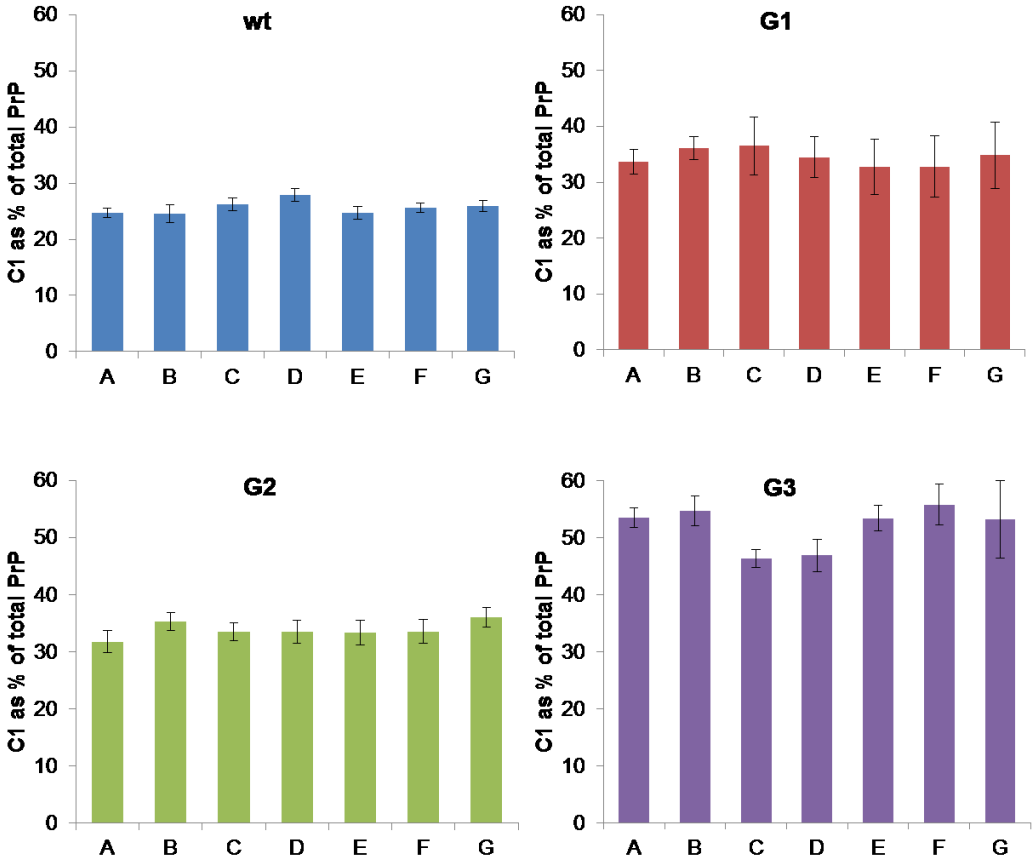

Figure 3.15. C1 levels in different brain regions
Densitometry was carried out on immunoblots of different brain regions. C1 levels for each brain region for each genotype were measured as a percentage of total PrP (4-8 brains per genotype carried out in duplicate). Brain regions **A** Cerebellum, **B** Brain stem, **C** Dorsal Raphe, **D** Hippocampus, **E** Cortex, **F** Thalamus, **G** Septum. There was no significant difference in C1 levels between brain regions selected (ANOVA).

3.3.10 GPI anchoring of PrP to the cell surface

The decrease in total PrP may also be due to susceptibility to other proteases and cleavage events. Membrane associated PrP was separated from non-membrane associated PrP to establish that the GlycoD mutants are GPI anchored. All glycoforms were found predominantly in the membrane associated pellet (Figure 3.16). A small amount of PrP was detected in non-membrane associated fractions; however this did not show a change in molecular weight expected by loss of the GPI anchor (Figure 3.17; B).

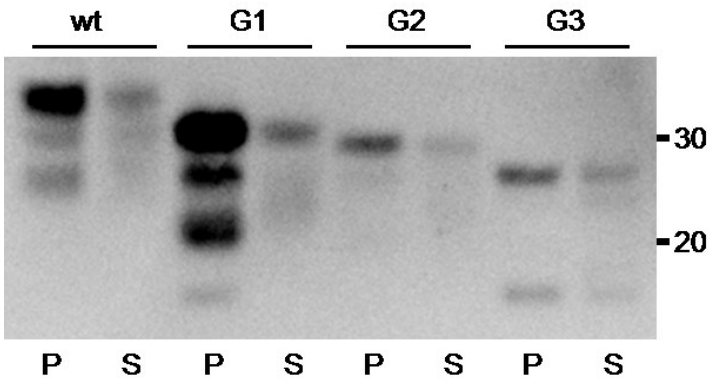

Figure 3.16 Separation of membrane associated and non-associated PrP^C
10% brain homogenate was centrifuged to separate into a membrane associated pellet fraction and a non-membrane supernatant fraction (n=5 per genotype). Fractions were run on an immunoblot and probed with anti-PrP mAb BC6 (0.01µg/ml). Brain homogenates show that PrP^C from all genotypes were predominantly found in the membrane associated pellet.

In order to see whether a PrP glycoform is more prone to C-terminal shedding a phosphatidylinositol-specific phospholipase C (PI-PLC) was used to cleave PrP^C from the GPI anchor to release it from the membrane (Figure 3.17).

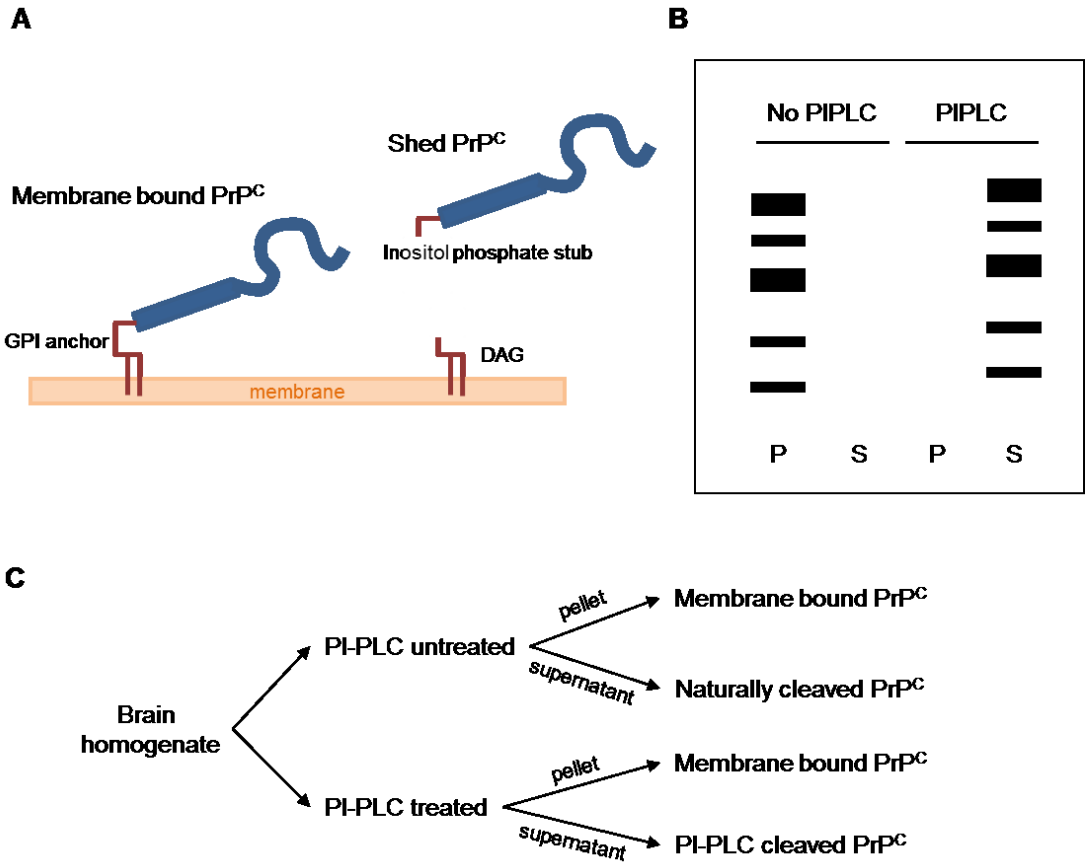

Figure 3.17 PI-PLC cleavage of GPI anchored PrP^C
(A) Diagram showing membrane bound PrP^C and shed PrP^C after PI-PLC cleavage (B) The expected immunoblot patterns of wild type PrP^C after PI-PLC treatment. PI-PLC untreated sample contains membrane bound PrP^C found in the pellet fraction, P. PI-PLC treated sample is comprised of shed PrP^C which is found in the supernatant fraction. Shed PrP^C is ~3kDa heavier than GPI anchored PrP^C due to the hydrophilic inositol phosphate stub (Stahl et al., 1987). (C) Diagram showing the collected fractions. Pellet fractions contain membrane associated PrP^C, which is not necessarily GPI anchored. Supernatant fractions contain cleaved PrP^C, untreated supernatant shows naturally shed PrP^C and PI-PLC shows GPI anchored PrP^C.

Temperature, incubation period and enzyme concentration were altered in order to optimise the technique. The different conditions tested did not fully cleave all of the GPI anchors from PrP^C as it was still detected in pellet fractions, which is GPI anchored, membrane associated PrP^C.

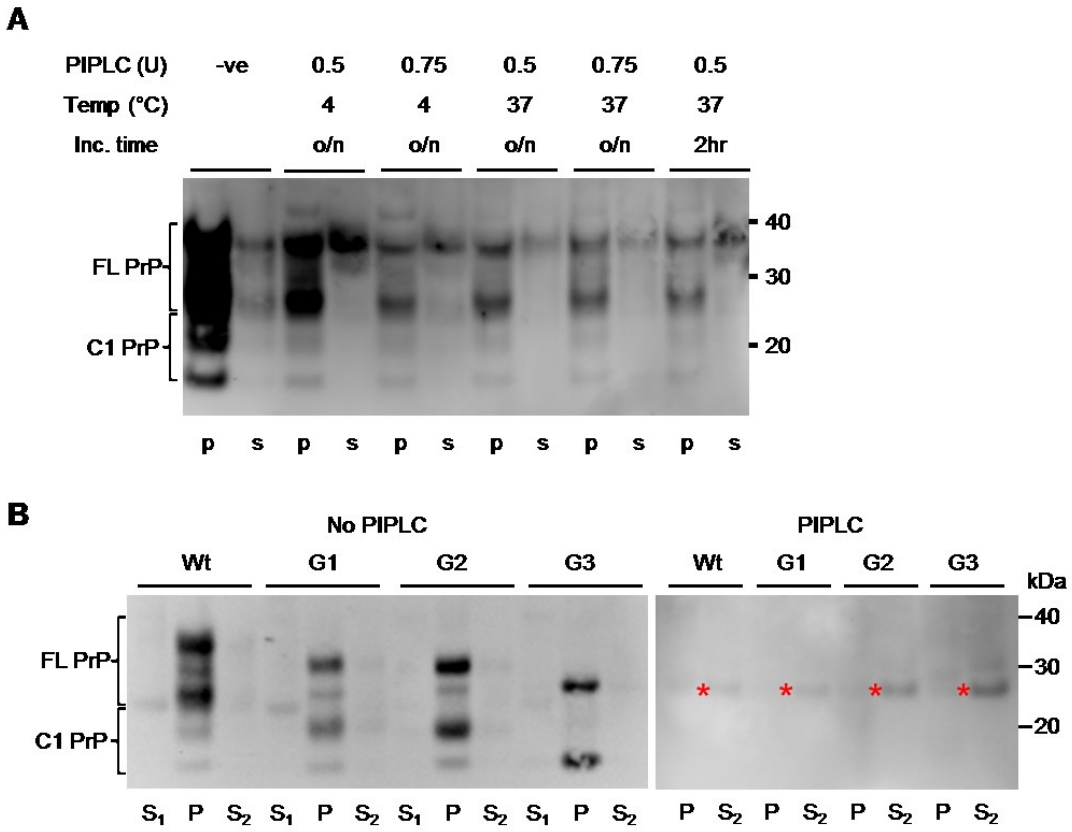

Figure 3.18 Determining PI-PLC incubation conditions
(A) A single 10% wild type homogenate was treated with different conditions in order to find the best conditions for shedding PrP^C. Temperature, incubation period and enzyme concentration were altered. P = pellet, PrP^C in this fraction is membrane associated; S_1 & S_2 = supernatant containing naturally secreted proteins; PrP^C in this fraction is not membrane associated. (B) 10% brain homogenates from GlycoD mice were treated with 0.5 U PI-PLC overnight at 37°C to cleave the GPI anchor (n=2). In untreated homogenate the PrP^C was predominantly found associated with the membrane in the pellet fraction. PrP^C was not detected in PI-PLC treated homogenates. Asterisks show IgG light chain detected in the absence of primary antibody.

All conditions showed a much stronger PrP signal in the pellet fraction than the supernatant fraction (Figure 3.18; A). PI-PLC treated samples showed a reduction in amount of membrane associated PrP in the pellet fraction, indicating that PrP^C had been cleaved from the membrane. However, only small amounts of shed PrP^C were detected in the supernatant fractions. With extended incubation at 37 °C all membrane associated PrP was cleaved but shed PrP was not detected in the supernatant fraction (Figure 3.18; B).

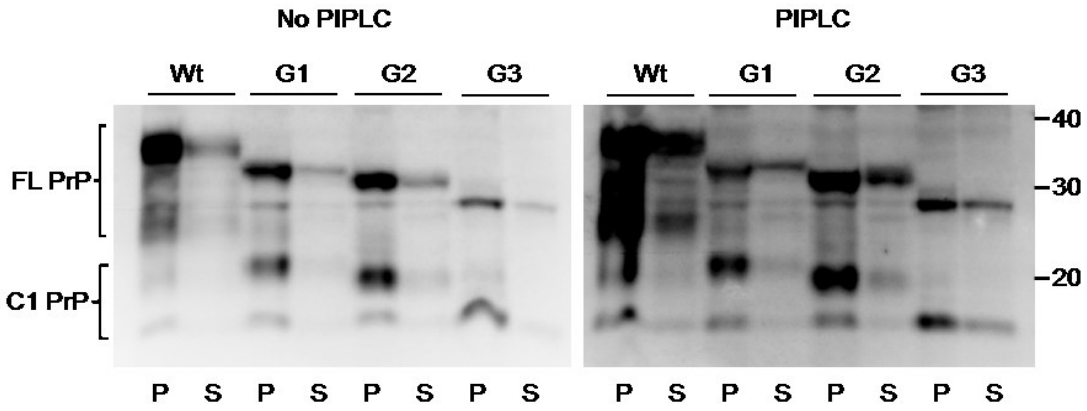

Figure 3.19 PI-PLC treatment of GlycoD mutants
10% brain homogenates from GlycoD mice were treated with 0.5 U PI-PLC for 2 hours at 37 °C to cleave the GPI anchor. Samples were also left untreated to see whether naturally cleaved PrP^C could be detected in the supernatant fraction. P = pellet, membrane associated fraction; S = supernatant, membrane released fraction.

PI-PLC treated samples showed that a large amount of PrP^C was still membrane bound and found in the pellet fraction. PrP^C was detected in the supernatant fraction and had a small shift in molecular weight indicating the loss of the GPI anchor.

Untreated homogenates (Figure 3.19, left hand panel) showed the majority of PrP^C was GPI anchored and found in the membranes. Small amounts of PrP^C were detected in the supernatant, although there was not an apparent shift in molecular weight. This most likely represented inefficient membrane separation.

3.3.11 Ratios of PrPC glycoforms

It is not known whether wild type PrP^C favours glycosylation of one site over the other. The prevention of glycosylation at one site may have consequences for the glycosylation of the other site therefore one monoglycosylated glycoform may be favoured over the other.

Under the PAGE conditions used previously in this chapter unglycosylated PrP cannot be easily distinguished from the diglycosylated C1 fragment. Electrophoresis on wild type mice was carried out for longer on an 18% polyacrylamide gel to allow the two

isoforms to separate so that they could be measured accurately. Densitometry was then carried out on all glycoforms for both full length and C1 fragments.

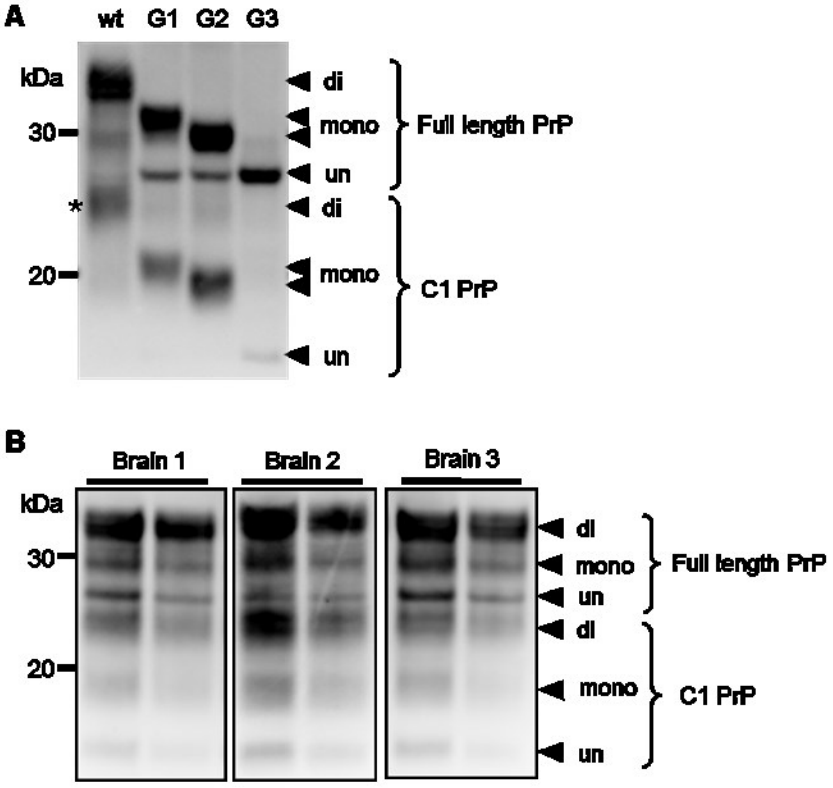

Figure 3.20. Glycoform composition of wild type PrP^{C}
An Immunoblot showing the separation of full length unglycosylated PrP and diglycosylated C1 PrP from a wild type brain. (A) All genotypes were compared side by side so that each band could be identified. Diglycosylated C1 is indicated by an asterisk (B) Immunoblots showing separation of three different wild type brains.

In order to identify the different bands of the wild type PrP after full separation of all isoforms all the bands were compared with the GlycoD mice on an immunoblot. The diglycosylated C1 band (marked with an asterisk) was only present in the wild type homogenate and was lower than the unglycosylated bands from the other genotypes (Figure 3.20, A). Densitometry was carried out to calculate the ratios of glycoforms in wild type, G1 and G2 mice. Three different mouse brains were used to assess the variability of glycoform ratios between animals (Figure 3.20, B).

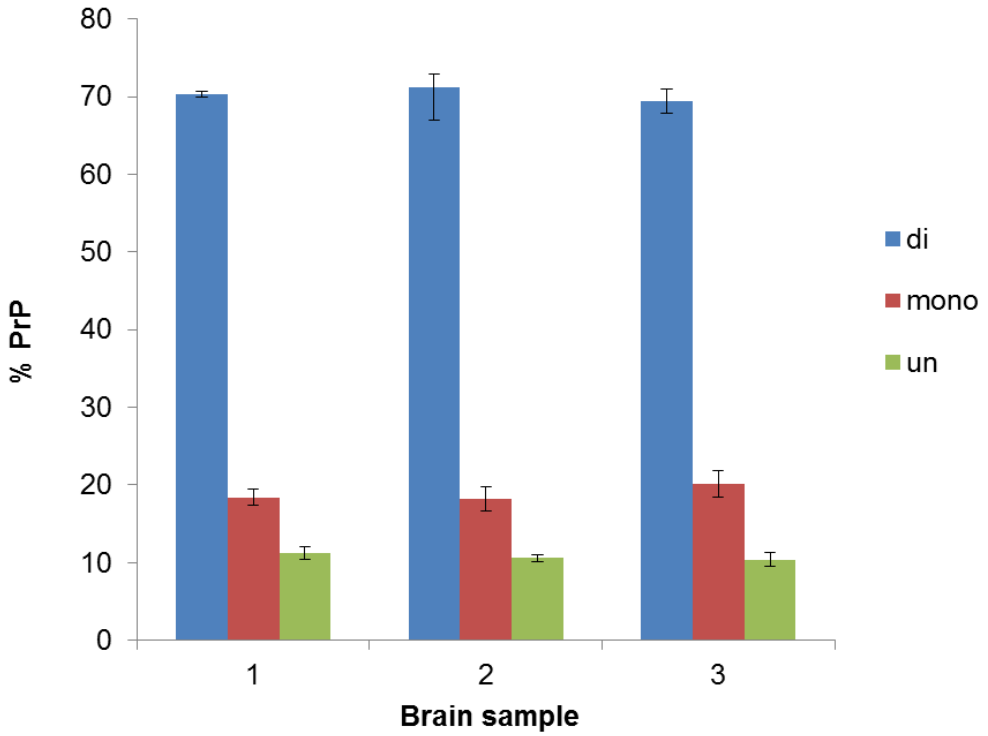

Figure 3.21 Consistent wild type glycoform ratios from mouse to mouse
Three different wild type mouse brains were homogenised and the glycoform ratios measured by densitometry. Ratios were calculated by combining values for full length and C1 bands for each glycoform. Each brain sample was run on 4-6 immunoblots.

Ratios were similar for each wild type animal tested; the predominant glycoform was diglycosylated PrP and the mono and unglycosylated were minor glycoforms (Figure 3.21).

To investigate how the glycoform ratios are changed in the GlycoD mice the ratios of the glycoforms were measured and compared with the wild type ratio data above. The ratios were calculated for each individual genotype and the values adjusted using the values in section 3.3.5 to give the relative amount of each glycoform for all of the genotypes.

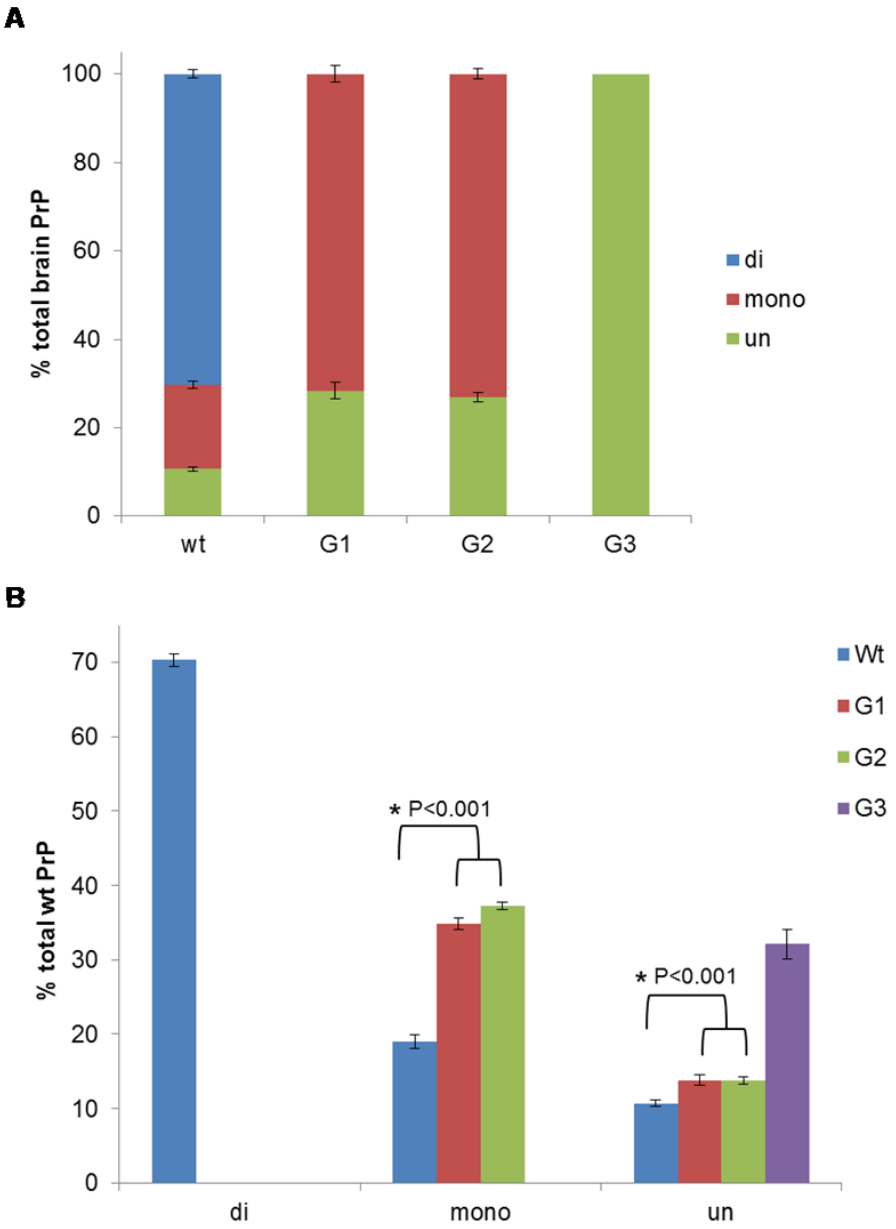

Figure 3.22 Ratios of glycoforms for GlycoD mice
Densitometry data was carried out on 3 brains for each genotype and used to calculate the amount of each glycoform present in wild type and in each mutant. (A) The ratio of each glycoform was measured by combining full length and C1 values for each glycoform in each genotype. (B) G1, G2 and G3 values were then adjusted to reflect the lower overall expression levels of PrP to give comparable levels of each of the glycoforms

There was no difference in the ratios of monoglycosylated to unglycosylated PrP between the G1 and G2 mice (Figure 3.22, A). 70% PrP^C was glycosylated for both G1 and G2 mutants. 30% PrP^C remained unglycosylated. There was significantly more

unglycosylated PrP in both G1 (T-test, P<0.001) and G2 (T-test, P<0.001) than the wild type mice. Very little animal to animal variation was observed.

G1 and G2 values were adjusted using the values obtained for total brain expression to reflect the overall lower expression levels of PrP in these mice so that they could be directly compared with wild type PrP (Figure 3.22). Although there is a much lower overall PrP level in the G1 and G2 mice there is a significant increase in unglycosylated PrP in the G1 (T-test, p<0.001) and G2 mice (T-test, p<0.05) compared to wild type.

3.3.12 Glycosylation site occupancy in wild type mice

It has been shown that in the GlycoD mice the monoglycosylated bands have different electrophoretic mobilities when separated by electrophoresis, depending upon the site glycosylated (Figure 3.3). Wild type monoglycosylated PrP can be seen as a doublet on an immunoblot under certain conditions. It is assumed that these represent the two different monoglycosylated isoforms as they have the same electrophoretic mobility as the G1 and G2 bands.

Wild type PrP^{C} was run on an 18% acrylamide gel to separate out the monoglycosylated PrP into a doublet to see whether each band contributes equally or whether there is a predominant monoglycosylated form. The two different monoglycosylated isoforms in wild type PrP are expressed at equal levels (Figure 3.23).

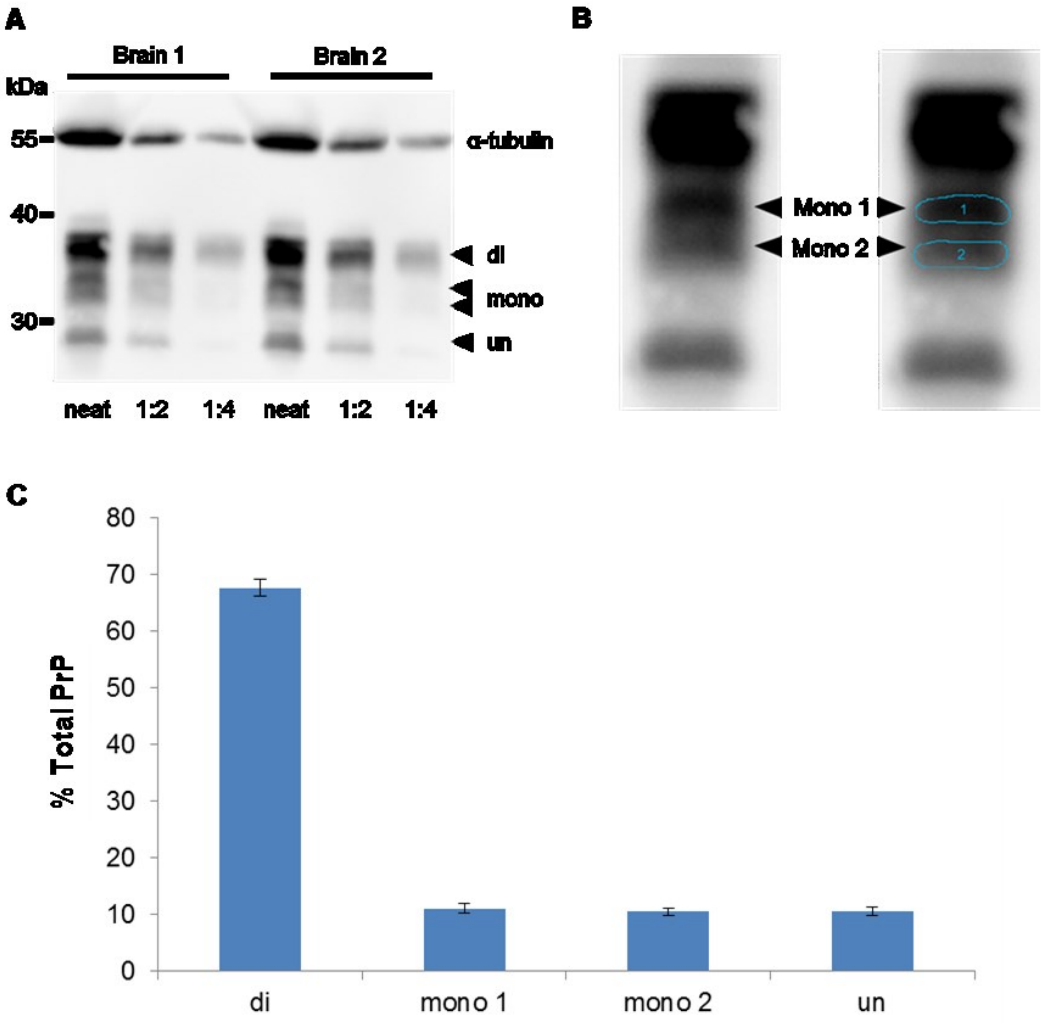

Figure 3.23 Separation of monoglycoforms in wild type PrP
(A) Immunoblot showing 2 different brain homogenates at different dilutions, showing the separation of the monoglycosylated PrP. (B) Higher contrast immunoblot showing the 2 monoglycosylated bands present in wild type PrP and with bands highlighted for densitometry. (C) Densitometry data shows that both monoglycosylated isoforms and the unglycosylated isoform are present at equal levels in wild type mice.

The level of site occupancy can be calculated for each site by combining the levels of diglycosylated PrP, at which both sites are occupied, and the specific monoglycosylated PrP. Both sites have 78% glycan occupancy suggesting that glycosylation happens equally at both sites (Figure 3.24).

The carbohydrates attached to PrP are large and heterogeneous and have not been fully elucidated. It was not possible to analyse the glycans to the level required to confirm

that the same range of glycans found on wild type PrP are also found on the GlycoD mutants and that the wild type bands correspond to the two different monoglycoforms.

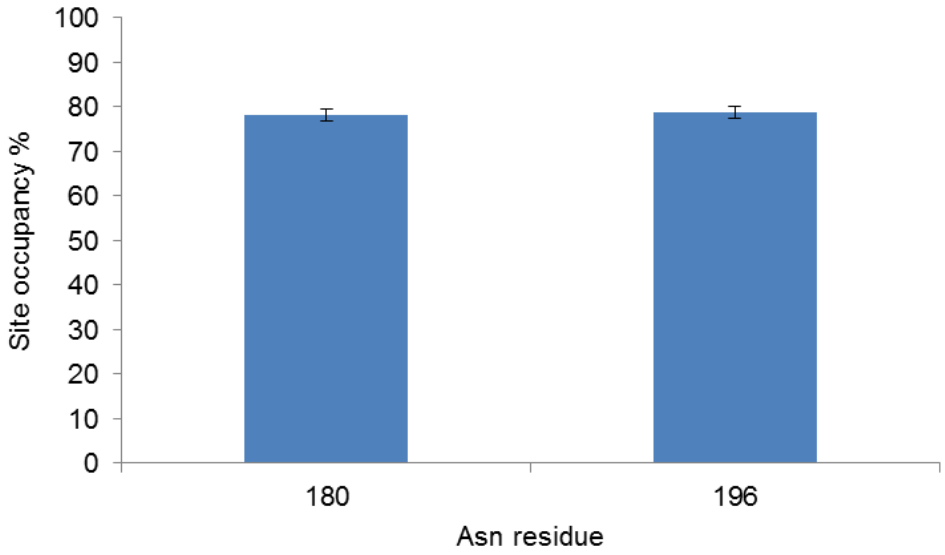

Figure 3.24 Glycan site occupancy of wild type PrP^C
The levels of each of the glycotypes in wild type mice can be used to calculate the level of site occupancy for each glycosylation site. The higher MW monoglycosylated band represents PrP with an occupied Asn 196, the lower MW represents PrP with an occupied Asn 180. Diglycosylated PrP has both sites occupied therefore each site can be calculate by the amount of diglycosylated and the relevant monoglycosylated PrP. Site occupancy was calculated for 3 mice on duplicate immunoblots.

3.4 Conclusions

3.4.1 Comparison of PrP Protein levels

PrP^C detected by immunoblot showed a reduction of total protein in all of the glycosylation deficient mutants. Removal of a single glycosylation site, either the first or the second reduced the PrP protein level by 50% whilst removing both glycosylation sites reduced levels by 70%.

During characterisation of the GlycoD mice it was reported that there was no difference in protein levels between the genotypes; however there were conflicting results with the different methods used to quantify PrP^C (Cancellotti et al., 2005). A quantitative method, DELFIA was used to assess expression levels using three different capture-

detection antibody pairs. This method showed that levels of PrP varied greatly depending upon the antibody pairs used and was in contradiction to the apparent reduction in protein determined by immunoblot.

This contradiction in expression levels is most likely due to the choice of monoclonal antibody pairs used for DELFIA and the epitopes they recognise. There is strong antibody dependant detection of PrP^{C} using monoclonal antibodies, which by their nature may only be detecting a subset of isoforms. One antibody chosen had an N-terminal epitope and only recognised the full length protein. This thesis showed that all of the antibodies within the C-terminal and central region of PrP^{C} were able to detect all isoforms and that the glycans did not hinder recognition.

In order to overcome the variability caused by antibody pairs this study used immunoblotting with a single antibody to measure expression levels. To ensure that all isoforms were being detected a range of monoclonal antibodies were tested. The consistent levels of PrP^{C} for all of the glycoforms with the different antibodies tested suggest that neither carbohydrates nor the mutations are influencing epitope availability for the antibodies selected.

It is possible that lack of glycans or the point mutation could cause the PrP^{C} to spontaneously adopt a different conformation or PrP^{Sc}-like properties that could not be detected by the monoclonal antibody selected. Single amino acid changes have been demonstrated to cause spontaneous misfolding of PrP^{C} *in vivo* and *in vitro* (Imran and Mahmood, 2011). The experiments conducted here make this unlikely to be the case here. PrP^{C} from the GlycoD mice showed the same solubility as wild type mice in low levels of guanidine hydrochloride and was PK sensitive. The monoclonal antibody selected (BC6) is able to detect the misfolded PrP^{Sc} in mice infected with different TSE agents so it is unlikely that any isoforms are missed. The GlycoD mice do not show any signs of spontaneous disease associated with abnormal protein folding when aged (Cancellotti et al., 2005), further adding strength to the argument that the reduction is not due to abnormally folded PrP.

Despite the Glyco D mutants showing decreased total PrP there was a negative correlation between the percentage of C1 and the total PrP expression level; wild type had the highest total protein level and the lowest level of alpha cleavage whilst G3 have the lowest expression but the highest level of alpha cleavage. The increased proportion of truncated PrP lends strength to the argument that the glycans provide protection against proteolysis. However; when the reduced levels of total PrP are taken into consideration the absolute levels of C1 are significantly lower in the GlycoD mutants than wild type mice, arguing against increased proteolysis. Alpha cleavage may be indirectly affected by glycosylation, which can influence the trafficking and turnover of PrP^C. The reduced PrP^C levels suggest that there is an increase in turnover in the GlycoD mutants, which could affect the exposure of PrP^C for proteolytic processing.

This study shows that the glycosylation regulates the levels of PrP^C post-translationally, either through increased stability and/or through altered trafficking. Removal of both glycosylation sites reduced PrP^C levels significantly more than removal of a single site. There was no difference between the two monoglycosylated PrPs for either total or truncated PrP, suggesting that both glycans exert the same effect.

3.4.2 Trafficking versus degradation

As expected for a gene targeted model the levels of *Prnp* mRNA in the GlycoD mutants are the same as in wild type mice indicating that the reduction of PrP^C is due to post-translational control. The reduction in the mutants may be due to increased turnover of the protein. Glycosylation is known to increase the half-life of many proteins through increasing stability, altering trafficking or through shielding from proteolytic degradation (Kundra and Kornfeld, 1999, Sola and Griebenow, 2009).

The glycoforms may have altered degradation susceptibilities due to the shielding properties of the glycans, which provide protection from degradation leading to overall reduced PrP levels in their absence. G3 mice lacking glycosylated PrP had the lowest PrP levels and wild type PrP with two glycans had the highest levels. The G3 mice also had the highest proportion of cleavage, suggesting that glycans offer some protection

against cleavage. The levels of G1 and G2 PrP^C are indistinguishable from each other, suggesting that the presence of just one glycan is sufficient to offer a degree of protection from proteolysis.

In addition to increased susceptibility to proteolysis a change in trafficking could also account for the reduced PrP levels and can act in two different ways, either through retention in the secretory pathway or through increased endocytosis. A lack of glycosylation may lead to retention in the secretory pathway and degradation as is seen with acetylcholinesterase in erythrocytes; unglycosylated protein is retained in the ER and not trafficked to the Golgi (Luk et al., 2012). Previous experiments have shown that unglycosylated PrP has a predominantly intracellular localisation (Salamat et al., 2011, Cancellotti et al., 2005), which may be due to retention in the ER or Golgi. However, monoglycosylated PrP showed no difference in localisation from wild type PrP and no difference depending upon the glycosylation site occupied (Cancellotti et al., 2005) indicating that a specific glycan is not required for trafficking to the membrane.

PrP^C has been shown to bind to many different lectins and receptors, potentially via the glycans. The trafficking is heavily influenced by receptor binding. PrP^C relies on binding partners to be internalised from the cell surface (Parkyn et al., 2008, Gauczynski et al., 2001, Zanata et al., 2002). A change or lack of glycosylation could increase the interactions with some of the receptors, changing the rate of internalisation of the protein. If PrP^C is on the cell surface for longer it is more likely to have a longer half-life (Nunziante et al., 2003).

Trafficking will need to be explored further to determine whether the reduction is due to an increased turnover or whether the protein is prevented from maturation and is degraded quickly. Half-life of PrP^C could be measured in primary cells from the different GlycoD mice. A decreased half-life would indicate more rapid degradation of the protein. Investigating the precise localisation of the PrP^C glycoforms will indicate whether the protein is retained in the secretory pathway or whether a large amount is directed to lysosomes for degradation.

3.4.3 PrPC in different brain regions

In this study there were no regional differences in total PrP^C levels or truncated PrP levels observed within wild type mice or any of the GlycoD mutants. All seven regions assessed had the same amount of PrP showing equal distribution of PrP^C throughout the brain. The glycoform ratios were not measured in the brain regions of wild type mice; however, the equal distribution throughout the brain in the GlycoD mutants indicates that none of the regions preferentially produced a particular glycoform.

There was a trend for lower PrP^C expression levels in the brain stem and to a lesser extent the cerebellum. This reduction could be due to fewer cells or few synapses in these regions. Both are predominantly white matter regions, containing highly myelinated axons, which have been shown to be almost completely unlabelled for PrP^C (Ford et al., 2002a). The brain stem had less total protein than other brain regions measured. This may reflect the high levels of myelinated axons and fewer synapses in the white matter tracts.

It was reasonable to speculate that the different brain regions would express different levels of PrP^C due to the different neuronal subtypes present in each region and the preference for glycoforms. PrP^C protein in the brain is predominantly neuronal and protein levels vary depending on the neuronal subtype despite the high levels of *Prnp* mRNA in all neurons (Ford et al., 2002a). This study indicated that there were no regional differences in any of the genotypes but may be limited by the technique used. Microdissection of the mouse brain takes relatively large areas of the brain, encompassing many different cell types. The cells may express different levels of PrP but for a heterogeneous mixture of cells the differences may be too subtle to detect.

Studies have used IHC to look at distribution throughout the mouse brain. In one study regional differences were observed; the hippocampus and cortex had particularly high levels of protein, whilst the cerebellum and brain stem had low levels (Liu et al., 2001). In another study histoblots of wild type mice showed very weak staining and no differences in regional PrP^C expression levels and differences in expression levels were

only observed in transgenic mice overexpressing PrP^C (Herms et al., 1999). Regional variations in mouse brain were described using immunoblotting (Liu et al., 2001) however quantification was not carried out and no assessment was made for variability of protein loaded, therefore the variations seen in brain regions may be more subtle once total protein levels were controlled for.

There is a lack of consensus on PrP^C distribution in the mouse brain, possibly hindered by the techniques used and the difficulty in detecting PrP^C. Regional differences in PrP^C were mostly detected by histology, where tissue processing has a huge impact upon antibody detection. The use of monoclonal antibodies in IHC can reduce the amount of PrP^C detected due to antigen availability. Epitopes may be buried or difficult to access in certain tissues, especially as the protein is in its native state. Antigens may be lost during fixation and tissue processing, such as harsh antigen retrieval treatments. There are contradictions in the literature about PrP^C distribution in brain using the same antibody, mAb 8H4. PrP^C was detected in Purkinje cells in one study (Laine et al., 2001) but not in another (Liu et al., 2001). During an immunoblot tissue is disrupted and PrP is denatured, potentially allowing equal epitope availability of all PrP molecules; however PrP^C cannot be assigned to individual cell types.

There was no difference in cleavage levels between different brain regions in any of the GlycoD mutants. The enzyme(s) responsible for alpha cleavage has/have not been elucidated and data from this thesis support that the enzyme(s) is/are ubiquitously expressed throughout the brain. Several enzymes have been proposed as candidate enzymes for alpha cleavage but it seems likely that there are several enzymes with the ability to perform alpha cleavage (Liang and Kong, 2012). Different neuronal cell types may use different enzymes for alpha cleavage however the overall cleavage levels may be similar for each cell type or brain region because of the multitude of enzymes available. Additionally there may be very subtle differences in brain regions that are not detectable using immunoblots and densitometry.

3.4.4 The role of truncated PrP

The significance of the truncated PrP is not understood therefore the implication of enhanced cleavage in the GlycoD mutants is difficult to elucidate. A high variability of alpha cleavage levels can be seen depending upon species, PrP sequence and age of animal (Laffont-Proust et al., 2006). Healthy humans displayed 30-50% C1 in brain and cleavage increased with age. In some humans and non-human primates C1 is the major PrP^C isoform (Laffont-Proust et al., 2005). It is not known whether full length PrP undergoes cleavage to create fragments with distinct functions or whether the C1/N1 fragments serve to regulate the functions of full length PrP, or even a combination of the two.

The N-terminal of PrP^C mediates some of the proposed functions such as copper binding at the synapse (Brown, 2003) and signal transduction (Vassallo et al., 2005) thus cleavage may be a regulatory mechanism of PrP^C. Signal transduction is increased by copper binding and membrane perturbation (Haigh et al., 2009). Copper binds to the octarepeat region of the N-terminal and many ligands bind to the N-terminal to assist in movement of PrP out of the lipid rafts or movement of ligands into lipid rafts (Parkyn et al., 2008). Alpha cleavage removes the N-terminal and reduces the amount of functionally active full length PrP.

Both C1 and N1 have been shown to be biologically active fragments. Cells overexpressing C1 had an increased cytotoxic response to staurosporine leading to the conclusion that C1 possesses pro-apoptotic functions (Sunyach et al., 2007), however mice expressing C1 alone showed no neurotoxicity (Westergard et al., 2011). This discrepancy could be due to treatment with pro-apoptotic agents; C1 enhances susceptibility to pro-apoptotic stimuli but is not neurotoxic under normal conditions. This susceptibility change could be due to down regulation of neuroprotective signal transduction caused by high levels of C1. Increased N1, which is believed to have neuroprotective properties, preventing cell death were not detected in the C1 overexpressing cells (Guillot-Sestier et al., 2009). N1 is produced at the same time as C1 but is secreted so is difficult to detect and may be more rapidly degraded.

It is difficult to judge the likely effects of reduced C1 levels or increased C1 proportions without understanding the role C1 is playing. If truncated PrP fragments are acting as regulators for full length PrP then it is likely that the proportions of full length and C1 are critical. If C1 and N1 have specific functions then the overall C1 level is likely to become more important.

The increased proportion of C1 in the GlycoD mutants may influence PrP localisation in some cell types. The N-terminal has been shown to be important for several different binding partners, such as LRP1 which is involved in internalisation (Parkyn et al., 2008). Truncated PrP^C lacking the N-terminal should not be able to be internalised as readily as full length PrP^C and should accumulate on the cell surface.

3.4.5 C-terminal Shedding of PrPC

The point mutations introduced in the GlycoD mutants do not influence GPI anchoring as all PrP^C glycoforms were detected in the membrane associated pellet. All glycoforms possess a GPI signal sequence and the GPI anchor is attached at translation into the ER, hence it is a reasonable assumption that the membrane associated PrP^C is attached by a GPI anchor.

Naturally shed PrP^C was not detected in PI-PLC untreated homogenate. PrP^C was detected in the non-membrane fraction but a lack of molecular weight change indicated that this is more likely to be due to inefficient separation. A study using Syrian hamster brain showed that ~10% PrP^C is lacking the lipid moiety of the GPI anchor (Borchelt et al., 1993) thus a small amount of naturally shed PrP would be expected in the GlycoD mice. Naturally shed PrP^C may be lower in mouse than hamster or levels may have been too low to detect by immunoblot.

Treatment with PI-PLC reduced GPI anchored PrP^C but cleaved PrP^C was not always detected. Only a small amount of shed PrP^C could be detected and sometimes none at all. Low levels of cleaved PrP^C could be detected for some samples when the proteins were concentrated and PrP^C was also strongly detected in the membrane associated

pellet fraction. It has been reported that PI-PLC treatment significantly reduces detection on immunoblot, probably due to the negatively charged GPI stub preventing efficient binding to non-specific membranes, such as PVDF (Nishina and Supattapone, 2007). Inefficient binding to the transfer membrane may lead to bound protein levels below the detection limit of an immunoblot. Immunoprecipitation would allow concentration specifically of PrP^C and allow higher concentrations of PrP to be immunoblotted, increasing detection.

3.4.6 Occupancy of glycosylation sites

Wild type PrP shows glycan site occupancy of 78% for each glycosylation site, indicating that neither site influenced glycosylation of the other site. Wild type PrP is usually analysed as three glycoforms, without distinguishing between the two mono-glycoforms so it was not known whether glycosylation was favoured at a particular site. The equal site glycosylation showed that wild type PrP does not favour one monoglycosylated glycoform over the other.

The occupancy of the glycosylation sites and the ratios of glycoforms may have implications on the function of the different isoforms. Many functions have been proposed for PrP^C, from a role in cell signalling to cell survival and neuronal excitability. The importance of the existence of the different glycoforms of PrP^C for function or cell biology is unknown but the diverse functions proposed for PrP^C and the multiple isoforms may indicate separate functions for different isoforms.

In general glycosylation at one site does not determine the glycosylation of another (Opdenakker et al., 1993). Glycosylation of the rabies virus glycoprotein Asn-37 is highly inefficient, possibly due to inaccessibility to glycosylation enzymes but is not significantly increased when other glycosylation sites are deleted (Shakin-Eshleman et al., 1992). Although not common there are examples of different glycosylation sites on the same protein with the ability to influence other glycosylation sites. Human protein C has four potential glycosylation sites which each impart different features. Glycosylation at Asn97 influences the level of core glycosylation at Asn329 (Grinnell et

al., 1991). Glycosylation can slow down folding of the protein allowing a longer exposure of other glycosylation consensus sites to the glycosylation enzymes. Glycosylation is not required for correct folding of PrP; however the glycosylation sites of PrP are close together and the presence of a glycan may hinder accessibility to the other glycosylation site.

Glycosylation is predominantly used as a mechanism to alter the properties of the protein such as improving the activity or stability rather than completely changing the function. Enzymes lacking glycosylation are usually more active, presumably due to steric hindrance of the active site by large glycans, whereas the same glycosylated enzyme is more stable and has a longer half-life (Stevenson et al., 1993). A cell may possess a mixture of the unglycosylated and glycosylated forms of an enzyme to modulate the activity under different cellular conditions. Under stress a cell may rapidly turn over highly active enzyme and maintain less active enzyme (Stevenson et al., 1993). PrP^C has been shown to protect neurons against oxidative stress potentially through beta cleavage (Watt and Hooper, 2005) therefore the multiple glycoforms may be necessary to initiate a correct response. A glycoform may be preferentially selected under stress conditions to increase cleavage and facilitate a more rapid response.

The glycoforms may represent inefficient glycosylation rather than possess individual functions. G1 and G2 mice showed an increase in the amount of unglycosylated PrP compared to the wild type mice. Even when adjusted to reflect the lower overall expression levels the monoglycosylated mutants still expressed significantly higher levels of unglycosylated PrP than wild type mice. PrP null mice only show very subtle adverse phenotypes such as an altered circadian rhythm, increased susceptibility to seizures and neurons are more prone to stress (Tobler et al., 1996, Roucou et al., 2004, Walz et al., 1999). The GlycoD mice have not been subjected to phenotype testing so it may be that a change in glycoform ratios would lead to phenotypes under rigorous testing which may indicate functions of the glycoforms.

In conclusion prevention of glycosylation at one or both sites significantly reduces PrP^C levels. The reduction is due to post-translational processing and may be a result of

increased susceptibility to degradation or altered trafficking and turnover of unglycosylated and monoglycosylated PrP^C. There is no difference in regional levels of PrP^C throughout the wild type brain and the disruption of glycosylation in the GlycoD mutants does not change the distribution of PrP^C.

4 Localisation of PrP^C

4.1 Aims

Disruption of glycosylation decreases the total protein levels of PrP^C and increases the proportion of truncated protein. This chapter aims to assess the overall distribution of PrP^C within the cell and identify whether the glycoforms have an altered ultra-structural localisation of PrP^C on the cell surface. Altered PrP localisation in the GlycoD mutants could account for the changes in protein levels, and influence the function of the protein.

4.2 Introduction

PrP^C is a membrane bound protein localised predominantly on the cell surface with a dynamic and complex lifecycle. It is processed through the secretory pathway and delivered to the cell surface where it is continuously recycled into endosomes and back to the cell surface. Several functions have been proposed which are dependent upon cell surface PrP^C, such as copper buffering at the pre-synapse (Vassallo and Herms, 2003), promotion of neurite outgrowth (Santuccione et al., 2005) and signal transduction (Roffe et al., 2010). PrP^C lacks a transmembrane domain to interact with cytoplasmic proteins therefore interactions with binding partners are important in carrying out some proposed functions or to allow endocytosis.

Recycling of PrP^C relies on binding partners for endocytosis. Interactions with binding partners are therefore important determinants of cellular localisation (Taylor and Hooper, 2007). Glycosylation can affect the localisation in two different ways, either through trafficking to the cell surface or through interactions with binding partners. Glycosylation is important for membrane trafficking for several glycoproteins, such as the rat luteinizing hormone receptor (Clouser and Menon, 2005) and acetylcholinesterase in erythrocytes (Luk et al., 2012). Previous studies with the GlycoD mice have shown that G1 and G2 mice have predominantly cell surface PrP^C, similar to wild type mice, but an increased proportion of intracellular PrP^C. However G3

PrP^C was mainly intracellular indicating that the glycans of PrP^C may have a role in determining the localisation (Cancellotti et al., 2005).

In addition to glycan interactions the unstructured N-terminal also plays a role in internalisation. The N-terminal domain has been proposed as the ligand binding domain for many partners such as LRP1 (Parkyn et al., 2008) and NCAM (Schmitt-Ulms et al., 2001). Deletion of the N-terminal portion of PrP^C reduces internalisation and turnover, suggesting an important role of the highly conserved N-terminal in trafficking and localisation of the protein (Nunziante et al., 2003). The GlycoD mutants have an increased proportion of truncated PrP lacking the N terminal [Chapter 3] so it may be expected that the G1 and G2 mutants have a higher proportion of cell surface PrP^C than wild type mice.

The localisation of the different glycoforms may help to explain the reduced PrP^C levels and the increased proportion of truncated protein demonstrated in previous chapters. The previous study in the GlycoD mutants used immunofluorescence and was not sensitive enough to determine exact localisation so it was not known which intracellular compartments contain PrP^C and the quantities in each organelle type (Cancellotti et al., 2005). It was also not known whether any unglycosylated PrP^C reached the cell surface in the G3 mice. This study will employ electron microscopy to determine the localisation of PrP^C. Electron microscopy allows a greater magnification than confocal microscopy and cell structures can be identified by their morphology. Individual PrP molecules can be identified and their location can be determined by identification of the cell structures. This will allow PrP to be quantified for each organelle, allowing more subtle differences between the GlycoD mice to be identified than immunofluorescence.

PrP^C is difficult to detect at physiological levels using IHC, even in the CNS. Trafficking and localisation has previously been studied in overexpressing models in order to be able to detect PrP^C easily.However, overexpression is not an ideal system for studying PrP cell biology. Saturation of the intracellular transport mechanisms can lead to abnormal intracellular localisation. Overexpression can also lead to toxicity through misfolding and oligomerisation. The localisation will be investigated *in vitro* using

primary cells derived from stem cells of GlycoD mutant embryos to allow PrP to be studied at physiological levels. Previous studies investigated PrP *in vivo* (Cancellotti et al., 2005) however cells will be used in this study in order to confirm that localisation is the same as *in vivo* and in order to establish a system to investigate the trafficking of PrP^C. Primary cells were chosen over immortalised cells as PrP^C has been shown to be involved in neuroprotection against oxidative stress and signal transduction, which may be altered during immortalisation.

The brain consists of both neuronal and glial cells, such as microglia, astrocytes and oligodendrocytes. Glial cells account for a large number of cells in the brain and interact with neurons to provide a support system (Montgomery, 1994). While many studies have concentrated exclusively on neuronal PrP *Prnp* mRNA can also be detected in astrocytes *in vivo* and in isolated microglia cultured *in vitro* (Brown et al., 1990). Astrocytes express much lower levels of PrP^C than neurons and it is not clear whether the function and location of PrP in astrocytes differs from that in neurones (Witusik et al., 2007, Brown, 2004). Trafficking and turnover of PrP^C is likely to be cell specific (Fivaz et al., 2002), therefore establishing individual cultures will allow the localisation of PrP^C in glia and neurons to be analysed.

The glycosylation may not only change the localisation of PrP within the cell but also within the membrane. The GPI anchor causes PrP^C to associate with small, organised microdomains of the membrane known as lipid rafts (Sarnataro et al., 2004) however, PrP^C must bind ligands in order to move out of lipid raft regions and initiate internalisation via clathrin coated pits (Sunyach et al., 2003). The presence or absence of glycans at a particular site may assist ligand binding and increase the amount of PrP^C found in non-raft regions. There may be a different ultra-structural localisation of the glycoforms which may affect the rate of internalisation and therefore the turnover of the protein.

This chapter will investigate the localisation of PrP^C in the GlycoD mice in order to determine whether the glycans influence localisation within the cell and within the membrane.

4.3 Results

4.3.1 Primary cell cultures

In order to identify the localisation of PrP^C primary neuronal and glial cell cultures were derived from the GlycoD mice. Cultures were differentiated from pluripotent stem cells taken from E17 day embryos. Neuronal cultures were established using the neuronal growth factor B-27, which promotes neuronal growth and discourages glial differentiation (Brewer et al., 1993). Glial cultures were established using foetal bovine serum and the glial growth factor, G5 (Vermeiren et al., 2005). Differentiation occurred after 24 hours for glial cells and after 3 days for neuronal cells. Neuronal cultures were cultured for at least 7 days to allow dendritic growth and maturity.

Cells were identified initially by morphology then by ICC to establish that pure cultures were obtained. A neuron specific cytoskeletal marker, microtubule associated binding protein 2 (MAP-2), was used to confirm neurons (Figure 5.1). An astrocyte specific cell marker, Glial fibrillary acidic protein (GFAP) was used to confirm glial cultures (Figure 5.1). Neurons expressed high levels of MAP-2 but no detectable GFAP, showing that they were pure neuronal cultures. Glial cultures expressed high levels of GFAP.

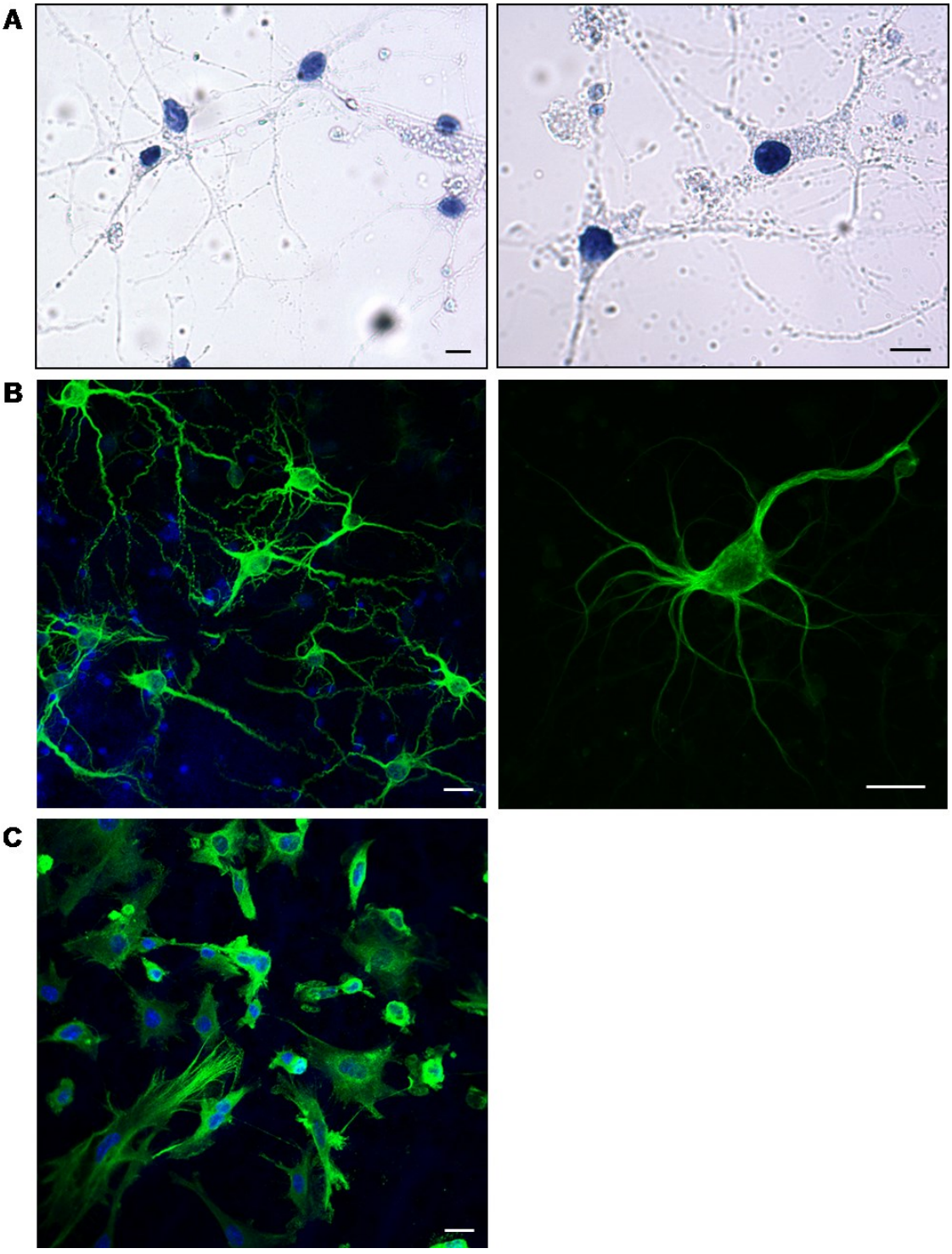

Figure 4.1. Primary cell cultures
(A) Brightfield images of 7 day old haematoxylin stained neurons, showing the characteristic morphology of neurons with dendrites and axons. Cells are initially identified by this morphology. (B) Immunofluorescence of primary neurons showing cytoskeleton (MAP2, green) (C) Immunofluorescence of primary glia stained with GFAP (green). Cells are much larger and flatter than neurons and lack dendrites. Scale bar shows 20 μm.

Characterisation of primary neuronal cultures was carried out to establish whether neurons were mature. Immunofluoresence was used to look at expression of VAMP2, a protein involved in the docking and/or fusion of synaptic vesicles with the presynaptic membrane and GABA, a neurotransmitter involved in the elongation of neurites and the formation of synapses.

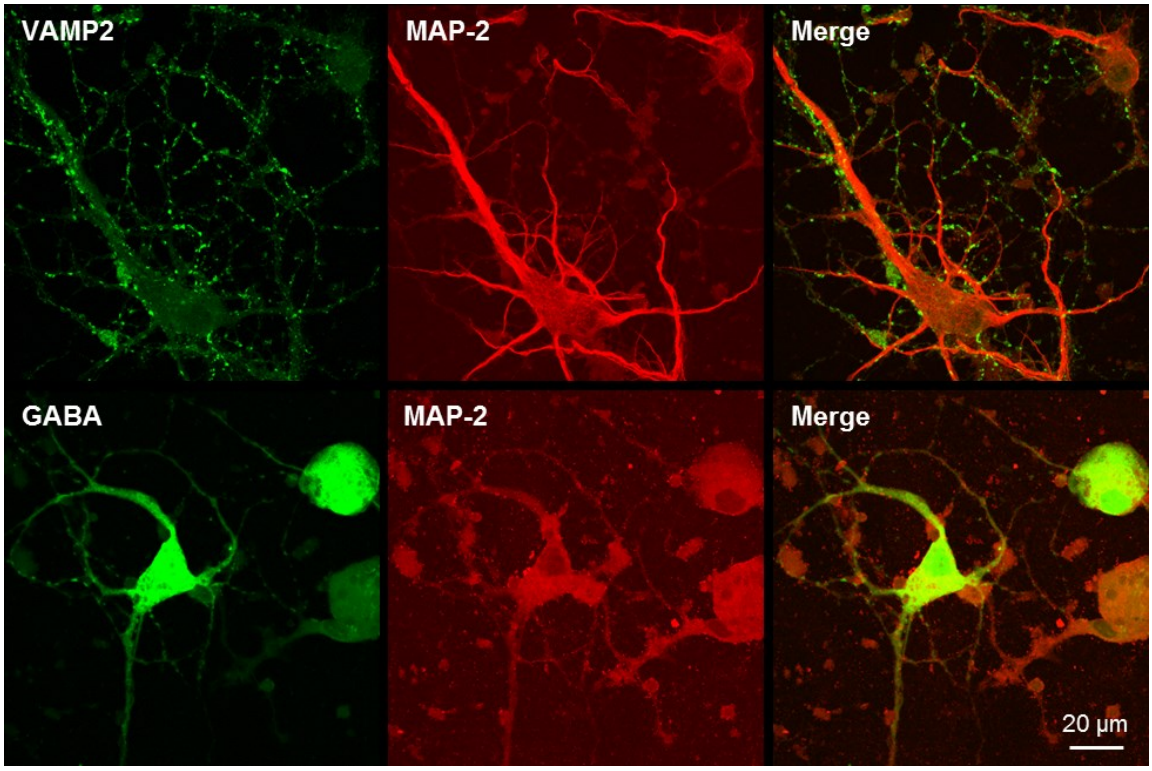

Figure 4.2. Characterisation of primary neuronal cultures
Immunofluorescence of wild type neurons at 10 days showing expression of synaptic vesicles. MAP-2 showed that cells are neuronal and makes the individual dendrites and cell bodies visible to allow localisation of VAMP2 and GABA. VAMP2 is a synaptic vesicle marker showing pre-synaptic vesicles along the dendrites. The GABA neurotransmitter showed variable staining for different neurons and was mainly cytoskeletal.

Cells expressed both VAMP2 and GABA, suggesting that the neurons are mature and expressing synaptic vesicles (Figure 4.2). VAMP2 appeared to be on the cell surface along dendrites, as expected of a vesicle protein. GABA showed weaker staining and variable levels were seen for different neurons.

Cultures showed a low level of differentiated cells and a high level of undifferentiated cells and cellular debris, creating an unfavourable culture environment and reducing the

amount of time the differentiated cells could be kept alive. In addition to the toxicity created by debris and dying cells the low cell density of differentiated cells also hindered culture survival. Neurons that were isolated from other neurons in the culture dish were unable to form connections with other neurons and did not survive for longer than four days. Neurons in clusters that had formed connections between cells could survive for up to 14 days. Neuronal cultures were used for immunofluorescence and electron microscopy at 7-14 days.

A second approach was taken for generating neuronal cultures. The cells isolated from embryos were cultured into neurospheres in order to create stocks of neuronal precursors, which could then be differentiated into neurons. Neurospheres were disrupted to create a single cell suspension and then cultured into differentiated neurons. Less debris and more neuronal differentiation were observed; however success rates in creating neuronal cultures were still less than 50%. Most cultures did not differentiate and once differentiated many cultures did not survive 14 days.

Neuronal cultures were difficult to establish and only 10% cultures were successfully differentiated. Cells did not always differentiate after three weeks of incubation in culture conditions. Undifferentiated cells were adherent and were shown to be viable by trypan blue exclusion. These cells showed no neuronal morphology and remained small and round. ICC showed that they did not express either neuronal or glial markers or PrP^{C}.

4.3.2 PrPC detection in primary cells by immunocytochemistry

Immunofluorescence has been previously used to detect localisation in whole brain slices and showed an altered localisation, particularly in G3 mice (Cancellotti et al., 2005). To establish whether the primary neurons were reflecting the differences in PrP^{C} localisation seen *in vivo* the same method was used to detect PrP^{C} in neuronal cultures. Due to the reported low levels of PrP^{C} in astrocytes three different anti-PrP antibodies were tested to determine whether PrP^{C} could be detected in astrocytes.

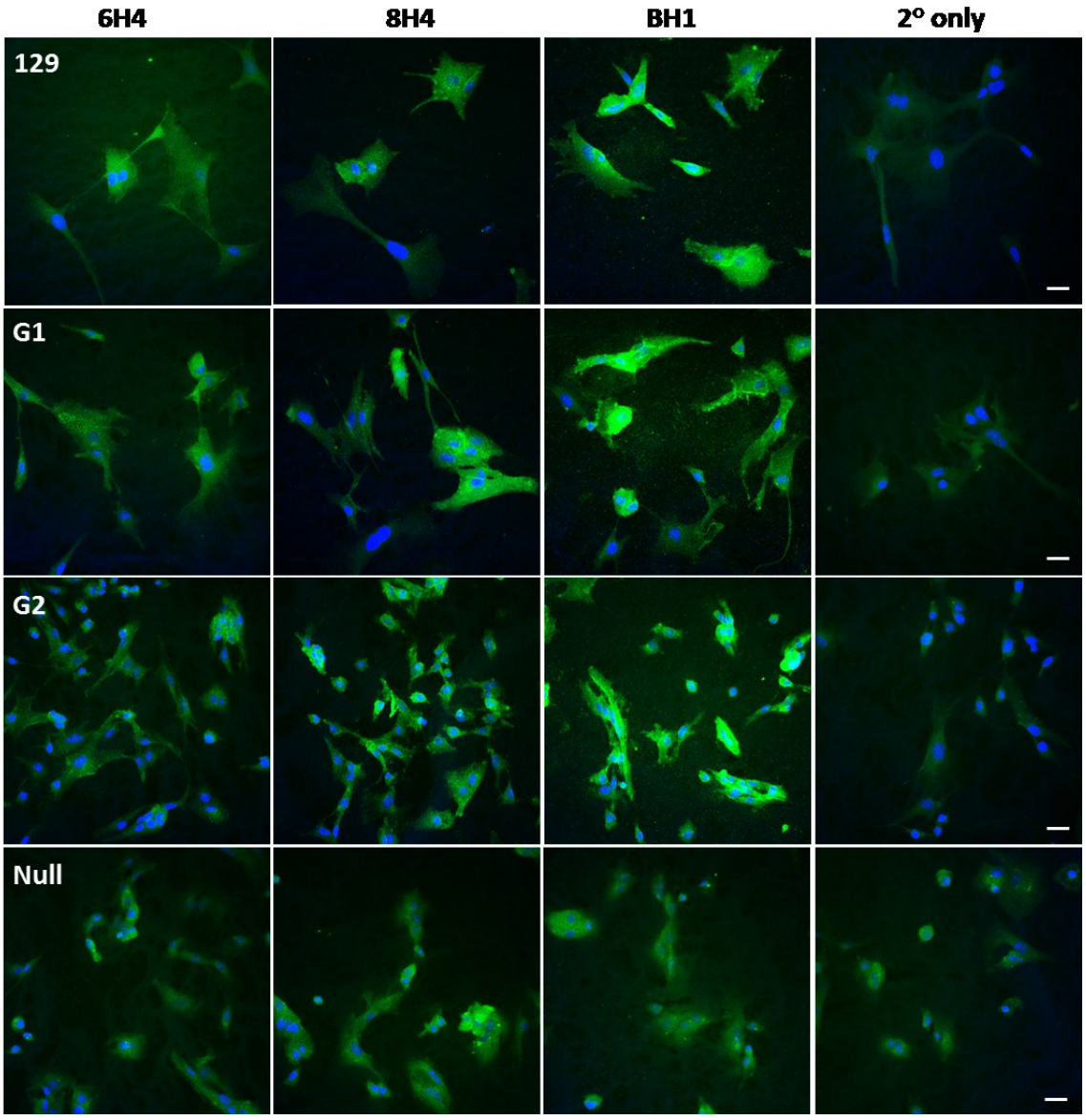

Figure 4.3. Immunofluorescence of astrocytes using different anti-PrP antibodies
Astrocytes were labelled with three different anti-PrP mAbs; 6H4, 8H4 and BH1 at concentrations described (Table 2.2). 6 cultures per genotype were tested with each antibody. No difference in staining was seen between the three different antibodies for specificity of sensitivity. There was no difference between PrP null and PrP expressing cells in PrP fluorescence. The reduced staining in cells that were not treated with anti-PrP antibodies suggests non-specific binding of the primary antibodies. Scale bar shows 20 µm.

Astrocyte cells showed very little difference in staining intensity between the PrP expressing cells and null cells (Figure 4.3), suggesting that there is a level of non-specific binding with all three different antibodies. There were low levels of background staining and possible autofluorescence in cells when primary antibody was omitted.

When antibody concentration was reduced to try to reduce non-specific binding the signal was too weak to differentiate from background.

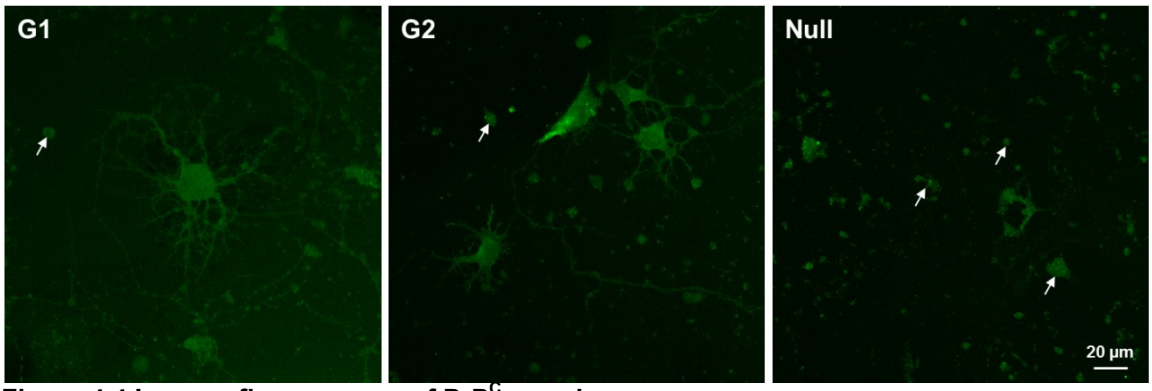

Figure 4.4 Immunofluorescence of PrP^C on primary neurons
Primary neurons were labelled with the anti-PrP mAb 6H4 at concentrations described in Chapter 2. Neurons showed low levels of staining that was difficult to differentiate from background staining and autofluorescence. Null neurons did not show any PrP specific labelling of neurons however there was staining and autofluorescence seen from debris and undifferentiated cells in all cultures (shown by white arrows).

Neurons showed weak immunofluorescence with PrP antibodies. In all genotypes there was considerable autofluorescence and non-specific binding, especially of undifferentiated cells and cellular debris found in the cultures (Figure 4.4). Immunofluorescence was carried out on two different cultures of G1, G2 and null neurons. To reduce the non-specific signal semi-thin sections were used rather than whole cells. Cells were fixed and scraped from the culture dish to form a cell pellet and debris and small undifferentiated cells were removed by centrifugation.

Semi-thin sections were performed on a single culture of each genotype and showed specific PrP fluorescence on wild type and GlycoD neurons that was not observed in null neurons (Figure 4.5). The semi-thin sections reflected the expression levels observed previously by biochemical methods; wild type neurons showed the strongest PrP fluorescence and the GlycoD mutants showed reduced PrP fluorescence.

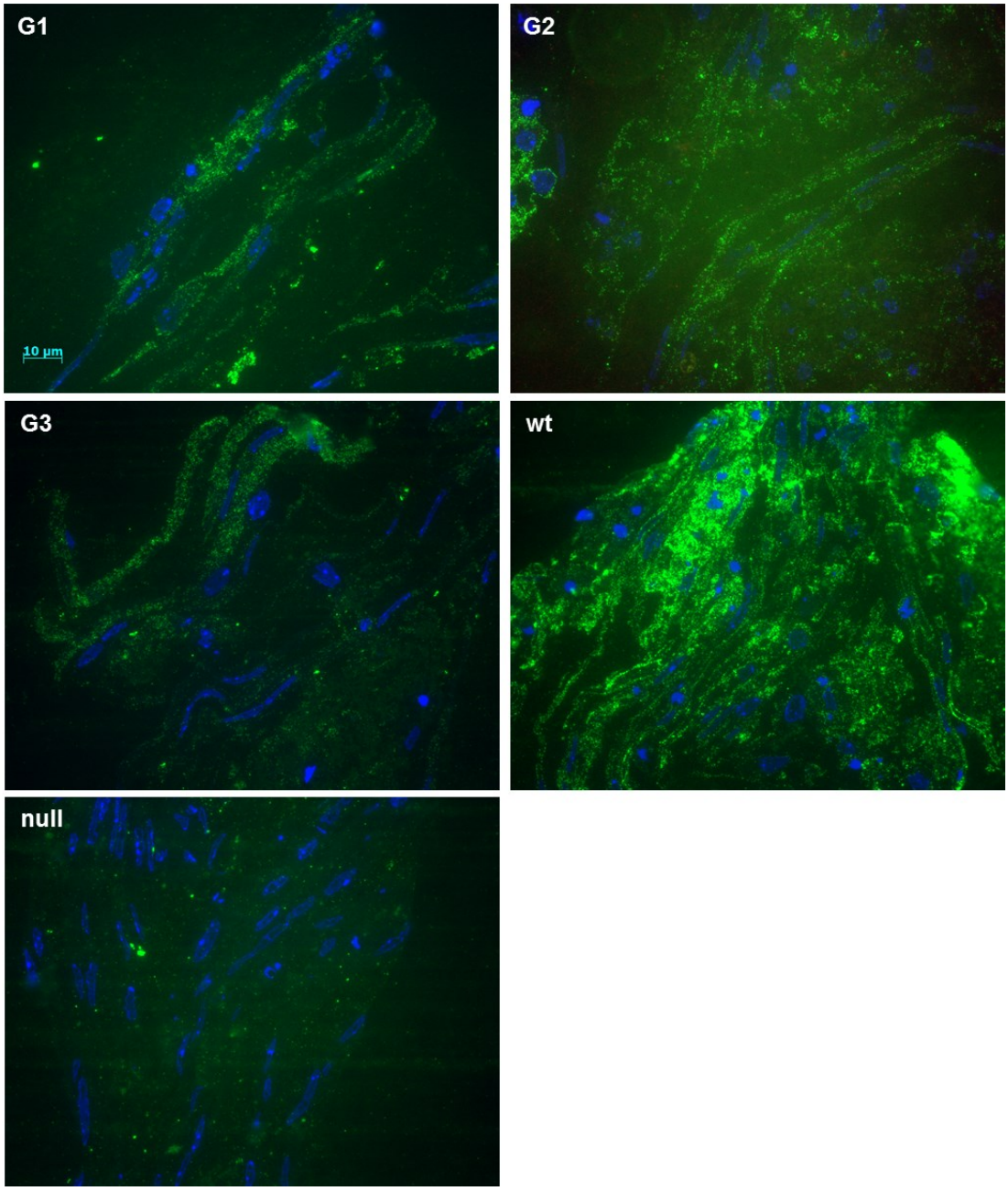

Figure 4.5. PrP staining of semi-thin sections of primary neuronal cultures
Immunofluorescence of primary neurons to visualise PrP^C using anti-PrP mAb F4-31. Staining is much stronger in wild type PrP than in the mutants but is present in all genotypes except for null. Very little background fluorescence was observed in null cells.

Immunofluorescence was not sensitive enough to investigate PrP localisation in cell cultures. PrP^C was difficult to detect by ICC in all cell cultures. PrP^C could be detected on neuronal cultures however fluorescence was weak due to the low expression level. In glial cells it was not possible to detect PrP^C in astrocytes. Electron microscopy was

therefore undertaken in favour of immunofluorescence as individual PrP molecules could be identified and quantified to determine localisation.

4.3.3 Localisation of PrPC on neurons by cryo-electron microscopy

Cryo-electron microscopy was carried out in collaboration with Sue Godsave at the Netherlands Cancer Institute, Amsterdam.

Due to the low detection of PrP^C during immunofluorescence, two antibodies which have demonstrated high sensitivity, mAbs BC6 and F4-31 were used for electron microscopy to determine the optimal detection. Gold was detected on all membranes in all genotypes, allowing electron microscopy to be used to identify PrP^C localisation. There was heterogeneous labelling of PrP in neurons; some expressed high levels and others little or no detectable PrP^C.

Ten micrographs were taken for each genotype from two different neuronal cultures with both antibodies selecting cells that had high levels of PrP^C labelling. The micrographs were grouped by genotypes and blinded. The total gold particles were counted and gold associated with membranes (within 20 nm) were assigned to plasma membrane, Golgi, ER or to vesicles (Figure 4.6). If the structure was not identifiable due to section planes it was counted as a vesicle.

PrP^C null neurons were used as a control for non-specific binding of the primary antibodies, as non-specificity was a problem with immunofluorescence. Neurons showed low levels of gold labelling of the nucleus and occasionally mitochondria (Figure 4.6, C). Gold particles associated with these structures were discounted as non-specific labelling as this was also observed in the null neurons in the absence of gold labelling on other membranes. Null neurons did not show labelling of other membranes such as the plasma membrane or the Golgi (Figure 4.11).

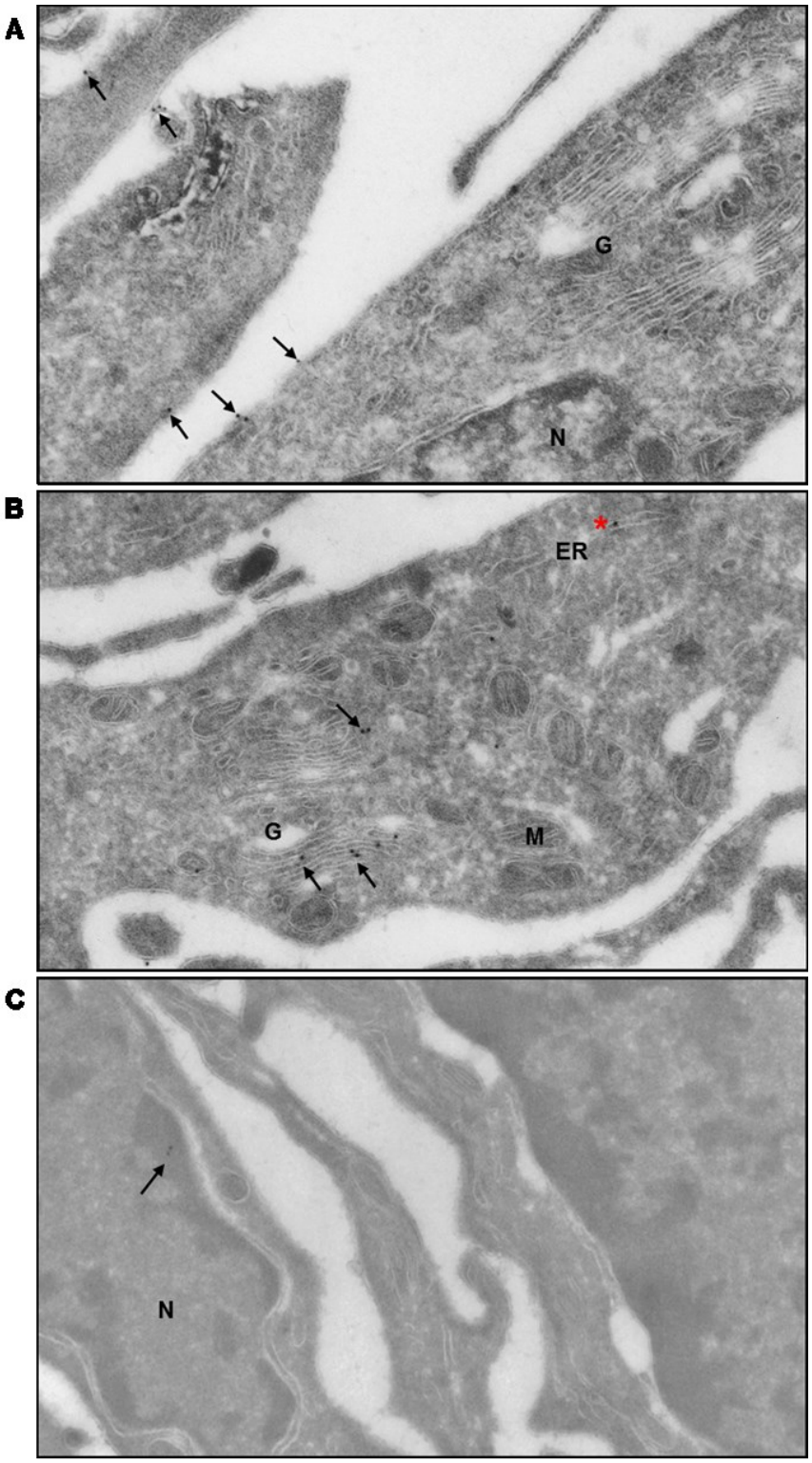

Figure 4.6. PrP^{C} associated with different cellular structures
Cryo-electron micrographs showing PrP^{C} labelling on primary neurons using mAb F4-31 (A) Gold labelling of plasma membrane localised PrP^{C} (arrows) (B) Labelling of PrP^{C} on internal membranes. Arrows show PrP^{C} in the Golgi apparatus. Red asterisk shows ER associated gold particle. (C) Non-specific labelling of nucleus seen on a null neuron. **G** Golgi, **ER** Endoplasmic reticulum, **N** nucleus, **M** mitochondria

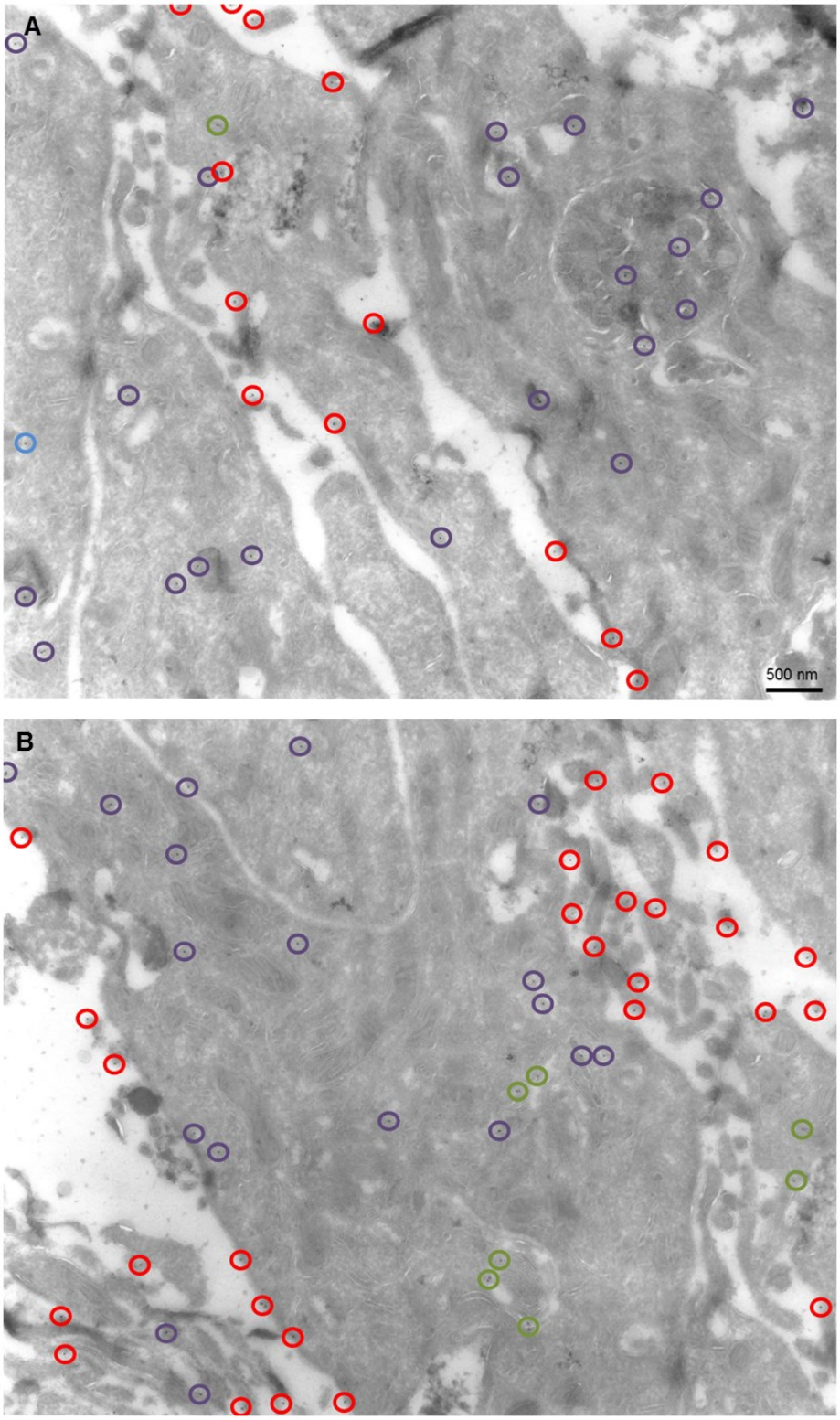

Figure 4.7 Micrographs of wild type neurons
Wild type neurons labelled with anti PrP antibody F4-31 and 10nm gold particles. (A) Micrograph showing predominantly cell body and large dendrites (B) Micrograph showing small dendrites. PrP bound gold particles circled; Red = cell surface, green = Golgi, purple = internal membranes.

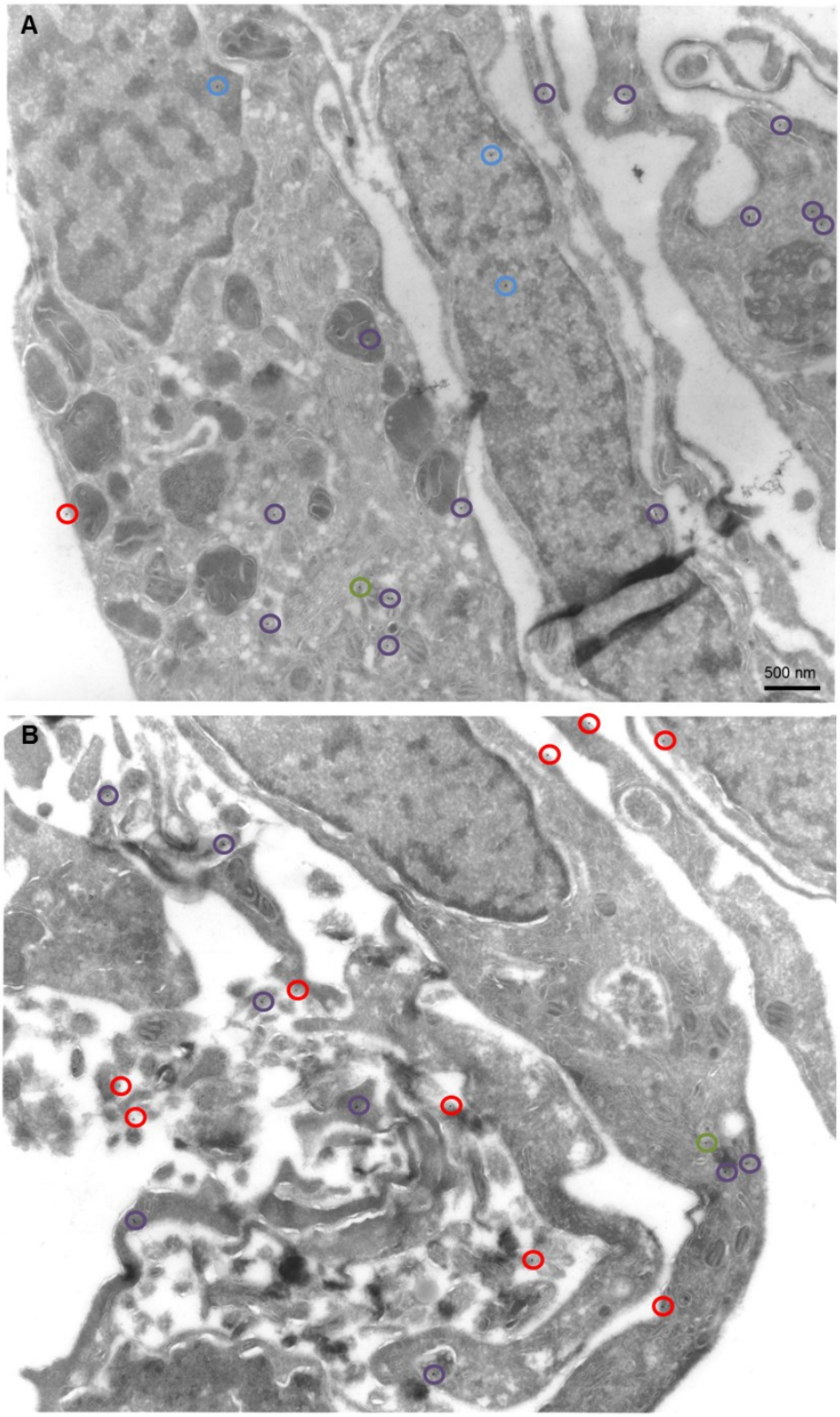

Figure 4.8 Micrographs of G1 neurons
G1 neurons labelled with anti PrP antibody F4-31 and 10nm gold particles. (A) Micrograph sowing predominantly cell body and large dendrites (B) Micrograph showing small dendrites. PrP bound gold particles circled; Red = cell surface, green = Golgi, purple = internal membranes, blue = non-specific.

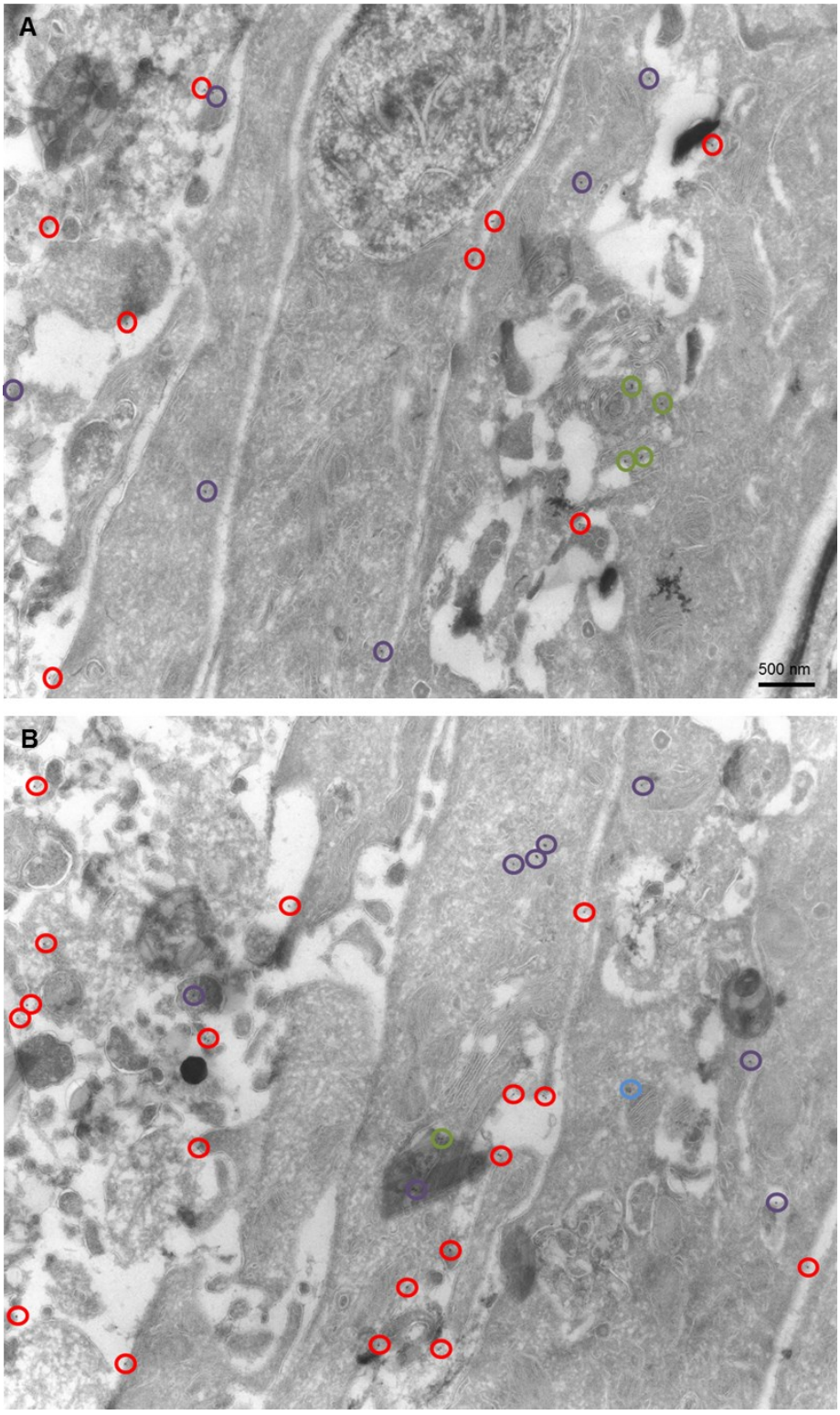

Figure 4.9 Micrographs of G2 neurons
G2 neurons labelled with anti PrP antibody F4-31 and 10nm gold particles. (A) Micrograph showing predominantly cell body and large dendrites (B) Micrograph showing small dendrites. PrP bound gold particles circled; Red = cell surface, green = Golgi, purple = internal membranes, blue = non-specific.

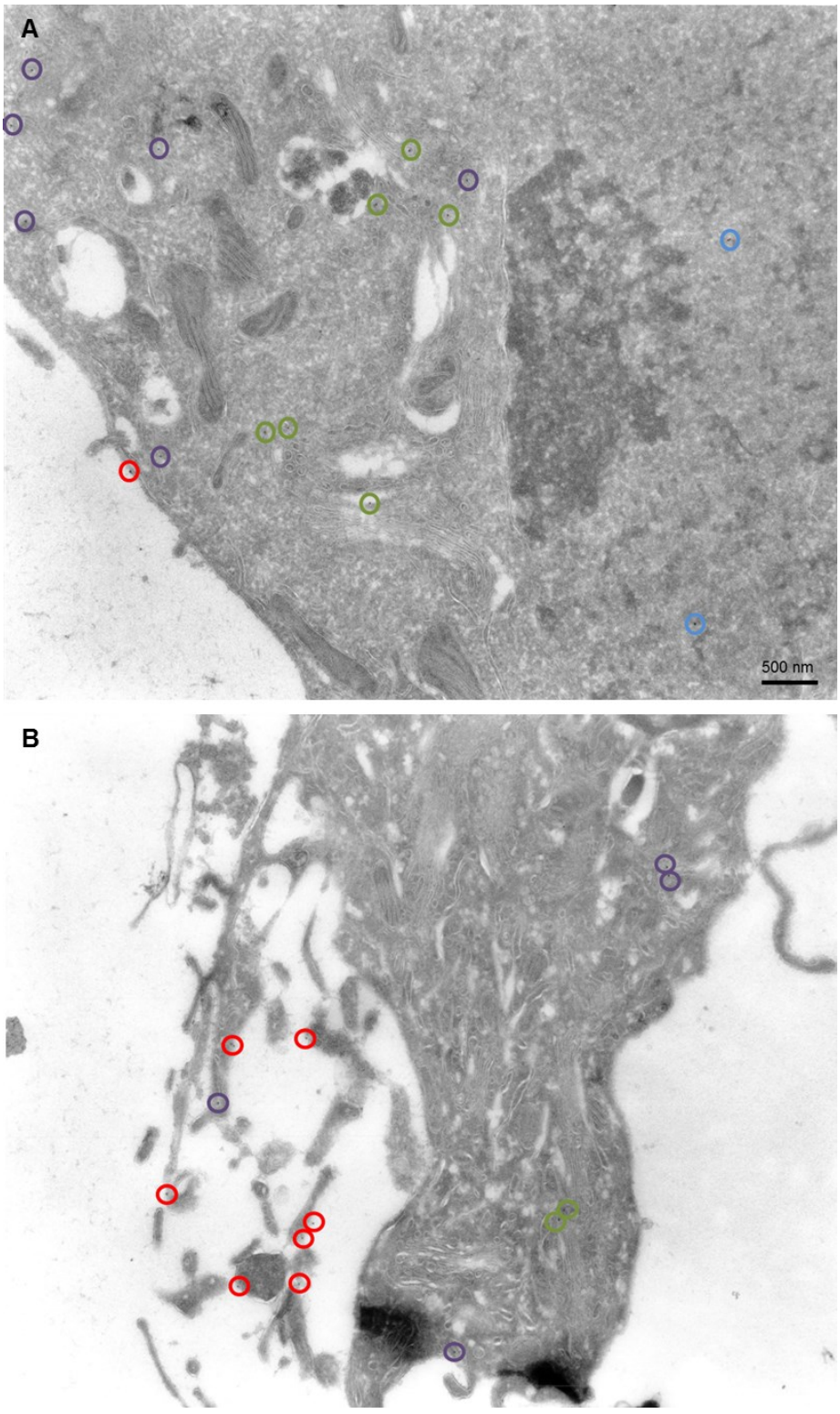

Figure 4.10 Micrographs of G3 neurons
G3 neurons labelled with anti PrP antibody F4-31 and 10nm gold particles. (A) Micrograph showing predominantly cell body (B) Micrograph showing small dendrites. PrP bound gold particles circled; Red = cell surface, green = Golgi, purple = internal membranes, blue = non-specific.

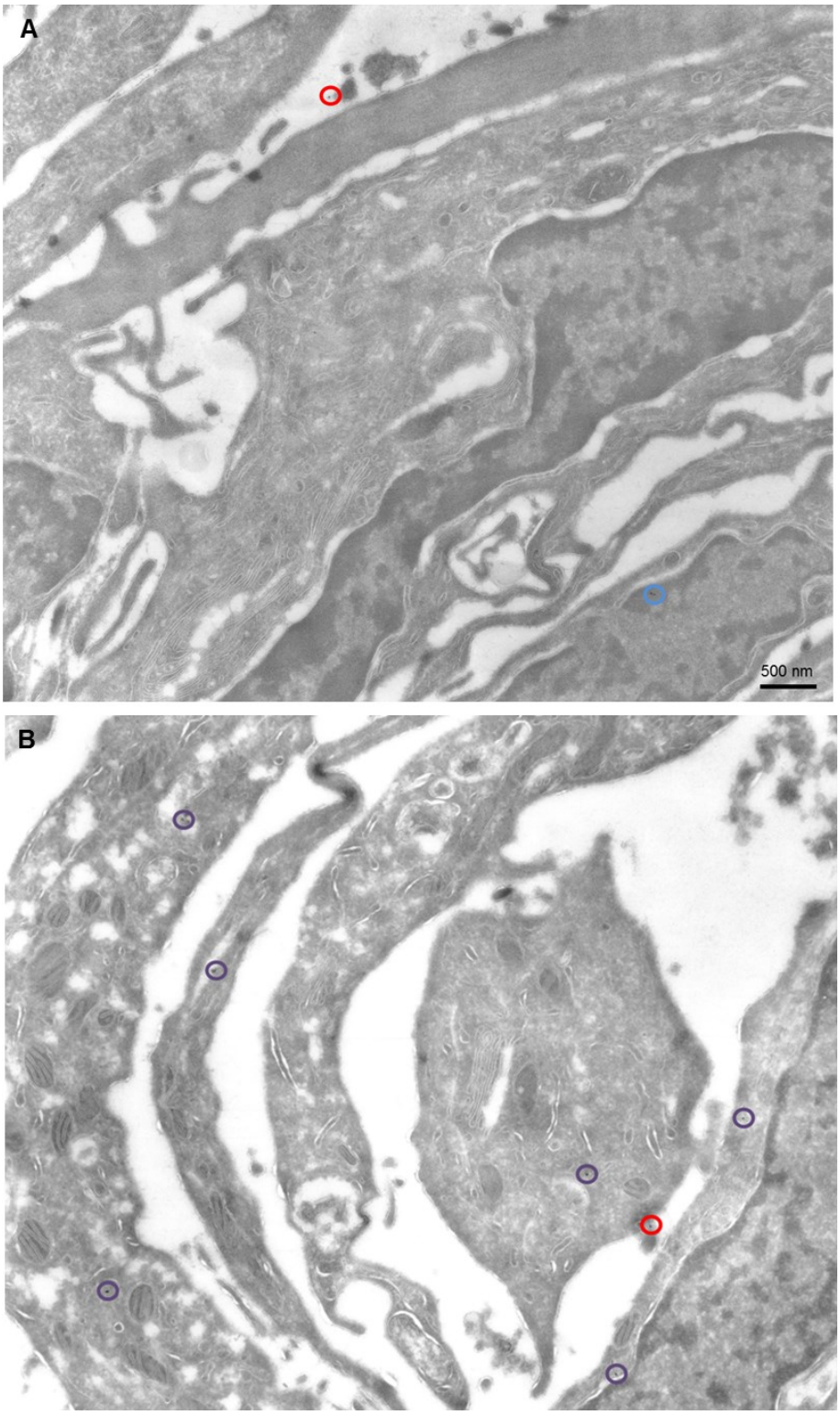

Figure 4.11 Background labelling in null neurons and low level labelling in G3 neurons
Neurons labelled with anti PrP antibody F4-31 and 10nm gold particles. (A) Null neurons with non-specific binding of the nucleus (blue) and a plasma membrane (red) (B) Labelling in G3 neurons was just above background labelling seen in null neurons. Intracellular labelling = purple, plasma membrane = red

Observations about the PrP^C labelling were made using the micrographs before quantification to gain an impression of the distribution. Gold labelling showed reduced PrP^C in all GlycoD neurons, particularly the G3 neurons, reflecting the reduced expression described in Chapter 3.

As expected, wild type neurons showed labelling predominantly on the cell surface with less PrP on the Golgi and ER membranes (Figure 4.7). G1 and G2 neurons also showed substantial plasma membrane labelling but a higher amount of Golgi labelling than wild type neurons, especially in the G2 cells (Figure 4.8 and Figure 4.9). PrP^C was found on all cell membranes in G3 cells. Gold labelling on the plasma membrane was very low and most PrP^C tended to be associated with internal membranes. There appeared to be a high level of Golgi associated PrP^C (Figure 4.10).

PrP^C localisation in neuronal cultures reflected the localisation observed in murine brains suggesting that primary cell cultures are a good model for studying the ultrastructural localisation of PrP^C in the GlycoD mutants. Using electron microscopy to detect PrP^C it was observed that there was a high variability in labelling of neurons for PrP^C within the same genotype. Some neurons had high levels of PrP^C labelling whilst some showed little or no labelling. Different neuronal types express different levels of PrP *in vivo* (Ford et al., 2002a) therefore the variability from cell to cell could indicate that cultures comprise a mixed neuronal type population. Immunofluorescence to detect GABA in the neuronal cultures showed some strongly positive neurons and others with only weak positivity (Figure 4.2) which also indicated different neuronal types. Cultures were created from whole brains and given a pan-neuronal growth factor rather than establishing a single neuronal type as it was possible that PrP^C had a different localisation for different cells.

4.3.4 Quantification of PrPC labelling by electron microscopy

Preliminary impressions of the micrographs showed a difference in PrP^C labelling of the different GlycoD neurons.Therefore, the gold particles were counted and quantified to allow a more accurate description of the localisation. Monoclonal antibody F4-31

showed the highest level of labelling so was chosen for quantification. To eliminate the variability of size of organelles the labelling density was calculated to show gold per μm membrane. Membranes were measured using a 1.2cm square grid and counting the number of times a membrane bisected the grid lines. Labelling density was calculated using the formula

Gold labelling density = gold/(grid intersections*distance between grid lines)

Labelling was quantified for plasma membrane and intracellular organelles using a semi-random method. Whole cells are too large to be captured on a single micrograph; therefore certain structures may be biased. An individual micrograph may favour plasma membrane if axons and dendrites are captured, equally a micrograph with cell bodies would be expected to be predominantly Golgi and under-represent plasma membrane. To avoid bias five micrographs that had predominantly plasma membrane and five micrographs that had predominantly Golgi and internal membranes were taken so that all structures were represented during quantification. Due to low gold labelling for all genotypes the gold counts were combined for all micrographs of the same genotype.

Gold labelling could not be accurately quantified for G3 neurons due to the overall low levels of labelling.

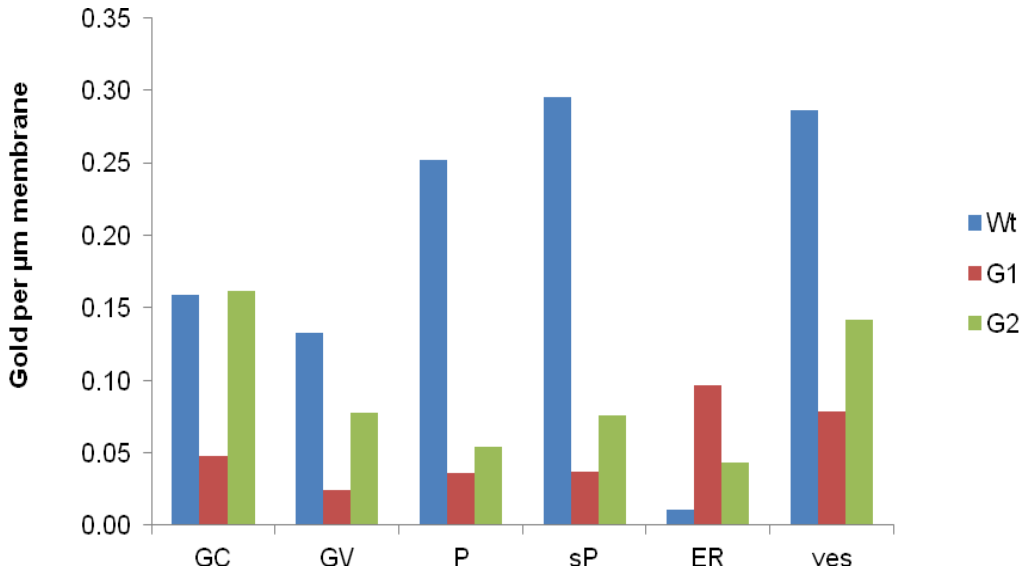

Figure 4.12. PrP^C labelling in different cell regions
Labelling density was carried out to measure the amount of gold per µm membrane. GC=Golgi cisternae; GV= Golgi vesicles; P=plasma membrane, cell body &processes > 200 nm across; sP = plasma membrane of processes up to 200 nm across; ER = endoplasmic reticulum; ves = other vesicles, outer membrane. Both G1 and G2 have a 5-fold reduction of PrP^C on the cell surface. Wild type and G1 neurons have similar amounts of PrP on non-Golgi internal membranes whilst G2 and wild type have similar amounts of Golgi associated PrP^C.

Wild type neurons had the highest labelling density for all membranes except the ER, which reflects the higher expression observed in Chapter 3 (Figure 4.13). G2 had a higher labelling density than G1 for all membranes except the ER. Wild type neurons showed almost three times more labelling on the cell surface in comparison to the GlycoD mutants and twice as much PrP^C in vesicles. All GlycoD mutants express less PrP therefore it is not unexpected that mutants showed reduced labelling along membranes. Due to the low levels of PrP and high variability between micrographs no significant difference after statistical analysis was seen for any membrane for any genotype.

The differences in PrP^C levels made comparisons between genotypes difficult. The labelling densities were used to calculate the distribution of gold throughout the cell for each individual genotype. Labelling of each membrane was calculated as a percentage of total PrP for each genotype.

Labelling density was combined from ER and vesicle membranes and expressed as other internal membranes. ER membranes can be hard to identify from micrographs if the membrane is bisected at an unfavourable angle thus it is likely that some ER gold counts are included as vesicles rather than ER. Small and large dendrites were also combined to show total surface PrP^C.

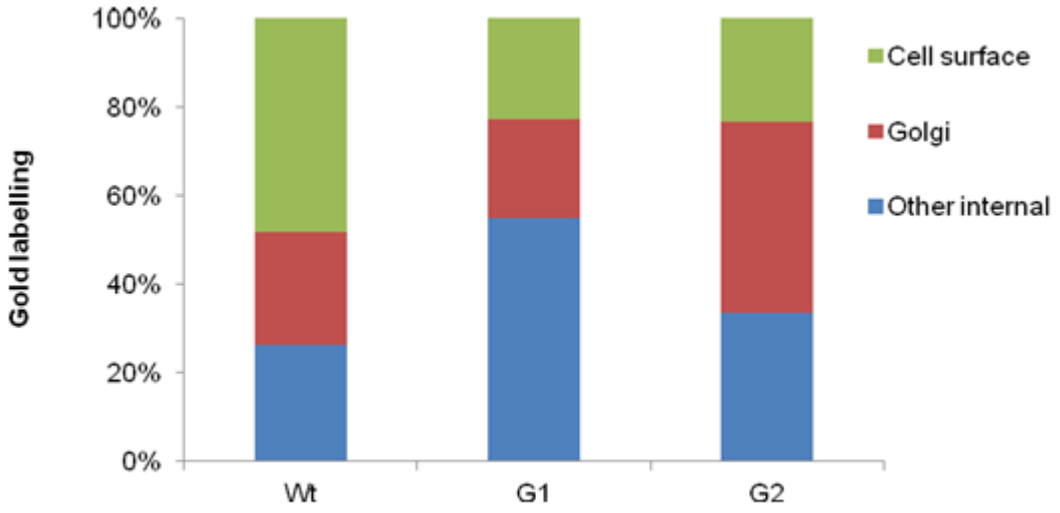

Figure 4.13. Distribution of PrP^C in different cell regions
Labelling density of PrP^C from 10 micrographs was used to calculate the percentage of PrP^C on each membrane. 50% wild type PrP is found on the cell surface, whilst only 20% is found on the cell surface of G1 or G2 neurons. G2 cells had larger amounts of Golgi labelling than both wild type and G1 cells, which had similar amounts. G1 cells had much higher labelling of PrP^C on other internal membranes. This could represent either newly synthesised immature PrP^C or mature PrP^C that has been internalised from the cell surface.

Surface PrP^C was reduced in GlycoD mutants. Almost half of the PrP^C in wild type neurons was localised to the cell surface, whereas G1 and G2 only had around 20% on the cell surface. G2 mutants have a larger proportion of Golgi associated PrP^C than both G1 and wild type neurons (Figure 4.13), although gold labelling of the Golgi was at similar levels in wild type and G2 neurons. G1 cells have a higher proportion of internal PrP^C that is not associated with the Golgi. This may represent PrP^C retained in the ER or may represent PrP^C in endocytic vesicles.

PrP^C localisation in neuronal cultures reflected the localisation observed in murine brains suggesting that primary cell cultures are a good model for looking at the ultrastructural localisation of PrP^C in the GlycoD mutants.

4.3.5 Endo H sensitive PrPC in wild type, G1 and G2 mice

Electron microscopy showed that G1 and G2 mice had higher labelling of the ER than wild type mice (Figure 4.12), however ER can be difficult to identify on micrographs. It is likely that some ER labelling from the micrographs was not identified as ER and labelling was included with other vesicles. In order to confirm this increase in the mutants PrP^C in the ER was detected biochemically using Endo H to remove mannose rich oligosaccharides. Endo H is only able to remove the immature glycans that are present in the ER and not the mature glycans that are modified in the Golgi. Localisation of the glycoforms appeared to be the same in brain and cells (Figure 4.13) (Cancellotti et al., 2005) therefore brains were used to look at the amount of immature PrP^C in the ER.

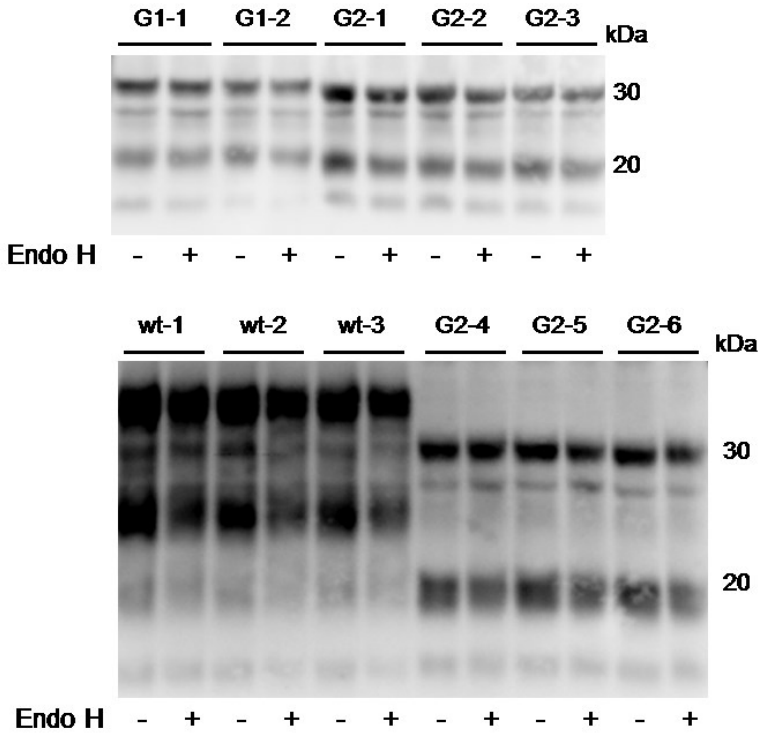

Figure 4.14 Immunoblots of Endo H treated PrP^C
10% brain homogenates were treated with and without 2500 Units Endo H for 24 hours and then run on an immunoblot. Three different mice per genotype were assessed in triplicate. Densitometry was carried out to compare the ratios of the glycoforms before and after treatment with Endo H.

Brain homogenate was divided into two and one aliquot treated with Endo H for 24 hours. Densitometry was carried out on immunoblots for all glycoform bands (Figure 4.14). Endo H sensitive PrP^C was detected as a decrease in diglycosylated PrP for wild type mice and a decrease in monoglycosylated PrP for G1 and G2 mutants when compared with untreated homogenates.

Immunoblots showed a very subtle difference that was difficult to assess without quantification. After Endo H treatment the diglycosylated (wild type) and monoglycosylated (G1 and G2) bands were reduced and the unglycosylated bands were increased as immature glycans were removed. Wild type mice showed a slight increase in monoglycosylated and unglycosylated PrP as glycans were removed from diglycosylated PrP

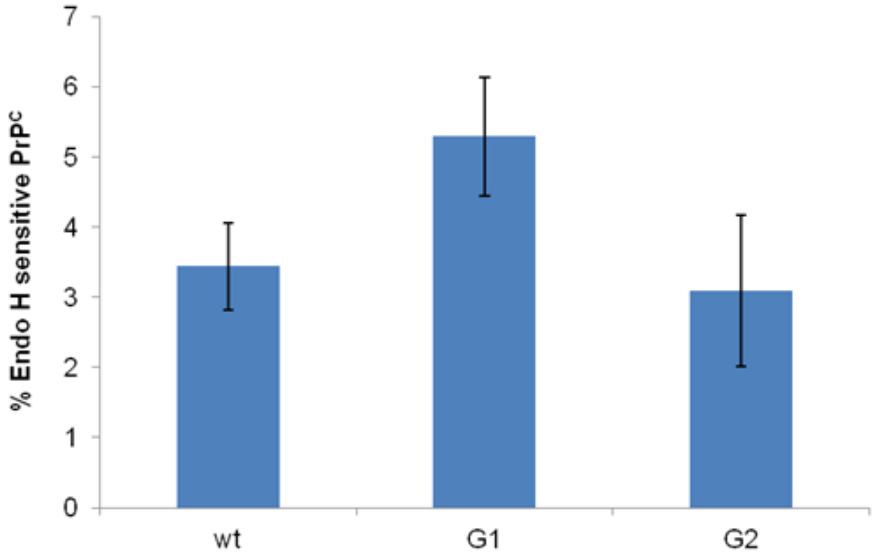

Figure 4.15 Level of Endo H sensitive PrP^C
Densitometry was carried out on immunoblots to calculate the change in each glycoform after treatment with 20,000U Endo H for 24 hours. Changes were very subtle, between 3 and 5% and not significant for any genotype. G1 mice had a higher level of Endo H sensitive PrP^C than wild type or G2 mice.

Although there was no significant difference between the genotypes the G1 mice tended to have more Endo H sensitive PrP than the wild type and G2 (Figure 4.15). There was no difference between G2 and wild type, suggesting that the level of PrP^C in the ER is the same for both genotypes. This result reflects the increase of PrP^C in the ER of G1 mice determined by electron microscopy.

4.3.6 Lipid raft isolation

The GPI anchor localises PrP to the lipid rafts, however binding partners cause PrP to move out of the lipid rafts for internalisation, which may be affected by the glycosylation status of PrP. To investigate the ultra-structural localisation of PrP^C lipid rafts were isolated from non-lipid raft membrane regions based on the selective insolubility of rafts in the presence of detergent at 4 °C, then separated out on a sucrose gradient. Fractions were collected and probed on an immunoblot to detect PrP^C (Expected fractions shown in Figure 4.16).

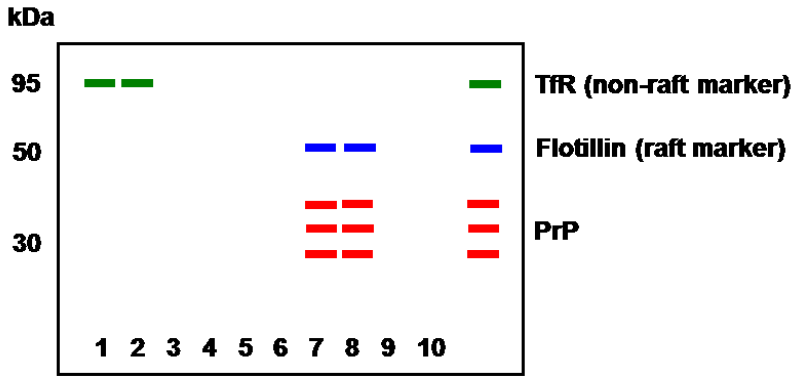

Figure 4.16. Expected lipid raft isolation profile on an immunoblot
Diagram showing expected western blot after lipid raft isolation on a sucrose gradient. Fraction 1 is the bottom of the gradient and fraction 10 is the top. Insoluble proteins, such as the raft marker and PrP will float to the 5-30% gradient interface, which is seen in fractions 7 and 8. There are many more soluble proteins, such as the non-raft marker so these will float with the denser gradient in fractions 1 and 2.

Lipid rafts are preferentially isolated from cell cultures rather than brains, due to the high myelin content in tissues which can contaminate lipid rafts and hinder separation on the gradient (Persaud-Sawin et al., 2009). Due to difficulties in culturing neurons in large quantities limited amounts of cell cultures were available and were prioritised for electron microscopy studies. Brain material was readily available in sufficient quantities hence lipid rafts were isolated using a method developed for brain material.

A variety of factors influence the detergent insolubility and physical separation of membrane regions therefore several conditions were changed to optimise separation (described below).

4.3.6.1 The effect of temperature on separation

Membrane regions are separated based on the differential solubility at 4 °C. At 37 °C both lipid rafts and non-raft regions are soluble; however at 4 °C lipid rafts become insoluble and non-rafts remain soluble.

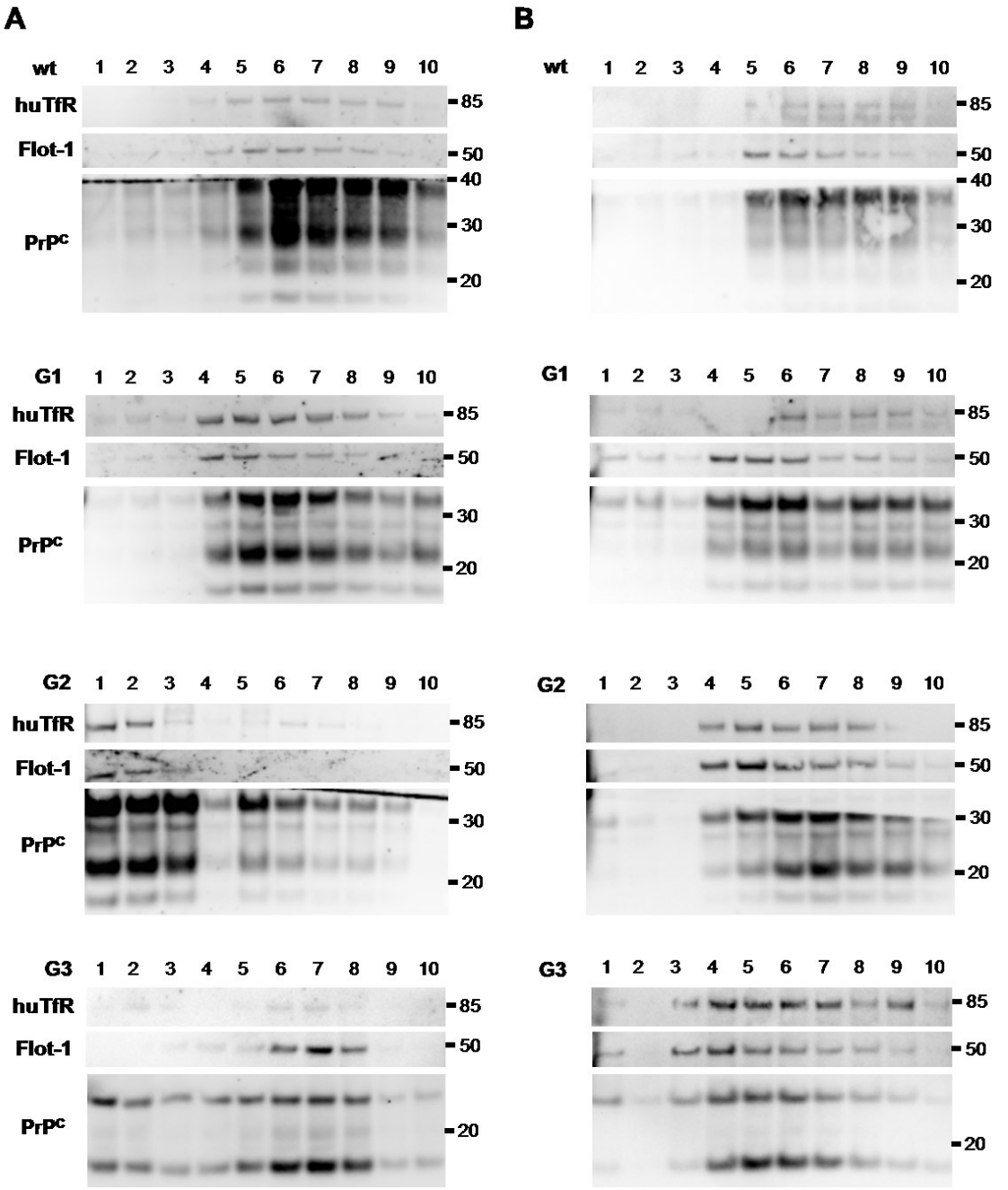

Figure 4.17 Comparison of solubilisation at 4 °C or 37 °C
Immunoblots of each genotype of gradients carried out at (A) 4 °C and (B) 37 °C. All 4 genotypes were carried out at the same time for each temperature but different brains were used for the different temperatures. Transferrin receptor (huTfR), the non-raft marker is shown in the top panel; flotillin (Flot-1), the raft marker is shown in the centre panel and PrP^C is shown in the bottom panel. Fraction 1 is the bottom of the gradient and fraction 10 is the top of the gradient.

Separation was carried out at 4 °C as described by (Parkin et al., 1997) (Figure 4.17, A). When solubilised at 4 °C PrP was found in most membrane fractions but there was no separation of raft and non-raft proteins. In an attempt to improve separation the method

was carried out at 37 °C using a more physiological buffer that is thought to stabilise the membranes better (Chen et al., 2009) (Figure 4.17, B).

Isolation was carried out four times using two different brains at each temperature. Isolation at 37 °C appeared to show the genotypes to be more similar with each other than at 4 °C; however neither protocol showed separation of the raft and non-raft markers and PrP was predominantly localised with both markers. This suggests that temperature may play a role in gradient formation and the speed the sample floats up the gradient rather than solubilisation. At 4 °C the sample may take longer to float to the appropriate density, producing the variable results and proteins found in the lower fractions for some gradients.

4.3.6.2 The effect of gradient on separation

Soluble and insoluble proteins are separated by floatation on a discontinuous sucrose gradient, made up of 30% and 70% sucrose. The majority of the membranes and membrane bound proteins are soluble and have a low buoyancy therefore sink to the bottom of the sucrose gradients and are found in fractions 1-3. Insoluble proteins are found at the gradient interface.

Three different brains were separated on a gradient in quadruplet and the number of fractions PrP^C was detected in was very variable within the same brain homogenate. PrP^C was detected in either a few discreet fractions or in all fractions along the gradient.

The refractive index was measured for each fraction to establish that a gradient was being formed and maintained during centrifugation (Figure 4.18). A discontinuous gradient was present at 0 and 4 hours. After 18 hours at 100,000 x *g* the sucrose had formed a continuous gradient without an interface between the different sucrose solutions.

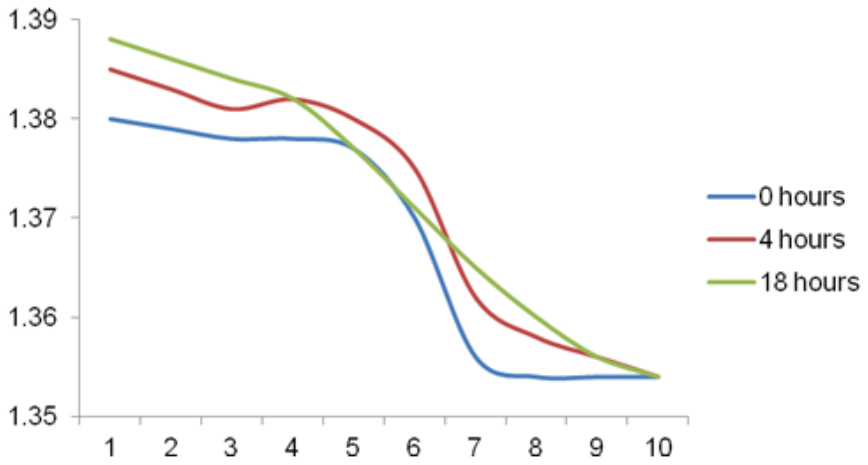

Figure 4.18 The influence of centrifugation time on gradient type
A sucrose gradient was set up as described in the methods but without adding homogenate and centrifuged for different lengths of time. The refractive index was measured for each fraction to assess the density gradient. All sucrose solutions formed a gradient. The initial sucrose solutions formed a discontinuous gradient and this was still present after 4 hours. After 18 hours of centrifugation the gradient had changed to a continuous gradient. (n=4 per centrifugation time)

Initially a sucrose gradient was set up with equal volumes of 30% and 70% sucrose, however PrP was found in fractions 2 to 7 without a gap between raft and non-raft proteins (Figure 4.19, A). To improve separation the gradient was set up with three times the amount of 70% sucrose so that the gradient interface and lipid raft proteins were in fractions 7-8 (Figure 4.19, B). A 3:1 sucrose gradient showed a shift in the fractions that PrP^C was seen in which would improve the separation of the raft and non-raft proteins.

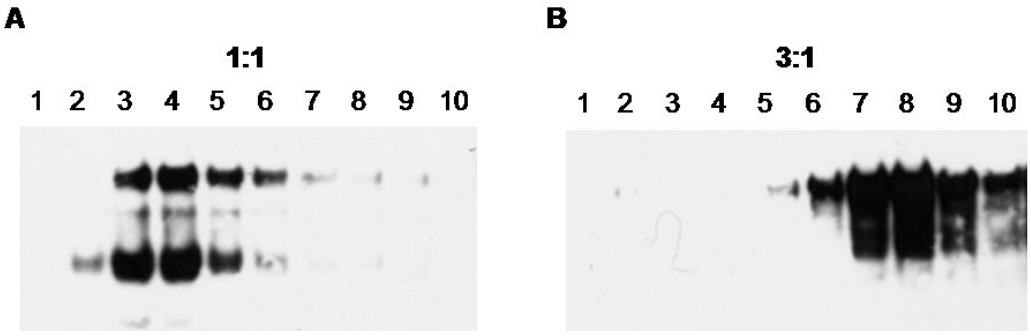

Figure 4.19 Different sucrose gradients change the interface fractions
Immunoblots showing insoluble wild type PrP at the gradient interface with (A) an equal volume of 70% and 30% sucrose and (B) 3:1 ratio of 70% sucrose to 30% sucrose. A 1:1 gradient showed PrP predominantly in fractions 3-5 whilst a 3:1 gradient moved the interface to fractions 7-9 allowing a clearer separation from soluble proteins found at the bottom of the gradient.

4.3.6.3 The effect of detergent concentration

The detergent concentration plays a role in the solubility of rafts; too little and non-raft membranes are not solubilised, too much and rafts become solubilised. Different dilutions of detergent were tested in duplicate on the same wild type homogenate to identify the best detergent concentration (Figure 4.20).

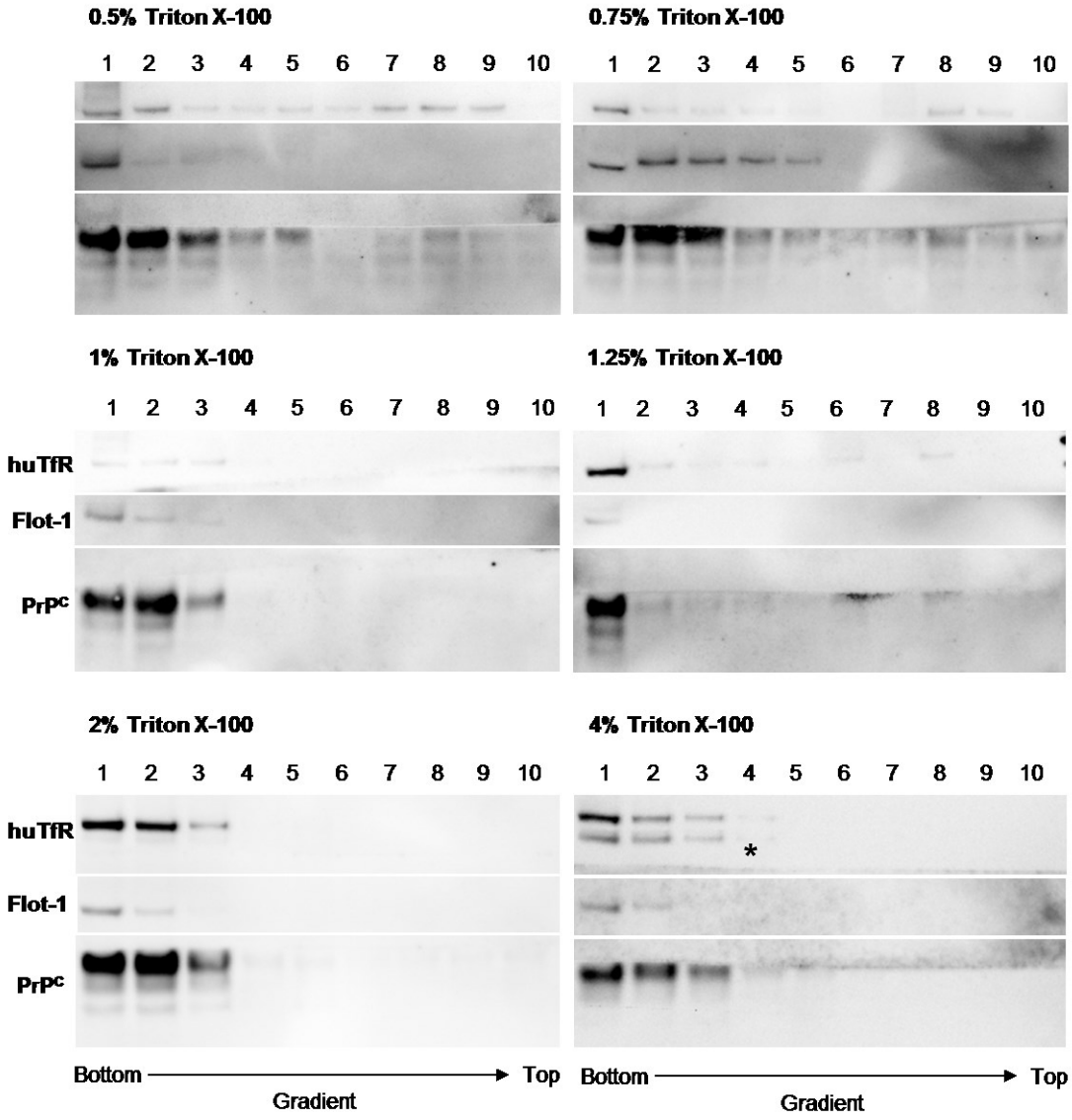

Figure 4.20 The effect of detergent level on the solubility of PrP^C
Wild type brain homogenates were solubilised at 37 °C with different concentrations of Triton X-100 and separated on a discontinuous gradient. 1% is the standard level of detergent described in the protocols used. Higher levels of detergent reduced the number of fractions PrP was found in, although PrP was found in the soluble fractions with all detergent concentrations used. The transferrin receptor was seen as a doublet with 4% detergent (labelled with asterisk). The lower band probably corresponds to a degradation product (Vidal et al., 1997) and was observed in some immunoblots but not others.

Adjusting the protein:detergent ratio altered the fractions that PrP was found in; however it did not alter the differential solubilisation of membrane regions. It was not possible to isolate lipid rafts from non-raft regions of the membrane using whole brains. There was a high variability and lack of reproducibility seen in isolating lipid rafts and

there was no difference in localisation of raft and non-raft markers during fractionation therefore it was not possible to assign PrP to a raft or non-raft fraction.

Isolation of rafts using detergent has been controversial. It has been reported that detergents may create rafts as artefacts of the preparation (Lichtenberg et al., 2005), redistribute gangliosides and alter raft properties (Heffer-Lauc et al., 2005) or interfere with organelles and raft integrity (Suneja et al., 2006). Different detergents can yield different subsets of detergent resistant membranes with unique properties (Chen et al., 2007). Another GPI anchored protein, Thy-1, was found in distinct lipid rafts from PrP^C (Brugger et al., 2004). Different methods have been developed which bypass the use of detergents however there was still significant membrane contamination of raft fractions and low yield (Song et al., 1996, Smart et al., 1995, Macdonald and Pike, 2005).

4.4 Conclusions

4.4.1 Localisation of PrPC

Glycosylation of PrP^C has the ability to alter localisation of the protein within the neurons. Glycosylation is not essential for cell surface expression but the GlycoD mutants have demonstrated that it is important for efficient surface expression. All glycoforms can be trafficked to the cell surface as a small amount of G3 PrP^C was seen on the plasma membrane.

Previous localisation work on the GlycoD mice has shown that unglycosylated PrP in the G3 mice was intracellular (Cancellotti et al., 2005). This study has shown that although G3 PrP is predominantly intracellular a small amount is localised to the cell surface. Many of the proposed functions of PrP require cell surface PrP therefore the presence of unglycosylated surface PrP^C suggest that unglycosylated PrP is able to carry out these functions.

Previous studies using G1 and G2 mice showed PrP expressed on the cell surface but a higher proportion of intracellular PrP in comparison to wild type mice (Cancellotti et

al., 2005). Co-localisation with ER and Golgi markers indicated that PrP was most likely in the Golgi. Electron microscopy in this study showed that G1 and G2 mice had a reduction in cell surface PrP^C. There was no difference in the amount of surface PrP^C between G1 and G2 cells; however there appeared to be a difference in internal localisation suggesting that glycans at the different sites influence trafficking.

G1 neurons showed a higher level of ER associated PrP^C by cryo-electron microscopy than G2 neurons. An increase in Endo H sensitive PrP^C was also seen, albeit subtle. This ER associated PrP in the G1 mutants likely represents protein that is retained in the secretory pathway prior to being trafficked to the cell surface as the glycans retained the sensitivity to Endo H and had not yet been matured in the Golgi. G2 mice showed a similar proportion of PrP^C in the ER as wild type neurons; however 40% PrP^C associated with the Golgi. The high proportion of Golgi PrP could be a reflection of slower trafficking to the cell surface or a higher proportion of retrograde transport back into the Golgi from the cell surface.

Localisation *in vivo* was determined using immunofluorescence and confocal microscopy (Cancellotti et al., 2005) thus the sensitivity was not enough to see the exact localisation or to quantify the amounts of PrP on the cell surface. This study employed electron microscopy to increase sensitivity and to allow quantification of PrP^C on the different membranes, allowing differences in G1 and G2 mice to be identified.

The glycan at the first site, which is abolished in G1 mutants, may assist transition of PrP^C from the ER to the Golgi. A mutation in the human PrP gene, T183A, abolishes the first glycosylation site and causes familial CJD (Grasbon-Frodl et al., 2004, Nitrini et al., 1997). Similar to G1 neurons, murine PrP with a T182A mutation is predominantly localised in the ER, and has been shown to have a shorter half-life than wild type PrP (Campana et al., 2006). However, T182A PrP is partially protease resistant whereas G1 PrP remains PK sensitive. G2 neurons had a higher proportion of Golgi-associated PrP^C than G1 cells, so unlike G1 cells PrP is not being retained in the ER.

PrP^C localised to the cell surface is distributed equally to small processes (<200 nm) and to cell bodies and larger processes (>200 nm) in wild type neurons. Surface labelling was also equally distributed between large and small processes for the G1 and G2 mutants. PrP^C is reported to localise to synapses (Herms et al., 1999) therefore it would be expected that smaller processes would be heavily labelled and larger processes less so. PrP^C also localised along developing axons and dendrites *in vivo* (Moya et al., 2000). Neuronal cultures showed limited viability and a lifespan of less than 14 days therefore were used at 7-10 days old and axons were potentially still growing.

It was not possible in this study to identify the proportion of PrP^C associated with lipid rafts in the GlycoD mice. In hindsight, isolation of lipid rafts would only identify large differences in localisation due to the complex trafficking of PrP^C. In wild type cells a proportion of PrP is found in lipid rafts and a proportion in non-lipid rafts due to the dynamic cycling of PrP^C. PrP^C is predominantly found in lipid raft regions but in neurons has the ability to move into non-raft regions to be internalised. Around 20% of PrP is always found in the insoluble pellet found at the bottom of the gradient, representing PrP attached to internal membranes, such as the Golgi and ER, which are difficult to disrupt [personal communication with R. Morris, Kings College London].

It is not known whether the different glycoforms have different localisations in wild type cells. It is possible that the wild type glycoforms detected are an artefact of detecting the protein in various stages of its life cycle. Very few antibodies that differentially recognise the glycoforms are available and have not been used to investigate localisation of the different glycoforms therefore it is not known where the different glycoforms are localised in wild type cells. The GlycoD mice have shown that all glycoforms can be expressed on the cell surface therefore are all likely to be functioning proteins rather than intermediates.

4.4.2 Retention in the ER versus rapid endocytosis

The increase in internal PrP in the GlycoD mutants may be due either to retention in the secretory pathway or rapid endocytosis from the cell surface. PrP^C has a dynamic life-

cycle; it is processed through the secretory pathway and delivered to the cell surface where it is rapidly endocytosed with a half-life of ~20 minutes before being trafficked back to the cell surface (Shyng et al., 1993). PrP^C interacts with many different proteins in order to traffic correctly and glycosylation and cleavage of PrP influences these interactions.

A lack of glycans did not prevent cell surface PrP in G3 cells indicating that glycosylation is not essential for cell surface expression. Loss of glycosylation can slow down trafficking to the cell surface, as is seen with the vascular endothelial growth factor (VEGF) (Yeo et al., 1991) and the C3b/C4b receptor (Lublin et al., 1986). Site directed mutagenesis to remove *N*-linked glycosylation of the yeast protein *MFα1* precursor protein delays transit from the ER to the Golgi (Caplan et al., 1991). Intracellular *MFα1* precursor protein was also exposed to some proteolytic degradation so overall protein level was reduced (Caplan et al., 1991).

Increased proportion of PrP^C in the secretory pathway suggests that glycosylation may play a role in trafficking of PrP^C to the surface. PrP lacking a single glycosylation site had a higher proportion of PrP^C associated with ER and Golgi. G1 PrP showed a greater amount of immature Endo H sensitive glycans which indicates that PrP is retained in the secretory pathway rather than recycling back to the ER and Golgi. PrP^C from the GlycoD mutants did not show any properties associated with misfolded protein [Chapter 3] and structural studies have shown that the glycans impart little or no structure (Hornemann et al., 2004) so it is doubtful that partially or unglycosylated PrP is retained in the ER due to misfolding and triggering of the unfolded protein response (UPR). The monoglycosylated PrP^C may be retained in the ER to increase exposure to the glycosylation enzymes and increase the probability of further glycosylation.

Although the GlycoD mutants showed an increased proportion of protein in the secretory pathway they had less PrP labelling than wild type neurons. This may indicate that protein is being delivered to the cell surface at the same rate in all mice but that it is endocytosed and degraded much quicker in the mutants. It has also been shown that a substantial amount of PrP is found in non-raft membranes and internalised through

clathrin mediated endocytosis (Sunyach et al., 2003, Laine et al., 2001). In order to move out of raft regions PrP^C is dependent upon ligand binding to transmembrane proteins to 'piggy back' into clathrin coated pits. The glycans of PrP^C may influence the binding ability and therefore the rate of endocytosis of each of the glycoforms. The overall reduction of PrP^C protein but not mRNA [Chapter 3] suggests that the GlycoD mutants have an increased level of degradation. The GlycoD mutants show no spontaneously misfolded protein so degradation is likely to be after endocytosis rather than through ER mediated degradation.

The recycling and trafficking of PrP^C means it is not possible to definitively conclude whether PrP^C in the Golgi is being retained or recycled using the electron microscopy localisation data on its own. PrP^C is endocytosed and can be trafficked back to the ER and Golgi through interactions with Rab proteins, small GTPases that regulate vesicular transport in endocytosis and exocytosis (Zerial and McBride, 2001). Different Rabs are associated with different trafficking, for example Rab5 is associated with clathrin-coated vesicles and early endosomes (Bucci et al., 1992, Stenmark et al., 1995) whilst Rab6 is involved in retrograde transport from the Golgi to the ER (White et al., 1999). Co-localisation with the different Rabs would help to indicate whether a protein was transported. Labelling surface PrP^C and pulse-chasing the cells would also give an indication of the trafficking and whether the mutant protein is retained or rapidly endocytosed.

The GlycoD mutants have an increased proportion of truncated PrP^C lacking the N-terminal [Chapter 4]. This region has been shown to assist in internalisation and alter the level of cell surface PrP (Shyng et al., 1995, Nunziante et al., 2003). It would be expected that GlycoD mutants would have a higher level of surface PrP due to truncated PrP that cannot be endocytosed, however the mutants have less surface PrP than wild type mice. It was not possible to differentiate between full length and truncated PrP so it is not known whether surface PrP is truncated in the mutants. C1 on the cell surface may be shed through C-terminal cleavage more efficiently in the mutants leading to reduced surface PrP.

This chapter has shown that glycosylation at either site influences the localisation of PrP^C to the cell surface. Glycosylation is not required for cell surface expression however removal of one or both glycosylation sites reduces the proportion of cell surface PrP. The glycans are likely to assist in correct trafficking to the cell surface as an increased proportion of PrP^C is localised intracellularly within the secretory pathway in the GlycoD mice.

5 *In vitro* amplification of PrP glycoforms

5.1 Aims

Conversion of PrP^{C} to PrP^{Sc} during TSE disease is influenced by the exposure to PrP^{Sc} and the physical interaction with the molecules. Previous chapters have investigated how glycosylation can alter the exposure of PrP^{C} by changing the localisation and levels of protein. This chapter aims to identify the effect of glycosylation on the physical interaction with PrP^{Sc} to initiate conversion. The efficiency of the different glycoforms to convert to PrP^{Sc} and the ability to act as a template for protein misfolding and fibrillisation will be investigated using an *in vitro* conversion method.

5.2 Introduction

PrP^{C} is essential for TSE disease and one of the central events is the conversion of host PrP^{C} to the disease associated PrP^{Sc}. Conversion of PrP^{C} to PrP^{Sc} is thought to occur via a direct interaction between the two (Horiuchi and Caughey, 1999). All glycoforms are able to convert to PrP^{Sc} however the presence of the glycans alters the efficiency of conversion.

Glycosylation may affect the conversion through altering the kinetics of conversion. Helix 2 and 3 are important regions for amyloid formation and are believed to be the initiation sites of PrP^{C} to PrP^{Sc} transition (Yamaguchi et al., 2008, Chen and Thirumalai, 2013). The first glycosylation site lies within helix 2 and presence of the glycan has been shown to reduce the rate of fibril formation by stabilising the intra-molecular disulphide bond formation (Bosques and Imperiali, 2003). G1 and G3 mice lack glycans at this site therefore would be expected to form fibrils faster than wild type and G2 mice.

The sequence homogeneity between PrP^{C} and PrP^{Sc} has been shown to be important for conversion and may contribute to the interspecies barrier observed with some TSEs (Kocisko et al., 1995). Homogenous seeding is more effective than heterogeneous

seeding, thus seeding mouse PrP^{C} with mouse PrP^{Sc} gives more efficient conversion than seeding hamster PrP^{C} with mouse PrP^{Sc} (Kocisko et al., 1995). The effect of glycosylation homogeneity has also been shown to be significant but is secondary to PrP sequence in determining compatibility for conversion *in vitro* (Priola and Lawson, 2001). The cell free conversion assay showed that unglycosylated mouse PrP^{C} was converted more efficiently than glycosylated mouse PrP^{C} with a hamster PrP^{Sc} seed (Priola and Lawson, 2001). Glycosylation prevented efficient binding of PrP^{C} to PrP^{Sc} but did not appear to influence the conversion efficiency (Priola and Lawson, 2001).

Several *in vitro* conversion assays have been developed to try to understand the prion hypothesis, the conversion of PrP^{C} to PrP^{Sc} and to aid in identifying the infectious agent. These assays use a small seed from infectious material as a template to induce refolding and fibrillisation of PrP^{C} under different biophysical conditions.

In this thesis the quaking induced conversion (QuIC) assay will be used to investigate the effect of glycosylation on the efficiency of conversion. The assay uses small amount of PrP^{Sc} to seed conversion with recombinant PrP^{C} in excess as a substrate (Figure 5.1). Initially the QuIC assay was carried out and amplification measured by immunoblotting assay products (Atarashi et al., 2008); however the technique was improved by the addition of thioflavin T (Orru et al., 2009). The amyloid fibrils formed during conversion bind to thioflavin T and fluorescence is enhanced. Fluorescence is measured throughout the incubation, giving a real time measurement of amplification (Orru et al., 2009). Real-time QuIC will be used in this thesis but will be referred to simply as QuIC. The *in vitro* conversion product will be described as PrP^{res} rather than PrP^{Sc} as the conversion product is not necessarily the same as PrP^{Sc} generated in disease. The assay produces PrP which is PK resistant but is not able to cause TSE disease when inoculated into mice to date.

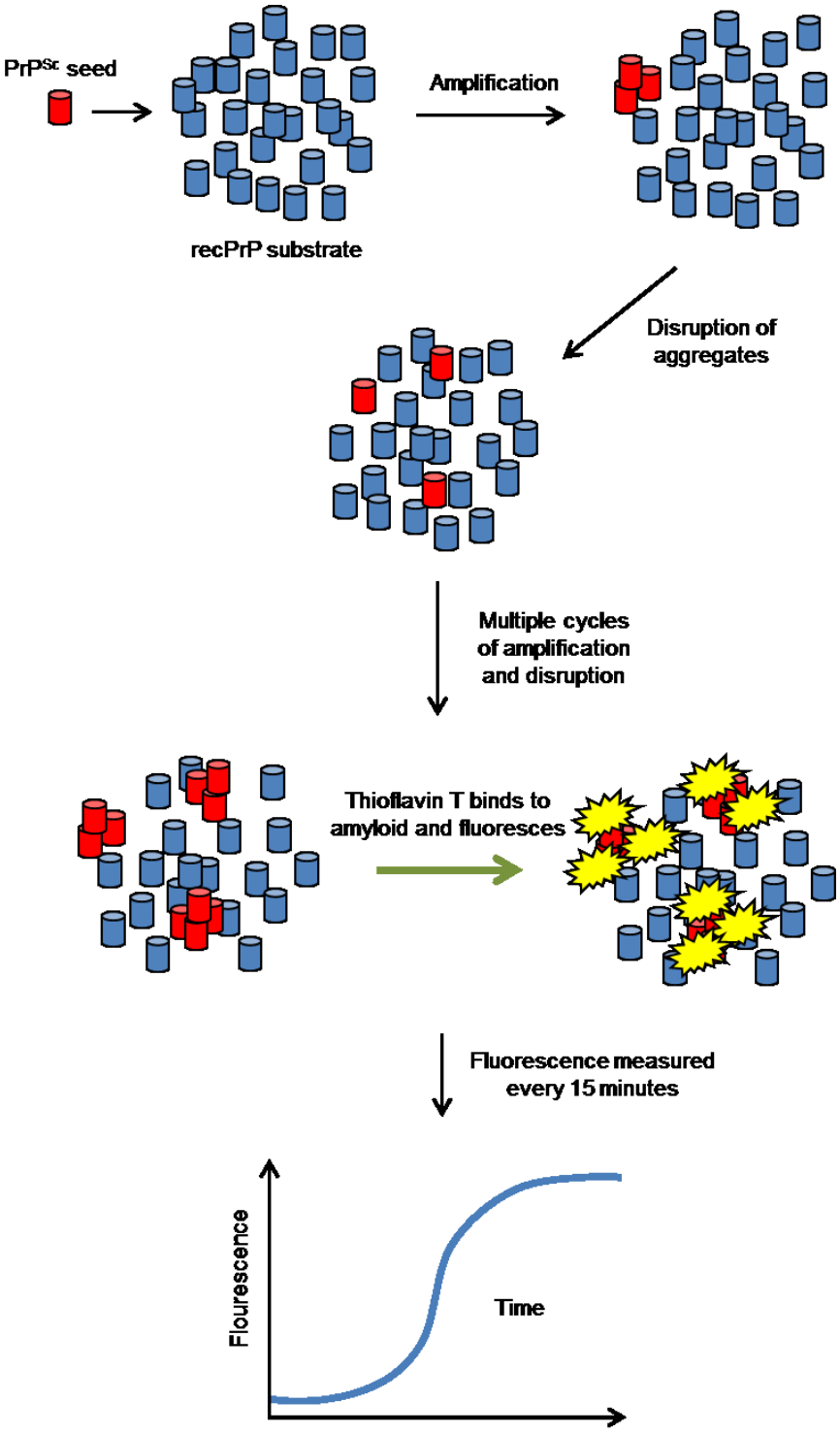

Figure 5.1 The real-time quaking induced conversion assay
A small amount of PrP^{Sc} (seed) is added to an excess of recombinant PrP (substrate). A double orbital shaker shakes the samples for 1 minute and then rests for one minute at 42 °C. Recombinant PrP binds to the PrP^{Sc} seed and is converted to PrP^{res}. Agitating the sample disrupts PrP^{res} aggregates, generating more PrP^{res} seeds for conversion. As recombinant PrP is converted to PrP^{res} it forms amyloid fibrils, which causes enhanced fluorescence of Thioflavin T. This fluorescence is measured every 15 minutes over a 60 hour period and can be plotted on a graph to show real-time amplification of PrP^{res}.

Previous studies using the GlycoD mice have shown that both host PrP^{C} and donor PrP^{Sc} glycosylation influence TSE disease (Tuzi et al., 2008, Cancellotti et al., 2013). The previous chapters of this thesis have demonstrated that the cell biology of PrP^{C} is altered for the different glycoforms, which will impact the interactions of PrP^{C} and PrP^{Sc} and influence the disease susceptibility observed in the *in vivo* TSE experiments using the GlycoD mice. The QuIC assay can be used as a model for the *in vivo* infections to investigate the conversion of PrP^{C} in the GlycoD mutants. The *in vitro* nature of the assay allows confounding factors from the *in vivo* experiments, such as the differences in localisation and protein levels to be removed. The amount of substrate for conversion is in excess in the QuIC assay and can be normalised between the genotypes so that reduced protein levels are not limiting conversion.

This chapter will address the efficiency of converting the different glycoforms of PrP^{C} (representing wild type TSE inoculation into a GlycoD mouse) and the ability of the different glycoforms of PrP^{Sc} in initiating conversion (representing GlycoD TSE inoculation into a wild type mouse). 79A has been chosen as the TSE strain for the QuIC assay as it is a well characterised strain in the GlycoD mice and all genotypes are susceptible to disease. Incubation time and pathology were different in the genotypes, suggesting that glycosylation may influence the ability to convert to PrP^{res} (Tuzi et al., 2008).

Recombinant PrP is unglycosylated therefore the effect of glycosylation on conversion of the different PrP^{C} glycoforms cannot be studied using recombinant PrP. The QuIC assay will be adapted to use brain homogenate as a substrate and conditions tested to allow amplification of the glycoforms of PrP^{C}. Recombinant hamster-sheep chimeric PrP will be used to assess the efficiency of the different glycoforms to initiate conversion. The first 114 amino acids (23-137) are Syrian hamster PrP sequence, the last 93 amino acids (141-234) are sheep PrP sequence from the R_{154} Q_{171} polymorph. The recombinant PrP construct was provided by B. Caughey (National Institute of Allergy and Infectious Diseases, NIH, USA) and the protein produced by R. Alejo-Blanco, (The Roslin Institute, The University of Edinburgh) and J. Alibhai (The Roslin Institute, The University of Edinburgh) as described in (Orru et al., 2009).

The PrP^{Sc} from all but the G3 mice are a heterogeneous mixture of glycoforms therefore it is not possible to examine the interactions of the individual glycoforms. It is important to consider that the different glycoforms may interact with each other and therefore the ratio of glycoforms may affect the conversion. GlycoD mice heterozygous for the wild type allele were also used as a seed to assess how the ratios of the glycoforms can change conversion. The heterozygous mice have a wild type allele thus produce all of the glycoforms; however they do not produce as much diglycosylated PrP so have a different ratio of glycoforms from wild type mice.

5.3 Results

5.3.1 Quaking induced conversion assay

The aim of the QuIC assay in this thesis was to identify the ability of the glycans to affect fibrillisation of the prion protein. The ability of PrP^{C} to convert to PrP^{res} can be assessed by the lag time to fibrillisation, the rate of fibrillisation and the total amount of fibrillisation.

The QuIC assay measures fluorescence produced by thioflavin T binding to amyloid. However, there is an upper limit to detection which is usually reached during the assay. The amount of fluorescence produced does not always correspond to the amount of PrP^{res} detected by immunoblotting of the QuIC product. Different strains are thought to arise from different conformations therefore the different conformations may have differing abilities to cause thioflavin fluorescence. The different glycoforms may also have different conformations as they show different strain characteristics after challenge with 79A (Cancellotti et al., 2013). This means that amount of fluorescence is not a suitable measurement for the efficiency of conversion.

The lag time was used to assess the ability of the glycoforms of PrP^{Sc} to initiate conversion. Using the GlycoD PrP^{Sc} as a seed for recombinant PrP allows the glycoforms to be assessed in initiating conversion; however as recombinant PrP is converted to PrP^{res} it provides more seed for further conversion. Therefore glycosylation

is only influencing conversion at the beginning of the assay. The lag time measures the first conversion events, which will be influenced by the glycans.

The fluorescence was measured every 15 minutes and values plotted on a graph. The time to seed was determined by comparing the graph of the fluorescence and the individual fluorescence readings and looking at when the readings started to steadily increase from the average baseline reading. The fluorescence decreased after the first time point and fluctuated until amplification occurred. The baseline was calculated by taking an average from the third to the sixth fluorescent reading.

5.3.1.1 PrPSc seed

The PrP^{Sc} seed was created from a wild type mouse and GlycoD mice that were challenged with the mouse adapted TSE strain 79A as all GlycoD mice were susceptible to this strain. Mice had been inoculated with 79A from C57 mice and 10% brain homogenates were prepared from mice culled in the terminal stage of clinical disease that were confirmed to be pathologically positive for disease.

Due to limited numbers of animals from previous transmission studies only one terminal animal from each genotype was used as a seed so it is not known whether there is any animal to animal variability in seeding ability. Terminal animals have different amounts of deposition between and within genotypes. To overcome this PrP^{Sc} seed was measured and adjusted so that the same amount of PrP^{Sc} was used for each reaction. This should eliminate animal variation within a genotype.

5.3.1.2 Normalising PrPSc seed

Each mouse used to create the PrP^{Sc} seed had different levels of PrP^{Sc} deposition in the brain, therefore different concentrations of PrP^{Sc} seed. It would be expected that a higher concentration of seed would cause conversion to have a shorter lag time as there

is more material to initiate conversion. Serial dilutions of seed were prepared in order to validate that reducing the amount of seed increased the lag time.

Seeding with both wild type and G1 PrP^{Sc} showed that reducing the amount of seed increased the length of time it took to seed the conversion (Figure 5.2). The highest dilution was the fastest to seed, however the lower the dilution the less difference there was in time to seed. In the wild type seed there was no difference between the time to seed at 10^{-6} and 10^{-7}, showing that a higher dilution will give better sensitivity and is more likely to detect differences than lower dilutions.

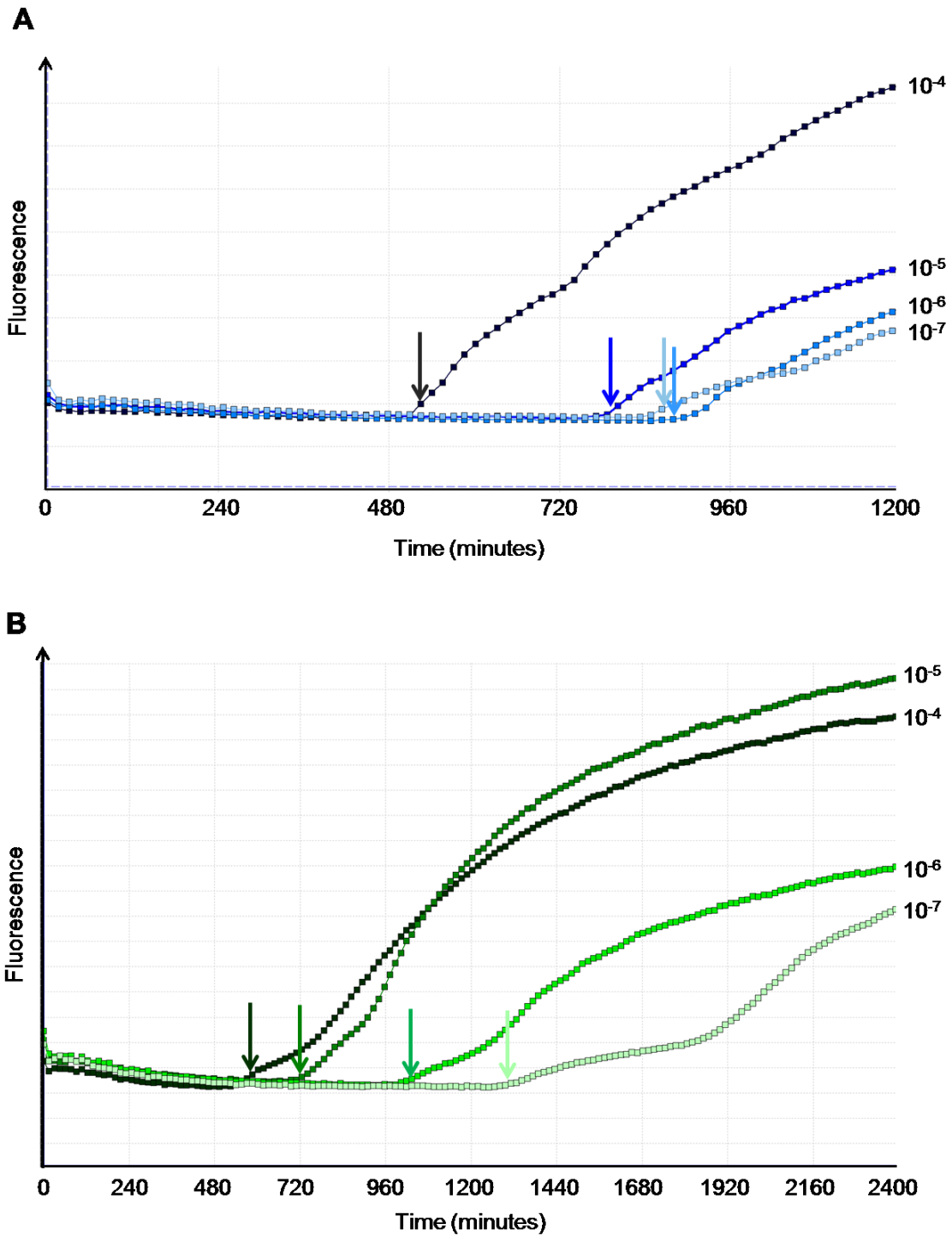

Figure 5.2 Effect of seed dilution on seeding times
Two different 10% homogenate seeds from 79A terminally infected mice (**A** wt; **B** G1) were serially diluted from 10^{-4} to 10^{-7} and used in the QuIC assay. Fluorescence was measured every 15 minutes and an average of 4 repeats calculated. The time to seeding was measured and is marked with an arrow for each dilution. Both seeds show that the more dilute the seed the longer the time to seeding. There was very little difference in time to seeding for lower dilutions in the wild type seed.

The concentration of seed affects the time to seeding therefore the amount of PrP^{Sc} was normalised for each genotype of homogenate used as a seed. To measure PrP^{Sc} brain homogenates were treated with PK at 37 ˚C for 75 minutes to remove the PrP^{C} and then run on an immunoblot which was scanned using a near infrared imager and densitometry carried out on each sample. A recombinant PrP standard was included to allow the software to calculate the quantity of PrP^{Sc} in each of the samples.

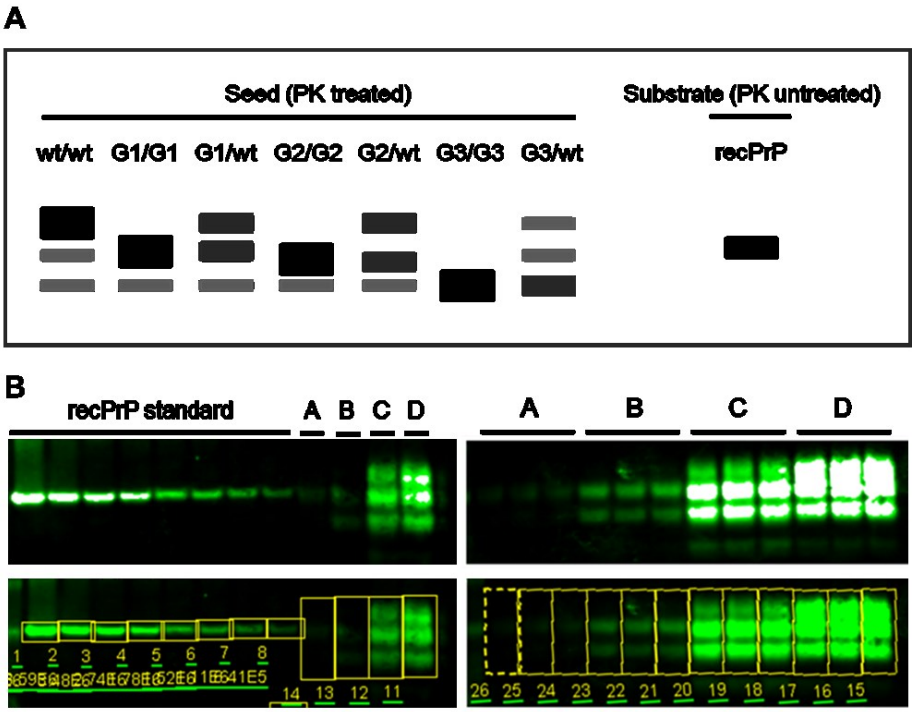

Figure 5.3 Quantification of PrP^{Sc} in 79A infected mice
Homozygous GlycoD mice and GlycoD mice heterozygous for the wild type allele were used as seed. (A) Expected PrP^{Sc} banding pattern for each of the genotypes on an immunoblot. The homozygous GlycoD did not have all of the glycoforms. The heterozygous mice had all of the glycoforms but in different ratios to the wild type mice. (B) 10% Brain homogenates from clinically positive mice infected with 79A were treated with 50 µg/ml Proteinase K for 75 minutes at 37 °C to remove PrP^{C}. Samples were run on fluorescent immunoblots in quadruplet and scanned using a near-infra red scanner. A standard of known recombinant PrP was also run on the same immunoblot so that quantification by densitometry could be carried out. Each sample had the same area highlighted and fluorescence was measured. The top row shows the over-exposed immnoblots so that all samples can be seen easily by eye. The bottom row shows the same immunoblots at a shorter exposure and the areas marked for quantification. The imager software was used to quantify each band. **A** wild type with very little PrP^{Sc}; **B** G1 mouse; **C** G2/wt mouse; **D** wt mouse.

PrP^{Sc} was quantified for each sample on at least two immunoblots. Loading controls, such as α-tubulin, were digested by PK so could not be used to control for differences in

sample loading. The replicates showed that there was little variation in loading the sample onto the gel. Once the concentration of PrP^{Sc} of each of the genotype was calculated they were diluted to the same quantity as the lowest sample.

5.3.1.3 Controls and spontaneous fibrillisation

Spontaneous fibrillisation is a concern of the QuIC assay and has been seen in uninfected controls. This questions whether there is true seeding of PrP^{Sc} or whether the samples can spontaneously misfold under QuIC conditions. For each QuIC run several controls were included to rule out spontaneous PrP^{res} (PrP^{spon}) contamination in infected samples. A recombinant only control was used in quadruplet to ensure that the recombinant was not spontaneously forming PrP^{res} during the assay. A normal brain homogenate seed control of each homozygous genotype was included to ensure that no other proteins in the brains were causing PrP to form amyloid fibrils.

PrP^{spon} was seen infrequently in some of the controls (less than 3 per 20 controls). PrPspon was never seen in all replicates of a single control. True amplification of PrP^{res} and PrP^{spon} could be differentiated as infected samples were positive before 24 hours but PrP^{spon} was never seen before 24 hours (Figure 5.4). Recombinant C showed amplification at around 8 hours however PrP^{spon} was not observed until after 30 hours.

Different batches of recombinant were tested to assess whether they formed PrP^{spon} at different efficiencies. Three different recombinants, all hamster-sheep chimeras, were initially at different concentrations but were diluted to 0.1mg/ml in the assay. Recombinant PrP strongly influences the QuIC reaction; all batches of recombinant PrP are produced using the same method and equipment by R. Alejo-Blanco and J Alibhai yet there was variation between the conversion times for PrP^{res} and in PrP^{spon} formation (Figure 5.4).

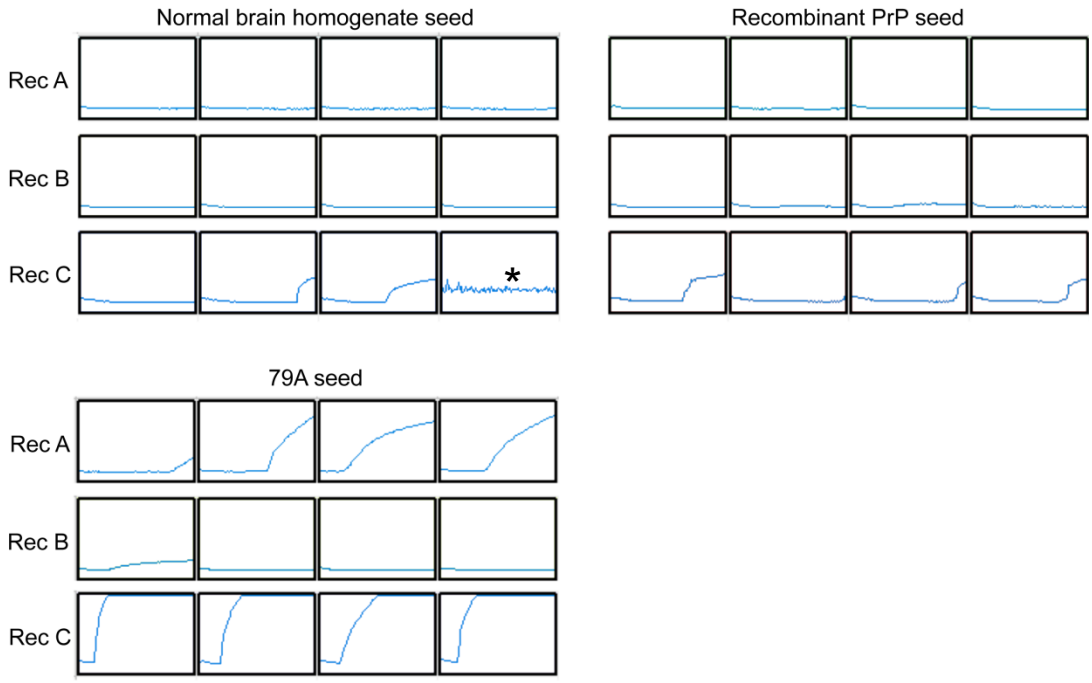

Figure 5.4 Recombinant PrP variation on PrP^{spon} formation
Three different batches of hamster-sheep recombinant was used as substrate in the QuIC assay. Each box shows thioflavin T fluorescence over 60 hours and represents an individual well. Each sample was run in quadruplet using the same recombinant master mix and seed. Recombinants A and B showed no PrP^{spon} formation with NBH or recombinant PrP as a seed. Recombinant C showed PrP^{spon} 5 out of 7 wells with uninfected seed.

Recombinant A showed no spontaneous PrP^{res} in any of the uninfected samples and all infected repeats showed amplification. Recombinant B did not show spontaneous PrP^{res} but did not amplify the infected sample within 60 hours, so would not be appropriate for amplifying infected PrP^{Sc} seed. Recombinant C showed formation of spontaneous PrP^{res} in 5 out of 7 controls; however it was possible to distinguish between PrP^{spon} and amplification by the difference in lag time. One well showed an erratic fluorescence (marked with an asterisk) which was possibly caused by condensation on the plate preventing accurate fluorescence readings and was discounted

5.3.2 The ability of the glycoforms to initiate conversion

To establish whether the glycosylation affects the ability to initiate conversion the QuIC assay was carried out with normalised seed from brain homogenate of each of the GlycoD mice to identify whether any glycoforms were more efficient at seeding conversion of recombinant PrP to PrP^{res}.

The QuIC was carried out using 6-10 repeats for each genotype of PrP^{Sc} seed per assay. The assay was carried out six times using recombinant PrP from three different batches, each one for two assays. The lag time was calculated for each repeat and combined for all assays to produce an average for each genotype (Table 5.1).

Table 5.1 Time in minutes for different glycoforms to seed PrP^{res} conversion in recombinant PrP (n=26-45)

	Mean seeding time (minutes)						
	wt	**G1/G1**	**G1/wt**	**G2/G2**	**G2/wt**	**G3/G3**	**G3/wt**
Mean	845	816	746	440	451	718	808
sem	48	55	29	26	28	39	52

There was a significant difference between the seeding times for the genotypes (ANOVA, $p<0.001$). G2/G2 and G2/wt had significantly shorter seeding times compared to the other genotypes ($p<0.05$). There is no significant difference between any of the other genotypes.

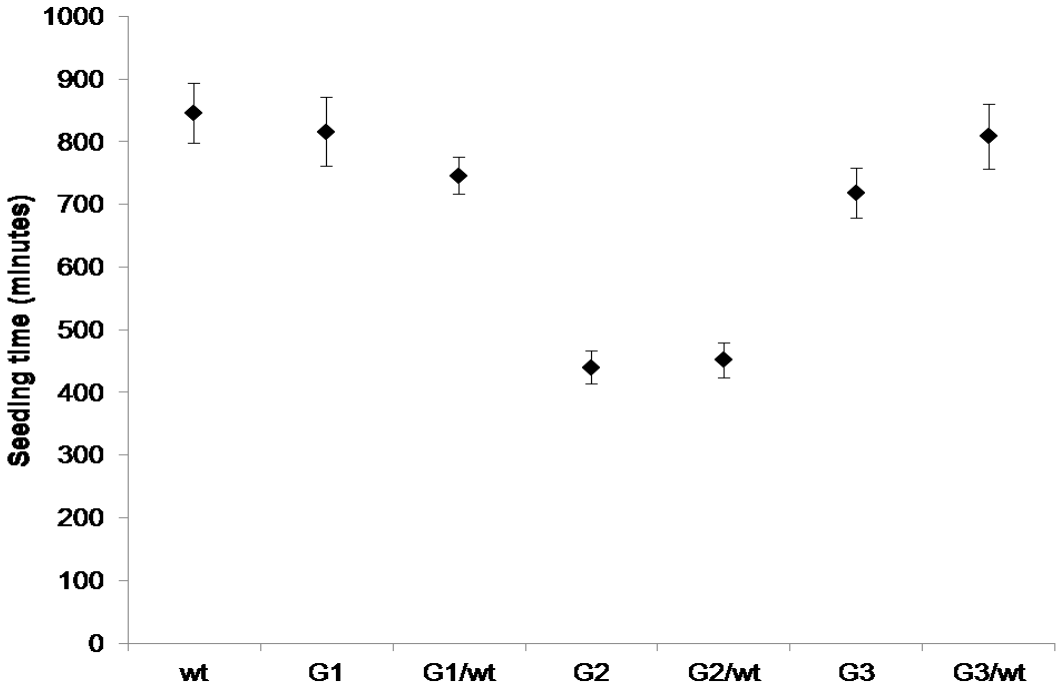

Figure 5.5 Seeding times of PrP^{Sc} from different GlycoD mice
PrP^{Sc} from 79A terminal brains from GlycoD mice was quantified and diluted so that all seed homogenates contained the same amount of PrP^{Sc}. The QuIC assay was carried out with 2µl normalised homogenate to seed conversion of 0.1 mg/ml recombinant PrP; shaking for 1 minute, resting for 1 minute at 42 °C for 60 hours (n=26-45). The time to seed was measured as the first fluorescent reading above the baseline reading taken at 0 minutes. The mean was taken for the time to seed from all values from all recombinants.

It was expected that unglycosylated PrP^{Sc} would seed fastest as it lacked glycans to hinder binding to the recombinant PrP, however there was no significant difference between diglycosylated and unglycosylated PrP. G2 PrP increased the seeding efficiency significantly (Figure 5.5), suggesting that the glycan at the first site may assist in seeding conversion. There was no difference in seeding time for mice homozygous or heterozygous for the G2 allele indicating that G2 PrP only needs to be slightly increased to allow efficient seeding.

5.3.3 Recombinant PrP batch effect

To assess whether variation in seeding times could be influenced by the batch of recombinant PrP the assays were analysed for each recombinant batch separately. Batch to batch variation was seen during optimisation of the QuIC assay and affected the time to seed with a 79A positive control and the generation of PrP^{spon} (Figure 5.4). It is not

known why different batches were more efficient at conversion however the lack of significance when all assays are combined may be due to variability in seeding times caused by the different recombinant batches.

Table 5.2 Time (mins) for each genotype to seed PrP^{res} amplification for different batches of recombinant PrP

Rec	Mean seeding time (sem)						
	wt	G1/G1	G1/wt	G2/G2	G2/wt	G3/G3	G3/wt
1	568 (68)	838 (93)	698 (49)	465 (48)	387 (68)	804 (68)	625 (77)
2	935 (37)	743 (66)	862 (41)	322 (15)	487 (18)	810 (35)	742 (24)
3	1194 (57)	1208 (115)	620 (22)	568 (34)	486 (47)	452 (15)	1254 (47)

Reproducibility was good between replicates of the same recombinant PrP substrate however there was a significant variation in seeding times for different batches of recombinant PrP (ANOVA, $p<0.001$; Table 5.2). The different efficiencies of conversion with different recombinant batches (Figure 5.4) would be expected to affect each genotype equally so the overall seeding times would be quicker or slower but the patterns in seeding times for the different genotypes would remain constant. However the relationships in seeding times were different for the different batches of recombinants, despite being produced in the same way.

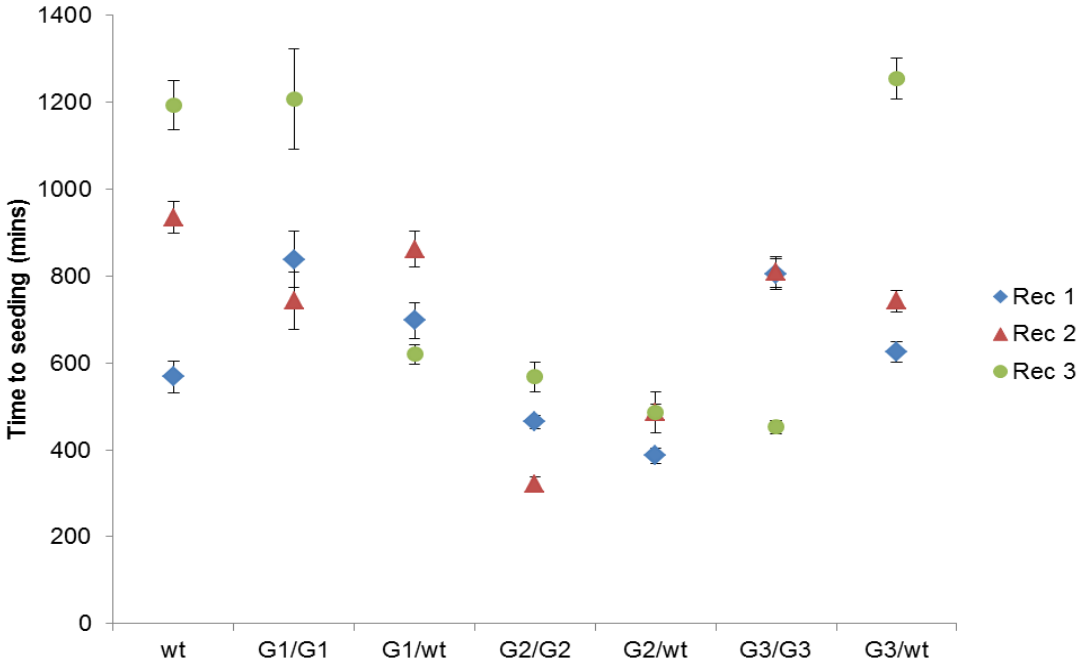

Figure 5.6 Seeding times of different glycoforms with different recombinant PrP
PrP^{Sc} from 79A terminal brains from GlycoD mice was quantified and diluted so that all seed homogenates contained the same amount of PrP^{Sc}. The QuIC assay was carried out with 2 µl normalised homogenate to seed conversion of 0.1 mg/ml recombinant PrP; shaking for 1 minute, resting for 1 minute at 42 °C for 60 hours. The time to seed was measured as the first fluorescent reading above the baseline reading taken at 0 minutes. A mean was taken for all replicates for each recombinant to allow comparison between recombinant batches.

Recombinant 1 showed that G2 mice had the quickest time to seed, followed closely by wild type mice and then G3 and G1. Mutants with a G2 allele were significantly faster than G1/G1, G1/wt and G3/G3 mutants to seed conversion ($p<0.05$). Heterozygous mice had quicker seeding times compared to their homozygous GlycoD mutant counterparts. Adding a wild type allele to the GlycoD mutants appeared to reduce the time of PrP^{Sc} to seed. This suggests that diglycosylated PrP^{Sc} is converting recombinant PrP more efficiently than the other glycoforms.

Recombinant 2 showed that G2 PrP was the fastest to seed followed by G1, G3 and then wild type PrP. As seen with the recombinant 1 G2/G2 PrP^{Sc} seeded significantly faster ($p<0.05$) than all other genotypes and G2/wt seeded significantly faster ($p<0.05$) than all other genotypes, except G2/G2. Wild type PrP^{Sc} seeded significantly slower than G1/G1, G3/wt, G2/G2 and G2/wt seeds ($p<0.05$). Heterozygous G1 and G2 mice had slower seeding times compared to their homozygous GlycoD mutant counterparts.

Adding a wild type allele to these GlycoD mutants increased the time of PrP^{Sc} to seed. This suggests that diglycosylated PrP^{Sc} is converting recombinant PrP less efficiently than the other glycoforms. G3 and G3 heterozygous mice showed the same patterns as seen with recombinant 1 and adding deglycosylated PrP reduced seeding time.

Recombinant 3 showed two different groups of seeding times; G1/wt, G2/G2, G2/wt and G3/G3 had faster seeding times and were significantly different to G3/wt, G1/G1 and wild type PrP^{Sc} (ANOVA, $p<0.001$). There was no pattern between the heterozygous and homozygous counterparts for each genotype. There was a higher variation in seeding times for each genotype with recombinant 3.

There is a difference in seeding efficiencies of the different GlycoD mice that can be reproducibly measured using the QuIC assay. G2 was consistently the fastest glycoform to seed conversion with all three of the recombinant PrPs tested.

Table 5.3 Rankings for the seeding efficiencies of the genotypes with different recombinant PrP (1 is most efficient)

Rec	Ranking of seeding efficiency						
	wt	G1/G1	G1/wt	G2/G2	G2/wt	G3/G3	G3/wt
1	2	4	3	1	1	4	3
2	4	2	3	1	1	3	2
3	2	2	1	1	1	1	2

The order of the genotypes to convert was different for each batch of recombinant (Table 5.3). The rankings show that G2 PrP is consistently the fastest, however with one recombinant the unglycosylated PrP was the fastest to seed and with another it was the slowest.

5.3.4 Brain homogenate as the substrate for the QuIC assay

The QuIC assay was used to assess the ability of each of the glycoforms to convert into PrP^{res}. The *in vivo* data has shown differences in susceptibility when the GlycoD mice were challenged with 79A, which may be due to the glycans altering the ability of PrP^{C} to convert to PrP^{Sc}.

The QuIC assay has been developed using unglycosylated recombinant protein as the conversion substrate therefore cannot be used to assess conversion of the glycoforms. Normal brain homogenate was tested as a substitute for recombinant PrP to allow the glycoforms to be converted. Initially wild type and null brain homogenate were used in order to optimise conditions. Serial dilutions were used for the substrate to assess the brain homogenate concentration that allowed the best conversion.

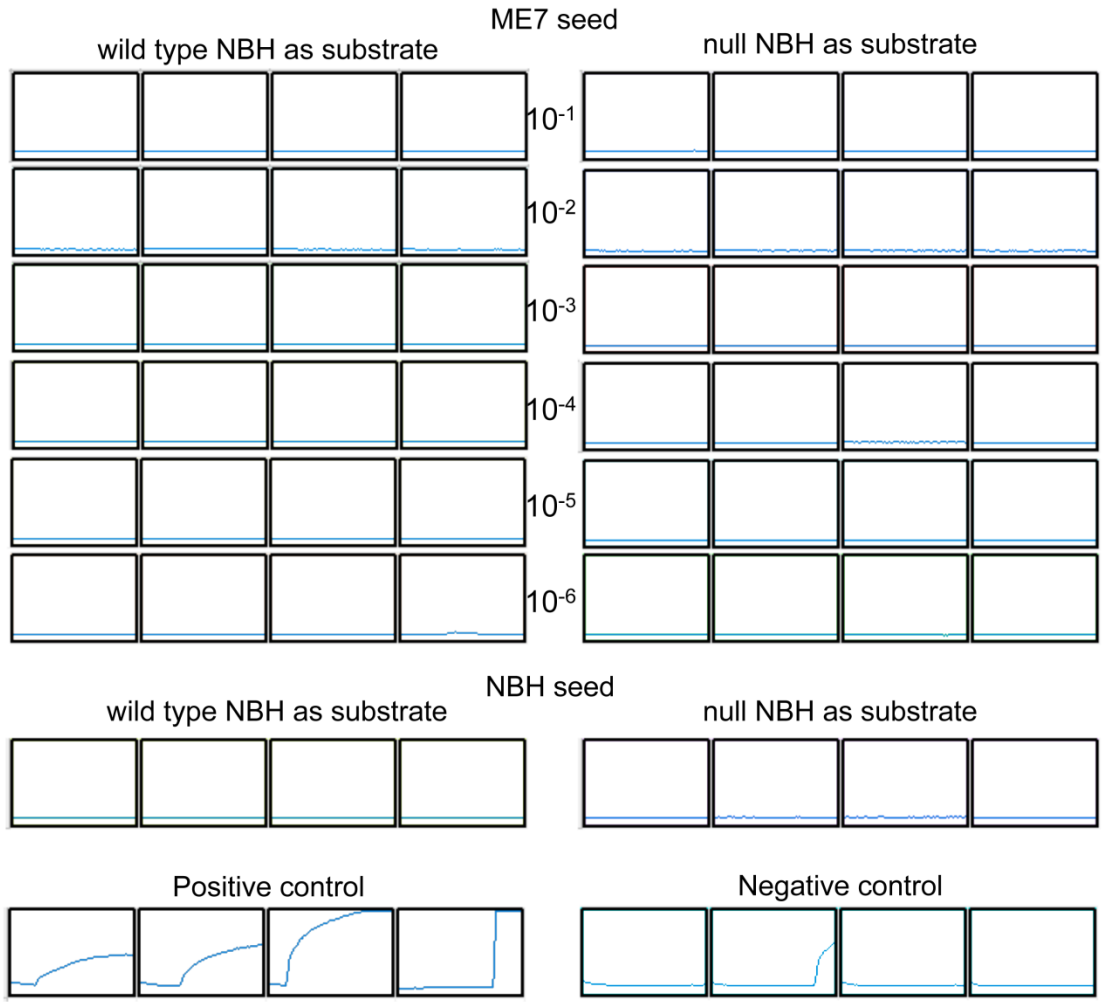

Figure 5.7 Normal brain homogenate as a substrate for the QuIC assay
10% normal brain homogenate was used as a substrate for the QuIC assay using an ME7 seed that had previously been used in a QuIC assay. Uninfected brain was used as a seed to control for spontaneous PrP^{res}. The positive control is an ME7 (10^{-3}) seed in 0.1 mg/ml recombinant PrP substrate and the negative control is 0.1 mg/ml recombinant PrP substrate without any seed. Each condition was carried out in quadruplet and fluorescence was measured every 15 minutes over 60 hours. There was no PrP^{res} amplification in any of the dilutions using normal brain homogenate as a substrate.

No seeding or amplification was seen with any of the wild type normal brain homogenates as a substrate for conversion (Figure 5.7). Amplification was seen in the positive controls (recombinant PrP as a substrate) showing that the ME7 seed was able to initiate conversion. Amplification of ME7 was not possible with crude brain homogenate as a substrate and may be inhibited by a component of the homogenate.

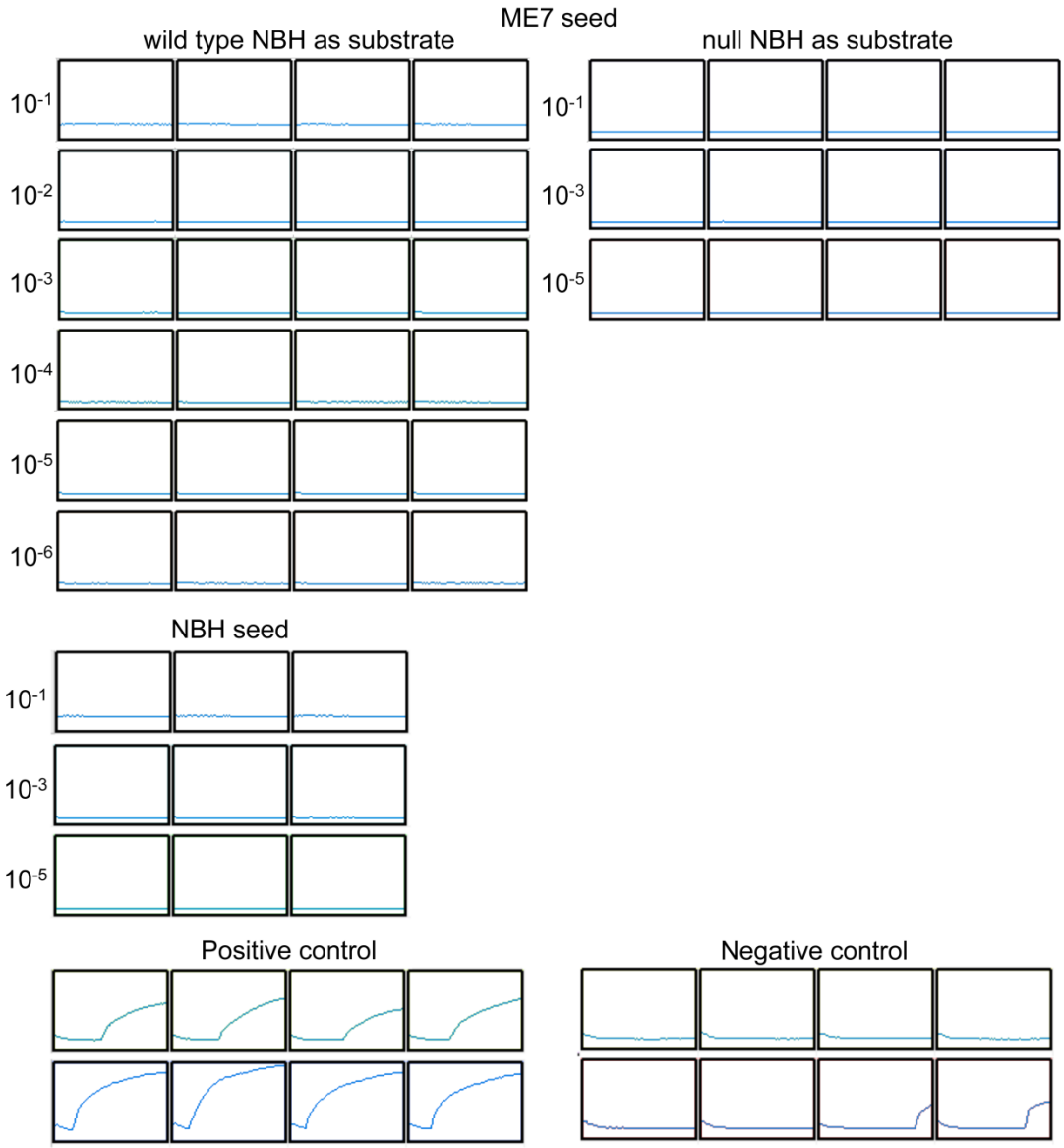

Figure 5.8 Quic assay with PI-PLC treated substrate
10% normal brain homogenate was treated for 36 hours with 0.5 U PI-PLC to release PrP^{C} from the membrane. Membrane depleted brain homogenate was used as a substrate for the QuIC assay using an ME7 seed. Uninfected brain was used as a seed to control for spontaneous PrP^{res}. The positive control is an ME7 (10^{-3}) seed in 0.1 mg/ml recombinant PrP substrate and the negative control is an uninfected brain (10^{-3}) seed in 0.1 mg/ml recombinant PrP substrate. Two different recombinant substrates were used for both controls. Each condition was carried out in quadruplet and fluorescence was measured every 15 minutes over 60 hours. There was no PrP^{res} amplification in any of the dilutions using normal brain homogenate as a substrate.

It has been suggested that lipids may inhibit conversion in the QuIC assay. PrP^{C} prepared from homogenate is membrane associated and brains are lipid rich due to myelin. To address this normal brain homogenate was treated with PI-PLC to release the protein from the membrane in order to try to reduce the amount of lipids present in

the substrate. 10% homogenates were treated with PI-PLC for 36 hours to ensure full cleavage and released protein separated from the membranes by centrifugation. Protein was concentrated to provide as much substrate possible. Total protein was not measured initially as very little substrate was generated

Even with reduced lipids there was no amplification seen with normal brain homogenate as a substrate for conversion (Figure 5.8). Crude brain homogenate was not a suitable substrate for the QuIC assay and further purification of PrP^{C} from brain homogenate may be required to allow amplification of the glycoforms using QuIC.

5.4 Conclusions

This study is the first to investigate the effect of the glycoform acting as a template for conversion. Homology between seed and substrate has been shown to be important for conversion (Priola and Lawson, 2001) but only the effect of glycosylation of the substrate, which undergoes conformational change, has been studied. The results presented here suggest that the glycan at the first site may assist in initiating conversion as PrP^{Sc} from G2 mice were able to initiate conversion faster than other genotypes. The first glycan lies within helix 2 of PrP^{C} and has been shown to stabilise the intra-molecular disulphide bond formation. The glycan may also stabilise PrP^{Sc} aggregates, allowing a more stable seed or providing a better template for PrP^{C}. The delay in seeding for the other genotypes may indicate that the second site is inhibiting conversion.

If the glycan at the first site is assisting in conversion then it would be expected that wild type PrP^{Sc}, which also contains PrP with the first site glycosylated would be more efficient at converting PrP^{Sc} than the G1 and G3 which lack this glycan. However, with the exception of G3 the different genotypes are heterogeneous mixtures of the glycoforms therefore the ratios of the glycoforms in wild type PrP^{Sc} may prevent differences being detected.

Differences were not observed in the ability to initiate conversion between wild type, G1 and G3 mice, which is in contradiction to the incubation periods seen with 79A in the GlycoD mice. This lack of difference suggests that environmental exposure of PrP^{C} to PrP^{Sc} may be more important than the physical interactions between the two molecules in determining disease susceptibility. The altered localisation and reduced expression levels described in previous chapters may contribute more to the increased incubation period than the ability to be initiate conversion to PrP^{Sc}.

The similarity in seeding times may indicate that the glycans do not impart any effect on conversion. The effect of glycosylation on conversion was secondary to PrP sequence (Priola and Lawson, 2001) therefore the differences observed in the G2 seeding times in this study may be due to the sequence differences between the recombinant PrP and PrP^{Sc} seed. The batch of recombinant PrP had a huge effect on the outcome of the assay and a single recombinant showed differences between the genotypes. It is not understood why a batch effect was seen with the different recombinant despite being produced using the same method. Further investigation is needed to determine whether there is a true difference in seeding times or whether it is an effect caused by the recombinant. Different species of recombinant need to be tested to eliminate the variation seen with recombinant PrP and to assess whether the differences in seeding are species specific and likely to account for differences between the GlycoD mutants seen in TSE disease. A recombinant mouse PrP would need to be used with these PrP^{Sc} seeds to identify whether the differences seen were due to glycosylation or PrP sequence.

Conversion assays all have different limitations therefore other assays could be tested in conjunction with the QuIC assay to give a more rounded view of conversion. PMCA has been shown to produce infectious PrP^{res} and can use either crude homogenate or recombinant as a substrate for conversion (Shikiya and Bartz, 2011, Barria et al., 2009). However the conditions for PMCA are less standardised and the technique is more variable than the QuIC assay. Cells can be used to study conversion and amplification of PrP^{res} in more physiological conditions, however few cell lines exist which are can be persistently infected and do not always show toxicity of PrP^{Sc}.

5.4.1 Limitations of the QuIC assay

There are several limitations of using an *in vitro* assay that must be considered when relating *in vitro* results to *in vivo* data. The PrP^{res} generated during QuIC has yet to be shown to be infectious, suggesting that the QuIC assay is not a true representation of the conversion process *in vivo*. The lack of infectivity may be due to a cofactor required for infectivity which is not supplied in the QuIC assay.

The QuIC assay detects PrP^{res} that is in an amyloid conformation, however PrP^{Sc} exists in several different forms *in vivo*; from small oligomers to larger fibrils and amyloid (Silveira et al., 2005). The different aggregates are all associated with infectivity (Silveira et al., 2005) but it is not known which aggregate is the infectious species, or whether all PrP^{Sc} aggregates are equally involved in disease. Amyloid is not characteristic of every TSE strain therefore the QuIC assay may not be relevant to all strains.

Due to the *in vitro* nature of the QuIC assay other factors which may influence conversion during disease are not accounted for. The glycans may influence the ability to bind and convert to PrP^{Sc} but the localisation of the protein will also influence whether PrP^{C} comes into contact with PrP^{Sc}. It is thought that cell surface PrP is important for conversion (Goold et al., 2011) therefore the reduced cell surface PrP^{C} in the GlycoD mice will limit the amount of PrP available for conversion.

Although PrP^{Sc} is a defining feature of TSEs the role of PrP^{Sc} in disease is poorly understood. There is a lack of correlation between PrP^{Sc} deposition and disease. Models exist that have large amounts of aggregated PrP but lack disease symptoms (Chesebro et al., 2005, Piccardo et al., 2007), equally there are models that exist with little or no detectable PrP^{Sc} but succumb to clinical disease and are highly infectious (Barron et al., 2007). The amount of PrP^{res} produced during the QuIC may not correlate with disease susceptibility.

Despite the limitations mentioned above the QuIC assay provides a useful tool to study the interactions of the glycoforms during conversion and taken together with the cell biology of the different glycoforms can be potentially used to explain differences in TSE susceptibility and pathology.

This chapter has demonstrated that the glycoforms have a different ability in initiating conversion with recombinant PrP. G2 PrP^{Sc} was more efficient at seeding amplification than the other genotypes. This is the first time that a difference between G1 and G2 mice has been observed that could account for the difference in disease susceptibility in these mice, showing that the glycans may have differing effects during conversion.

6 Discussion

6.1 Glycosylation and cell biology of PrP^C

Glycosylation is an important post-translational modification. The addition of glycans can change the property of the protein without having to encode this change in the genome and the complex structures of glycans can provide extra diversity to the glycoprotein (Varki and Sharon, 2009). The glycosylation sites of PrP are highly conserved across species suggesting an important role in either the protein's cell biology or function (Lee et al., 2003, Kim et al., 2004). This thesis demonstrates that although glycosylation is not essential for the health or survival of transgenic mice it influences the localisation and expression of PrP^C, which in turn could influence normal function and TSE susceptibility.

Gene targeted mutants were employed here to investigate the effect of glycosylation on the cell biology of PrP^C. The GlycoD mice have PrP^C with selectively abolished glycosylation expressed under the same physiological conditions as wild type PrP. This unique system allows the complexity of the glycoforms and the effects of the individual glycosylation sites to be studied by isolating the individual glycoforms.

The data presented here demonstrates that glycosylation has an effect on the localisation and protein levels of PrP^C. Removal of either the first (G1) or the second (G2) glycosylation site produced changes in cell biology that were almost indistinguishable from each other. Disruption of both glycosylation sites (G3) produced a more extreme phenotype than removal of a single site.

Interestingly there was very little difference in cell biology between the two monoglycosylated glycoforms. The lack of differences between G1 and G2 mice indicate that both glycosylation sites have a similar effect on determining the cell biology. The glycosylation sites of PrP^C are close together and are occupied by similar oligosaccharides (Stimson et al., 1999) therefore interactions that alter the localisation and trafficking may not be selective with the first or second site, just by the presence of

a single glycan. The glycosylation sites are likely to shield similar areas from proteolytic degradation, thus there is no difference in the degradation of the monoglycosylated glycoforms.

The function of PrP^C remains elusive and it is not known whether the different glycoforms have unique functions or even if all glycoforms are functioning. The differences observed in the cell biology of the different glycoforms can indicate whether the glycoforms are likely to carry out specific functions.

6.1.1 The effect of glycosylation on protein levels

This is the first time that it has been demonstrated that removal of either one or both of the glycosylation sites of PrP^C reduces PrP protein levels [Chapter 3]. Removal of a single glycosylation site reduced protein by 50% and complete removal of glycosylation reduced protein levels to around 32% total protein of that in wild type mice. The decrease of PrP^C in the GlycoD mutants may limit the ability to perform its normal functions.

Real-time PCR of the *Prnp* gene [Chapter 3] and previous northern blot analysis (Cancellotti et al., 2005) showed that PrP mRNA levels in the brain were the same for all GlycoD mutants as in wild type mice. This showed that the reduction of protein was due to post-translational regulation rather than transcriptional regulation. It also demonstrates that down regulation of PrP^C does not feed-back and regulate the level of transcription in the CNS.

In addition to the different glycoforms, truncated isoforms are also present *in vivo*. There are several cleavage events possible for PrP but the predominant one under normal physiological conditions is alpha cleavage. The data shown here demonstrates an increased proportion of the alpha cleavage product, C1, when a glycosylation site is abolished [Chapter 3]. In the wild type mice 25% of PrP underwent alpha cleavage and was detected as a C1 fragment. G1 and G2 mice had ~35% as the C1 isoform and up to 50% in G3 mice.

The proportion of C1 is increased in the GlycoD mice but the absolute levels of C1 are reduced slightly. The relative levels of C1 in the GlycoD mutants are also preserved whether a single glycosylation site or both are abolished. This increase in proportion of C1 but the preservation of the absolute levels of C1 suggests that truncation and the products have an important role in the function of PrP^C.

N1 has been shown to be neuroprotective both *in vitro* and *in vivo* by down regulating the p53 pathway (Guillot-Sestier et al., 2009) and protective against Aβ toxicity in cell culture (Guillot-Sestier et al., 2012). C1 enhances susceptibility to pro-apoptotic conditions but is not neurotoxic under normal conditions. The glycoforms may exist to balance the production of the neuroprotective N1 fragment and the full length PrP. Diglycosylated PrP had higher protein levels indicating that it was degraded less readily, either through trafficking or through protection against proteolytic enzymes; however it produced less N1. The unglycosylated and monoglycosylated glycoforms were able to contribute the same amount of C1/N1 but were degraded more readily hence they do not contribute so much towards full length PrP. The full length PrP may function more efficiently with both glycans present whereas the N1 does not possess glycans therefore the presence or absence of glycans on the full length has no bearing on the function of N1.

6.1.2 The effect of glycosylation on localisation

In order to define the localisation of the glycoforms electron microscopy was used to quantify the amount of PrP associated with different cell membranes. This study shows that glycosylation of PrP^C is not essential for cell surface expression however removal of either of the glycosylation sites significantly reduces the presence of PrP^C on the cell surface. Previous studies showed that abolition of both glycosylation sites caused retention of PrP^C inside the cell (Cancellotti et al., 2005)[F. Wiseman; PhD thesis 2007]. This study allowed localisation to be investigated at a higher resolution to identify whether unglycosylated PrP could be localised to the cell surface and showed small amounts of PrP^C on the plasma membrane.

G1 and G2 mutants showed reduced surface PrP^C and a higher proportion of intracellular PrP^C associated with the ER and Golgi. Previous data using the GlycoD mice had shown that removal of a single glycosylation site appeared to increase the proportion of intracellular PrP but that the protein was still predominantly on the plasma membrane (Cancellotti et al., 2005) in contrast to other PrP glycosylation deficient mutants, which showed intracellular retention of PrP^C in cell models (Rogers et al., 1990). The limited resolution of immunofluorescence may account for the differences between the studies. The method used here was able to quantify PrP on the different membranes and showed that cell surface PrP^C only accounted for 20% of total PrP in both G1 and G2 neurons. The intracellular distribution was also slightly different between G1 and G2 mice indicating that the different glycans assist with trafficking at different points through the secretory pathway.

The altered localisation in the GlycoD mutants is likely due to the changes in the ability to interact with other proteins. PrP^C relies on ligands for trafficking, particularly for endocytosis. The ligands bound to PrP^C determine the method of internalisation, and have the potential to determine the destination.

The location of PrP^C in the cell can influence the ability to carry out different functions. The glycosylation can change function through either modulating the interactions with other proteins or through changing the localisation, and therefore the availability of ligands. The glycosylation of PrP may influence the ability to bind with ligands through direct recognition of the glycans by lectins (Gabius, 1994) or through shielding of binding domains on the peptide. The multiple ligands demonstrated for PrP^C could induce different trafficking and signalling thus allowing the multiple functions proposed.

Several functions have been proposed for PrP^C in neurons and many rely on the cell surface localisation in order to carry out these functions. PrP has been implicated in signal transduction however the reduced cell surface expression of PrP^C in the GlycoD mutants may have a limited ability to initiate signal transduction. Different signal

transduction pathways can be activated by the binding of different partners (Arsenault et al., 2012). PrP^C interacts with the intracellular Fyn kinase when associated with lipid rafts and caveolin-1 although the mechanism is undetermined (Mouillet-Richard et al., 2000). PrP^C also binds to astrocyte-secreted stress-inducible protein 1 (Stip-1) in lipid rafts modulating the pool of cellular proteins needed for proper neuronal function through the PI3K–Akt–mTOR and ERK1/2 pathways (Roffe et al., 2010, Caetano et al., 2008). PrP^C interacts with the neural cell adhesion molecule (NCAM) in cis and trans to recruit NCAM into lipid rafts and activate $p59^{fyn}$ to promote neurite outgrowth.

PrP^C has also been implicated in copper homeostasis at the synaptic cleft. PrP^C binds copper at the cell surface which promotes endocytosis to allow maintenance of copper in the pre-synaptic cytosol and buffering against toxic levels of copper (Vassallo and Herms, 2003).

The reduced cell surface PrP^C indicates that the glycoforms may be less efficient at carrying out the functions of PrP^C. The functions of PrP^C are associated with cell survival and growth, therefore monitoring and responding to the cell environment is important to allow the correct response. The glycoforms may exist to allow a response to environmental changes and therefore the GlycoD mutants may be less able to adapt to change.

6.1.3 Localisation and protein levels

The altered localisation of the GlycoD mutants observed in Chapter 4 may result in the reduced expression levels observed in Chapter 3 through several mechanisms. The localisation of the PrP^C will influence the exposure to other cellular proteins, such as degradation enzymes, ligands and the alpha cleavage enzymes. Interactions with enzymes can reduce the protein levels directly through degradation whilst interactions with ligands can reduce proteins indirectly through altering trafficking and degradation.

It is not known whether the increased proportion of intracellular PrP in the GlycoD mutants is due to retention in the secretory pathway or due to rapid endocytosis from the

cell surface. The GlycoD mutants had an increased proportion of intracellular PrP but the level of intracellular PrP was slightly less than in the wild type mice. The increased proportion of intracellular PrP is likely due to a decrease in cell surface PrP^C caused by more rapid endocytosis from the cell surface. PrP^C that has been endocytosed is exposed to degradation enzymes, reducing protein levels.

PrP is continuously recycled between the cell surface and endocytic vesicles before degradation. Endocytosis is mediated by binding partners, which are influenced by the glycans attached to PrP^C. The Glycans of diglycosylated PrP^C may bind to surface proteins, such as galectins which prevent endocytosis.

The increased Endo H sensitive PrP in G1 mice [Chapter 4] suggests that this glycoform is retained in the ER rather than being retro-translocated back to the ER. The delay in trafficking to the cell surface may push PrP^C in the G1 mice to be targeted for degradation without being trafficked to the cell surface.

The altered localisation of PrP^C in the GlycoD mice can affect the amount of protein through a change in alpha cleavage levels. Alpha cleavage has been proposed to occur in the late Golgi (Walmsley et al., 2009) or in the early endocytic compartments (Shyng et al., 1993). The almost normal levels of C1 detected in the GlycoD mutants despite the reduced level of total PrP^C suggests that the increased proportion of intracellular PrP allows the alpha cleavage to occur at the same rate in all genotypes.

6.1.4 PrPC in the peripheral nervous system

PrP^C is expressed selectively and at lower levels in tissues outside the CNS (Ford et al., 2002b) however PrP^C has been shown to be important for peripheral myelin maintenance in the PNS (Bremer et al., 2010). PrP null mice showed a chronic demyelinating polyneuropathy in peripheral nerves as mice aged. Maintenance of myelin was dependent upon axonally expressed PrP^C with the ability to undergo alpha cleavage (Bremer et al., 2010). The lack of myelinopathy in the CNS suggests that PrP^C has different functions in different tissues.

In a limited study G3 mice surprisingly showed no peripheral myelinopathy despite the reduce expression of CNS PrP^C and the alteration in cellular localisation no changes were seen in sciatic nerves (PNS) or optic nerves (CNS) of aged G3 mice, however null mice showed dysfunctional myelin in the sciatic nerves but not the optic nerves [Iremonger unpublished observation]. The expression of PrP^C in the periphery of the G3 mice was not assessed although the lack of glycosylation showed a change in cell biology in the CNS that would be expected to be mirrored in the PNS.

Alpha cleavage is important in the function of PrP^C in the PNS (Bremer et al., 2010) suggesting that either the N1 or C1 fragments were essential for peripheral myelin maintenance. Rescue was also dependent upon axonal PrP^C showing cross talk between neurons and myelin producing Schwann cells and an effect of PrP^C in trans (Bremer et al., 2010). This thesis has shown that surface PrP^C is vastly reduced in the GlycoD mutants therefore the ability of the C1 fragment to act in trans would be reduced in G3 mutants. However there was no peripheral myelinopathy phenotype in the G3 mice showing the reduced surface C1 has no effect in the PNS. The overall amount of C1 and presumably N1 is only slightly reduced in the G3 mice therefore it is more likely that the secreted N1 is acting as the factor for myelin maintenance.

6.2 Glycosylation and TSE disease susceptibility

Glycosylation of PrP is thought to be important in TSE disease as it is believed that the glycans may encrypt strain characteristics through modulation of protein conformation. The GlycoD mice provided a tool to study the effect of glycosylation on TSE disease and allow a direct comparison of the effects on disease of the two different glycosylation sites. Previous work has shown that both glycosylation of host PrP^C and donor PrP^{Sc} can influence disease (Cancellotti et al., 2013). The glycosylation status of the host can change the susceptibility to disease with different TSE strains, altering incubation periods and pathology.

PrP^{C} and its conversion into the disease associated isoform PrP^{Sc} is poorly understood but is central to TSE pathogenesis (Weissmann et al., 1994). PrP^{Sc} is generated by direct interaction and a template conversion of host PrP^{C} to PrP^{Sc} therefore two factors can influence conversion; the physical interaction and ability of PrP^{Sc} to induce conformational change and the environmental factors that determine the exposure of PrP^{C} to PrP^{Sc}.

This thesis has investigated the effect of glycosylation on the normal isoform of PrP and the role of the glycans in the interactions of PrP^{C} and PrP^{Sc} during an *in vitro* conversion process. The glycans can significantly alter the localisation and expression levels of the PrP^{C} isoforms. The data collected in this thesis can be used to elucidate the contributions of the cell biology and the interactions of the glycans during conversion in the changes seen in the altered susceptibilities of the GlycoD mice during TSE disease.

6.2.1 The effect of glycosylation on incubation period and disease susceptibility

The increased incubation period and resistance in the GlycoD mutants may be accounted for by the altered localisation shown in Chapter 4 and by the decrease in full length PrP demonstrated in Chapters 3.

All GlycoD mice have significantly reduced levels of PrP^{C} which has been shown to influence TSE disease incubation time. There is an inverse correlation with the amount of PrP and the incubation period. Heterozygous mice which only carry a single *Prnp* gene ($PrP^{-/+}$) have significantly longer incubation times than mice carrying two copies of the gene (Bueler et al., 1993, Manson et al., 1994b). The absence of PrP renders an animal resistant to TSEs (Manson et al., 1994b).

PrP^{C} levels correlate to incubation period thus all GlycoD mice would be expected to have an increased incubation period. It would be expected that as G1 and G2 mice have the same PrP levels that they would also have the same incubation periods and G3 have an increased incubation period. Although there is an increase in incubation period the

PrP levels do not correlate completely suggesting that other factors are also influencing incubation period. It would be expected that reducing PrP^C levels by 50% would double the incubation time. Previous experiments with heterozygous mice showed that challenge with TSE strain 301C increased the incubation period by 150 days (Manson et al., 1994b), however G1 and G2 mice had the same amount of PrP^C as the heterozygous mice yet the incubation time is increased by 340 days in G2 mice and G1 mice are resistant. G3 mice were also resistant to 301C (Table 1.6).

Challenge of the GlycoD mice with 79A produced disease in all genotypes but showed an increased incubation time. A reduction of PrP^C by two thirds in G3 mice increased the incubation period by 290 days. G1 and G2 mice had half the amount of PrP^C however the incubation period was only increased by 50 and 20 days respectively (Table 1.6).

Another factor influencing the incubation period is the localisation of PrP^C within the cell. All GlycoD mice showed a decrease in cell surface PrP^C, which is believed to be essential during conversion. The conversion site of PrP^C to PrP^{Sc} has yet to be clearly defined but it has been proposed that PrP^C must reach the cell surface in order to be converted (Goold et al., 2011, Arnold et al., 1995, Kenward et al., 1992). Tagged PrP^C has been shown to convert rapidly upon exposure to external PrP^{Sc} on the cell surface before being endocytosed (Goold et al., 2011). Conversion has also been shown to take place in endocytic vesicles after endocytosis from the cell surface (Marijanovic et al., 2009). The GlycoD mice had an increased proportion of PrP^C associate with the ER and Golgi, suggesting retention in the secretory pathway. This PrP^C will not be as readily converted because it will not come into contact with PrP^{Sc} until it has been expressed on the cell surface.

6.2.2 Differences between G1 and G2 mice

The cell biology investigated in this thesis has revealed very little difference between the G1 and G2 mice in the localisation of PrP^C [Chapter 4], the amount of total PrP and

the levels of proteolytic cleavage [Chapter 3]. However the disease susceptibility is very different for G1 and G2 mice (Table 1.6).

G1 mice had half the amount of PrP^C than wild type mice yet were resistant to five of the six strains tested and showed a resistance similar to G3 mice. This is perhaps not surprising considering that in addition to reduced PrP^C it is also mislocalised and very little PrP is found on the cell surface. Interestingly G2 mice had an incubation period equal to wild type mice in ME7 despite expressing 50% less protein and a reduced level of cell surface PrP. G2 mice were also susceptible to sCJD when all other mice, including wild type mice, were resistant.

The localisation study showed a subtle difference in localisation between the two monoglycosylated PrPs [Chapter 4] and may explain the differences between G1 and G2 mice. Both monoglycosylated PrPs had the same amount of intracellular PrP^C but different distributions. The differences between the intracellular localisation could be influencing the differences in susceptibility seen in between the G1 and G2 mice. PrP glycosylated at the second site (G1) showed a higher level of immature PrP^C in the ER whilst PrP glycosylated at the first site showed a higher proportion in the Golgi [Chapter 5]. The primary site of conversion to PrP^{Sc} is the plasma membrane (Goold et al., 2011) however intracellular compartments of the endocytic compartments have also been identified as potential conversion sites (Borchelt et al., 1992, Marijanovic et al., 2009, Veith et al., 2009). PrP^C is recycled from the cell surface into different endocytic compartments and can undergo retrograde transport back to the Golgi [reviewed in (Linden et al., 2008)]. PrP in the Golgi is more likely to be exposed to PrP^{Sc} that has undergone retrograde translocation and subsequently be converted than PrP in the ER. G1 mice have more non-Golgi associated PrP, which could be due to ER retention, so less mature PrP^C to convert.

Conversion of PrP^C is dependent on intact lipid rafts and *in vitro* conversion is enhanced by cofactors found in lipid rafts (Goold et al., 2011, Abid et al., 2010). While it was not possible here to isolate lipid rafts or identify the ultrastructural localisation of the different glycoforms within the membrane, this could account for differences in TSE

disease susceptibility. PrP^{C} is predominantly found in lipid rafts but moves out of raft regions when bound to some ligands in order to be internalised. Glycans have the ability to interact with ligands therefore the absence of glycans at either site may hinder interactions. It is possible that G2 PrP is present in lipid rafts for longer period of time, allowing more conversion to PrP^{Sc}.

G2 mice have more Golgi associated PrP^{C} than wild type mice, which could represent a faster synthesis and turnover of PrP, so that although there is less total PrP^{C}, during TSE infection there is a faster supply of PrP^{C} which can be converted. This may explain why G2 mice have reduced incubation periods compared to wild type mice

6.2.3 The effect of glycosylation on PrPSc deposition

This thesis examined the expression levels and alpha cleavage levels in several brain regions in an attempt to determine whether these regions preferentially expressed PrP^{C} in the GlycoD mutants and whether this corresponded to differences seen in PrP^{Sc} deposition during TSE disease. This study showed that there was no difference in expression of PrP^{C} or levels of alpha cleavage in different brain regions for any of the GlycoD mice, indicating that the change in regional deposition of PrP^{Sc} was not due to differing levels of regional PrP^{C}.
PrP^{Sc} deposition was changed in the GlycoD mice with some TSE strains (Tuzi et al., 2008). G3 mice showed deposits of amyloid plaques whereas wild type mice showed diffuse deposition of PrP^{Sc}. It has been proposed that different TSE strains may be targeted to a particular subset of cells within the brain which leads to accumulation of the PrP^{Sc} glycoform that is most abundant in those cell types. The GlycoD mutants suggest that different brain regions do not preferentially express a particular glycoform and that the overall levels of each glycoform is maintained despite the different cell types for each region.

The equal distribution of PrP^{C} throughout the brain suggests that the cell biology of PrP^{C} does not determine the targeting of PrP^{Sc} deposition. The strain targeting may be determined by another co-factor required for conversion which is found in different

brain regions, such as a ligand found in a particular cell type that allows PrP^{C} to interact with PrP^{Sc}.

The QuIC assay showed no difference in the ability of the glycoforms to fibrillise and form amyloid *in vitro*. Amyloid formation has been proposed as a protective mechanism during protein misfolding diseases (Silveira et al., 2005, Treusch et al., 2009) therefore it would be expected that glycoforms with a better ability to form amyloid would provide resistance to disease. G3 mice showed amyloid plaques *in vivo* however *in vitro* there was no difference in the efficiency of forming amyloid between G3 mice and mice that do not form amyloid *in vivo.*

6.2.4 The role of alpha cleavage in TSE disease

Cleavage plays an important role during TSE disease as well as the normal cell biology of PrP^{C}. The increased alpha cleavage in the GlycoD mice [Chapter 3] is likely to have a two-fold effect on disease; reduced full length PrP available for conversion and a higher proportion of C1 to act as an inhibitor of conversion. G3 mice were the least susceptible to TSEs and had the highest proportion of C1.

Alpha cleavage has been shown to be an important factor for TSE disease susceptibility. The proportion of PrP^{C} that underwent alpha cleavage correlated with the increased resistance in all GlycoD mutants. The same influence has been observed in other species. C1 levels have been linked to decreased susceptibility both *in vitro* and *in vivo*. Increased C1 levels have been correlated with decreased susceptibility to scrapie in sheep (Campbell et al., 2013).

It is believed that C1 is unable to convert to the protease resistant disease isoform during TSE disease as the cleavage occurs in the cytotoxic $PrP^{106\text{-}126}$ peptide (Chen et al., 1995) and C1 was not detected in PK treated immunoblots detecting PrP^{Sc}. Mice only expressing C1 were resistant to disease and did not accumulate abnormal protein (Westergard et al., 2011). However, C1 can fibrillise *in vitro* (Campbell et al., 2013). Due to the increased proportion of C1 the G3 mice had the smallest amount of full

length PrP of all the genotypes. The reduction of full length PrP could account for the increased resistance to TSE as there is less PrP^{C} available for conversion to PrP^{Sc}. The G1 and G2 mice also had reduced levels of full length PrP and decreased susceptibility to disease in comparison to wild type mice.

C1 acts as a dominant negative inhibitor for conversion therefore the higher proportion of C1 in the GlycoD mice provided a higher level of inhibition (Westergard et al., 2011). Studies using TgC1 mice showed that co-expression of a transgene for full length PrP delayed disease onset indicating that an increased proportion of C1 increases incubation period (Westergard et al., 2011). The proportion of C1 has been shown to affect disease *in vitro* and *in vivo*. Studies in overexpressing cell cultures have shown that the proportion of C1 was important in protecting against the M1000 strain (Lewis et al., 2009).

This protective effect of the alpha cleavage and its catabolites could provide a therapeutic target for disease. Increasing the levels of alpha cleavage *in vivo* would reduce the amount of full length PrP^{C} available for conversion to PrP^{Sc}. Introduction of the C1 fragment would also act as an inhibitor for conversion, decreasing conversion and potentially increasing incubation period.

6.2.5 The role of glycosylation during conversion

All glycoforms have the ability to convert to the disease associated isoform however this thesis demonstrates that there are different efficiencies of initiating conversion for the GlycoD mice [Chapter 5]. Glycosylation at the first site appeared to increase the efficiency of conversion over other glycoforms.

The increased efficiency to seed PrP^{Sc} by G2 mice may help to explain the incubation periods in some TSE strains. The changes in cell biology demonstrated here for G2 mice would predict that incubation times would be more similar to G1 mice, with increased incubation periods and resistance. However, G2 mice had much shorter incubation periods than expected for all TSE strains. G2 mice had the same incubation

period as wild type mice when challenged with ME7 even though they had half the amount of PrP^{C}. This may be a reflection of the increased efficiency in conversion in reducing the incubation period.

This study showed that unglycosylated PrP is no more efficient at seeding the conversion than diglycosylated PrP [Chapter 5]. There was no difference in the seeding ability of G1 and G3 mice, which display the greatest amount of resistance to most TSE strains and the wild type mice, which are the most susceptible. Glycosylation can increase stability therefore reducing a proteins ability to aggregate (Kayser et al., 2011, Banks, 2011) so it would be expected that unglycosylated PrP would be more efficient at conversion. *In vitro* conversion assays have shown that unglycosylated PrP converts more readily than diglycosylated PrP, presumably because the glycans hinder binding of PrP^{C} to PrP^{Sc}. However, in one study the glycosylation had no influence when the sequence of PrP^{C} was the same as PrP^{Sc} (Priola and Lawson, 2001). This suggests that the differences in susceptibilities are more influenced by the changes in cell biology seen in the GlycoD mutants than the interactions of the glycoforms during conversion.

However, this study only examined the ability to initiate conversion and not the ability to sustain conversion. The partially glycosylated glycoforms may have different efficiencies for conversion once a substantial amount of seed is present. It is also important to consider interactions between different glycoforms when interpreting seeding data from *in vitro* conversion using the GlycoD mice. Only G3 mice have a homogeneous protein all others are a heterogeneous mixture of different glycoforms. G1 and G2 PrP is a mixture of mono and unglycosylated PrP and wild type mice have a mixture of all glycoforms. Different prion strains require different glycoforms to propagate PrP^{Sc} in the *in vitro* conversion assay, PMCA (Nishina et al., 2006). The efficiency of conversion was also dependent upon the interactions of the different glycoforms.

PrP^{Sc} exists in several different aggregation states from small oligomers to large amyloid aggregates. G1 and G3 mice showed amyloid plaques with some TSE strains, suggesting that the absence of the first glycosylation site promotes amyloid formation.

Amyloid has been proposed to be a protective mechanism in protein misfolding diseases (Treusch et al., 2009) by sequestering the misfolded protein away from the toxic smaller oligomers. Although there was very little difference in seeding times between wild type, G1 and G3 PrP in *in vitro* conversion the increased resistance in the G1 and G3 mice could be due to the production of amyloid preferentially over smaller oligomers.

6.3 Final conclusions

This is the first time that the effect of PrP glycosylation has been studied in relation to the normal cell biology of the protein. This thesis has demonstrated that the glycosylation of PrP^C infuences the cell biology of the protein post-translationally. The study demonstrates that the glycans are likely to play a role in cell surface expression [Chapter 4] and are also responsible for shielding against proteolysis [Chapter 3]. Removal of a single glycan causes a reduction in PrP^C levels, an increased proportion of cleavage products and a more intracellular localisation. There are very subtle differences between a single glycan at either site, which perhaps reflects the spatial closeness of the two sites and the similarities of the glycans attached to either site. A complete lack of glycosylation causes a more extreme change than removal of a single glycan.

This thesis has shown that in addition to influencing the normal cell biology the glycosylation of host PrP^C has a role in determining susceptibility to TSE disease and incubation period through several mechanisms. A reduction in susceptibility may be in part due to the reduced availability of full length PrP^C on the cell surface available for conversion. The increased proportion of the neuroprotective N1 peptide and the dominant negative inhibitor, C1, may also help to increase resistance when glycans are lacking.

This study is the first to show that despite the similarities in protein levels and cell surface localisation between the two monoglycoforms there is a vast difference in susceptibility and disease outcome with different TSE strains. This indicates that although cell biology influences TSE disease it is not the sole determinant. A limited

study has shown that the presence of a glycan at the first site can increase the ability of PrP^{Sc} to initiate conversion.

6.4 Future work

There is a need to further understand the cell biology of the normal cellular prion protein and its isoforms. PrP is highly conserved through several species suggesting an important function yet PrP^{C} is not essential for development and survival. Several functions in neuronal development and survival have been proposed which could be carried out by different isoforms. The GlycoD mutants could be used to look at candidate binding partners, such as laminin receptor precursor 1 and NCAM (Parkyn et al., 2008, Santuccione et al., 2005) and the interactions with the different glycoforms. This could help to elucidate whether functions are carried out by particular glycoforms.

PrP^{C} has been implicated Alzheimer's disease (AD), another protein misfolding disease thus understanding the biology and function of PrP^{C} may also identify therapeutic targets for AD as well as TSE diseases. PrP^{C} is thought to be a high affinity binding partner of amyloid-β (Aβ) oligomers and N1 has been shown to protect against toxic Aβ oligomers (Beland et al., 2012, Nieznanski et al., 2012, Gimbel et al., 2010, Um et al., 2012).

PrP^{C} has a dynamic trafficking and lifecycle and the differences between the GlycoD mice in total PrP expression and cell surface expression could be due to altered trafficking or turnover. This study looked at localisation as a snapshot therefore it is difficult to know whether PrP from the GlycoD mice is retained in the secretory pathway or whether it is endocytosed more efficiently from the cell surface. Primary cultures can be used to further investigate the rate of endocytosis from the plasma membrane. Cell cultures can also be used to investigate the half-life and degradation mechanism of each glycoform.

The GlycoD mice are a useful tool to study the glycoforms separately but it would be useful to be able to identify the different PrP^C glycoforms in wild type mice. The GlycoD mutants show a dramatic change in cell biology but it is not known whether this is reflected in wild type mice where the glycoforms can potentially interact with each other. 30% of PrP in wild type mice is incompletely glycosylated but it is not known whether this represents PrP in the secretory pathway which will go on to be fully glycosylated and delivered to the cell surface or whether this is PrP at the cell surface. Cell compartments of wild type mice could be separated to identify the ratios of glycoforms in each cell compartment and identify whether monoglycosylated and unglycosylated PrP localisation is reflected from the GlycoD mice.

This study has demonstrated that the localisation and expression of PrP^C are not the only factors to influence conversion to PrP^{Sc}. This study showed that the different glycoforms had differing abilities to initiate conversion with the QuIC assay. However, the PrP^C for conversion was from a different species and showed batch to batch differences. This assay could be carried out using mouse recombinant PrP to assess whether it is a more appropriate substrate. To further investigate the influence of the glycans on the proteins ability to undergo conversion the GlycoD PrP could be used as a substrate for other *in vitro* conversion assays, such as the PMCA.

The work produced in this thesis has highlighted the complexity of the cell biology of the prion protein and the many aspects of PrP^C which influence TSE disease. The cell biology of PrP^C is a major contributor to susceptibility and could potentially be used to design therapeutic targets of TSEs. Insight into the cell biology of PrP^C may lead to understanding of the function, which could, in turn, help to identify whether the neurotoxic mechanism in disease is through loss or gain of function.

References

ABID, K., MORALES, R. & SOTO, C. 2010. Cellular factors implicated in prion replication. *FEBS Lett,* 584**,** 2409-14.

AEBI, M., BERNASCONI, R., CLERC, S. & MOLINARI, M. 2010. N-glycan structures: recognition and processing in the ER. *Trends Biochem Sci,* 35**,** 74-82.

AGUZZI, A. & HEIKENWALDER, M. 2005. Prions, cytokines, and chemokines: a meeting in lymphoid organs. *Immunity,* 22**,** 145-54.

AISINA, R., MUKHAMETOVA, L., GERSHKOVICH, K. & VARFOLOMEYEV, S. 2005. The role of carbohydrate side chains of plasminogen in its activation by staphylokinase. *Biochim Biophys Acta,* 1725**,** 370-6.

ALFA CISSE, M., SUNYACH, C., SLACK, B. E., FISHER, A., VINCENT, B. & CHECLER, F. 2007. M1 and M3 muscarinic receptors control physiological processing of cellular prion by modulating ADAM17 phosphorylation and activity. *J Neurosci,* 27**,** 4083-92.

ALPER, T., CRAMP, W. A., HAIG, D. A. & CLARKE, M. C. 1967. Does the agent of scrapie replicate without nucleic acid? *Nature,* 214**,** 764-6.

ALTMEPPEN, H. C., PROX, J., PUIG, B., KLUTH, M. A., BERNREUTHER, C., THURM, D., JORISSEN, E., PETROWITZ, B., BARTSCH, U., DE STROOPER, B., SAFTIG, P. & GLATZEL, M. 2011. Lack of a-disintegrin-and-metalloproteinase ADAM10 leads to intracellular accumulation and loss of shedding of the cellular prion protein in vivo. *Mol Neurodegener,* 6**,** 36.

ALTMEPPEN, H. C., PUIG, B., DOHLER, F., THURM, D. K., FALKER, C., KRASEMANN, S. & GLATZEL, M. 2012. Proteolytic processing of the prion protein in health and disease. *Am J Neurodegener Dis,* 1**,** 15-31.

ARMENDARIZ, A. D., GONZALEZ, M., LOGUINOV, A. V. & VULPE, C. D. 2004. Gene expression profiling in chronic copper overload reveals upregulation of Prnp and App. *Physiol Genomics,* 20**,** 45-54.

ARNOLD, J. E., TIPLER, C., LASZLO, L., HOPE, J., LANDON, M. & MAYER, R. J. 1995. The abnormal isoform of the prion protein accumulates in late-endosome-like organelles in scrapie-infected mouse brain. *J Pathol,* 176**,** 403-11.

ARONOFF-SPENCER, E., BURNS, C. S., AVDIEVICH, N. I., GERFEN, G. J., PEISACH, J., ANTHOLINE, W. E., BALL, H. L., COHEN, F. E., PRUSINER, S. B. & MILLHAUSER, G. L. 2000. Identification of the Cu2+ binding sites in the N-terminal domain of the prion protein by EPR and CD spectroscopy. *Biochemistry,* 39**,** 13760-71.

ARSENAULT, R. J., LI, Y., POTTER, A., GRIEBEL, P. J., KUSALIK, A. & NAPPER, S. 2012. Induction of ligand-specific PrP (C) signaling in human neuronal cells. *Prion,* 6**,** 477-88.

ATARASHI, R., WILHAM, J. M., CHRISTENSEN, L., HUGHSON, A. G., MOORE, R. A., JOHNSON, L. M., ONWUBIKO, H. A., PRIOLA, S. A. & CAUGHEY, B. 2008. Simplified ultrasensitive prion detection by recombinant PrP conversion with shaking. *Nat Methods,* 5**,** 211-2.

AZZALIN, A., FERRARA, V., ARIAS, A., CERRI, S., AVELLA, D., PISU, M. B., NANO, R., BERNOCCHI, G., FERRETTI, L. & COMINCINI, S. 2006. Interaction between the cellular prion (PrPC) and the 2P domain K+ channel TREK-1 protein. *Biochem Biophys Res Commun,* 346**,** 108-15.

BALDWIN, M. A., PAN, K. M., NGUYEN, J., HUANG, Z., GROTH, D., SERBAN, A., GASSET, M., MEHLHORN, I., FLETTERICK, R. J., COHEN, F. E. & ET AL. 1994. Spectroscopic characterization of conformational differences between PrPC and PrPSc: an alpha-helix to beta-sheet transition. *Philos Trans R Soc Lond B Biol Sci,* 343**,** 435-41.

BANKS, D. D. 2011. The effect of glycosylation on the folding kinetics of erythropoietin. *J Mol Biol,* 412**,** 536-50.

BARNEWITZ, K., MARINGER, M., MITTEREGGER, G., GIESE, A., BERTSCH, U. & KRETZSCHMAR, H. A. 2006. Unaltered prion protein cleavage in plasminogen-deficient mice. *Neuroreport,* 17**,** 527-30.

BARR, J. B., SOMERVILLE, R. A., CHUNG, Y. L. & FRASER, J. R. 2004. Microdissection: a method developed to investigate mechanisms involved in transmissible spongiform encephalopathy pathogenesis. *BMC Infect Dis,* 4**,** 8.

BARRIA, M. A., MUKHERJEE, A., GONZALEZ-ROMERO, D., MORALES, R. & SOTO, C. 2009. De novo generation of infectious prions in vitro produces a new disease phenotype. *PLoS Pathog,* 5**,** e1000421.

BARRON, R. M., CAMPBELL, S. L., KING, D., BELLON, A., CHAPMAN, K. E., WILLIAMSON, R. A. & MANSON, J. C. 2007. High titers of transmissible spongiform encephalopathy infectivity associated with extremely low levels of PrPSc in vivo. *J Biol Chem,* 282**,** 35878-86.

BASLER, K., OESCH, B., SCOTT, M., WESTAWAY, D., WALCHLI, M., GROTH, D. F., MCKINLEY, M. P., PRUSINER, S. B. & WEISSMANN, C. 1986. Scrapie and cellular PrP isoforms are encoded by the same chromosomal gene. *Cell,* 46**,** 417-28.

BECK, K. E., VICKERY, C. M., LOCKEY, R., HOLDER, T., THORNE, L., TERRY, L. A., DENYER, M., WEBB, P., SIMMONS, M. M. & SPIROPOULOS, J. 2012. The interpretation of disease phenotypes to identify TSE strains following murine bioassay: characterisation of classical scrapie. *Vet Res,* 43**,** 77.

BELAND, M., MOTARD, J., BARBARIN, A. & ROUCOU, X. 2012. PrP(C) homodimerization stimulates the production of PrPC cleaved fragments PrPN1 and PrPC1. *J Neurosci,* 32**,** 13255-63.

BENVEGNU, S., POGGIOLINI, I. & LEGNAME, G. 2010. Neurodevelopmental expression and localization of the cellular prion protein in the central nervous system of the mouse. *J Comp Neurol,* 518**,** 1879-91.

BERANGER, F., MANGE, A., GOUD, B. & LEHMANN, S. 2002. Stimulation of PrP(C) retrograde transport toward the endoplasmic reticulum increases accumulation of PrP(Sc) in prion-infected cells. *J Biol Chem,* 277**,** 38972-7.

BERG, D. T., BURCK, P. J., BERG, D. H. & GRINNELL, B. W. 1993. Kringle glycosylation in a modified human tissue plasminogen activator improves functional properties. *Blood,* 81**,** 1312-22.

BERINGUE, V., BENCSIK, A., LE DUR, A., REINE, F., LAI, T. L., CHENAIS, N., TILLY, G., BIACABE, A. G., BARON, T., VILOTTE, J. L. & LAUDE, H. 2006. Isolation from cattle of a prion strain distinct from that causing bovine spongiform encephalopathy. *PLoS Pathog,* 2**,** e112.

BERINGUE, V., MALLINSON, G., KAISAR, M., TAYEBI, M., SATTAR, Z., JACKSON, G., ANSTEE, D., COLLINGE, J. & HAWKE, S. 2003. Regional

heterogeneity of cellular prion protein isoforms in the mouse brain. *Brain,* 126**,** 2065-73.
BORCHELT, D. R., ROGERS, M., STAHL, N., TELLING, G. & PRUSINER, S. B. 1993. Release of the cellular prion protein from cultured cells after loss of its glycoinositol phospholipid anchor. *Glycobiology,* 3**,** 319-29.
BORCHELT, D. R., TARABOULOS, A. & PRUSINER, S. B. 1992. Evidence for synthesis of scrapie prion proteins in the endocytic pathway. *J Biol Chem,* 267**,** 16188-99.
BOSQUES, C. J. & IMPERIALI, B. 2003. The interplay of glycosylation and disulfide formation influences fibrillization in a prion protein fragment. *Proc Natl Acad Sci U S A,* 100**,** 7593-8.
BOSSERS, A., BELT, P., RAYMOND, G. J., CAUGHEY, B., DE VRIES, R. & SMITS, M. A. 1997. Scrapie susceptibility-linked polymorphisms modulate the in vitro conversion of sheep prion protein to protease-resistant forms. *Proc Natl Acad Sci U S A,* 94**,** 4931-6.
BOUNHAR, Y., MANN, K. K., ROUCOU, X. & LEBLANC, A. C. 2006. Prion protein prevents Bax-mediated cell death in the absence of other Bcl-2 family members in Saccharomyces cerevisiae. *FEMS Yeast Res,* 6**,** 1204-12.
BOUNHAR, Y., ZHANG, Y., GOODYER, C. G. & LEBLANC, A. 2001. Prion protein protects human neurons against Bax-mediated apoptosis. *J Biol Chem,* 276**,** 39145-9.
BOUZAMONDO-BERNSTEIN, E., HOPKINS, S. D., SPILMAN, P., UYEHARA-LOCK, J., DEERING, C., SAFAR, J., PRUSINER, S. B., RALSTON, H. J., 3RD & DEARMOND, S. J. 2004. The neurodegeneration sequence in prion diseases: evidence from functional, morphological and ultrastructural studies of the GABAergic system. *J Neuropathol Exp Neurol,* 63**,** 882-99.
BRAGASON, B. T. & PALSDOTTIR, A. 2005. Interaction of PrP with NRAGE, a protein involved in neuronal apoptosis. *Mol Cell Neurosci,* 29**,** 232-44.
BREMER, J., BAUMANN, F., TIBERI, C., WESSIG, C., FISCHER, H., SCHWARZ, P., STEELE, A. D., TOYKA, K. V., NAVE, K. A., WEIS, J. & AGUZZI, A. 2010. Axonal prion protein is required for peripheral myelin maintenance. *Nat Neurosci,* 13**,** 310-8.
BREWER, G. J., TORRICELLI, J. R., EVEGE, E. K. & PRICE, P. J. 1993. Optimized survival of hippocampal neurons in B27-supplemented Neurobasal, a new serum-free medium combination. *J Neurosci Res,* 35**,** 567-76.
BROWN, D. R. 2003. Prion protein expression modulates neuronal copper content. *J Neurochem,* 87**,** 377-85.
BROWN, D. R. 2004. Role of the prion protein in copper turnover in astrocytes. *Neurobiol Dis,* 15**,** 534-43.
BROWN, D. R., IORDANOVA, I. K., WONG, B. S., VENIEN-BRYAN, C., HAFIZ, F., GLASSSMITH, L. L., SY, M. S., GAMBETTI, P., JONES, I. M., CLIVE, C. & HASWELL, S. J. 2000. Functional and structural differences between the prion protein from two alleles prnp(a) and prnp(b) of mouse. *Eur J Biochem,* 267**,** 2452-9.
BROWN, D. R., NICHOLAS, R. S. & CANEVARI, L. 2002. Lack of prion protein expression results in a neuronal phenotype sensitive to stress. *J Neurosci Res,* 67**,** 211-24.

BROWN, D. R., SCHMIDT, B. & KRETZSCHMAR, H. A. 1996. Role of microglia and host prion protein in neurotoxicity of a prion protein fragment. *Nature,* 380**,** 345-7.

BROWN, H. R., GOLLER, N. L., RUDELLI, R. D., MERZ, G. S., WOLFE, G. C., WISNIEWSKI, H. M. & ROBAKIS, N. K. 1990. The mRNA encoding the scrapie agent protein is present in a variety of non-neuronal cells. *Acta Neuropathol,* 80**,** 1-6.

BROWN, P., GIBBS, C. J., JR., RODGERS-JOHNSON, P., ASHER, D. M., SULIMA, M. P., BACOTE, A., GOLDFARB, L. G. & GAJDUSEK, D. C. 1994. Human spongiform encephalopathy: the National Institutes of Health series of 300 cases of experimentally transmitted disease. *Ann Neurol,* 35**,** 513-29.

BROWNLEE, A. 1940. Histo-Pathological Studies of Scrapie, an Obscure Disease of Sheep. *The Veterinary Journal,* 96**,** 254-264.

BRUCE, M. E. 2003. TSE strain variation. *Br Med Bull,* 66**,** 99-108.

BRUGGER, B., GRAHAM, C., LEIBRECHT, I., MOMBELLI, E., JEN, A., WIELAND, F. & MORRIS, R. 2004. The membrane domains occupied by glycosylphosphatidylinositol-anchored prion protein and Thy-1 differ in lipid composition. *J Biol Chem,* 279**,** 7530-6.

BUCCI, C., PARTON, R. G., MATHER, I. H., STUNNENBERG, H., SIMONS, K., HOFLACK, B. & ZERIAL, M. 1992. The small GTPase rab5 functions as a regulatory factor in the early endocytic pathway. *Cell,* 70**,** 715-28.

BUDKA, H., AGUZZI, A., BROWN, P., BRUCHER, J. M., BUGIANI, O., GULLOTTA, F., HALTIA, M., HAUW, J. J., IRONSIDE, J. W., JELLINGER, K. & ET AL. 1995. Neuropathological diagnostic criteria for Creutzfeldt-Jakob disease (CJD) and other human spongiform encephalopathies (prion diseases). *Brain Pathol,* 5**,** 459-66.

BUELER, H., AGUZZI, A., SAILER, A., GREINER, R. A., AUTENRIED, P., AGUET, M. & WEISSMANN, C. 1993. Mice devoid of PrP are resistant to scrapie. *Cell,* 73**,** 1339-47.

BUELER, H., FISCHER, M., LANG, Y., BLUETHMANN, H., LIPP, H. P., DEARMOND, S. J., PRUSINER, S. B., AGUET, M. & WEISSMANN, C. 1992. Normal development and behaviour of mice lacking the neuronal cell-surface PrP protein. *Nature,* 356**,** 577-82.

CAETANO, F. A., LOPES, M. H., HAJJ, G. N., MACHADO, C. F., PINTO ARANTES, C., MAGALHAES, A. C., VIEIRA MDE, P., AMERICO, T. A., MASSENSINI, A. R., PRIOLA, S. A., VORBERG, I., GOMEZ, M. V., LINDEN, R., PRADO, V. F., MARTINS, V. R. & PRADO, M. A. 2008. Endocytosis of prion protein is required for ERK1/2 signaling induced by stress-inducible protein 1. *J Neurosci,* 28**,** 6691-702.

CALZOLAI, L., LYSEK, D. A., PEREZ, D. R., GUNTERT, P. & WUTHRICH, K. 2005. Prion protein NMR structures of chickens, turtles, and frogs. *Proc Natl Acad Sci U S A,* 102**,** 651-5.

CAMPANA, V., SARNATARO, D., FASANO, C., CASANOVA, P., PALADINO, S. & ZURZOLO, C. 2006. Detergent-resistant membrane domains but not the proteasome are involved in the misfolding of a PrP mutant retained in the endoplasmic reticulum. *J Cell Sci,* 119**,** 433-42.

CAMPANA, V., SARNATARO, D. & ZURZOLO, C. 2005. The highways and byways of prion protein trafficking. *Trends Cell Biol,* 15**,** 102-11.
CAMPBELL, L., GILL, A. C., MCGOVERN, G., JALLAND, C. M., HOPKINS, J., TRANULIS, M. A., HUNTER, N. & GOLDMANN, W. 2013. The PrP(C) C1 fragment derived from the ovine A136R154R171PRNP allele is highly abundant in sheep brain and inhibits fibrillisation of full-length PrP(C) protein in vitro. *Biochim Biophys Acta,* 1832**,** 826-36.
CANCELLOTTI, E., BARRON, R. M., BISHOP, M. T., HART, P., WISEMAN, F. & MANSON, J. C. 2007. The role of host PrP in Transmissible Spongiform Encephalopathies. *Biochim Biophys Acta,* 1772**,** 673-80.
CANCELLOTTI, E., BRADFORD, B. M., TUZI, N. L., HICKEY, R. D., BROWN, D., BROWN, K. L., BARRON, R. M., KISIELEWSKI, D., PICCARDO, P. & MANSON, J. C. 2010. Glycosylation of PrPC determines timing of neuroinvasion and targeting in the brain following transmissible spongiform encephalopathy infection by a peripheral route. *J Virol,* 84**,** 3464-75.
CANCELLOTTI, E., MAHAL, S. P., SOMERVILLE, R., DIACK, A., BROWN, D., PICCARDO, P., WEISSMANN, C. & MANSON, J. C. 2013. Post-translational changes to PrP alter transmissible spongiform encephalopathy strain properties. *EMBO J.*
CANCELLOTTI, E., WISEMAN, F., TUZI, N. L., BAYBUTT, H., MONAGHAN, P., AITCHISON, L., SIMPSON, J. & MANSON, J. C. 2005. Altered glycosylated PrP proteins can have different neuronal trafficking in brain but do not acquire scrapie-like properties. *J Biol Chem,* 280**,** 42909-18.
CAPLAN, S., GREEN, R., ROCCO, J. & KURJAN, J. 1991. Glycosylation and structure of the yeast MF alpha 1 alpha-factor precursor is important for efficient transport through the secretory pathway. *J Bacteriol,* 173**,** 627-35.
CAUGHEY, B. & BARON, G. S. 2006. Prions and their partners in crime. *Nature,* 443**,** 803-10.
CHAVAN, M., YAN, A. & LENNARZ, W. J. 2005. Subunits of the translocon interact with components of the oligosaccharyl transferase complex. *J Biol Chem,* 280**,** 22917-24.
CHEN, J. & THIRUMALAI, D. 2013. Helices 2 and 3 Are the Initiation Sites in the PrP(C) --> PrP(SC) Transition. *Biochemistry,* 52**,** 310-9.
CHEN, S., MANGE, A., DONG, L., LEHMANN, S. & SCHACHNER, M. 2003. Prion protein as trans-interacting partner for neurons is involved in neurite outgrowth and neuronal survival. *Mol Cell Neurosci,* 22**,** 227-33.
CHEN, S. G., TEPLOW, D. B., PARCHI, P., TELLER, J. K., GAMBETTI, P. & AUTILIO-GAMBETTI, L. 1995. Truncated forms of the human prion protein in normal brain and in prion diseases. *J Biol Chem,* 270**,** 19173-80.
CHEN, X., JEN, A., WARLEY, A., LAWRENCE, M. J., QUINN, P. J. & MORRIS, R. J. 2009. Isolation at physiological temperature of detergent-resistant membranes with properties expected of lipid rafts: the influence of buffer composition. *Biochem J,* 417**,** 525-33.
CHEN, X., MORRIS, R., LAWRENCE, M. J. & QUINN, P. J. 2007. The isolation and structure of membrane lipid rafts from rat brain. *Biochimie,* 89**,** 192-6.
CHESEBRO, B. 1998. BSE and prions: uncertainties about the agent. *Science,* 279**,** 42-3.

CHESEBRO, B., TRIFILO, M., RACE, R., MEADE-WHITE, K., TENG, C., LACASSE, R., RAYMOND, L., FAVARA, C., BARON, G., PRIOLA, S., CAUGHEY, B., MASLIAH, E. & OLDSTONE, M. 2005. Anchorless prion protein results in infectious amyloid disease without clinical scrapie. *Science,* 308**,** 1435-9.

CHIESA, R., PICCARDO, P., GHETTI, B. & HARRIS, D. A. 1998. Neurological illness in transgenic mice expressing a prion protein with an insertional mutation. *Neuron,* 21**,** 1339-51.

CHITI, F. & DOBSON, C. M. 2006. Protein misfolding, functional amyloid, and human disease. *Annu Rev Biochem,* 75**,** 333-66.

CLOUSER, C. L. & MENON, K. M. 2005. N-linked glycosylation facilitates processing and cell surface expression of rat luteinizing hormone receptor. *Mol Cell Endocrinol,* 235**,** 11-9.

COITINHO, A. S., ROESLER, R., MARTINS, V. R., BRENTANI, R. R. & IZQUIERDO, I. 2003. Cellular prion protein ablation impairs behavior as a function of age. *Neuroreport,* 14**,** 1375-9.

COLLING, S. B., COLLINGE, J. & JEFFERYS, J. G. 1996. Hippocampal slices from prion protein null mice: disrupted Ca(2+)-activated K+ currents. *Neurosci Lett,* 209**,** 49-52.

COLLING, S. B., KHANA, M., COLLINGE, J. & JEFFERYS, J. G. 1997. Mossy fibre reorganization in the hippocampus of prion protein null mice. *Brain Res,* 755**,** 28-35.

COLLINGE, J. 2001. Prion diseases of humans and animals: their causes and molecular basis. *Annu Rev Neurosci,* 24**,** 519-50.

COLLINGE, J., SIDLE, K. C., MEADS, J., IRONSIDE, J. & HILL, A. F. 1996. Molecular analysis of prion strain variation and the aetiology of 'new variant' CJD. *Nature,* 383**,** 685-90.

COLLINGE, J., WHITTINGTON, M. A., SIDLE, K. C., SMITH, C. J., PALMER, M. S., CLARKE, A. R. & JEFFERYS, J. G. 1994. Prion protein is necessary for normal synaptic function. *Nature,* 370**,** 295-7.

COME, J. H., FRASER, P. E. & LANSBURY, P. T., JR. 1993. A kinetic model for amyloid formation in the prion diseases: importance of seeding. *Proc Natl Acad Sci U S A,* 90**,** 5959-63.

CUNNINGHAM, C., DEACON, R., WELLS, H., BOCHE, D., WATERS, S., DINIZ, C. P., SCOTT, H., RAWLINS, J. N. & PERRY, V. H. 2003. Synaptic changes characterize early behavioural signs in the ME7 model of murine prion disease. *Eur J Neurosci,* 17**,** 2147-55.

DEARMOND, S. J. & PRUSINER, S. B. 2003. Perspectives on prion biology, prion disease pathogenesis, and pharmacologic approaches to treatment. *Clin Lab Med,* 23**,** 1-41.

DEARMOND, S. J., QIU, Y., SANCHEZ, H., SPILMAN, P. R., NINCHAK-CASEY, A., ALONSO, D. & DAGGETT, V. 1999. PrPc glycoform heterogeneity as a function of brain region: implications for selective targeting of neurons by prion strains. *J Neuropathol Exp Neurol,* 58**,** 1000-9.

DEMARCO, M. L. & DAGGETT, V. 2009. Characterization of cell-surface prion protein relative to its recombinant analogue: insights from molecular dynamics

simulations of diglycosylated, membrane-bound human prion protein. *J Neurochem,* 109**,** 60-73.
DEVASAHAYAM, M., CATALINO, P. D., RUDD, P. M., DWEK, R. A. & BARCLAY, A. N. 1999. The glycan processing and site occupancy of recombinant Thy-1 is markedly affected by the presence of a glycosylphosphatidylinositol anchor. *Glycobiology,* 9**,** 1381-7.
DIARRA-MEHRPOUR, M., ARRABAL, S., JALIL, A., PINSON, X., GAUDIN, C., PIETU, G., PITAVAL, A., RIPOCHE, H., ELOIT, M., DORMONT, D. & CHOUAIB, S. 2004. Prion protein prevents human breast carcinoma cell line from tumor necrosis factor alpha-induced cell death. *Cancer Res,* 64**,** 719-27.
DONNE, D. G., VILES, J. H., GROTH, D., MEHLHORN, I., JAMES, T. L., COHEN, F. E., PRUSINER, S. B., WRIGHT, P. E. & DYSON, H. J. 1997. Structure of the recombinant full-length hamster prion protein PrP(29-231): the N terminus is highly flexible. *Proc Natl Acad Sci U S A,* 94**,** 13452-7.
DRICKAMER, K. & TAYLOR, M. E. 1998. Evolving views of protein glycosylation. *Trends Biochem Sci,* 23**,** 321-4.
DRISALDI, B., COOMARASWAMY, J., MASTRANGELO, P., STROME, B., YANG, J., WATTS, J. C., CHISHTI, M. A., MARVI, M., WINDL, O., AHRENS, R., MAJOR, F., SY, M. S., KRETZSCHMAR, H., FRASER, P. E., MOUNT, H. T. & WESTAWAY, D. 2004. Genetic mapping of activity determinants within cellular prion proteins: N-terminal modules in PrPC offset pro-apoptotic activity of the Doppel helix B/B' region. *J Biol Chem,* 279**,** 55443-54.
EDENHOFER, F., RIEGER, R., FAMULOK, M., WENDLER, W., WEISS, S. & WINNACKER, E. L. 1996. Prion protein PrPc interacts with molecular chaperones of the Hsp60 family. *J Virol,* 70**,** 4724-8.
ERMONVAL, M., MOUILLET-RICHARD, S., CODOGNO, P., KELLERMANN, O. & BOTTI, J. 2003. Evolving views in prion glycosylation: functional and pathological implications. *Biochimie,* 85**,** 33-45.
ETTAICHE, M., PICHOT, R., VINCENT, J. P. & CHABRY, J. 2000. In vivo cytotoxicity of the prion protein fragment 106-126. *J Biol Chem,* 275**,** 36487-90.
FABER, H. R. & MATTHEWS, B. W. 1990. A mutant T4 lysozyme displays five different crystal conformations. *Nature,* 348**,** 263-6.
FARQUHAR, C. F., DORNAN, J., SOMERVILLE, R. A., TUNSTALL, A. M. & HOPE, J. 1994. Effect of Sinc genotype, agent isolate and route of infection on the accumulation of protease-resistant PrP in non-central nervous system tissues during the development of murine scrapie. *J Gen Virol,* 75 (Pt 3)**,** 495-504.
FERNANDES, H., COHEN, S. & BISHAYEE, S. 2001. Glycosylation-induced conformational modification positively regulates receptor-receptor association: a study with an aberrant epidermal growth factor receptor (EGFRvIII/DeltaEGFR) expressed in cancer cells. *J Biol Chem,* 276**,** 5375-83.
FEVRIER, B., VILETTE, D., ARCHER, F., LOEW, D., FAIGLE, W., VIDAL, M., LAUDE, H. & RAPOSO, G. 2004. Cells release prions in association with exosomes. *Proc Natl Acad Sci U S A,* 101**,** 9683-8.
FISCHER, M., RULICKE, T., RAEBER, A., SAILER, A., MOSER, M., OESCH, B., BRANDNER, S., AGUZZI, A. & WEISSMANN, C. 1996. Prion protein (PrP)

with amino-proximal deletions restoring susceptibility of PrP knockout mice to scrapie. *EMBO J,* 15**,** 1255-64.
FIVAZ, M., VILBOIS, F., THURNHEER, S., PASQUALI, C., ABRAMI, L., BICKEL, P. E., PARTON, R. G. & VAN DER GOOT, F. G. 2002. Differential sorting and fate of endocytosed GPI-anchored proteins. *EMBO J,* 21**,** 3989-4000.
FLECHSIG, E., SHMERLING, D., HEGYI, I., RAEBER, A. J., FISCHER, M., COZZIO, A., VON MERING, C., AGUZZI, A. & WEISSMANN, C. 2000. Prion protein devoid of the octapeptide repeat region restores susceptibility to scrapie in PrP knockout mice. *Neuron,* 27**,** 399-408.
FORD, M. J., BURTON, L. J., LI, H., GRAHAM, C. H., FROBERT, Y., GRASSI, J., HALL, S. M. & MORRIS, R. J. 2002a. A marked disparity between the expression of prion protein and its message by neurones of the CNS. *Neuroscience,* 111**,** 533-51.
FORD, M. J., BURTON, L. J., MORRIS, R. J. & HALL, S. M. 2002b. Selective expression of prion protein in peripheral tissues of the adult mouse. *Neuroscience,* 113**,** 177-92.
FORLONI, G., ANGERETTI, N., CHIESA, R., MONZANI, E., SALMONA, M., BUGIANI, O. & TAGLIAVINI, F. 1993. Neurotoxicity of a prion protein fragment. *Nature,* 362**,** 543-6.
FOURNIER, J. G., ESCAIG-HAYE, F., BILLETTE DE VILLEMEUR, T. & ROBAIN, O. 1995. Ultrastructural localization of cellular prion protein (PrPc) in synaptic boutons of normal hamster hippocampus. *C R Acad Sci III,* 318**,** 339-44.
FUJII, S., NISHIURA, T., NISHIKAWA, A., MIURA, R. & TANIGUCHI, N. 1990. Structural heterogeneity of sugar chains in immunoglobulin G. Conformation of immunoglobulin G molecule and substrate specificities of glycosyltransferases. *J Biol Chem,* 265**,** 6009-18.
GABIUS, H. J. 1994. Non-carbohydrate binding partners/domains of animal lectins. *Int J Biochem,* 26**,** 469-77.
GABRIEL, J. M., OESCH, B., KRETZSCHMAR, H., SCOTT, M. & PRUSINER, S. B. 1992. Molecular cloning of a candidate chicken prion protein. *Proc Natl Acad Sci U S A,* 89**,** 9097-101.
GAMBETTI, P., PARCHI, P. & CHEN, S. G. 2003. Hereditary Creutzfeldt-Jakob disease and fatal familial insomnia. *Clin Lab Med,* 23**,** 43-64.
GASSET, M., BALDWIN, M. A., LLOYD, D. H., GABRIEL, J. M., HOLTZMAN, D. M., COHEN, F., FLETTERICK, R. & PRUSINER, S. B. 1992. Predicted alpha-helical regions of the prion protein when synthesized as peptides form amyloid. *Proc Natl Acad Sci U S A,* 89**,** 10940-4.
GAUCZYNSKI, S., PEYRIN, J. M., HAIK, S., LEUCHT, C., HUNDT, C., RIEGER, R., KRASEMANN, S., DESLYS, J. P., DORMONT, D., LASMEZAS, C. I. & WEISS, S. 2001. The 37-kDa/67-kDa laminin receptor acts as the cell-surface receptor for the cellular prion protein. *EMBO J,* 20**,** 5863-75.
GAVIER-WIDEN, D., STACK, M. J., BARON, T., BALACHANDRAN, A. & SIMMONS, M. 2005. Diagnosis of transmissible spongiform encephalopathies in animals: a review. *J Vet Diagn Invest,* 17**,** 509-27.
GIBBONS, R. A. & HUNTER, G. D. 1967. Nature of the scrapie agent. *Nature,* 215**,** 1041-3.

GILCH, S., WINKLHOFER, K. F., GROSCHUP, M. H., NUNZIANTE, M., LUCASSEN, R., SPIELHAUPTER, C., MURANYI, W., RIESNER, D., TATZELT, J. & SCHATZL, H. M. 2001. Intracellular re-routing of prion protein prevents propagation of PrP(Sc) and delays onset of prion disease. *EMBO J,* 20**,** 3957-66.

GIMBEL, D. A., NYGAARD, H. B., COFFEY, E. E., GUNTHER, E. C., LAUREN, J., GIMBEL, Z. A. & STRITTMATTER, S. M. 2010. Memory impairment in transgenic Alzheimer mice requires cellular prion protein. *J Neurosci,* 30**,** 6367-74.

GO, E. P., IRUNGU, J., ZHANG, Y., DALPATHADO, D. S., LIAO, H. X., SUTHERLAND, L. L., ALAM, S. M., HAYNES, B. F. & DESAIRE, H. 2008. Glycosylation site-specific analysis of HIV envelope proteins (JR-FL and CON-S) reveals major differences in glycosylation site occupancy, glycoform profiles, and antigenic epitopes' accessibility. *J Proteome Res,* 7**,** 1660-74.

GOOLD, R., RABBANIAN, S., SUTTON, L., ANDRE, R., ARORA, P., MOONGA, J., CLARKE, A. R., SCHIAVO, G., JAT, P., COLLINGE, J. & TABRIZI, S. J. 2011. Rapid cell-surface prion protein conversion revealed using a novel cell system. *Nat Commun,* 2**,** 281.

GRANER, E., MERCADANTE, A. F., ZANATA, S. M., FORLENZA, O. V., CABRAL, A. L., VEIGA, S. S., JULIANO, M. A., ROESLER, R., WALZ, R., MINETTI, A., IZQUIERDO, I., MARTINS, V. R. & BRENTANI, R. R. 2000a. Cellular prion protein binds laminin and mediates neuritogenesis. *Brain Res Mol Brain Res,* 76**,** 85-92.

GRANER, E., MERCADANTE, A. F., ZANATA, S. M., MARTINS, V. R., JAY, D. G. & BRENTANI, R. R. 2000b. Laminin-induced PC-12 cell differentiation is inhibited following laser inactivation of cellular prion protein. *FEBS Lett,* 482**,** 257-60.

GRASBON-FRODL, E., LORENZ, H., MANN, U., NITSCH, R. M., WINDL, O. & KRETZSCHMAR, H. A. 2004. Loss of glycosylation associated with the T183A mutation in human prion disease. *Acta Neuropathol,* 108**,** 476-84.

GRIFFITH, J. S. 1967. Self-replication and scrapie. *Nature,* 215**,** 1043-4.

GRINNELL, B. W., WALLS, J. D. & GERLITZ, B. 1991. Glycosylation of human protein C affects its secretion, processing, functional activities, and activation by thrombin. *J Biol Chem,* 266**,** 9778-85.

GU, Y., VERGHESE, S., MISHRA, R. S., XU, X., SHI, Y. & SINGH, N. 2003. Mutant prion protein-mediated aggregation of normal prion protein in the endoplasmic reticulum: implications for prion propagation and neurotoxicity. *J Neurochem,* 84**,** 10-22.

GUILLOT-SESTIER, M. V., SUNYACH, C., DRUON, C., SCARZELLO, S. & CHECLER, F. 2009. The alpha-secretase-derived N-terminal product of cellular prion, N1, displays neuroprotective function in vitro and in vivo. *J Biol Chem,* 284**,** 35973-86.

GUILLOT-SESTIER, M. V., SUNYACH, C., FERREIRA, S. T., MARZOLO, M. P., BAUER, C., THEVENET, A. & CHECLER, F. 2012. alpha-Secretase-derived fragment of cellular prion, N1, protects against monomeric and oligomeric amyloid beta (Abeta)-associated cell death. *J Biol Chem,* 287**,** 5021-32.

HAIGH, C. L., LEWIS, V. A., VELLA, L. J., MASTERS, C. L., HILL, A. F., LAWSON, V. A. & COLLINS, S. J. 2009. PrPC-related signal transduction is influenced by copper, membrane integrity and the alpha cleavage site. *Cell Res,* 19**,** 1062-78.

HALABAN, R., MOELLMANN, G., TAMURA, A., KWON, B. S., KUKLINSKA, E., POMERANTZ, S. H. & LERNER, A. B. 1988. Tyrosinases of murine melanocytes with mutations at the albino locus. *Proc Natl Acad Sci U S A,* 85**,** 7241-5.

HANSON, S. R., CULYBA, E. K., HSU, T. L., WONG, C. H., KELLY, J. W. & POWERS, E. T. 2009. The core trisaccharide of an N-linked glycoprotein intrinsically accelerates folding and enhances stability. *Proc Natl Acad Sci U S A,* 106**,** 3131-6.

HARPER, J. D. & LANSBURY, P. T., JR. 1997. Models of amyloid seeding in Alzheimer's disease and scrapie: mechanistic truths and physiological consequences of the time-dependent solubility of amyloid proteins. *Annu Rev Biochem,* 66**,** 385-407.

HARRIS, D. A. 2003. Trafficking, turnover and membrane topology of PrP. *Br Med Bull,* 66**,** 71-85.

HASEGAWA, M., ORITA, T., KOJIMA, T., TOMONOH, K., HIRATA, Y. & OCHI, N. 1992. Improvement in the heterogeneous N-termini and the defective N-glycosylation of human interleukin-6 by genetic engineering. *Eur J Biochem,* 210**,** 9-12.

HECKER, R., TARABOULOS, A., SCOTT, M., PAN, K. M., YANG, S. L., TORCHIA, M., JENDROSKA, K., DEARMOND, S. J. & PRUSINER, S. B. 1992. Replication of distinct scrapie prion isolates is region specific in brains of transgenic mice and hamsters. *Genes Dev,* 6**,** 1213-28.

HEFFER-LAUC, M., LAUC, G., NIMRICHTER, L., FROMHOLT, S. E. & SCHNAAR, R. L. 2005. Membrane redistribution of gangliosides and glycosylphosphatidylinositol-anchored proteins in brain tissue sections under conditions of lipid raft isolation. *Biochim Biophys Acta,* 1686**,** 200-8.

HERMS, J., TINGS, T., GALL, S., MADLUNG, A., GIESE, A., SIEBERT, H., SCHURMANN, P., WINDL, O., BROSE, N. & KRETZSCHMAR, H. 1999. Evidence of presynaptic location and function of the prion protein. *J Neurosci,* 19**,** 8866-75.

HOLSCHER, C., BACH, U. C. & DOBBERSTEIN, B. 2001. Prion protein contains a second endoplasmic reticulum targeting signal sequence located at its C terminus. *J Biol Chem,* 276**,** 13388-94.

HOLSCHER, C., DELIUS, H. & BURKLE, A. 1998. Overexpression of nonconvertible PrPc delta114-121 in scrapie-infected mouse neuroblastoma cells leads to trans-dominant inhibition of wild-type PrP(Sc) accumulation. *J Virol,* 72**,** 1153-9.

HORIUCHI, M. & CAUGHEY, B. 1999. Specific binding of normal prion protein to the scrapie form via a localized domain initiates its conversion to the protease-resistant state. *EMBO J,* 18**,** 3193-203.

HORNEMANN, S., SCHORN, C. & WUTHRICH, K. 2004. NMR structure of the bovine prion protein isolated from healthy calf brains. *EMBO Rep,* 5**,** 1159-64.

HSIAO, K. K., SCOTT, M., FOSTER, D., GROTH, D. F., DEARMOND, S. J. & PRUSINER, S. B. 1990. Spontaneous neurodegeneration in transgenic mice with mutant prion protein. *Science,* 250**,** 1587-90.

HULSMEIER, A. J., PAESOLD-BURDA, P. & HENNET, T. 2007. N-glycosylation site occupancy in serum glycoproteins using multiple reaction monitoring liquid chromatography-mass spectrometry. *Mol Cell Proteomics,* 6**,** 2132-8.

HUNDT, C., PEYRIN, J. M., HAIK, S., GAUCZYNSKI, S., LEUCHT, C., RIEGER, R., RILEY, M. L., DESLYS, J. P., DORMONT, D., LASMEZAS, C. I. & WEISS, S. 2001. Identification of interaction domains of the prion protein with its 37-kDa/67-kDa laminin receptor. *EMBO J,* 20**,** 5876-86.

HUNTER, G. D., GIBBONS, R. A., KIMBERLIN, R. H. & MILLSON, G. C. 1969. Further studies of the infectivity and stability of extracts and homogenates derived from scrapie affected mouse brains. *J Comp Pathol,* 79**,** 101-8.

HUNTER, G. D. & MILLSON, G. C. 1967. Attempts to release the scrapie agent from tissue debris. *J Comp Pathol,* 77**,** 301-7.

IKEDA, S., KOBAYASHI, A. & KITAMOTO, T. 2008. Thr but Asn of the N-glycosylation sites of PrP is indispensable for its misfolding. *Biochem Biophys Res Commun,* 369**,** 1195-8.

IMPERIALI, B. & O'CONNOR, S. E. 1999. Effect of N-linked glycosylation on glycopeptide and glycoprotein structure. *Curr Opin Chem Biol,* 3**,** 643-9.

IMRAN, M. & MAHMOOD, S. 2011. An overview of human prion diseases. *Virol J,* 8**,** 559.

JACKSON, G. S., HOSSZU, L. L., POWER, A., HILL, A. F., KENNEY, J., SAIBIL, H., CRAVEN, C. J., WALTHO, J. P., CLARKE, A. R. & COLLINGE, J. 1999. Reversible conversion of monomeric human prion protein between native and fibrilogenic conformations. *Science,* 283**,** 1935-7.

JAMIESON, E., JEFFREY, M., IRONSIDE, J. W. & FRASER, J. R. 2001. Apoptosis and dendritic dysfunction precede prion protein accumulation in 87V scrapie. *Neuroreport,* 12**,** 2147-53.

JARRETT, J. T. & LANSBURY, P. T., JR. 1993. Seeding "one-dimensional crystallization" of amyloid: a pathogenic mechanism in Alzheimer's disease and scrapie? *Cell,* 73**,** 1055-8.

JIMENEZ-HUETE, A., LIEVENS, P. M., VIDAL, R., PICCARDO, P., GHETTI, B., TAGLIAVINI, F., FRANGIONE, B. & PRELLI, F. 1998. Endogenous proteolytic cleavage of normal and disease-associated isoforms of the human prion protein in neural and non-neural tissues. *Am J Pathol,* 153**,** 1561-72.

KANAANI, J., PRUSINER, S. B., DIACOVO, J., BAEKKESKOV, S. & LEGNAME, G. 2005. Recombinant prion protein induces rapid polarization and development of synapses in embryonic rat hippocampal neurons in vitro. *J Neurochem,* 95**,** 1373-86.

KAYSER, V., CHENNAMSETTY, N., VOYNOV, V., FORRER, K., HELK, B. & TROUT, B. L. 2011. Glycosylation influences on the aggregation propensity of therapeutic monoclonal antibodies. *Biotechnol J,* 6**,** 38-44.

KENWARD, N., LASZLO, L., LANDON, M., FERGUSSON, J., LOWE, J., MCDERMOTT, H., HOPE, J., BROWN, J. & MAYER, R. J. 1992. A role for lysosomes in scrapie pathogenesis. *Biochem Soc Trans,* 20**,** 265S.

KIM, B. M., KIM, H., RAINES, R. T. & LEE, Y. 2004. Glycosylation of onconase increases its conformational stability and toxicity for cancer cells. *Biochem Biophys Res Commun,* 315**,** 976-83.

KIM, S. J. & HEGDE, R. S. 2002. Cotranslational partitioning of nascent prion protein into multiple populations at the translocation channel. *Mol Biol Cell,* 13**,** 3775-86.

KIMBERLIN, R. H. & WALKER, C. A. 1979. Pathogenesis of mouse scrapie: dynamics of agent replication in spleen, spinal cord and brain after infection by different routes. *J Comp Pathol,* 89**,** 551-62.

KIMBERLIN, R. H., WALKER, C. A. & FRASER, H. 1989. The genomic identity of different strains of mouse scrapie is expressed in hamsters and preserved on reisolation in mice. *J Gen Virol,* 70 (Pt 8)**,** 2017-25.

KOBAYASHI, Y. & SUZUKI, Y. 2012. Evidence for N-glycan shielding of antigenic sites during evolution of human influenza A virus hemagglutinin. *J Virol,* 86**,** 3446-51.

KOCISKO, D. A., COME, J. H., PRIOLA, S. A., CHESEBRO, B., RAYMOND, G. J., LANSBURY, P. T. & CAUGHEY, B. 1994. Cell-free formation of protease-resistant prion protein. *Nature,* 370**,** 471-4.

KOCISKO, D. A., PRIOLA, S. A., RAYMOND, G. J., CHESEBRO, B., LANSBURY, P. T., JR. & CAUGHEY, B. 1995. Species specificity in the cell-free conversion of prion protein to protease-resistant forms: a model for the scrapie species barrier. *Proc Natl Acad Sci U S A,* 92**,** 3923-7.

KORNBLATT, J. A., MARCHAL, S., REZAEI, H., KORNBLATT, M. J., BALNY, C., LANGE, R., DEBEY, M. P., HUI BON HOA, G., MARDEN, M. C. & GROSCLAUDE, J. 2003. The fate of the prion protein in the prion/plasminogen complex. *Biochem Biophys Res Commun,* 305**,** 518-22.

KRISTIANSEN, M., DERIZIOTIS, P., DIMCHEFF, D. E., JACKSON, G. S., OVAA, H., NAUMANN, H., CLARKE, A. R., VAN LEEUWEN, F. W., MENENDEZ-BENITO, V., DANTUMA, N. P., PORTIS, J. L., COLLINGE, J. & TABRIZI, S. J. 2007. Disease-associated prion protein oligomers inhibit the 26S proteasome. *Mol Cell,* 26**,** 175-88.

KUCZIUS, T., GRASSI, J., KARCH, H. & GROSCHUP, M. H. 2007a. Binding of N- and C-terminal anti-prion protein antibodies generates distinct phenotypes of cellular prion proteins (PrPC) obtained from human, sheep, cattle and mouse. *FEBS J,* 274**,** 1492-502.

KUCZIUS, T. & GROSCHUP, M. H. 1999. Differences in proteinase K resistance and neuronal deposition of abnormal prion proteins characterize bovine spongiform encephalopathy (BSE) and scrapie strains. *Mol Med,* 5**,** 406-18.

KUCZIUS, T., KOCH, R., KEYVANI, K., KARCH, H., GRASSI, J. & GROSCHUP, M. H. 2007b. Regional and phenotype heterogeneity of cellular prion proteins in the human brain. *Eur J Neurosci,* 25**,** 2649-55.

KUNDRA, R. & KORNFELD, S. 1999. Asparagine-linked oligosaccharides protect Lamp-1 and Lamp-2 from intracellular proteolysis. *J Biol Chem,* 274**,** 31039-46.

KURSCHNER, C. & MORGAN, J. I. 1995. The cellular prion protein (PrP) selectively binds to Bcl-2 in the yeast two-hybrid system. *Brain Res Mol Brain Res,* 30**,** 165-8.

KURSCHNER, C. & MORGAN, J. I. 1996. Analysis of interaction sites in homo- and heteromeric complexes containing Bcl-2 family members and the cellular prion protein. *Brain Res Mol Brain Res,* 37**,** 249-58.

KUWAHARA, C., TAKEUCHI, A. M., NISHIMURA, T., HARAGUCHI, K., KUBOSAKI, A., MATSUMOTO, Y., SAEKI, K., YOKOYAMA, T., ITOHARA, S. & ONODERA, T. 1999. Prions prevent neuronal cell-line death. *Nature,* 400**,** 225-6.

LAFFONT-PROUST, I., FAUCHEUX, B. A., HASSIG, R., SAZDOVITCH, V., SIMON, S., GRASSI, J., HAUW, J. J., MOYA, K. L. & HAIK, S. 2005. The N-terminal cleavage of cellular prion protein in the human brain. *FEBS Lett,* 579**,** 6333-7.

LAFFONT-PROUST, I., HASSIG, R., HAIK, S., SIMON, S., GRASSI, J., FONTA, C., FAUCHEUX, B. A. & MOYA, K. L. 2006. Truncated PrP(c) in mammalian brain: interspecies variation and location in membrane rafts. *Biol Chem,* 387**,** 297-300.

LAINE, J., MARC, M. E., SY, M. S. & AXELRAD, H. 2001. Cellular and subcellular morphological localization of normal prion protein in rodent cerebellum. *Eur J Neurosci,* 14**,** 47-56.

LATARJET, R., MUEL, B., HAIG, D. A., CLARKE, M. C. & ALPER, T. 1970. Inactivation of the scrapie agent by near monochromatic ultraviolet light. *Nature,* 227**,** 1341-3.

LAZARINI, F., CASTELNAU, P., CHERMANN, J. F., DESLYS, J. P. & DORMONT, D. 1994. Modulation of prion protein gene expression by growth factors in cultured mouse astrocytes and PC-12 cells. *Brain Res Mol Brain Res,* 22**,** 268-74.

LAZARINI, F., DESLYS, J. P. & DORMONT, D. 1991. Regulation of the glial fibrillary acidic protein, beta actin and prion protein mRNAs during brain development in mouse. *Brain Res Mol Brain Res,* 10**,** 343-6.

LEE, I. Y., WESTAWAY, D., SMIT, A. F., WANG, K., SETO, J., CHEN, L., ACHARYA, C., ANKENER, M., BASKIN, D., COOPER, C., YAO, H., PRUSINER, S. B. & HOOD, L. E. 1998. Complete genomic sequence and analysis of the prion protein gene region from three mammalian species. *Genome Res,* 8**,** 1022-37.

LEE, T. K., KOH, A. S., CUI, Z., PIERCE, R. H. & BALLATORI, N. 2003. N-glycosylation controls functional activity of Oatp1, an organic anion transporter. *Am J Physiol Gastrointest Liver Physiol,* 285**,** G371-81.

LEWIS, V., HILL, A. F., HAIGH, C. L., KLUG, G. M., MASTERS, C. L., LAWSON, V. A. & COLLINS, S. J. 2009. Increased proportions of C1 truncated prion protein protect against cellular M1000 prion infection. *J Neuropathol Exp Neurol,* 68**,** 1125-35.

LI, A., CHRISTENSEN, H. M., STEWART, L. R., ROTH, K. A., CHIESA, R. & HARRIS, D. A. 2007. Neonatal lethality in transgenic mice expressing prion protein with a deletion of residues 105-125. *EMBO J,* 26**,** 548-58.

LI, A. & HARRIS, D. A. 2005. Mammalian prion protein suppresses Bax-induced cell death in yeast. *J Biol Chem,* 280**,** 17430-4.

LIANG, J. & KONG, Q. 2012. alpha-Cleavage of cellular prion protein. *Prion,* 6**,** 453-60.

LICHTENBERG, D., GONI, F. M. & HEERKLOTZ, H. 2005. Detergent-resistant membranes should not be identified with membrane rafts. *Trends Biochem Sci,* 30**,** 430-6.

LINDEN, R., MARTINS, V. R., PRADO, M. A., CAMMAROTA, M., IZQUIERDO, I. & BRENTANI, R. R. 2008. Physiology of the prion protein. *Physiol Rev,* 88**,** 673-728.

LIU, T., ZWINGMAN, T., LI, R., PAN, T., WONG, B. S., PETERSEN, R. B., GAMBETTI, P., HERRUP, K. & SY, M. S. 2001. Differential expression of cellular prion protein in mouse brain as detected with multiple anti-PrP monoclonal antibodies. *Brain Res,* 896**,** 118-29.

LIVI, G. P., LILLQUIST, J. S., MILES, L. M., FERRARA, A., SATHE, G. M., SIMON, P. L., MEYERS, C. A., GORMAN, J. A. & YOUNG, P. R. 1991. Secretion of N-glycosylated interleukin-1 beta in Saccharomyces cerevisiae using a leader peptide from Candida albicans. Effect of N-linked glycosylation on biological activity. *J Biol Chem,* 266**,** 15348-55.

LLOYD, S. E., THOMPSON, S. R., BECK, J. A., LINEHAN, J. M., WADSWORTH, J. D., BRANDNER, S., COLLINGE, J. & FISHER, E. M. 2004. Identification and characterization of a novel mouse prion gene allele. *Mamm Genome,* 15**,** 383-9.

LOPES, M. H., HAJJ, G. N., MURAS, A. G., MANCINI, G. L., CASTRO, R. M., RIBEIRO, K. C., BRENTANI, R. R., LINDEN, R. & MARTINS, V. R. 2005. Interaction of cellular prion and stress-inducible protein 1 promotes neuritogenesis and neuroprotection by distinct signaling pathways. *J Neurosci,* 25**,** 11330-9.

LUBLIN, D. M., GRIFFITH, R. C. & ATKINSON, J. P. 1986. Influence of glycosylation on allelic and cell-specific Mr variation, receptor processing, and ligand binding of the human complement C3b/C4b receptor. *J Biol Chem,* 261**,** 5736-44.

LUK, W. K., CHEN, V. P., CHOI, R. C. & TSIM, K. W. 2012. N-linked glycosylation of dimeric acetylcholinesterase in erythrocytes is essential for enzyme maturation and membrane targeting. *FEBS J,* 279**,** 3229-39.

LYSEK, D. A., SCHORN, C., NIVON, L. G., ESTEVE-MOYA, V., CHRISTEN, B., CALZOLAI, L., VON SCHROETTER, C., FIORITO, F., HERRMANN, T., GUNTERT, P. & WUTHRICH, K. 2005. Prion protein NMR structures of cats, dogs, pigs, and sheep. *Proc Natl Acad Sci U S A,* 102**,** 640-5.

MA, J., WOLLMANN, R. & LINDQUIST, S. 2002. Neurotoxicity and neurodegeneration when PrP accumulates in the cytosol. *Science,* 298**,** 1781-5.

MACDONALD, J. L. & PIKE, L. J. 2005. A simplified method for the preparation of detergent-free lipid rafts. *J Lipid Res,* 46**,** 1061-7.

MANGE, A., BERANGER, F., PEOC'H, K., ONODERA, T., FROBERT, Y. & LEHMANN, S. 2004. Alpha- and beta- cleavages of the amino-terminus of the cellular prion protein. *Biol Cell,* 96**,** 125-32.

MANSON, J., WEST, J. D., THOMSON, V., MCBRIDE, P., KAUFMAN, M. H. & HOPE, J. 1992. The prion protein gene: a role in mouse embryogenesis? *Development,* 115**,** 117-22.

MANSON, J. C., CANCELLOTTI, E., HART, P., BISHOP, M. T. & BARRON, R. M. 2006. The transmissible spongiform encephalopathies: emerging and declining epidemics. *Biochem Soc Trans,* 34**,** 1155-8.

MANSON, J. C., CLARKE, A. R., HOOPER, M. L., AITCHISON, L., MCCONNELL, I. & HOPE, J. 1994a. 129/Ola mice carrying a null mutation in PrP that abolishes mRNA production are developmentally normal. *Mol Neurobiol,* 8**,** 121-7.

MANSON, J. C., CLARKE, A. R., MCBRIDE, P. A., MCCONNELL, I. & HOPE, J. 1994b. PrP gene dosage determines the timing but not the final intensity or distribution of lesions in scrapie pathology. *Neurodegeneration,* 3**,** 331-40.

MARIJANOVIC, Z., CAPUTO, A., CAMPANA, V. & ZURZOLO, C. 2009. Identification of an intracellular site of prion conversion. *PLoS Pathog,* 5**,** e1000426.

MARINO, K., BONES, J., KATTLA, J. J. & RUDD, P. M. 2010. A systematic approach to protein glycosylation analysis: a path through the maze. *Nat Chem Biol,* 6**,** 713-23.

MARTINS, V. R., MERCADANTE, A. F., CABRAL, A. L., FREITAS, A. R. & CASTRO, R. M. 2001. Insights into the physiological function of cellular prion protein. *Braz J Med Biol Res,* 34**,** 585-95.

MCLENNAN, N. F., BRENNAN, P. M., MCNEILL, A., DAVIES, I., FOTHERINGHAM, A., RENNISON, K. A., RITCHIE, D., BRANNAN, F., HEAD, M. W., IRONSIDE, J. W., WILLIAMS, A. & BELL, J. E. 2004. Prion protein accumulation and neuroprotection in hypoxic brain damage. *Am J Pathol,* 165**,** 227-35.

MCMAHON, H. E., MANGE, A., NISHIDA, N., CREMINON, C., CASANOVA, D. & LEHMANN, S. 2001. Cleavage of the amino terminus of the prion protein by reactive oxygen species. *J Biol Chem,* 276**,** 2286-91.

MCNALLY, K. L., WARD, A. E. & PRIOLA, S. A. 2009. Cells expressing anchorless prion protein are resistant to scrapie infection. *J Virol,* 83**,** 4469-75.

MEAD, S. 2006. Prion disease genetics. *Eur J Hum Genet,* 14**,** 273-81.

MIELE, G., ALEJO BLANCO, A. R., BAYBUTT, H., HORVAT, S., MANSON, J. & CLINTON, M. 2003. Embryonic activation and developmental expression of the murine prion protein gene. *Gene Expr,* 11**,** 1-12.

MONTGOMERY, D. L. 1994. Astrocytes: Form, Functions, and Roles in Disease. *Veterinary Pathology Online,* 31**,** 145-167.

MOORE, R. C., LEE, I. Y., SILVERMAN, G. L., HARRISON, P. M., STROME, R., HEINRICH, C., KARUNARATNE, A., PASTERNAK, S. H., CHISHTI, M. A., LIANG, Y., MASTRANGELO, P., WANG, K., SMIT, A. F., KATAMINE, S., CARLSON, G. A., COHEN, F. E., PRUSINER, S. B., MELTON, D. W., TREMBLAY, P., HOOD, L. E. & WESTAWAY, D. 1999. Ataxia in prion protein (PrP)-deficient mice is associated with upregulation of the novel PrP-like protein doppel. *J Mol Biol,* 292**,** 797-817.

MORILLAS, M., SWIETNICKI, W., GAMBETTI, P. & SUREWICZ, W. K. 1999. Membrane environment alters the conformational structure of the recombinant human prion protein. *J Biol Chem,* 274**,** 36859-65.

MOSER, M., COLELLO, R. J., POTT, U. & OESCH, B. 1995. Developmental expression of the prion protein gene in glial cells. *Neuron,* 14**,** 509-17.

MOUILLET-RICHARD, S., ERMONVAL, M., CHEBASSIER, C., LAPLANCHE, J. L., LEHMANN, S., LAUNAY, J. M. & KELLERMANN, O. 2000. Signal transduction through prion protein. *Science,* 289**,** 1925-8.

MOYA, K. L., SALES, N., HASSIG, R., CREMINON, C., GRASSI, J. & DI GIAMBERARDINO, L. 2000. Immunolocalization of the cellular prion protein in normal brain. *Microsc Res Tech,* 50**,** 58-65.

MURAMOTO, T., DEARMOND, S. J., SCOTT, M., TELLING, G. C., COHEN, F. E. & PRUSINER, S. B. 1997. Heritable disorder resembling neuronal storage disease in mice expressing prion protein with deletion of an alpha-helix. *Nat Med,* 3**,** 750-5.

NASLAVSKY, N., STEIN, R., YANAI, A., FRIEDLANDER, G. & TARABOULOS, A. 1997. Characterization of detergent-insoluble complexes containing the cellular prion protein and its scrapie isoform. *J Biol Chem,* 272**,** 6324-31.

NEUENDORF, E., WEBER, A., SAALMUELLER, A., SCHATZL, H., REIFENBERG, K., PFAFF, E. & GROSCHUP, M. H. 2004. Glycosylation deficiency at either one of the two glycan attachment sites of cellular prion protein preserves susceptibility to bovine spongiform encephalopathy and scrapie infections. *J Biol Chem,* 279**,** 53306-16.

NICO, P. B., DE-PARIS, F., VINADE, E. R., AMARAL, O. B., ROCKENBACH, I., SOARES, B. L., GUARNIERI, R., WICHERT-ANA, L., CALVO, F., WALZ, R., IZQUIERDO, I., SAKAMOTO, A. C., BRENTANI, R., MARTINS, V. R. & BIANCHIN, M. M. 2005. Altered behavioural response to acute stress in mice lacking cellular prion protein. *Behav Brain Res,* 162**,** 173-81.

NIEZNANSKI, K., CHOI, J. K., CHEN, S., SUREWICZ, K. & SUREWICZ, W. K. 2012. Soluble prion protein inhibits amyloid-beta (Abeta) fibrillization and toxicity. *J Biol Chem,* 287**,** 33104-8.

NIEZNANSKI, K., NIEZNANSKA, H., SKOWRONEK, K. J., OSIECKA, K. M. & STEPKOWSKI, D. 2005a. Direct interaction between prion protein and tubulin. *Biochem Biophys Res Commun,* 334**,** 403-11.

NIEZNANSKI, K., RUTKOWSKI, M., DOMINIK, M. & STEPKOWSKI, D. 2005b. Proteolytic processing and glycosylation influence formation of porcine prion protein complexes. *Biochem J,* 387**,** 93-100.

NISHINA, K. A., DELEAULT, N. R., MAHAL, S. P., BASKAKOV, I., LUHRS, T., RIEK, R. & SUPATTAPONE, S. 2006. The stoichiometry of host PrPC glycoforms modulates the efficiency of PrPSc formation in vitro. *Biochemistry,* 45**,** 14129-39.

NISHINA, K. A. & SUPATTAPONE, S. 2007. Immunodetection of glycophosphatidylinositol-anchored proteins following treatment with phospholipase C. *Anal Biochem,* 363**,** 318-20.

NITRINI, R., ROSEMBERG, S., PASSOS-BUENO, M. R., DA SILVA, L. S., IUGHETTI, P., PAPADOPOULOS, M., CARRILHO, P. M., CARAMELLI, P., ALBRECHT, S., ZATZ, M. & LEBLANC, A. 1997. Familial spongiform encephalopathy associated with a novel prion protein gene mutation. *Ann Neurol,* 42**,** 138-46.

NORSTROM, E. M., CIACCIO, M. F., RASSBACH, B., WOLLMANN, R. & MASTRIANNI, J. A. 2007. Cytosolic prion protein toxicity is independent of cellular prion protein expression and prion propagation. *J Virol,* 81**,** 2831-7.

NUNZIANTE, M., GILCH, S. & SCHATZL, H. M. 2003. Essential role of the prion protein N terminus in subcellular trafficking and half-life of cellular prion protein. *J Biol Chem,* 278**,** 3726-34.
OESCH, B., WESTAWAY, D., WALCHLI, M., MCKINLEY, M. P., KENT, S. B., AEBERSOLD, R., BARRY, R. A., TEMPST, P., TEPLOW, D. B., HOOD, L. E. & ET AL. 1985. A cellular gene encodes scrapie PrP 27-30 protein. *Cell,* 40**,** 735-46.
OHTSUBO, K. & MARTH, J. D. 2006. Glycosylation in cellular mechanisms of health and disease. *Cell,* 126**,** 855-67.
OPDENAKKER, G., RUDD, P. M., PONTING, C. P. & DWEK, R. A. 1993. Concepts and principles of glycobiology. *FASEB J,* 7**,** 1330-7.
ORRU, C. D., WILHAM, J. M., HUGHSON, A. G., RAYMOND, L. D., MCNALLY, K. L., BOSSERS, A., LIGIOS, C. & CAUGHEY, B. 2009. Human variant Creutzfeldt-Jakob disease and sheep scrapie PrP(res) detection using seeded conversion of recombinant prion protein. *Protein Eng Des Sel,* 22**,** 515-21.
PAN, K. M., BALDWIN, M., NGUYEN, J., GASSET, M., SERBAN, A., GROTH, D., MEHLHORN, I., HUANG, Z., FLETTERICK, R. J., COHEN, F. E. & ET AL. 1993. Conversion of alpha-helices into beta-sheets features in the formation of the scrapie prion proteins. *Proc Natl Acad Sci U S A,* 90**,** 10962-6.
PANTERA, B., BINI, C., CIRRI, P., PAOLI, P., CAMICI, G., MANAO, G. & CASELLI, A. 2009. PrP(c) activation induces neurite outgrowth and differentiation in PC12 cells: role for caveolin-1 in the signal transduction pathway. *J Neurochem*.
PARKIN, E. T., HUSSAIN, I., TURNER, A. J. & HOOPER, N. M. 1997. The amyloid precursor protein is not enriched in caveolae-like, detergent-insoluble membrane microdomains. *J Neurochem,* 69**,** 2179-88.
PARKIN, E. T., WATT, N. T., TURNER, A. J. & HOOPER, N. M. 2004. Dual mechanisms for shedding of the cellular prion protein. *J Biol Chem,* 279**,** 11170-8.
PARKYN, C. J., VERMEULEN, E. G., MOOTOOSAMY, R. C., SUNYACH, C., JACOBSEN, C., OXVIG, C., MOESTRUP, S., LIU, Q., BU, G., JEN, A. & MORRIS, R. J. 2008. LRP1 controls biosynthetic and endocytic trafficking of neuronal prion protein. *J Cell Sci,* 121**,** 773-83.
PATTISON, I. H. & MILLSON, G. C. 1961. Scrapie produced experimentally in goats with special reference to the clinical syndrome. *J Comp Pathol,* 71**,** 101-9.
PEDEN, A. H. & IRONSIDE, J. W. 2004. Review: pathology of variant Creutzfeldt-Jakob disease. *Folia Neuropathol,* 42 Suppl A**,** 85-91.
PERETZ, D., WILLIAMSON, R. A., MATSUNAGA, Y., SERBAN, H., PINILLA, C., BASTIDAS, R. B., ROZENSHTEYN, R., JAMES, T. L., HOUGHTEN, R. A., COHEN, F. E., PRUSINER, S. B. & BURTON, D. R. 1997. A conformational transition at the N terminus of the prion protein features in formation of the scrapie isoform. *J Mol Biol,* 273**,** 614-22.
PERINI, F., VIDAL, R., GHETTI, B., TAGLIAVINI, F., FRANGIONE, B. & PRELLI, F. 1996. PrP27-30 is a normal soluble prion protein fragment released by human platelets. *Biochem Biophys Res Commun,* 223**,** 572-7.
PERSAUD-SAWIN, D. A., LIGHTCAP, S. & HARRY, G. J. 2009. Isolation of rafts from mouse brain tissue by a detergent-free method. *J Lipid Res,* 50**,** 759-67.

PICCARDO, P., MANSON, J. C., KING, D., GHETTI, B. & BARRON, R. M. 2007. Accumulation of prion protein in the brain that is not associated with transmissible disease. *Proc Natl Acad Sci U S A,* 104**,** 4712-7.
PIRO, J. R., HARRIS, B. T., NISHINA, K., SOTO, C., MORALES, R., REES, J. R. & SUPATTAPONE, S. 2009. Prion protein glycosylation is not required for strain-specific neurotropism. *J Virol,* 83**,** 5321-8.
PORTO-CARREIRO, I., FEVRIER, B., PAQUET, S., VILETTE, D. & RAPOSO, G. 2005. Prions and exosomes: from PrPc trafficking to PrPsc propagation. *Blood Cells Mol Dis,* 35**,** 143-8.
POWELL, L. M. & PAIN, R. H. 1992. Effects of glycosylation on the folding and stability of human, recombinant and cleaved alpha 1-antitrypsin. *J Mol Biol,* 224**,** 241-52.
PRADO, M. A., ALVES-SILVA, J., MAGALHAES, A. C., PRADO, V. F., LINDEN, R., MARTINS, V. R. & BRENTANI, R. R. 2004. PrPc on the road: trafficking of the cellular prion protein. *J Neurochem,* 88**,** 769-81.
PRAUS, M., KETTELGERDES, G., BAIER, M., HOLZHUTTER, H. G., JUNGBLUT, P. R., MAISSEN, M., EPPLE, G., SCHLEUNING, W. D., KOTTGEN, E., AGUZZI, A. & GESSNER, R. 2003. Stimulation of plasminogen activation by recombinant cellular prion protein is conserved in the NH2-terminal fragment PrP23-110. *Thromb Haemost,* 89**,** 812-9.
PRIOLA, S. A. & LAWSON, V. A. 2001. Glycosylation influences cross-species formation of protease-resistant prion protein. *EMBO J,* 20**,** 6692-9.
PRUSINER, S. B. 1982. Novel proteinaceous infectious particles cause scrapie. *Science,* 216**,** 136-44.
PRUSINER, S. B. 1991. Molecular biology of prion diseases. *Science,* 252**,** 1515-22.
PRUSINER, S. B. 1998. Prions. *Proc Natl Acad Sci U S A,* 95**,** 13363-83.
PRUSINER, S. B., GROTH, D. F., BOLTON, D. C., KENT, S. B. & HOOD, L. E. 1984. Purification and structural studies of a major scrapie prion protein. *Cell,* 38**,** 127-34.
QIN, K., ZHAO, L., TANG, Y., BHATTA, S., SIMARD, J. M. & ZHAO, R. Y. 2006. Doppel-induced apoptosis and counteraction by cellular prion protein in neuroblastoma and astrocytes. *Neuroscience,* 141**,** 1375-88.
RANSOHOFF, R. M. & PERRY, V. H. 2009. Microglial physiology: unique stimuli, specialized responses. *Annu Rev Immunol,* 27**,** 119-45.
RAYMOND, G. J., BOSSERS, A., RAYMOND, L. D., O'ROURKE, K. I., MCHOLLAND, L. E., BRYANT, P. K., 3RD, MILLER, M. W., WILLIAMS, E. S., SMITS, M. & CAUGHEY, B. 2000. Evidence of a molecular barrier limiting susceptibility of humans, cattle and sheep to chronic wasting disease. *EMBO J,* 19**,** 4425-30.
RIEK, R., HORNEMANN, S., WIDER, G., BILLETER, M., GLOCKSHUBER, R. & WUTHRICH, K. 1996. NMR structure of the mouse prion protein domain PrP(121-321). *Nature,* 382**,** 180-2.
ROBERTSON, C., BOOTH, S. A., BENIAC, D. R., COULTHART, M. B., BOOTH, T. F. & MCNICOL, A. 2006. Cellular prion protein is released on exosomes from activated platelets. *Blood,* 107**,** 3907-11.
ROESLER, R., WALZ, R., QUEVEDO, J., DE-PARIS, F., ZANATA, S. M., GRANER, E., IZQUIERDO, I., MARTINS, V. R. & BRENTANI, R. R. 1999.

Normal inhibitory avoidance learning and anxiety, but increased locomotor activity in mice devoid of PrP(C). *Brain Res Mol Brain Res,* 71**,** 349-53.
ROFFE, M., BERALDO, F. H., BESTER, R., NUNZIANTE, M., BACH, C., MANCINI, G., GILCH, S., VORBERG, I., CASTILHO, B. A., MARTINS, V. R. & HAJJ, G. N. 2010. Prion protein interaction with stress-inducible protein 1 enhances neuronal protein synthesis via mTOR. *Proc Natl Acad Sci U S A,* 107**,** 13147-52.
ROGERS, M., TARABOULOS, A., SCOTT, M., GROTH, D. & PRUSINER, S. B. 1990. Intracellular accumulation of the cellular prion protein after mutagenesis of its Asn-linked glycosylation sites. *Glycobiology,* 1**,** 101-9.
ROSSI, D., COZZIO, A., FLECHSIG, E., KLEIN, M. A., RULICKE, T., AGUZZI, A. & WEISSMANN, C. 2001. Onset of ataxia and Purkinje cell loss in PrP null mice inversely correlated with Dpl level in brain. *EMBO J,* 20**,** 694-702.
ROUCOU, X., GAINS, M. & LEBLANC, A. C. 2004. Neuroprotective functions of prion protein. *Journal of Neuroscience Research,* 75**,** 153-161.
RUDD, P. M., WORMALD, M. R., WING, D. R., PRUSINER, S. B. & DWEK, R. A. 2001. Prion glycoprotein: structure, dynamics, and roles for the sugars. *Biochemistry,* 40**,** 3759-66.
RYOU, C. 2007. Prions and prion diseases: fundamentals and mechanistic details. *J Microbiol Biotechnol,* 17**,** 1059-70.
SAKAGUCHI, S., KATAMINE, S., NISHIDA, N., MORIUCHI, R., SHIGEMATSU, K., SUGIMOTO, T., NAKATANI, A., KATAOKA, Y., HOUTANI, T., SHIRABE, S., OKADA, H., HASEGAWA, S., MIYAMOTO, T. & NODA, T. 1996. Loss of cerebellar Purkinje cells in aged mice homozygous for a disrupted PrP gene. *Nature,* 380**,** 528-31.
SALAMAT, M. K., DRON, M., CHAPUIS, J., LANGEVIN, C. & LAUDE, H. 2011. Prion propagation in cells expressing PrP glycosylation mutants. *J Virol,* 85**,** 3077-85.
SANTUCCIONE, A., SYTNYK, V., LESHCHYNS'KA, I. & SCHACHNER, M. 2005. Prion protein recruits its neuronal receptor NCAM to lipid rafts to activate p59fyn and to enhance neurite outgrowth. *J Cell Biol,* 169**,** 341-54.
SARNATARO, D., CAMPANA, V., PALADINO, S., STORNAIUOLO, M., NITSCH, L. & ZURZOLO, C. 2004. PrP(C) association with lipid rafts in the early secretory pathway stabilizes its cellular conformation. *Mol Biol Cell,* 15**,** 4031-42.
SCHMITT-ULMS, G., LEGNAME, G., BALDWIN, M. A., BALL, H. L., BRADON, N., BOSQUE, P. J., CROSSIN, K. L., EDELMAN, G. M., DEARMOND, S. J., COHEN, F. E. & PRUSINER, S. B. 2001. Binding of neural cell adhesion molecules (N-CAMs) to the cellular prion protein. *J Mol Biol,* 314**,** 1209-25.
SCHNEIDER, B., MUTEL, V., PIETRI, M., ERMONVAL, M., MOUILLET-RICHARD, S. & KELLERMANN, O. 2003. NADPH oxidase and extracellular regulated kinases 1/2 are targets of prion protein signaling in neuronal and nonneuronal cells. *Proc Natl Acad Sci U S A,* 100**,** 13326-31.
SCOTT, M., FOSTER, D., MIRENDA, C., SERBAN, D., COUFAL, F., WALCHLI, M., TORCHIA, M., GROTH, D., CARLSON, G., DEARMOND, S. J., WESTAWAY, D. & PRUSINER, S. B. 1989. Transgenic mice expressing

hamster prion protein produce species-specific scrapie infectivity and amyloid plaques. *Cell,* 59**,** 847-57.
SHAKIN-ESHLEMAN, S. H., REMALEY, A. T., ESHLEMAN, J. R., WUNNER, W. H. & SPITALNIK, S. L. 1992. N-linked glycosylation of rabies virus glycoprotein. Individual sequons differ in their glycosylation efficiencies and influence on cell surface expression. *J Biol Chem,* 267**,** 10690-8.
SHIKIYA, R. A. & BARTZ, J. C. 2011. In vitro generation of high-titer prions. *J Virol,* 85**,** 13439-42.
SHMERLING, D., HEGYI, I., FISCHER, M., BLATTLER, T., BRANDNER, S., GOTZ, J., RULICKE, T., FLECHSIG, E., COZZIO, A., VON MERING, C., HANGARTNER, C., AGUZZI, A. & WEISSMANN, C. 1998. Expression of amino-terminally truncated PrP in the mouse leading to ataxia and specific cerebellar lesions. *Cell,* 93**,** 203-14.
SHYNG, S. L., HEUSER, J. E. & HARRIS, D. A. 1994. A glycolipid-anchored prion protein is endocytosed via clathrin-coated pits. *J Cell Biol,* 125**,** 1239-50.
SHYNG, S. L., HUBER, M. T. & HARRIS, D. A. 1993. A prion protein cycles between the cell surface and an endocytic compartment in cultured neuroblastoma cells. *J Biol Chem,* 268**,** 15922-8.
SHYNG, S. L., MOULDER, K. L., LESKO, A. & HARRIS, D. A. 1995. The N-terminal domain of a glycolipid-anchored prion protein is essential for its endocytosis via clathrin-coated pits. *J Biol Chem,* 270**,** 14793-800.
SHYU, W. C., CHEN, C. P., SAEKI, K., KUBOSAKI, A., MATUSMOTO, Y., ONODERA, T., DING, D. C., CHIANG, M. F., LEE, Y. J., LIN, S. Z. & LI, H. 2005. Hypoglycemia enhances the expression of prion protein and heat-shock protein 70 in a mouse neuroblastoma cell line. *J Neurosci Res,* 80**,** 887-94.
SHYU, W. C., LIN, S. Z., SAEKI, K., KUBOSAKI, A., MATSUMOTO, Y., ONODERA, T., CHIANG, M. F., THAJEB, P. & LI, H. 2004. Hyperbaric oxygen enhances the expression of prion protein and heat shock protein 70 in a mouse neuroblastoma cell line. *Cell Mol Neurobiol,* 24**,** 257-68.
SILVEIRA, J. R., RAYMOND, G. J., HUGHSON, A. G., RACE, R. E., SIM, V. L., HAYES, S. F. & CAUGHEY, B. 2005. The most infectious prion protein particles. *Nature,* 437**,** 257-61.
SIRACUSA, L. D., SILAN, C. M., JUSTICE, M. J., MERCER, J. A., BAUSKIN, A. R., BEN-NERIAH, Y., DUBOULE, D., HASTIE, N. D., COPELAND, N. G. & JENKINS, N. A. 1990. A molecular genetic linkage map of mouse chromosome 2. *Genomics,* 6**,** 491-504.
SMART, E. J., YING, Y. S., MINEO, C. & ANDERSON, R. G. 1995. A detergent-free method for purifying caveolae membrane from tissue culture cells. *Proc Natl Acad Sci U S A,* 92**,** 10104-8.
SOLA, R. J. & GRIEBENOW, K. 2009. Effects of glycosylation on the stability of protein pharmaceuticals. *J Pharm Sci,* 98**,** 1223-45.
SOLOMON, I. H., KHATRI, N., BIASINI, E., MASSIGNAN, T., HUETTNER, J. E. & HARRIS, D. A. 2011. An N-terminal polybasic domain and cell surface localization are required for mutant prion protein toxicity. *J Biol Chem,* 286**,** 14724-36.
SOMERVILLE, R. A. 1999. Host and transmissible spongiform encephalopathy agent strain control glycosylation of PrP. *J Gen Virol,* 80 (Pt 7)**,** 1865-72.

SOMERVILLE, R. A., HAMILTON, S. & FERNIE, K. 2005. Transmissible spongiform encephalopathy strain, PrP genotype and brain region all affect the degree of glycosylation of PrPSc. *J Gen Virol,* 86**,** 241-6.

SONG, K. S., LI, S., OKAMOTO, T., QUILLIAM, L. A., SARGIACOMO, M. & LISANTI, M. P. 1996. Co-purification and direct interaction of Ras with caveolin, an integral membrane protein of caveolae microdomains. Detergent-free purification of caveolae microdomains. *J Biol Chem,* 271**,** 9690-7.

SPIELHAUPTER, C. & SCHATZL, H. M. 2001. PrPC directly interacts with proteins involved in signaling pathways. *J Biol Chem,* 276**,** 44604-12.

SPUDICH, A., FRIGG, R., KILIC, E., KILIC, U., OESCH, B., RAEBER, A., BASSETTI, C. L. & HERMANN, D. M. 2005. Aggravation of ischemic brain injury by prion protein deficiency: role of ERK-1/-2 and STAT-1. *Neurobiol Dis,* 20**,** 442-9.

STAHL, N., BORCHELT, D. R., HSIAO, K. & PRUSINER, S. B. 1987. Scrapie prion protein contains a phosphatidylinositol glycolipid. *Cell,* 51**,** 229-40.

STENMARK, H., BUCCI, C. & ZERIAL, M. 1995. Expression of Rab GTPases using recombinant vaccinia viruses. *Methods Enzymol,* 257**,** 155-64.

STEVENSON, S. C., WANG, S., DENG, L. & TALL, A. R. 1993. Human plasma cholesteryl ester transfer protein consists of a mixture of two forms reflecting variable glycosylation at asparagine 341. *Biochemistry,* 32**,** 5121-6.

STIMSON, E., HOPE, J., CHONG, A. & BURLINGAME, A. L. 1999. Site-specific characterization of the N-linked glycans of murine prion protein by high-performance liquid chromatography/electrospray mass spectrometry and exoglycosidase digestions. *Biochemistry,* 38**,** 4885-95.

SUNEJA, S. K., MO, Z. & POTASHNER, S. J. 2006. Phospho-CREB and other phospho-proteins: improved recovery from brain tissue. *J Neurosci Methods,* 150**,** 238-41.

SUNYACH, C., CISSE, M. A., DA COSTA, C. A., VINCENT, B. & CHECLER, F. 2007. The C-terminal products of cellular prion protein processing, C1 and C2, exert distinct influence on p53-dependent staurosporine-induced caspase-3 activation. *J Biol Chem,* 282**,** 1956-63.

SUNYACH, C., JEN, A., DENG, J., FITZGERALD, K. T., FROBERT, Y., GRASSI, J., MCCAFFREY, M. W. & MORRIS, R. 2003. The mechanism of internalization of glycosylphosphatidylinositol-anchored prion protein. *EMBO J,* 22**,** 3591-601.

TAGLIAVINI, F., PRELLI, F., PORRO, M., SALMONA, M., BUGIANI, O. & FRANGIONE, B. 1992. A soluble form of prion protein in human cerebrospinal fluid: implications for prion-related encephalopathies. *Biochem Biophys Res Commun,* 184**,** 1398-404.

TAKAHASHI, M., YOKOE, S., ASAHI, M., LEE, S. H., LI, W., OSUMI, D., MIYOSHI, E. & TANIGUCHI, N. 2008. N-glycan of ErbB family plays a crucial role in dimer formation and tumor promotion. *Biochim Biophys Acta,* 1780**,** 520-4.

TARABOULOS, A., ROGERS, M., BORCHELT, D. R., MCKINLEY, M. P., SCOTT, M., SERBAN, D. & PRUSINER, S. B. 1990. Acquisition of protease resistance by prion proteins in scrapie-infected cells does not require asparagine-linked glycosylation. *Proc Natl Acad Sci U S A,* 87**,** 8262-6.

TAYLOR, D. R. & HOOPER, N. M. 2006. The prion protein and lipid rafts. *Mol Membr Biol,* 23**,** 89-99.
TAYLOR, D. R. & HOOPER, N. M. 2007. The low-density lipoprotein receptor-related protein 1 (LRP1) mediates the endocytosis of the cellular prion protein. *Biochem J,* 402**,** 17-23.
TAYLOR, D. R., PARKIN, E. T., COCKLIN, S. L., AULT, J. R., ASHCROFT, A. E., TURNER, A. J. & HOOPER, N. M. 2009. Role of ADAMs in the ectodomain shedding and conformational conversion of the prion protein. *J Biol Chem,* 284**,** 22590-600.
TELLING, G. C., PARCHI, P., DEARMOND, S. J., CORTELLI, P., MONTAGNA, P., GABIZON, R., MASTRIANNI, J., LUGARESI, E., GAMBETTI, P. & PRUSINER, S. B. 1996. Evidence for the conformation of the pathologic isoform of the prion protein enciphering and propagating prion diversity. *Science,* 274**,** 2079-82.
TOBLER, I., GAUS, S. E., DEBOER, T., ACHERMANN, P., FISCHER, M., RULICKE, T., MOSER, M., OESCH, B., MCBRIDE, P. A. & MANSON, J. C. 1996. Altered circadian activity rhythms and sleep in mice devoid of prion protein. *Nature,* 380**,** 639-42.
TOMITA, M., FURTHMAYR, H. & MARCHESI, V. T. 1978. Primary structure of human erythrocyte glycophorin A. Isolation and characterization of peptides and complete amino acid sequence. *Biochemistry,* 17**,** 4756-70.
TREUMANN, A., LIFELY, M. R., SCHNEIDER, P. & FERGUSON, M. A. 1995. Primary structure of CD52. *J Biol Chem,* 270**,** 6088-99.
TREUSCH, S., CYR, D. M. & LINDQUIST, S. 2009. Amyloid deposits: protection against toxic protein species? *Cell Cycle,* 8**,** 1668-74.
TSUDA, T., IKEDA, Y. & TANIGUCHI, N. 2000. The Asn-420-linked sugar chain in human epidermal growth factor receptor suppresses ligand-independent spontaneous oligomerization. Possible role of a specific sugar chain in controllable receptor activation. *J Biol Chem,* 275**,** 21988-94.
TSUI-PIERCHALA, B. A., ENCINAS, M., MILBRANDT, J. & JOHNSON, E. M., JR. 2002. Lipid rafts in neuronal signaling and function. *Trends Neurosci,* 25**,** 412-7.
TUZI, N. L., CANCELLOTTI, E., BAYBUTT, H., BLACKFORD, L., BRADFORD, B., PLINSTON, C., COGHILL, A., HART, P., PICCARDO, P., BARRON, R. M. & MANSON, J. C. 2008. Host PrP glycosylation: a major factor determining the outcome of prion infection. *PLoS Biol,* 6**,** e100.
UM, J. W., NYGAARD, H. B., HEISS, J. K., KOSTYLEV, M. A., STAGI, M., VORTMEYER, A., WISNIEWSKI, T., GUNTHER, E. C. & STRITTMATTER, S. M. 2012. Alzheimer amyloid-beta oligomer bound to postsynaptic prion protein activates Fyn to impair neurons. *Nat Neurosci,* 15**,** 1227-35.
VAN DER KAMP, M. W. & DAGGETT, V. 2009. The consequences of pathogenic mutations to the human prion protein. *Protein Eng Des Sel,* 22**,** 461-8.
VAN DER KAMP, M. W. & DAGGETT, V. 2011. Molecular dynamics as an approach to study prion protein misfolding and the effect of pathogenic mutations. *Top Curr Chem,* 305**,** 169-97.
VARKI, A. 1993. Biological roles of oligosaccharides: all of the theories are correct. *Glycobiology,* 3**,** 97-130.

VARKI, A. & SHARON, N. 2009. Historical Background and Overview. *In:* VARKI, A., CUMMINGS, R. D., ESKO, J. D., FREEZE, H. H., STANLEY, P., BERTOZZI, C. R., HART, G. W. & ETZLER, M. E. (eds.) *Essentials of Glycobiology.* 2nd ed. Cold Spring Harbor (NY).

VASSALLO, N. & HERMS, J. 2003. Cellular prion protein function in copper homeostasis and redox signalling at the synapse. *J Neurochem,* 86**,** 538-44.

VASSALLO, N., HERMS, J., BEHRENS, C., KREBS, B., SAEKI, K., ONODERA, T., WINDL, O. & KRETZSCHMAR, H. A. 2005. Activation of phosphatidylinositol 3-kinase by cellular prion protein and its role in cell survival. *Biochem Biophys Res Commun,* 332**,** 75-82.

VEITH, N. M., PLATTNER, H., STUERMER, C. A., SCHULZ-SCHAEFFER, W. J. & BURKLE, A. 2009. Immunolocalisation of PrPSc in scrapie-infected N2a mouse neuroblastoma cells by light and electron microscopy. *Eur J Cell Biol,* 88**,** 45-63.

VERMEIREN, C., NAJIMI, M., MALOTEAUX, J. M. & HERMANS, E. 2005. Molecular and functional characterisation of glutamate transporters in rat cortical astrocytes exposed to a defined combination of growth factors during in vitro differentiation. *Neurochem Int,* 46**,** 137-47.

VETRUGNO, V., CARDINALE, A., FILESI, I., MATTEI, S., SY, M. S., POCCHIARI, M. & BIOCCA, S. 2005. KDEL-tagged anti-prion intrabodies impair PrP lysosomal degradation and inhibit scrapie infectivity. *Biochem Biophys Res Commun,* 338**,** 1791-7.

VIDAL, M., MANGEAT, P. & HOEKSTRA, D. 1997. Aggregation reroutes molecules from a recycling to a vesicle-mediated secretion pathway during reticulocyte maturation. *J Cell Sci,* 110 (Pt 16)**,** 1867-77.

VILOTTE, J. L., SOULIER, S., ESSALMANI, R., STINNAKRE, M. G., VAIMAN, D., LEPOURRY, L., DA SILVA, J. C., BESNARD, N., DAWSON, M., BUSCHMANN, A., GROSCHUP, M., PETIT, S., MADELAINE, M. F., RAKATOBE, S., LE DUR, A., VILETTE, D. & LAUDE, H. 2001. Markedly increased susceptibility to natural sheep scrapie of transgenic mice expressing ovine prp. *J Virol,* 75**,** 5977-84.

VINCENT, B., PAITEL, E., FROBERT, Y., LEHMANN, S., GRASSI, J. & CHECLER, F. 2000. Phorbol ester-regulated cleavage of normal prion protein in HEK293 human cells and murine neurons. *J Biol Chem,* 275**,** 35612-6.

VINCENT, B., PAITEL, E., SAFTIG, P., FROBERT, Y., HARTMANN, D., DE STROOPER, B., GRASSI, J., LOPEZ-PEREZ, E. & CHECLER, F. 2001. The disintegrins ADAM10 and TACE contribute to the constitutive and phorbol ester-regulated normal cleavage of the cellular prion protein. *J Biol Chem,* 276**,** 37743-6.

WADSWORTH, J. D. & COLLINGE, J. 2007. Update on human prion disease. *Biochim Biophys Acta,* 1772**,** 598-609.

WALMSLEY, A. R., WATT, N. T., TAYLOR, D. R., PERERA, W. S. & HOOPER, N. M. 2009. alpha-cleavage of the prion protein occurs in a late compartment of the secretory pathway and is independent of lipid rafts. *Mol Cell Neurosci,* 40**,** 242-8.

WALZ, R., AMARAL, O. B., ROCKENBACH, I. C., ROESLER, R., IZQUIERDO, I., CAVALHEIRO, E. A., MARTINS, V. R. & BRENTANI, R. R. 1999. Increased

sensitivity to seizures in mice lacking cellular prion protein. *Epilepsia,* 40**,** 1679-82.
WANG, X., BOWERS, S. L., WANG, F., PU, X. A., NELSON, R. J. & MA, J. 2009. Cytoplasmic prion protein induces forebrain neurotoxicity. *Biochim Biophys Acta,* 1792**,** 555-63.
WARD, H. J., HEAD, M. W., WILL, R. G. & IRONSIDE, J. W. 2003. Variant Creutzfeldt-Jakob disease. *Clin Lab Med,* 23**,** 87-108.
WATANABE, I., ZHU, J., RECIO-PINTO, E. & THORNHILL, W. B. 2004. Glycosylation affects the protein stability and cell surface expression of Kv1.4 but Not Kv1.1 potassium channels. A pore region determinant dictates the effect of glycosylation on trafficking. *J Biol Chem,* 279**,** 8879-85.
WATT, N. T. & HOOPER, N. M. 2005. Reactive oxygen species (ROS)-mediated beta-cleavage of the prion protein in the mechanism of the cellular response to oxidative stress. *Biochem Soc Trans,* 33**,** 1123-5.
WATT, N. T., TAYLOR, D. R., GILLOTT, A., THOMAS, D. A., PERERA, W. S. & HOOPER, N. M. 2005. Reactive oxygen species-mediated beta-cleavage of the prion protein in the cellular response to oxidative stress. *J Biol Chem,* 280**,** 35914-21.
WEISSMANN, C. 2002. Molecular genetics of transmissible spongiform encephalopathies: an introduction. *J Toxicol Sci,* 27**,** 69-77.
WEISSMANN, C., BUELER, H., FISCHER, M., SAILER, A., AGUZZI, A. & AGUET, M. 1994. PrP-deficient mice are resistant to scrapie. *Ann N Y Acad Sci,* 724**,** 235-40.
WESTAWAY, D., GOODMAN, P. A., MIRENDA, C. A., MCKINLEY, M. P., CARLSON, G. A. & PRUSINER, S. B. 1987. Distinct prion proteins in short and long scrapie incubation period mice. *Cell,* 51**,** 651-62.
WESTAWAY, D., MIRENDA, C. A., FOSTER, D., ZEBARJADIAN, Y., SCOTT, M., TORCHIA, M., YANG, S. L., SERBAN, H., DEARMOND, S. J., EBELING, C. & ET AL. 1991. Paradoxical shortening of scrapie incubation times by expression of prion protein transgenes derived from long incubation period mice. *Neuron,* 7**,** 59-68.
WESTERGARD, L., TURNBAUGH, J. A. & HARRIS, D. A. 2011. A naturally occurring C-terminal fragment of the prion protein (PrP) delays disease and acts as a dominant-negative inhibitor of PrPSc formation. *J Biol Chem,* 286**,** 44234-42.
WHITE, J., JOHANNES, L., MALLARD, F., GIROD, A., GRILL, S., REINSCH, S., KELLER, P., TZSCHASCHEL, B., ECHARD, A., GOUD, B. & STELZER, E. H. 1999. Rab6 coordinates a novel Golgi to ER retrograde transport pathway in live cells. *J Cell Biol,* 147**,** 743-60.
WHITTAL, R. M., BALL, H. L., COHEN, F. E., BURLINGAME, A. L., PRUSINER, S. B. & BALDWIN, M. A. 2000. Copper binding to octarepeat peptides of the prion protein monitored by mass spectrometry. *Protein Sci,* 9**,** 332-43.
WILLIAMS, E. S. 2003. Scrapie and chronic wasting disease. *Clin Lab Med,* 23**,** 139-59.
WILSON, C. M., KRAFT, C., DUGGAN, C., ISMAIL, N., CRAWSHAW, S. G. & HIGH, S. 2005. Ribophorin I associates with a subset of membrane proteins after their integration at the sec61 translocon. *J Biol Chem,* 280**,** 4195-206.

WITUSIK, M., GRESNER, S. M., HULAS-BIGOSZEWSKA, K., KRYNSKA, B., AZIZI, S. A., LIBERSKI, P. P., BROWN, P. & RIESKE, P. 2007. Neuronal and astrocytic cells, obtained after differentiation of human neural GFAP-positive progenitors, present heterogeneous expression of PrPc. *Brain Res,* 1186**,** 65-73.

YAMAGUCHI, K., MATSUMOTO, T. & KUWATA, K. 2008. Critical region for amyloid fibril formation of mouse prion protein: unusual amyloidogenic properties of the helix 2 peptide. *Biochemistry,* 47**,** 13242-51.

YANG, Y., CHEN, L., PAN, H. Z., KOU, Y. & XU, C. M. 2009. Glycosylation modification of human prion protein provokes apoptosis in HeLa cells in vitro. *BMB Rep,* 42**,** 331-7.

YEO, T. K., SENGER, D. R., DVORAK, H. F., FRETER, L. & YEO, K. T. 1991. Glycosylation is essential for efficient secretion but not for permeability-enhancing activity of vascular permeability factor (vascular endothelial growth factor). *Biochem Biophys Res Commun,* 179**,** 1568-75.

YUSA, S., OLIVEIRA-MARTINS, J. B., SUGITA-KONISHI, Y. & KIKUCHI, Y. 2012. Cellular prion protein: from physiology to pathology. *Viruses,* 4**,** 3109-31.

ZANATA, S. M., LOPES, M. H., MERCADANTE, A. F., HAJJ, G. N., CHIARINI, L. B., NOMIZO, R., FREITAS, A. R., CABRAL, A. L., LEE, K. S., JULIANO, M. A., DE OLIVEIRA, E., JACHIERI, S. G., BURLINGAME, A., HUANG, L., LINDEN, R., BRENTANI, R. R. & MARTINS, V. R. 2002. Stress-inducible protein 1 is a cell surface ligand for cellular prion that triggers neuroprotection. *EMBO J,* 21**,** 3307-16.

ZERIAL, M. & MCBRIDE, H. 2001. Rab proteins as membrane organizers. *Nat Rev Mol Cell Biol,* 2**,** 107-17.

ZHAO, H., KLINGEBORN, M., SIMONSSON, M. & LINNE, T. 2006. Proteolytic cleavage and shedding of the bovine prion protein in two cell culture systems. *Virus Res,* 115**,** 43-55.

ZLOTNIK, I. & RENNIE, J. C. 1963. Further observations on the experimental transmission of scrapie from sheep and goats to laboratory mice. *J Comp Pathol,* 73**,** 150-62.